

University of Groningen

Lipid carriers for endothelial-specific delivery of siRNA

Kowalski, Piotr Stanislaw

IMPORTANT NOTE: You are advised to consult the publisher's version (publisher's PDF) if you wish to cite from it. Please check the document version below.

Document Version

Publisher's PDF, also known as Version of record

Publication date:

2014

[Link to publication in University of Groningen/UMCG research database](#)

Citation for published version (APA):

Kowalski, P. S. (2014). Lipid carriers for endothelial-specific delivery of siRNA: From particle development to attenuation of inflammation [S.I.]: s.n.

Copyright

Other than for strictly personal use, it is not permitted to download or to forward/distribute the text or part of it without the consent of the author(s) and/or copyright holder(s), unless the work is under an open content license (like Creative Commons).

Take-down policy

If you believe that this document breaches copyright please contact us providing details, and we will remove access to the work immediately and investigate your claim.

Downloaded from the University of Groningen/UMCG research database (Pure): <http://www.rug.nl/research/portal>. For technical reasons the number of authors shown on this cover page is limited to 10 maximum.

Lipid carriers for endothelial-specific delivery of siRNA

From particle development to attenuation of inflammation

Printing of this thesis was financially supported by:

University of Groningen



University Medical Center Groningen



Synvolux Therapeutics



GUIDE



Cover design: Piotr Kowalski & Rianne Jongman

Lay-out: Rianne Jongman

Printed by: Lovebird design & printing solutions, Poland



© 2014, Piotr Kowalski

All rights reserved. No part of this publication may be reproduced or transmitted in any form or by any means without permission of the author.

ISBN (printed):978-90-367-6983-9

ISBN (digital): 978-90-367-6982-2



university of
groningen

Lipid carriers for endothelial-specific delivery of siRNA

From particle development to attenuation of inflammation

Proefschrift

ter verkrijging van de graad van doctor aan de
Rijksuniversiteit Groningen
op gezag van de
rector magnificus prof. dr. E. Sterken
en volgens besluit van het College voor Promoties.

De openbare verdediging zal plaatsvinden op

woensdag 14 mei 2014 om 16.15 uur

door

Piotr Stanisław Kowalski

geboren op 7 mei 1985
te Leżajsk, Polen

Promotor

Prof. dr. G. Molema

Copromotor

Dr. J.A.A.M. Kamps

Beoordelingscommissie

Prof. dr. A. Józkwicz

Prof. dr. A. Herrmann

Prof. dr. G. Storm

Paranimfen

Dr. M. van Meurs

Dr. J. Moser

CONTENTS

Chapter 1	Introduction and aims of the thesis	8
Chapter 2	Targeted siRNA Delivery to Diseased Microvascular Endothelial Cells — Cellular and Molecular Concepts <i>IUBMB Life. 2011 Aug;63(8):648-58.</i>	14
Chapter 3	A Critical Role for Egr-1 during Vascular Remodelling in Pulmonary Arterial Hypertension <i>Under revision for Cardiovascular research</i>	36
Chapter 4	Anti-VCAM-1 and Anti-E-selectin SAINT-O-Somes for Selective Delivery of siRNA into Inflammation-Activated Primary Endothelial Cells <i>Mol Pharm. 2013 Aug 5;10(8):3033-44.</i>	62
Chapter 5	Anti-VCAM-1 SAINT-O-Somes enable endothelial-specific delivery of siRNA and downregulation of inflammatory genes in activated endothelium in vivo <i>J Control Release. 2014 Jan 3;176C:64-75.</i>	88
Chapter 6	SAINT-Liposome-Polycation particles, a new carriers for improved delivery of siRNAs to inflamed endothelial cells <i>manuscript in preparation</i>	120
Chapter 7	Summary, Conclusions and Future perspectives	140
Chapter 8	Nederlandse samenvatting	154
Appendices	Streszczenie	160
	Curriculum Vitae	166
	List of publications	167
	Acknowledgements	168

Chapter 1

Introduction and aims of the thesis

Introduction

The endothelium is a specialized cell layer that forms the inner lining of blood vessels and is the key regulator of vascular homeostasis [1]. Endothelium functions not only as a barrier but it actively engages in the inflammatory process by recruiting leukocytes from the blood *via* the production of cytokines, chemokines and adhesion molecules [2]. Endothelial cells are therefore an attractive target for anti-inflammatory therapy specifically by virtue of their pivotal role in the pathology of (chronic) inflammatory diseases, including atherosclerosis, diabetes and sepsis [3, 4]. Various pharmacological approaches to counteract (endothelial) cell activation are already applied in the clinic and improve disease status, including corticosteroids, nonsteroidal anti-inflammatory drugs (NSAIDs), and inhibitors of NF κ B signaling, but existing therapies often carry a substantial risk of systemic toxicity due to the lack of cellular and molecular specificity [5].

Small interfering RNAs (siRNAs) are a class of new molecular drugs that offer high molecular specificity and potent silencing of disease associated genes [6]. The physicochemical properties of siRNAs demand their formulation into a delivery system that enables modification of the pharmacokinetic profile of the siRNA, reduces off-target toxicity, and improves the therapeutic index, thereby generating potent therapeutics [7, 8]. Lipid-based drug delivery has become an established technology platform and has gained considerable clinical acceptance due to its remarkable flexibility. Lipid-based carriers such as liposomes, can be manufactured in various sizes, tailored on demand to introduce cell specificity, can efficiently encapsulate small or macromolecules, and show low toxicity in clinical trials [9]. Among cationic lipids, SAINT-C18 (1-methyl-4-(*cis*-9-dioleyl)methyl-pyridiniumchloride) is a promising candidate for designing an efficient siRNA delivery system due to its capability to transfect cells in the presence of serum and with low toxicity [10]. Addition of SAINT-C18 amphiphile into formulation of conventional liposomes can potentially enhance their ability to efficiently encapsulate and intracellularly deliver siRNA with low toxicity, without reducing liposomes stability and target-specificity *in vivo*.

Aims of the thesis

This thesis focuses on the development of a lipid-based carrier suitable for endothelial-specific *in vivo* delivery of siRNA. We aimed to:

- design and characterize a liposomal targeted siRNA carrier system applying the cationic amphiphile SAINT-C18,
- study suitability of vascular cell adhesion protein 1 (VCAM-1) and E-selectin for targeted siRNA delivery into inflamed endothelium and validate molecular





- targets for siRNA mediated anti-inflammatory intervention,
- investigate the potential of the developed siRNA carriers to interfere with disease associated endothelial activation by knocking down relevant target genes *in vivo* and to demonstrate proof-of-concept of endothelial specific siRNA based anti-inflammatory therapy.

Outline of the thesis

Upon inflammatory stimulation, each organ displays a vascular bed specific expression pattern of cell adhesion molecules providing challenging opportunities to deliver drugs or siRNAs to organ specific (micro)vascular endothelial subsets. In **chapter 2** we introduce the general concept of endothelial heterogeneity and its consequences for targeted therapeutic intervention and discuss the key challenges for the development of an efficient and endothelial-specific siRNA delivery system that can effectively silence engagement of endothelial cells in the patho(physio)logy of disease.

Recently, the transcription factor Egr-1 was demonstrated to be upregulated in experimental neointimal pulmonary arterial hypertension (PAH) [11], that is characterized by the development of neointimal lesions in small pulmonary arteries, leading to increased right ventricular (RV) afterload and -failure [12]. In **chapter 3**, we aimed to uncover a novel role for Egr-1 as a molecular inducer for PAH development using catalytic oligodeoxynucleotides (DNAzymes) that bind to target RNA sequences resulting in specific RNA degradation. The effects of Egr-1 downregulation on pulmonary vascular remodeling were studied in experimental flow-associated PAH rats by i.v. administration of DNAzymes formulated with cationic lipid 1,2-dioleoyl-3-trimethylammonium-propane (DOTAP) and by application of the PPAR- γ ligand pioglitazone.

Despite significant progress with regard to the development of drug delivery devices, so far only a few types of carriers for siRNA delivery into endothelial cells have been developed. In **chapter 4** we embarked on an attempt to develop a targeted carrier for selective delivery of siRNA into inflamed endothelium by combining the cationic SAINT-C18 amphiphile with conventional liposome technology (so-called SAINT-O-Somes). To create specificity for inflamed endothelial cells, SAINT-O-Somes were harnessed with antibodies against VCAM-1 respectively E-selectin. Specificity of siRNA delivery and efficacy of VE-cadherin gene silencing was tested in TNF α activated primary endothelial cells *in vitro*. VE-cadherin gene expression is restricted to endothelial cells and maintained under TNF α stimulation making it a suitable model gene for our studies. Since little is known about the intracellular fate of siRNA delivery

systems internalized via VCAM-1 and E-selectin, we studied the intracellular trafficking of both siRNA and SAINT-O-Somes in the activated endothelial cells. SAINT-O-Somes were further characterized with regard to their physicochemical properties and suitability for *in vivo* siRNA delivery. Finally, we studied their pharmacokinetic behavior in C57Bl/6 mice.

In **chapter 5**, we continued to explore the potential of SAINT-O-Somes for *in vivo* application. We studied whether anti-VCAM-1 SAINT-O-Somes carrying siRNA were able to cell specifically downregulate gene expression in inflamed endothelium *in vivo*. Pharmacokinetic behavior, biodistribution, and *in vivo* toxicity of intravenously administered anti-VCAM-1 siRNA SAINT-O-Somes were investigated in a simple inflammation model, in mice challenged with TNF α . Focusing on kidneys as our organ of interest, we demonstrated the potential of anti-VCAM-1 siRNA SAINT-O-Somes to deliver VE-cadherin and NF κ B p65 (RelA) specific siRNAs to the inflamed renal microvasculature of TNF α challenged mice. Effects of endothelial specific RelA downregulation on the endothelial inflammatory response towards LPS were studied by laser microdissection of different vascular beds prior to analysis of gene expression.

To achieve effective gene silencing, siRNAs need to be released from the carrier into the cytoplasm, where it associates with the RNA-induced silencing complex (RISC). In **chapter 6**, we designed and characterized new SAINT-based siRNA carriers incorporating protamine, a small cationic protein used as a transfection enhancer, with the aim to improve the efficacy of *in vivo* gene silencing in endothelial cells by improved siRNA release. So called SAINT-liposome-polycation-DNA (S-LPD) and SAINT-liposome-polycation (S-LP) were formulated by combining SAINT:DOPE liposomes and protamine, complexed with siRNA and carrier DNA, or siRNA only. These particles were examined for size, stability and the influence of polyethyleneglycol grafting. *In vitro* Toxicity and VE-cadherin gene silencing efficacy of S-LPD and S-LP in endothelial cells was compared to conventional liposome-polycation-DNA particles based on DOTAP : Cholesterol liposomes [13].

Finally, in **chapter 7**, we summarize the results of the research presented in this thesis and discuss implications and perspectives for future development of targeted siRNA-based anti-inflammatory therapy.





References

1. T.J. Rabelink, H.C. de Boer, A.J. van Zonneveld, Endothelial activation and circulating markers of endothelial activation in kidney disease, *Nat Rev Nephrol*, 6 (2010) 404-414.
2. J.S. Pober, W.C. Sessa, Evolving functions of endothelial cells in inflammation, *Nat Rev Immunol*, 7 (2007) 803-815.
3. I. Tabas, C.K. Glass, Anti-inflammatory therapy in chronic disease: challenges and opportunities, *Science*, 339 (2013) 166-172.
4. D.C. Angus, The lingering consequences of sepsis: a hidden public health disaster?, *JAMA*, 304 (2010) 1833-1834.
5. J.M. Kuldo, K.I. Ogawara, N. Werner, S.A. Asgeirsdottir, J.A. Kamps, R.J. Kok, G. Molema, Molecular pathways of endothelial cell activation for (targeted) pharmacological intervention of chronic inflammatory diseases, *Curr Vasc Pharmacol*, 3 (2005) 11-39.
6. K.A. Whitehead, R. Langer, D.G. Anderson, Knocking down barriers: advances in siRNA delivery, *Nat Rev Drug Discov*, 8 (2009) 129-138.
7. R.L. Kanasty, K.A. Whitehead, A.J. Vegas, D.G. Anderson, Action and reaction: the biological response to siRNA and its delivery vehicles, *Mol Ther*, 20 (2012) 513-524.
8. Z. Cheng, A. Al Zaki, J.Z. Hui, V.R. Muzykantov, A. Tsourkas, Multifunctional nanoparticles: cost versus benefit of adding targeting and imaging capabilities, *Science*, 338 (2012) 903-910.
9. T.M. Allen, P.R. Cullis, Liposomal drug delivery systems: from concept to clinical applications, *Adv Drug Deliv Rev*, 65 (2013) 36-48.
10. I. van der Woude, A. Wagenaar, A.A. Meekel, M.B. ter Beest, M.H. Ruiters, J.B. Engberts, D. Hoekstra, Novel pyridinium surfactants for efficient, nontoxic in vitro gene delivery, *Proc Natl Acad Sci U S A*, 94 (1997) 1160-1165.
11. M.G. Dickinson, B. Bartelds, G. Molema, M.A. Borgdorff, B. Boersma, J. Takens, M. Weij, P. Wichers, H. Sietsma, R.M. Berger, Egr-1 expression during neointimal development in flow-associated pulmonary hypertension, *Am J Pathol*, 179 (2011) 2199-2209.
12. M. Rabinovitch, Molecular pathogenesis of pulmonary arterial hypertension, *J Clin Invest*, 122 (2012) 4306-4313.
13. S.D. Li, L. Huang, Targeted delivery of antisense oligodeoxynucleotide and small interference RNA into lung cancer cells, *Mol Pharm*, 3 (2006) 579-588.



Chapter 2

Targeted siRNA Delivery to Diseased Microvascular Endothelial Cells – Cellular and Molecular Concepts

Piotr S. Kowalski^{1*}, Niek G. J. Leus^{1*}, Gerrit L. Scherphof¹, Marcel H. J. Ruiters^{1,2}, Jan A. A. M. Kamps¹ and Grietje Molema¹

IUBMB Life. 2011 Aug;63(8):648-58.

¹*Department of Pathology & Medical Biology, Medical Biology section, Laboratory for Endothelial Biomedicine & Vascular Drug Targeting Research, University Medical Center, Groningen, University of Groningen, Groningen, The Netherlands*


²*Synvolux Therapeutics, Groningen, The Netherlands*

Summary

Increased insight in the role of endothelial cells in the pathophysiology of cancer, inflammatory and cardiovascular diseases, has drawn great interest in pharmacological interventions aiming at the endothelium in diseased sites. Their location in the body makes them suitable targets for therapeutic approaches based on targeted drug delivery. Functional heterogeneity of the microvascular bed in normal organ homeostasis has been appreciated for a long time, and more recent studies have revealed heterogeneity in endothelial reactivity to inflammatory stimuli as well. Upon stimulation, each organ displays a vascular bed specific pattern of cell adhesion molecules providing challenging opportunities to deliver drugs or small RNAs to organ specific (micro) vascular endothelial subsets. In this review we introduce general concepts of endothelial heterogeneity in relation to disease state and its consequences for targeted therapeutic interventions. Furthermore, we will describe novel approaches to interfere with endothelial cell engagement in disease with a main focus on siRNA therapeutics and currently used nonviral lipid and polymer-based siRNA delivery systems. The last part of this review addresses some technical issues that are essential in proving the concept of target mRNA knockdown in a vascular bed specific manner, and the further development of effective endothelial cell specific drug delivery devices.



Introduction



The endothelium is the cell layer that forms the inner lining of blood vessels. It is a spatially distributed system that extends to all organs and tissues of the body. The endothelium is a key regulator of vascular homeostasis and functions not only as a barrier but also acts as an active signal transducer for metabolic, hemodynamic and inflammatory input that modifies the function and morphology of the vessel wall [1]. Moreover, the smallest blood vessels engage in angiogenic processes that accompany wound healing, tissue repair, and solid tumor growth [2]. Depending on the location in the body, endothelial cells (ECs) display their own molecular make up that drives basic behavior as well as responses to inciting stimuli [3]. Along the vascular tree, major differences are observed in EC phenotype, permeability, endocytosis and transcytosis capacities, and responsiveness to activation. For example, brain microvasculature is an integral part of the impermeable blood brain barrier, whereas liver sinusoidal endothelial cells form a densely fenestrated sieve with support of a discontinuous basement membrane and engage in clearance of a variety of molecular entities from the circulation [4, 5]. Furthermore, endothelial cells aligning the postcapillary venules are primarily responsible for mediating leukocyte trafficking, whereas arteriolar endothelial cells regulate vasomotor tone [2].

Being a keeper of internal homeostasis, ECs are continuously sensing and responding to changes in the extracellular environment. They are the first cells exposed to proinflammatory stimuli associated with systemic diseases such as atherosclerosis, sepsis, diabetes, vasculitis and other (chronic) inflammatory disorders. The proinflammatory stimulus leads to activation of ECs, the status of which varies according to the nature of the activating factor and the location of the vascular bed [6]. For example, significant differences in response to proinflammatory stimuli such as tumor necrosis factor (TNF)- α are observed between venous and arteriolar endothelial cells [7]. Activated endothelium also accompanies the outgrowth of many tumors, where sustained formation of new blood vessels is one of the key factors leading to progression of the disease [8].

A variety of pharmacological approaches to counteract endothelial activation are already applied in the clinic, tested in clinical trials, or in preclinical development, including the potent inhibitors that affect receptor tyrosine kinase activation as well as specific kinases involved in the various signal transduction cascades [9]. Besides kinase inhibitors, drugs based on RNA interference (RNAi), i.e., small interfering RNAs (siRNAs), offer increased specificity and efficient gene silencing of disease-associated genes. Formulation of such drugs in a targeted delivery system would create potentially powerful gene silencing therapeutics with diminished side effects, and hold a great promise for successful treatment of chronic inflammatory diseases and cancer. In the

current review, we will focus on recent developments in the design of siRNA delivery approaches with the aim to therapeutically affect abnormal endothelium. We will introduce general consideration of endothelial heterogeneity in relation to disease state and its consequences for targeted therapeutic interventions. Next we will focus on drugs based on RNA interference, on their mechanisms of action and obstacles limiting application of siRNA in the clinic. We will provide an overview of currently used siRNA delivery systems designed to interfere with endothelial cell engagement in disease, with emphasis on nonviral approaches including lipids and polymers. In the last part, we will discuss the in vivo complexity of endothelial cell behavior and the difficulties encountered when attempting to mimic this in an in vitro setting. This calls for the use of new technologies that allow for endothelial gene expression analysis and studying targeted drug delivery devices in the complex environment of an organ.

Endothelial Heterogeneity and Abnormal ECs as Therapeutic Target

In recent years, the endothelium has become an attractive target for therapeutic intervention by virtue of its association with the pathophysiology of many diseases, its prevalence throughout the body, and its accessibility to intravenously administered agents [10]. Much effort has been dedicated to the development of drugs that inhibit endothelial cell activation to treat chronic inflammatory diseases, to disrupt tumor vasculature, or to halt angiogenesis. However, most of the drugs lack specificity for the endothelium, giving rise to adverse effects in other cells in the body. Formulation of highly potent drugs in EC specific delivery devices will be essential to provide these drugs with a potential for future clinical application [9, 11]. Critical for success of these approaches is the identification of target epitopes on the diseased endothelial cells as well as choosing the proper drug target and concurrent molecular entity for therapeutic effects. This justifies an approach in which knowledge of microvascular endothelial cell biology and pharmaceutical sciences are combined, as we do in our own research as well as in outlining the content of this review.

Endothelial cells are differentially regulated in diverse (micro)vascular beds and in time, giving rise to the phenomenon of endothelial cell heterogeneity. Structural and functional heterogeneity of endothelial cells is evident between arteries and veins as well as between the capillaries in the different organs. Not only do different endothelial cell subsets in one organ have a different phenotype and function related to organ physiology, they also behave differently under pathophysiologic stress. As a consequence, endothelial cells in various (micro)vascular beds express different proteins at different moments in time during disease initiation and development [4]. The differentially expressed determinants on the surface of disease-activated endothelium are excellent targets for drug delivery towards abnormal endothelium, and include molecules involved in leukocyte rolling and adhesion to the vascular wall during



the inflammatory process, and in other disease-related processes [12]. It should be noted, however, that many of these proteins are not homogeneously expressed by the endothelium but rather are (micro)vascular bed specific. Moreover, the kinetics of disease-induced target epitope expression may spatiotemporally differ between endothelial cell subsets in the diseased sites [13]. This could have either an advantageous or a detrimental effect with regard to specificity and/or extent of local accumulation of the drug delivery formulation.

Endothelial Adhesion Molecules as Targets for Inflamed Endothelium

Their position in the body makes the ECs one of the first cells to be exposed to systemic proinflammatory stimuli such as bacterial endotoxin (lipopolysaccharide, LPS), or systemically released cytokines such as TNF- α , interleukin (IL)-1, and IL-6. Exposure to these proinflammatory conditions leads to EC activation and expression of cell adhesion molecules and various other molecules associated with proinflammatory activation. Several of them can serve as molecular targets for siRNA delivery in pathologies such as atherosclerosis [vascular cell adhesion molecular-1 (VCAM-1), [14]], myocardial injury [P-selectin, [15]], glomerulonephritis (E-selectin, [16]); rheumatoid arthritis ($\alpha_v\beta_3$ integrin, E-selectin [17, 18]), and pulmonary inflammatory diseases (intercellular adhesion molecular-1 (ICAM-1), [19]).

Ideally, target epitope expression should be restricted to diseased endothelium, thereby preventing accumulation of a drug in nondiseased endothelium. E-selectin is one of the few molecules that meet this criterion. Moreover, it is not present on nonendothelial cells and its expression is dramatically upregulated during inflammation *in vivo*. The endothelial adhesion molecule expression induced by systemic stimuli varies between organs according to the nature of the stimulus and the origin of the vascular bed. Each organ displays a unique pattern of molecules providing further challenging opportunities to deliver drugs or small RNAs to organ specific (micro)vascular endothelial subsets (Fig. 1A). For example, van Meurs et al., observed E-selectin expression primarily in glomerular ECs in a study on microvascular activation following induction of systemic inflammation in a hemorrhagic shock mouse model. In contrast, VCAM-1 expression was induced in all vascular segments except in glomerular ECs [20].

Furthermore, it is important to note that target epitopes should reside at the exterior of the cell membrane of the target cells, that they are not avidly shed, and that they become internalized upon ligand binding and intracellularly processed when intracellular drug release is a prerequisite. E-selectin is an internalizing receptor that routes its ligands including antibodies and antibody modified-liposomes to the lysosomal compartment [21–23]. This feature substantially contributes to its outstanding quality as a target to be exploited for intracellular delivery of small RNAs. Also VCAM-1 and ICAM-1 are



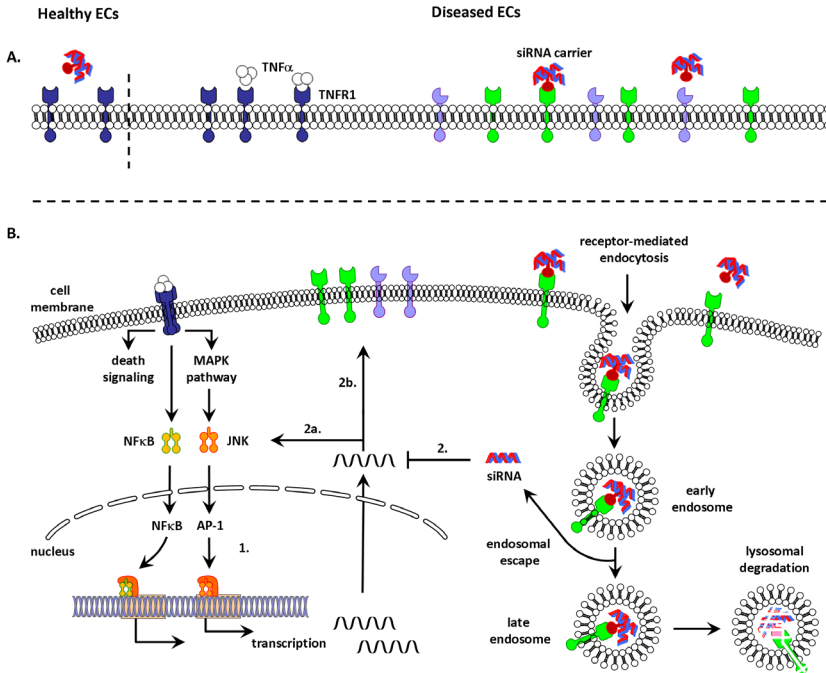


Figure 1. Simplified scheme of disease-associated cellular events that lead to endothelial cell activation and provide challenging opportunities for targeted siRNA delivery. (A) Microvascular endothelial cells (EC) are exposed to microenvironmental factors that differ from one vascular bed to the other, as a consequence of which their basic phenotype may vary. Exposure to proinflammatory conditions (e.g., TNF α or IL-1 β) leads to activation and expression of a variety of cell adhesion molecules and other determinants associated with disease which may vary between endothelial subsets. (B) The differentially expressed determinants on the surface of disease-activated endothelium are excellent targets for drug delivery to abnormal endothelium. The targeted siRNA carriers (e.g., lipoplexes, polyplexes, or liposomes) interact with cell surface receptors and are taken up into the target cells via receptor-mediated endocytosis. The resulting endocytotic vesicles fuse to form early endosomes. These mature into late endosomes which ultimately become part of the lysosomes, where proteins and nucleic acids are degraded by acid hydrolases. To achieve target gene silencing, siRNAs need to be released from the carrier and escape from the endosomes into the cytoplasm, where it associates with the RNAi machinery and directs the cleavage of target mRNAs. 1 The activated intracellular signal transduction cascade controls transcription factor activation and proinflammatory gene expression. 2. Once escaped from the endosomes, the siRNA incorporates into the RNA-induced silencing complex, is subsequently unwound, and next guided to the complementary site in the target mRNA. This leads to specific gene silencing of, for example, (2a) transcription factors (TFs) NF κ B or AP-1 to block downstream signaling pathways regulated by these TFs, or (2b) other determinants associated with disease activity.



internalizing receptors [24] and although their expression is not restricted to endothelial cells in inflamed sites, they can still be considered attractive targets, provided that the therapeutic advantages outweigh the undesired side effects of delivery of the drug into nondiseased endothelium.

Integrins $\alpha_v\beta_3$ and $\alpha_v\beta_5$ are interesting molecules to consider for targeted drug delivery to ECs as they are upregulated in physiological as well as pathological angiogenic vessels, and possess proangiogenic functions [11, 25, 26]. For example, peptides with the arginine glycine aspartic acid (RGD) amino acid sequence show high affinity for the $\alpha_v\beta_3$ -integrin, as do $\alpha_v\beta_3$ specific antibodies. During the past decade, RGD-peptides have become an established tool for the targeting of drugs and imaging agents to $\alpha_v\beta_3$ -integrin expressing ECs [27].

Small Interfering RNAs, a New Class of Therapeutics

Three decades ago, RNA was generally considered to be no more than just a passive intermediate transferring information from DNA to the protein-synthesizing machinery. The discovery of catalytic RNAs in the 1980s had a tremendous impact on this dogma. Small RNAs are key players in triggering post-transcriptional or translational gene silencing and nowadays they represent one of the most promising new classes of molecular target-specific therapeutics. There are two main groups of small RNAs, i.e., siRNA and micro RNA (miRNA), which are short double-stranded RNA (dsRNA) molecules generally composed of 21-23 (siRNA) or 18-25 (miRNA) nucleotides (nt). siRNA generally has perfect complementary sequence to its target messenger RNA (mRNA), leading to gene-specific degradation of the mRNA, in contrast miRNA has predominantly imperfect sequence complementarity in the 3' untranslated region of the target mRNA which leads to translational silencing without mRNA degradation [28, 29]. Mostly chemically synthesized siRNA molecules are used to silence target gene expression, exploiting the cells' endogenous RNAi processing machinery for further processing before hybridization with its target mRNA. Another method of mediating the RNAi effect involves exogenously administered vector-based short hairpin RNA (shRNA) which is transcribed in the nucleus, further processed and transported to the cytoplasm for silencing activity [30]. Although a vector-based shRNA system may have advantages such as robust and long term gene silencing in the transfected cell, its expression is hard to control with regard to length of time and efficiency. Moreover, vector-based shRNA require nuclear entry, which represents an additional hurdle in the overall mechanism of action. The use of exogenous siRNA results in direct gene silencing since it does not require additional processing. Furthermore, its effect is transient, which may be preferred in a therapeutic setting.

RNAi has become a widely used approach for silencing gene expression *in vitro* and *in vivo*, to study gene functions and elucidate molecular mechanisms in mammalian



cells. Both endogenously produced siRNAs and chemically synthesized siRNAs become assembled within a multisubunit ribonucleoprotein complex known as the RNA-induced silencing complex (RISC). Subsequently, the sense strand of the siRNA is removed, leaving the antisense strand to guide the ‘activated’ RISC to its site of action where it hybridizes with its target mRNA resulting in mRNA cleavage by the RNAi endonuclease Argonaute 2 [31]. This type of silencing occurs when siRNA molecules perfectly match their complementary target mRNA. The RISC complex can also guide and incorporate partially homologous siRNA strands to target mRNAs, causing translational repression of the particular mRNA present in the cytoplasm. In this case the siRNA acquires miRNA activity, and can control the expression of numerous target mRNAs at the translational level, which remains a critical issue for therapeutic applications of RNAi [32, 33]. The siRNA-loaded RISC is recycled for additional rounds of gene silencing activity. The rate of target cell divisions determines the persistence of siRNA, mediated gene silencing not of shRNA when stably incorporated in the DNA, since the siRNAs will be diluted after each cell division.

Apart from siRNA, gene silencing involving RNAi can also be achieved using so called DNA enzymes (deoxyribozymes) which can be perceived as molecular scissors containing a catalytic core of 15 deoxyribonucleotides that binds to and cleaves its target RNA (reviewed by [34]). Moreover, interference with miRNA pathways is possible by means of antisense oligonucleotides, which are complementary to the sense strand of the target miRNA duplex and block its processing (reviewed by [35]). RNAi based drugs may allow for specific silencing of a gene involved in downstream signaling of proinflammatory and pro-angiogenic stimuli, whereas interference with miRNA pathways may result in downregulation of multiple proinflammatory genes, both theoretically leading to suppression of inflammation. The recent discovery of miRNA involvement in tumor angiogenesis [36] furthermore paves the road for inhibitory miRNAs to be further developed for endothelium-specific therapy of cancer. For reasons of space limitations we will restrict ourselves in the next paragraphs to siRNA, although several of the concepts discussed may be applicable to other types of inhibitory RNAs as well.

siRNA Delivery Into Endothelial Cells

The first decade of targeted endothelial drug delivery research focused on the identification of molecular targets on the endothelial cells that are selectively expressed during disease development [27, 37]. Initially employed drugs include the cell death inducing molecules doxorubicin [38] and the proapoptotic heptapeptide dimer D(KLAKLAK)₂ [39]. Moreover, anti-inflammatory enzymes that provide anti-oxidant protection [40] and corticosteroids that inhibit intracellular signaling and concomitant proinflammatory gene expression [16, 22] have been formulated and were shown to



improve disease status. Also, targeted delivery of antisense oligonucleotides has been investigated in detail in the last 15 years [41]. The design of new siRNA delivery devices for future therapeutic application has benefitted and will continue to benefit from the knowledge gained by advancements in targeted delivery of these conventional drugs.

Unmodified and uncomplexed siRNAs (so-called naked si- RNAs) have a half-life in the blood of only a few minutes which limits their usefulness as a drug per se. They are rapidly eliminated by renal excretion and are also degraded with a $t_{1/2}$ 1 h by serum RNases [42]. Due to its relatively large molecular weight (13 kDa), polyanionic nature (40 negatively charged phosphate groups), and high hydrophilicity, naked siRNA will furthermore not passively cross the membrane of unperturbed cells. To apply siRNA for in vivo gene silencing, it either needs to be chemically modified or formulated and delivered to protect it from rapid clearance and degradation by serum RNases, to prevent activation of the immune system and interactions with other nontarget cells, and to allow cellular uptake, finally leading to participation in the RNAi pathway [43]. Formulation of siRNA in an advanced drug delivery system has the advantage that it does not affect the pharmacological potential of the siRNA, contrary to various forms of chemical modification.

Ideally, for in vivo application the siRNA needs to be efficiently formulated in carrier systems to contain sufficient amounts of siRNA and be stable to resist degradation or disassembly in the circulation. At the same time, carrier systems should allow efficient release of the cargo once the carrier arrives in the endocytotic vesicles and/or in the cytoplasm of the cells (discussed in more details by [44]). Physicochemical characteristics of the carrier such as composition, size and surface charge can handicap pharmacokinetic behavior by engaging in interactions with serum proteins including serum albumin, lipoproteins and immunoglobulins, which leads to clearance by cells of the reticulo-endothelial system (RES) in the spleen and liver [45]. To limit these interactions and prolong circulation half-life, the surface charge can be masked by covering the carrier with a hydrophilic polymer such as (poly)ethylene glycol (PEG) [46]. Recent work revealed that lipid-based particles containing high levels of PEG (10 mol%) are not taken up by the liver after systemic administration [47]. Moreover, different types of polymers, such as pH-sensitive or diffusible PEG variants are available for shielding off the vesicle surface. Such alterations provide increased carrier responsiveness to low pH and enhanced cytoplasmic release of its cargo [48]. Furthermore, it is possible to control the circulation time of particles by time dependent diffusion-mediated release of PEG shielding which can reduce side effects of formulations containing toxic drugs [49, 50].

Size and shape of the carrier also determine its fate in vivo. Most of the systems used for targeting endothelial cells have size ranging between 100–200 nm to minimize clearance from the circulation by renal filtration and liver uptake [51, 52]. Moreover,




several groups reported that nano-sized particles are more effective than microsized particles in targeting microcapillary sized vessels, where red blood cells (RBCs) preferentially line up in the center of the blood stream, thereby increasing nanoparticle contact with the vessel wall. They may, however, not be adequate for targeting to medium-to-large size blood vessels due to RBC-hindered margination which may decrease particle contact with the vessel wall [53, 54]. The shape of the carrier may also determine the extent and mode of interaction with the vascular wall and affect the rate of cellular uptake. Spherical nanoparticles are typically proposed for vasculature-targeted drug delivery by virtue of their relatively unrestricted capacity to navigate through the circulatory system bringing along minimal risk of vessel occlusion [10]. Furthermore, Muro et al., reported that *in vitro* endothelial ICAM-1-targeted $0.1 \times 1 \times 3 \mu\text{m}$ elliptical polystyrene disks exhibited four times slower uptake rates when compared to 0.1 and $5 \mu\text{m}$ diameter spheres [55].

To achieve specific delivery of siRNA to the desired endothelial subsets, carriers can be surface-modified with monoclonal antibodies, peptides, small-molecule ligands, or for example, aptamers, to recognize determinants on the cell surface. Antibodies and small antigen binding fragments have been studied most extensively for this purpose. A good ligand needs to be specific for a target expressed on the surface of ECs and should bind with sufficient capacity to promote internalization of drug loaded carrier to deliver therapeutically effective amounts of drug into the cells' interior. Furthermore, ligand-target molecule binding should avoid (prolonged) disruption or interference with normal functions of the target epitope [56]. Targeting endothelial cells can also be achieved by employing their basic functional heterogeneity without concomitant diseases activity. For example, liver sinusoidal endothelial cells, acting as scavengers specialized in the uptake of polyanionic macromolecules, could be efficiently reached by carriers conjugated with polyacetylated human serum albumin, a ligand for scavenger receptors [57]. Moreover, pulmonary endothelial cells which function as a nonthrombogenic semipermeable barrier and provide a vast surface for gas exchange, readily express high levels of thrombomodulin and angiotensin-converting enzyme at the cell surface as compared to other ECs, allowing effective preferential targeting [58, 59]. In addition, delivery to endothelium does not always require harnessing the carrier with a targeting ligand. Santel et al. reported that systemic administration of an siRNA complexed with a lipid-based carrier, creating a so called lipoplex, led to significant uptake of siRNA by endothelial cells in different organs. siRNA-lipoplexes were extensively taken up by the vasculature of the heart, lung, and liver resulting in RNAi mediated silencing of endothelial cell restricted genes CD31 and Tie2 [60].



Intracellular Fate of Endothelium Targeted Delivery Systems and Their Cargo



When a delivery system has reached the target endothelial cells, the carrier has to be internalized by the cell and release its content into the cytoplasm. Many carriers conjugated with ligands for extracellular receptors are internalized via endocytotic pathways leading to degradation, transcytosis, or sorting of internalized material to different cell compartments [58]. The type of pathway utilized depends on the target receptor, and the size and the nature of the drug carrier [44]. Clathrin-mediated uptake and caveolae-mediated uptake are two main mechanisms involved in endocytosis in ECs. The clathrin-mediated pathway mainly guides the delivery system to the endosomes with subsequent degradation in the lysosomes, whereas the caveolae-mediated pathway predominantly serves as an entry for transcytosis through endothelial monolayers that usually avoids lysosomal compartments [58]. Carriers targeting plasma membrane proteins like selectins are mainly taken up via clathrin-mediated endocytosis guiding the internalized content to the lysosomal degradation pathway within 2–4 h [22, 61]. On the other hand, ligands that bind to ICAM-1 were shown to enter ECs by a nonclassical endocytotic mechanism named cell adhesion molecule (CAM) mediated endocytosis. It requires formation of small multimeric complexes of the receptors and depends on target molecule clustering and size of the conjugates (100–300 nm). This mechanism also delivers materials to lysosomal compartments within 3 h [40, 62]. If the vesicular cargo enters the lysosomal degradation pathway, the initially formed early endosomes mature to more acidified (pH 5.0–6.0) late endosomes and eventually merge with lysosomes, rendering their content for degradation by lysosomal enzymes and low pH [63]. For siRNA delivery, however, endocytosis via the nondegradative route (e.g., caveolae-mediated pathway) likely leads to entrapment of the cargo in the endosomes [64].

We have shown that E-selectin targeted, lipid-based, conventional liposomes are extensively taken up by TNF- α activated HUVEC but also that they are degraded to a minor extent inside the endocytic vesicles of the endothelial cells [65]. Regardless of the entry pathway, a lack of endosomal escape generally leads to poor siRNA efficacy, thus carriers have to be able to release their siRNA before entering lysosomes and enable escape of intact siRNA from the endosomal compartment into the cytoplasm (Fig. 1B). To aid siRNA delivery, several mechanisms allowing penetration of the endosomal membrane before transfer to the lysosomal compartment have been proposed. Vesicle type carriers can be modified with pore forming peptides that are able to disturb the continuity of the bilayer by introducing a pore in the membrane, thereby facilitating release of endosomal contents. Those peptides are often based on naturally occurring toxins or venoms like diphtheria toxin or melittin, a major component of bee venom [64]. Cationic lipids can destabilize the endosomal membrane by inducing ‘flipping’ of anionic lipids in the endosomal bilayer, leading to formation of ion pairs

which facilitates vesicle fusion with the endosomal membrane and release of the cargo into the cytoplasm [66, 67]. Moreover, addition of a helper lipid with fusogenic properties [e.g., 1,2-dioleoyl-sn-glycero-3-phosphoethanolamine (DOPE)] to a carrier formulation can significantly improve content release and escape from the endosomes [68]. Furthermore, so called pH-sensitive carriers were developed by formulating DOPE with a pH-titrable lipid (displaying a pH-dependent charge) such as cholesteryl hemisuccinate (CHEMS) or by combination of cationic and anionic lipids in one lipid membrane. These formulations promoted content release by increased destabilization of the carrier in the endosomal compartment upon low pH [69]. In contrast, polymers like polyethylenimine (PEI) and polyamidoamine (PAM) can induce endosomolysis by the so called proton sponge effect. These polymers have a strong buffering capacity due to protonation of amino nitrogens upon endosome acidification. This invokes a high chloride ion influx into the endosome, causing osmotic swelling of the endosome and eventually endosome lysis [70].

Endothelial Cell Targeted siRNA Delivery Systems

Lipid-based systems have been used for the delivery of nucleic acids for over 20 years, starting with studies by Felgner et al. [71]. Liposomes and lipoplexes are the two main categories of lipid-based systems, although novel types of carriers such as stabilized nucleic acid-lipid particles (SNALP), lipid polycation-DNA nanoparticles (LPD) and lipid like molecules called lipidoids (extensively reviewed by [72]) have entered the stage in recent years. For siRNA delivery, liposomes and lipoplexes are usually composed of a cationic lipid, helper lipid (e.g., DOPE and/or cholesterol) and a (poly)ethylene glycolipid [44]. Liposomes consist of an aqueous core enclosed in a phospholipid bilayer with nucleic acids mainly entrapped in the central aqueous compartment. Liposomes have generally stable physicochemical characteristics, while lipoplexes are spontaneously formed via interaction of positively charged lipids and negatively charged nucleic acids which makes them more unstable [73]. The advantages of lipid-based systems are their low toxicity (several liposomal formulations are FDA approved), easy sizing to below 200 nm, and great flexibility in tailoring them on demand with targeting ligands. Lipid structures can be easily modified by coupling targeting ligands to improve their delivery potential or by adding pH-sensitive or fusogenic moieties to aid intracellular release of siRNA [41].

So far only a few types of carriers suitable for systemic siRNA delivery into endothelial cells have been developed (Table 1). Successful siRNA delivery to tumor endothelial cells expressing integrin $\alpha_v\beta_3$ using RGD based homing peptides has first been reported by Schiffelers et al. [74]. In this study, the siRNA that inhibited vascular endothelial growth factor receptor 1 (VEGFR2) expression was incorporated into self-assembling nanoparticles constructed with RGD-harnessed PEGylated polyethylenimine, after it





Table 1. Examples of non-viral systems suitable for siRNA delivery to endothelial cells

Validated	Delivery system	Chemical composition	Target epitope	Pharmacological target	Endothelial subset	Ref.
In vivo	polyplex	PEGylated branched PEI	integrin $\alpha_v\beta_3$	VEGFR2	Tumor vasculature	[74]
		Chitosan nanoparticles	integrin $\alpha_v\beta_3$	PLXDC1	Tumor vasculature	[79]
	lipoplex	AtuPlex (PEG-DSPE: AtuFECT01:DPhyPE) DDAB:chol	-	PECAM-1, PKN3	Tumor vasculature	[80, 60]
	liposome	SAINT-O-Somes (SAINT:POPC:Chol:PEG-DSPE)	E-selectin	VE-cadherin	HUVEC	[65]
	lipoplex	POPC:DAP:PEG-DMA SAINTarg (SAINT:DOPE)	-	Caveolin-1	Lung vasculature	[81]
			E-selectin	GAPDH	HUVEC	[82]
			E-selectin	VE cadherin	HUVEC	[76]

PEI, polyethyleneimine; PEG (poly)ethylene glycol; DPhyPE, 1,2-diphytanyl-sn-glycero-3-phosphoethanolamine; DSPE, 1,2-distearoyl-sn-glycero-3-phosphoethanolamine; DDAB, Dimethyldioctadecylammonium Bromide; SAINT, (1-methyl-4-(cis-9-dioleoyl)methyl-pyridiniumchloride); DOPE, 1,2-dioleoyl-sn-glycero-3-phosphoethanolamine; DAP, 1,2-dioleoyl-3-dimethylammonium-propane; DMA, 2-dimethylamino ethyl methacrylate; POPC, 1-palmitoyl-2-oleoyl-sn-glycero-3-phosphocholine; Chol, Cholesterol

was shown that formulation into conventional liposomes did not lead to target gene silencing. We recently developed two novel lipid-based systems which show potential for systemic siRNA delivery to activated endothelial cells. The first system is based on a lipoplex composed of the cationic amphiphilic lipid SAINT (1-methyl-4-(cis-9-dioleyl)methyl-pyridiniumchloride), a well established delivery agent of nucleotides and proteins, and the helper lipid DOPE [75]. To achieve specificity towards activated endothelium, SAINT was covalently coupled to a monoclonal anti-E-selectin antibody forming a construct referred to as SAINTarg. With this anti-E-selectin-SAINarg we were able to substantially enhance siRNA uptake, transfection specificity and efficacy of VE-cadherin down regulation in activated endothelial cells, as compared to transfection with a nontargeted SAINT formulation [76].

In addition, we have developed a novel generation of liposomes called SAINT-O-Somes, based on formulation of conventional long circulating liposomes by the addition of the cationic amphiphilic lipid SAINT. These liposomes harnessed with anti-Eselectin antibody showed specific uptake by activated endothelial cells, and displayed good size stability (100 nm in diameter) in the presence of serum, but were destabilized at lower pH as occurs in the endosomes of endothelial cells, thereby showing superior intracellular release of their content. We were able to efficiently encapsulate low molecular weight compounds such as doxorubicin and siRNA in these carrier systems, rendering this formulation an interesting candidate for systemic application [65].

Issues to be Addressed for Further Development of EC Specific Delivery Devices

Significant progress has been made in the last decade with regard to the development of endothelial cell specific drug delivery devices. Increased knowledge of the molecular changes within these cells during the onset and progression of disease has spurred identification of new potential targets on the cell membranes, while new molecular entities give rise to the design of novel carriers with important added value over conventional ones. Knowledge of the molecular control and pharmacology of microvascular endothelial cells remains, however, scarce. Basic heterogeneity in the control of EC behavior makes it highly likely that their responsiveness to ‘drugs’ is also microvascular bed dependent, although data to support this are only slowly emerging. Moreover, the loss of microenvironment driven EC behavior upon culturing the cells in vitro requires solid validation of in vitro molecular control or responsiveness to stimuli and pharmacological observations in the in vivo context (Fig. 2). This is only occasionally pursued, which is mostly due to the limited availability of methods to assess kinase activity, gene and protein expression in tissue biopsies, and to locate them specifically in the endothelium. As such, the choice of molecular target(s) allowing successful therapeutic interference by means of targeted siRNA approaches remains somewhat elusive.



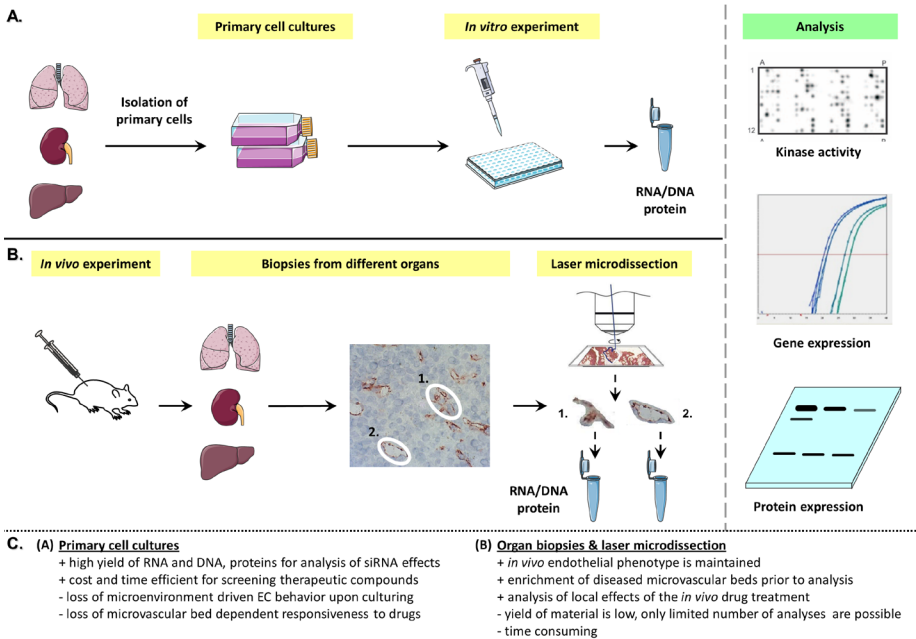


Figure 2. Experimental approaches to study the selectivity, intracellular delivery capacity and efficacy of endothelial targeted siRNA delivery systems *in vitro* and *in vivo*. Studying endothelial cell association, internalization and siRNA delivery using primary endothelial cell cultures (A) may be inadequate due to high rate of endothelial cell dedifferentiation upon *in vitro* culturing. This leads among others to loss of heterogenic behavior of ECs associated with the location of the microvascular bed *in vivo*. Laser microdissection (B) of ECs from specific microvascular segments in tissues is an essential technique to assist in the development of endothelial specific siRNA delivery devices, as it allows validation of local target gene knock down and studying downstream molecular consequences of gene knock down. The advantages and disadvantages of both approaches are summarized in (C).

After a drug delivery system carrying siRNA has been developed and properly optimized and sufficient siRNA can be delivered inside the target cell leading to the desired down regulation of the disease-associated target gene, novel technologies should be used to bring siRNA as therapeutic tool closer toward clinical application. Laser microdissection (LMD) of endothelial cells from specific microvascular segments in tissues allows compartmentalized analysis of gene expression and hence the examination of local effects of the targeted drug treatment [77]. LMD can be applied to both animal and human tissues and it allows for enrichment of endothelial cells from (micro)vascular segments which can be prior assessed histologically for disease activity. Combining targeted drug delivery systems carrying siRNA to selectively down regulate disease-associated genes in restricted microvascular segments with LMD-based validation of gene silencing in the target endothelial compartment represents not

just a powerful, but rather an essential strategy to provide proof of concept of in vivo siRNA delivery studies (Fig. 2).

Another technology that can significantly assist in further development of novel targeted delivery systems toward clinical application is precision-cut tissue slices. They closely resemble the organ from which it is prepared, with all cell types present in their original tissue-matrix configuration [78]. The circumstance that in tissue slices the architecture of the original organ is retained makes them an attractive tool for drug delivery studies. Using this system, we showed that anti-E-selectin-SAINTag specifically associated with activated endothelial cells in human kidney tissue slices subjected to inflammatory conditions, exactly following the expression pattern of E-selectin [76].

Furthermore, one should take into account the differences in behavior between primary endothelial cells and endothelial cell lines. Endothelial cell lines, for example, are easier to transfect and hence are often chosen for protein overexpression studies, yet they display quite some differences in phenotype and responsiveness compared to primary cells. Moreover, their internalization machinery is often more tumor cell like and less relevant to the uptake features of primary cells. Since primary endothelial cells are closest, though not identical, to endothelial cells in vivo, they should at one point in the design of targeted drug delivery systems be used to further validate binding, internalization and intracellular drug release characteristics.

Conclusions

Increased insight in the role of endothelial cells in the pathophysiology of cancer, inflammatory and cardiovascular diseases, has drawn great interest in the design of pharmacological interventions aiming at the endothelium in diseased sites. The effectiveness of drugs intended to affect diseased endothelium is however limited which is likely partly due to the existence of endothelial subset specific responsiveness to proinflammatory cytokines [6]. This heterogeneity on the other hand provides an opportunity for identification of disease-associated target epitopes expressed by vascular segment restricted endothelial cells as well as for selection of the proper drug target and concurrent drugs for therapeutic effects. Emerging therapeutic strategies based on RNAi have a great potential for therapeutic application. siRNAs can, however, not be directly applied for in vivo treatment of diseased endothelium due to a short half-life of the molecules, in the circulation, inability to pass the cellular membrane, high toxicity, and low cell selectivity. Formulation of these therapeutic molecules into delivery devices such as lipidbased or polymer-based systems targeted to diseased endothelial cells can provide them with a potential for further clinical application. Target determinants like E-selectin, VCAM-1, ICAM-1, and integrins with expression restricted to endothelial



cells and upregulated during inflammation or angiogenesis may help to achieve specific and safe delivery of drugs into EC subsets involved in diseases, thereby improving pharmacological efficacy. Widespread use of RNAi therapeutics for endothelial diseases requires a clinically suitable, safe and effective delivery vehicle. This can be achieved by developing new formulations and bio-materials (e.g., novel cationic lipids, polymers or pH-sensitive PEG) to avoid detection by cells of the RES and improve intracellular siRNA release properties of existing lipid or polymer-based systems. Combined research efforts in the field of microvascular endothelial cell biology and pharmaceutical sciences are crucial to achieve the final goal, that is, the development of an efficient and cell-specific siRNA drug delivery system that can be applied in the clinic to effectively silence endothelial cell engagement in the patho(physio)logy of disease.

Acknowledgements


This research was partly funded by the European Fund for Regional Development (EFRO), project number 068/073-Drug Delivery and Targeting. The authors declare no competing financial interests. M.H.J. Ruiters is CEO of Synvolux Therapeutics.

References

1. Rabelink, T. J., de Boer, H. C., and van Zonneveld, A. J. (2010) Endothelial activation and circulating markers of endothelial activation in kidney disease. *Nat. Rev. Nephrol.* 6, 404–414.
2. Poher, J. S. and Sessa, W. C. (2007) Evolving functions of endothelial cells in inflammation. *Nat. Rev. Immunol.* 7, 803–815.
3. Molema, G. (2010) Endothelial dysfunction and inflammation. In *Progress in Inflammation Research*, vol. 2 (Parnham, M., ed.). pp. 14–35, Springer, Basel.
4. Aird, W. C. (2007) Phenotypic heterogeneity of the endothelium: I. Structure, function, and mechanisms. *Circ. Res.* 100, 158–173.
5. Aird, W. C. (2007) Phenotypic heterogeneity of the endothelium: II. Representative vascular beds. *Circ. Res.* 100, 174–190.
6. Molema, G. (2010) Heterogeneity in endothelial responsiveness to cytokines, molecular causes, and pharmacological consequences. *Semin. Thromb. Hemost.* 36, 246–264.
7. Liu, M., Kluger, M. S., D'Alessio, A., Garcia-Cardena, G., and Poher, J. S. (2008) Regulation of arterial-venous differences in tumor necrosis factor responsiveness of endothelial cells by anatomic context. *Am. J. Pathol.* 172, 1088–1099.
8. Langenkamp, E. and Molema, G. (2009) Microvascular endothelial cell heterogeneity: general concepts and pharmacological consequences for anti-angiogenic therapy of cancer. *Cell Tissue Res.* 335, 205–222.
9. Kuldo, J. M., Ogawara, K. I., Werner, N., Asgeirsdottir, S. A., Kamps, J. A., et al. (2005) Molecular pathways of endothelial cell activation for (targeted) pharmacological intervention of chronic inflammatory diseases. *Curr. Vasc. Pharmacol.* 3, 11–39.
10. Huang, R. B., Mocherla, S., Heslinga, M. J., Charoenphol, P., and Eniola-Adefeso, O. (2010) Dynamic and cellular interactions of nanoparticles in vascular-targeted drug delivery (review). *Mol. Membr. Biol.* 27, 190–205.
11. Molema, G. (2008) Targeted drug delivery to


- the tumor neovasculature: concepts, advances, and challenges. In *Angiogenesis: An Integrative Approach From Science to Medicine*, Chapter 25 (Figg, W. D. and Folkman, J., eds). pp. 283–297, Springer Verlag, New York.
12. Kamps, J. A. A. M. and Molema, G. (2007) Targeting liposomes to endothelial cells in inflammatory diseases. In *Liposome Technology*, vol. 3 (Gregoriadis, G., ed). pp. 127–150, Informa Healthcare, New York.
 13. van Meurs, M., Kurniati, N. F., Wulfert, F. M., Asgeirsdottir, S. A., de Graaf, I. A., et al. (2009) Shock-induced stress induces loss of microvascular endothelial Tie2 in the kidney which is not associated with reduced glomerular barrier function. *Am. J. Physiol. Renal Physiol.* 297, F272–281.
 14. Deosarkar, S. P., Malgor, R., Fu, J., Kohn, L. D., Hanes, J., et al. (2008) Polymeric particles conjugated with a ligand to VCAM-1 exhibit selective, avid, and focal adhesion to sites of atherosclerosis. *Biotechnol. Bioeng.* 101, 400–407.
 15. Scott, R. C., Wang, B., Nallamothu, R., Pattillo, C. B., Perez-Liz, G., et al. (2007) Targeted delivery of antibody conjugated liposomal drugcarriers to rat myocardial infarction. *Biotechnol. Bioeng.* 96, 795–802.
 16. Asgeirsdottir, S. A., Kamps, J. A., Bakker, H. I., Zwiers, P. J., Heeringa, P., et al. (2007) Site-specific inhibition of glomerulonephritis progression by targeted delivery of dexamethasone to glomerular endothelium. *Mol. Pharmacol.* 72, 121–131.
 17. Koning, G. A., Schifflers, R. M., Wauben, M. H., Kok, R. J., Mastrobattista, E., et al. (2006) Targeting of angiogenic endothelial cells at sites of inflammation by dexamethasone phosphate-containing RGD peptide liposomes inhibits experimental arthritis. *Arthritis Rheum.* 54, 1198–1208.
 18. Hirai, M., Minematsu, H., Kondo, N., Oie, K., Igarashi, K., et al. (2007) Accumulation of liposome with Sialyl Lewis X to inflammation and tumor region: application to in vivo bio-imaging. *Biochem. Biophys. Res. Commun.* 353, 553–558.
 19. Ma, Z., Zhang, J., Alber, S., Dileo, J., Negishi, Y., et al. (2002) Lipidmediated delivery of oligonucleotide to pulmonary endothelium. *Am. J. Respir. Cell Mol. Biol.* 27, 151–159.
 20. van Meurs, M., Wulfert, F. M., Knol, A. J., De Haes, A., Houwertjes, M., et al. (2008) Early organ-specific endothelial activation during hemorrhagic shock and resuscitation. *Shock.* 29, 291–299.
 21. Kok, R. J., Everts, M., Asgeirsdottir, S. A., Meijer, D. K., and Molema, G. (2002) Cellular handling of a dexamethasone-anti-E-selectin immunoconjugate by activated endothelial cells: comparison with free dexamethasone. *Pharm. Res.* 19, 1730–1735.
 22. Everts, M., Kok, R. J., Asgeirsdottir, S. A., Melgert, B. N., Moolenaar, T. J., et al. (2002) Selective intracellular delivery of dexamethasone into activated endothelial cells using an E-selectin-directed immunoconjugate. *J. Immunol.* 168, 883–889.
 23. Everts, M., Koning, G. A., Kok, R. J., Asgeirsdottir, S. A., Vestweber, D., et al. (2003) In vitro cellular handling and in vivo targeting of Eselectin- directed immunoconjugates and immunoliposomes used for drug delivery to inflamed endothelium. *Pharm. Res.* 20, 64–72.
 24. Muro, S. (2007) Adhesion molecule-1 and vascular cell adhesion molecule- 1. In *Endothelial Biomedicine* (Aird, W., ed). pp. 1058–1070, Cambridge University press, New York.
 25. Dallabrida, S. M., De Sousa, M. A., and Farrell, D. H. (2000) Expression of antisense to integrin subunit beta 3 inhibits microvascular endothelial cell capillary tube formation in fibrin. *J. Biol. Chem.* 275, 32281–32288.
 26. Brooks, P. C., Clark, R. A., and Chersesh, D. A. (1994) Requirement of vascular integrin alpha v beta 3 for angiogenesis. *Science.* 264, 569–571.
 27. Schraa, A. J., Everts, M., Kok, R. J., Asgeirsdottir, S. A., Meijer, D. K., et al. (2002) Development of vasculature targeting strategies for the treatment of cancer and chronic inflammatory diseases. *Biotechnol. Annu. Rev.* 8, 133–165.
 28. Bartel, D. P. (2004) MicroRNAs: genomics, biogenesis, mechanism, and function. *Cell.* 116, 281–297.
 29. Garzon, R., Marcucci, G., and Croce, C. M. (2010) Targeting micro-RNAs in cancer: rationale, strategies and challenges. *Nat. Rev.*



- 
- Drug. Discov. 9, 775–789.
30. Rao, D. D., Vorhies, J. S., Senzer, N., and Nemunaitis, J. (2009) siRNA vs. shRNA: similarities and differences. *Adv. Drug Deliv. Rev.* 61, 746–759.
 31. Castanotto, D. and Rossi, J. J. (2009) The promises and pitfalls of RNA-interference-based therapeutics. *Nature*. 457, 426–433.
 32. Kaufmann, J., Ahrens, K., and Santel, A. (2010) RNA interference for therapy in the vascular endothelium. *Microvasc. Res.* 80, 286–293.
 33. Birmingham, A., Anderson, E., Sullivan, K., Reynolds, A., Boese, Q., et al. (2007) A protocol for designing siRNAs with high functionality and specificity. *Nat. Protoc.* 2, 2068–2078.
 34. Bhindi, R., Fahmy, R. G., Lowe, H. C., Chesterman, C. N., Dass, C. R., et al. (2007) Brothers in arms: DNA enzymes, short interfering RNA, and the emerging wave of small-molecule nucleic acid-based genesilencing strategies. *Am. J. Pathol.* 171, 1079–1088.
 35. Kota, S. K. and Balasubramanian, S. (2010) Cancer therapy via modulation of micro RNA levels: a promising future. *Drug. Discov. Today*. 15, 733–740.
 36. Anand, S., Majeti, B. K., Acevedo, L. M., Murphy, E. A., Mukthavaram, R., et al. (2010) MicroRNA-132-mediated loss of p120RasGAP activates the endothelium to facilitate pathological angiogenesis. *Nat. Med.* 16, 909–914.
 37. Molema, G., de Leij, L. F., and Meijer, D. K. (1997) Tumor vascular endothelium: barrier or target in tumor directed drug delivery and immunotherapy. *Pharm. Res.* 14, 2–10.
 38. Spragg, D. D., Alford, D. R., Greferath, R., Larsen, C. E., Lee, K. D., et al. (1997) Immunotargeting of liposomes to activated vascular endothelial cells: a strategy for site-selective delivery in the cardiovascular system. *Proc. Natl. Acad. Sci. USA.* 94, 8795–8800.
 39. Gerlag, D. M., Borges, E., Tak, P. P., Ellerby, H. M., Bredesen, D. E., et al. (2001) Suppression of murine collagen-induced arthritis by targeted apoptosis of synovial neovasculature. *Arthritis Res.* 3, 357–361.
 40. Muro, S., Cui, X., Gajewski, C., Murciano, J. C., Muzykantov, V. R., et al. (2003) Slow intracellular trafficking of catalase nanoparticles targeted to ICAM-1 protects endothelial cells from oxidative stress. *Am. J. Physiol. Cell Physiol.* 285, C1339–1347.
 41. Bartsch, M., Weeke-Klimp, A. H., Meijer, D. K., Scherphof, G. L., and Kamps, J. A. (2005) Cell-specific targeting of lipid-based carriers for ODN and DNA. *J. Liposome Res.* 15, 59–92.
 42. Dykxhoorn, D. M. and Lieberman, J. (2006) Knocking down disease with siRNAs. *Cell* 126, 231–235.
 43. Behlke, M. A. (2008) Chemical modification of siRNAs for in vivo use. *Oligonucleotides*. 18, 305–319.
 44. David, S., Pitard, B., Benoit, J. P., and Passirani, C. (2010) Non-viral nanosystems for systemic siRNA delivery. *Pharmacol. Res.* 62, 100–114.
 45. Simone, E., Ding, B. S., and Muzykantov, V. (2009) Targeted delivery of therapeutics to endothelium. *Cell Tissue Res.* 335, 283–300.
 46. Ogris, M. and Wagner, E. (2002) Targeting tumors with non-viral genedelivery systems. *Drug Discov. Today* 7, 479–485.
 47. Li, S. D., Chono, S., and Huang, L. (2008) Efficient gene silencing in metastatic tumor by siRNA formulated in surface-modified nanoparticles. *J. Controlled Release* 126, 77–84.
 48. Masson, C., Garinot, M., Mignet, N., Wetzter, B., Mailhe, P., et al. (2004) pH-sensitive PEG lipids containing orthoester linkers: new potential tools for nonviral gene delivery. *J. Controlled Release* 99, 423–434.
 49. Li, J. and Huang, L. (2010) Targeted delivery of RNAi therapeutics for cancer therapy. *Nanomedicine (Lond)* 5, 1483–1486.
 50. Fenske, D. B., MacLachlan, I., and Cullis, P. R. (2002) Stabilized plasmid-lipid particles: a systemic gene therapy vector. *Methods Enzymol.* 346, 36–71.
 51. Huang, L., Sullenger, B., and Juliano, R. (2011) The role of carrier size in the pharmacodynamics of antisense and siRNA oligonucleotides. *J. Drug Target.* 18, 567–574.
 52. Ding, B. S., Dziubla, T., Shuvaev, V. V., Muro, S., and Muzykantov, V. R. (2006) Advanced drug delivery systems that target the vascular

- endothelium. *Mol. Interv.* 6, 98–112.
53. Eckstein, E. C., Tilles, A. W., and Millero, F. J. III (1988) Conditions for the occurrence of large near-wall excesses of small particles during blood flow. *Microvasc. Res.* 36, 31–39.
 54. Charoenphol, P., Huang, R. B., and Eniola-Adefeso, O. (2010) Potential role of size and hemodynamics in the efficacy of vascular-targeted spherical drug carriers. *Biomaterials.* 31, 1392–1402.
 55. Muro, S., Garnacho, C., Champion, J. A., Lefterovich, J., Gajewski, C., et al. (2008) Control of endothelial targeting and intracellular delivery of therapeutic enzymes by modulating the size and shape of ICAM-1-targeted carriers. *Mol. Ther.* 16, 1450–1458.
 56. Kim, S. S., Garg, H., Joshi, A., and Manjunath, N. (2009) Strategies for targeted nonviral delivery of siRNAs in vivo. *Trends Mol. Med.* 15, 491–500.
 57. Kamps, J. A., Morselt, H. W., Swart, P. J., Meijer, D. K., and Scherphof, G. L. (1997) Massive targeting of liposomes, surface-modified with anionized albumins, to hepatic endothelial cells. *Proc. Natl. Acad. Sci. USA* 94, 11681–11685.
 58. Muro, S., Koval, M., and Muzykantov, V. (2004) Endothelial endocytic pathways: gates for vascular drug delivery. *Curr. Vasc. Pharmacol.* 2, 281–299.
 59. Kuruba, R., Wilson, A., Gao, X., and Li, S. (2009) Targeted delivery of nucleic-acid-based therapeutics to the pulmonary circulation. *AAPS J.* 11, 23–30.
 60. Santel, A., Aleku, M., Keil, O., Endruschat, J., Esche, V., et al. (2006) A novel siRNA-lipoplex technology for RNA interference in the mouse vascular endothelium. *Gene Ther.* 13, 1222–1234.
 61. Straley, K. S. and Green, S. A. (2000) Rapid transport of internalized P-selectin to late endosomes and the TGN: roles in regulating cell surface expression and recycling to secretory granules. *J. Cell Biol.* 151, 107–116.
 62. Muro, S., Wiewrodt, R., Thomas, A., Koniaris, L., Albelda, S. M., et al. (2003) A novel endocytic pathway induced by clustering endothelial ICAM-1 or PECAM-1. *J. Cell Sci.* 116, 1599–1609.
 63. Gluck, S. L. (1993) The vacuolar H⁺-ATPases: versatile proton pumps participating in constitutive and specialized functions of eukaryotic cells. *Int. Rev. Cytol.* 137C, 105–137.
 64. Medina-Kauwe, L. K., Xie, J., and Hamm-Alvarez, S. (2005) Intracellular trafficking of nonviral vectors. *Gene Ther.* 12, 1734–1751.
 65. Adrian, J. E., Morselt, H. W., Suss, R., Barnert, S., Kok, J. W., et al. (2010) Targeted SAINT-O-Somes for improved intracellular delivery of siRNA and cytotoxic drugs into endothelial cells. *J. Controlled Release* 144, 341–349.
 66. Xu, Y. and Szoka, F. C. Jr. (1996) Mechanism of DNA release from cationic liposome/DNA complexes used in cell transfection. *Biochemistry* 35, 5616–5623.
 67. Zelphati, O. and Szoka, F. C. Jr. (1996) Mechanism of oligonucleotide release from cationic liposomes. *Proc. Natl. Acad. Sci. USA* 93, 11493–11498.
 68. Wasungu, L. and Hoekstra, D. (2006) Cationic lipids, lipoplexes and intracellular delivery of genes. *J. Controlled Release* 116, 255–264.
 69. Karanth, H. and Murthy, R. S. (2007) pH-sensitive liposomes—principle and application in cancer therapy. *J. Pharm. Pharmacol.* 59, 469–483.
 70. Sonawane, N. D., Szoka, F. C. Jr., and Verkman, A. S. (2003) Chloride accumulation and swelling in endosomes enhances DNA transfer by polyamine-DNA polyplexes. *J. Biol. Chem.* 278, 44826–44831.
 71. Felgner, P. L., Gadek, T. R., Holm, M., Roman, R., Chan, H. W., et al. (1987) Lipofection: a highly efficient, lipid-mediated DNA-transfection procedure. *Proc. Natl. Acad. Sci. USA* 84, 7413–7417.
 72. Wu, S. Y. and McMillan, N. A. (2009) Lipidic systems for in vivo siRNA delivery. *AAPS J.* 11, 639–652.
 73. Gao, K. and Huang, L. (2009) Nonviral methods for siRNA delivery. *Mol. Pharm.* 6, 651–658.
 74. Schiffelers, R. M., Ansari, A., Xu, J., Zhou, Q., Tang, Q., et al. (2004) Cancer siRNA therapy by tumor selective delivery with ligand-targeted sterically stabilized nanoparticle. *Nucleic Acids Res.* 32, e149.



- 
75. van der Gun, B. T., Monami, A., Laarmann, S., Rasko, T., Slaska-Kiss, K., et al. (2007) Serum insensitive, intranuclear protein delivery by the multipurpose cationic lipid SAINT-2. *J. Controlled Release* 123, 228–238.
76. Asgeirsdottir, S. A., Talman, E. G., de Graaf, I. A., Kamps, J. A., Satchell, S. C., et al. (2010) Targeted transfection increases siRNA uptake and gene silencing of primary endothelial cells in vitro—a quantitative study. *J. Controlled Release* 141, 241–251.
77. Asgeirsdottir, S. A., Zwiers, P. J., Morselt, H. W., Moorlag, H. E., Bakker, H. I., et al. (2008) Inhibition of proinflammatory genes in anti-GBM glomerulonephritis by targeted dexamethasone-loaded AbEsel liposomes. *Am. J. Physiol. Renal Physiol.* 294, F554–F561.
78. de Graaf, I. A., Olinga, P., de Jager, M. H., Merema, M. T., de Kanter, R., et al. (2010) Preparation and incubation of precision-cut liver and intestinal slices for application in drug metabolism and toxicity studies. *Nat. Protoc.* 5, 1540–1551.
79. Han, H. D., Mangala, L. S., Lee, J. W., Shahzad, M. M., Kim, H. S., et al. (2010) Targeted gene silencing using RGD-labeled chitosan nanoparticles. *Clin. Cancer Res.* 16, 3910–3922.
80. Aleku, M., Fisch, G., Mopert, K., Keil, O., Arnold, W., et al. (2008) Atu027, a liposomal small interfering RNA formulation targeting protein kinase N3, inhibits cancer progression. *Cancer Res.* 68, 9788–9798.
81. Miyawaki-Shimizu, K., Predescu, D., Shimizu, J., Broman, M., Predescu, S., et al. (2006) siRNA-induced caveolin-1 knockdown in mice increases lung vascular permeability via the junctional pathway. *Am. J. Physiol. Lung Cell Mol. Physiol.* 290, L405–413.
82. Auguste, D. T., Furman, K., Wong, A., Fuller, J., Armes, S. P., et al. (2008) Triggered release of siRNA from poly(ethylene glycol)-protected, pH-dependent liposomes. *J. Controlled Release* 130, 266–274.



Chapter 3

A Critical Role for Egr-1 during Vascular Remodelling in Pulmonary Arterial Hypertension

Michael G. Dickinson¹, Piotr S. Kowalski^{2*}, Beatrijs Bartelds^{1*}, Marinus A.J. Borgdorff¹, Diederik van der Feen¹, Hannie Sietsma³, Grietje Molema², Jan A.A.M. Kamps², Rolf M.F. Berger¹, *Authors contributed equally

Under revision for Cardiovascular research

¹Center for Congenital Heart Diseases, Department of Pediatric Cardiology, Beatrix Children's Hospital, University Medical Center Groningen, University of Groningen, the Netherlands.

²Department of Pathology and Medical Biology, Medical Biology Section, University Medical Center Groningen (UMCG), University of Groningen, The Netherlands.

³Department of Pathology and Medical Biology, Pathology Section, University Medical Center Groningen (UMCG), University of Groningen, The Netherlands.

Abstract

Aims: Pulmonary arterial hypertension (PAH) is characterized by development of unique neointimal lesions in small pulmonary arteries, leading to increased right ventricular (RV) afterload and failure. Novel therapeutic strategies are needed that target these neointimal lesions. Recently, the transcription factor Egr-1 was demonstrated to be upregulated early in experimental neointimal PAH. Its effect on disease development, however, is unknown. We aimed to uncover a novel role for Egr-1 as a molecular inductor for disease development in PAH.

Methods and results: In experimental flow-associated PAH in rats, we investigated the effects of Egr-1 downregulation on pulmonary vascular remodelling, including neointimal development, and disease progression. Intravenous administration of catalytic oligodeoxynucleotides (DNAzymes) resulted in downregulation of pulmonary vascular Egr-1 expression. Compared to vehicle or scrambled-DNAzymes, DNAzymes attenuated pulmonary vascular remodelling, including the development of occlusive neointimal lesions. Selective downregulation of Egr-1 *in vivo* led to reduced expression of vascular PDGF-B, TGF- β , IL-6 and p53 resulting in a reduction of vascular proliferation and increased apoptosis. DNAzyme treatment further attenuated pulmonary vascular resistance, right ventricular systolic pressure and right ventricular hypertrophy. In contrast, in non-neointimal PH rodents DNAzyme treatment had no effect on pulmonary vascular and RV remodelling. Finally, pharmacological inhibition of Egr-1 with pioglitazone, a PPAR- γ ligand, attenuated vascular remodelling including of neointimal development.

Conclusions: These results indicate that Egr-1 governs pulmonary vascular remodelling and the development of characteristic vascular neointimal lesions in flow-associated PAH. Egr-1 is therefore a potential target for future PAH treatment.

Translational perspective

PAH is characterized by the development of unique neointimal lesions. PAH is regarded incurable when these neointimal lesions have formed. New therapeutic strategies are needed that target these neointimal lesions. Here we investigated whether Egr-1 could be such a target. We show that a) Egr-1 governs pulmonary neointimal development in experimental PAH and b) Egr-1 is a putative new treatment target for PAH patients.



Introduction

Pulmonary arterial hypertension (PAH) is a fatal and progressive form of pulmonary hypertension with, so far, unknown origin [1]. It is characterized by the development of unique so called neointimal lesions that result vascular proliferation and apoptotic dysregulation [2]. PAH is considered irreversible when these neointimal lesions have formed [3], and eventually results in death due to right ventricular (RV) failure [4,5]. Current treatment strategies may beneficially affect disease progression but certainly do not result in curing of the disease. Therefore, new treatment strategies are needed that target this irreversible form of pulmonary vascular proliferation.

In PAH associated with congenital heart diseases, the role of increased pulmonary blood flow is seen as an important trigger [6,7]. In experimental PAH models the addition of increased pulmonary blood flow has extensively been shown to induce neointimal development that reflects human PAH more truly than the monocrotaline or chronic hypoxia PH models [6,8]. Still, the mechanism by which increased blood flow leads to neointimal development and subsequently RV failure is unknown.

For this study, we hypothesized that the transcription factor Egr-1 (early growth response protein 1) is an important pathogenic inductor for neointimal development in PAH. Recently, we identified Egr-1 to be upregulated by increased pulmonary blood flow in the pulmonary vessels [9,10]. Furthermore, we confirmed Egr-1 to be upregulated in human end-stage PAH [9].

The transcription factor Egr-1 is known to play a major role in a variety of cardiovascular processes including systemic arterial remodelling [11,12]. However it is unknown whether *in vivo* downregulation of Egr-1 will beneficially affect PAH progression. Targeting Egr-1 *in vivo* has previously been described using pharmacological treatment (including PPAR- γ ligands [13,14]) or using specific gene silencing methods, including so-called DNAzymes (DNAzymes). DNAzymes are catalytic oligodeoxynucleotides that are able to bind to specific RNA sequences resulting in RNA degradation [15,16]. These DNAzymes exhibit greater catalytic efficiency than oligonucleotides such as ribozymes and are more stable in serum *in vivo*. For this study we therefore investigated whether *in vivo* downregulation of Egr-1, using both DNAzymes and the PPAR- γ ligand pioglitazone, would prevent the development of pulmonary vascular neointimal lesions in rats with flow-associated PAH.

Materials and methods

DNAzyme preparation

DNAzymes (Double RP-HPLC purification, phosphodiester backbone and inverted T at 3' terminus for increased stability; Trilink Biotechnologies, Santa Cruz CA, USA)



were sequenced as followed: Egr-1 DNAzyme (ED5; Figure 1): 5'-CCG CTG CCA GGC TAG CTA CAA CGA CCC GGA CGT Ti-3'; scrambled (inactive) DNAzyme (ED5scr): GCC AGC CGC GGC TAG CTA CAA CGA TGG CTC CAC Ti-3', as described previously [17]. Based on our result from a pilot study, the cationic lipid 1,2-dioleoyl-3-trimethylammonium-propane (DOTAP) was used as the transfection carrier as described in the online supplement.

PAH Animal model

The Institutional Animal Care and Use Committee approved animal care and experiments. One hundred twenty-three male Wistar rats (270-300g) were used. Experimental flow-associated PAH was created using a monocrotaline injection (60 mg/kg) followed by an abdominal aortocaval (av) shunt one week later, as described previously [9,10,18].

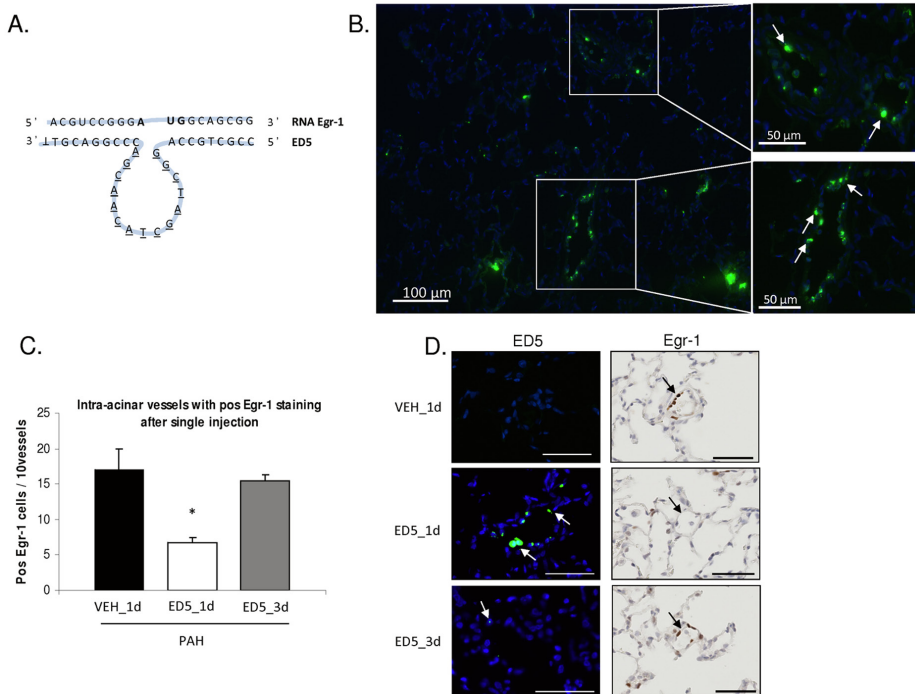



Figure 1. ED5 in the pulmonary vasculature. A) Schematic representation of the DNAzyme targeting Egr-1 (ED5). This molecule, with a phosphodiester backbone and an inverted T at 3' terminus, consists of a catalytic core (underline) and 2 recognition arms that attaches to the Egr-1 translational start site [17]. B) Vascular localization of ED5 24 hours after injection. ED5 was commercially labelled with 6FAM, combined with DOTAP and injected into the jugular vein. Positive fluorescent signalling was mainly seen in the vascular bed. Both pre- and intra-acinar vessels showed positive signalling for ED5. C) Single ED5 injection resulted in a decrease of vascular Egr-1 expression after 1 day. This effect was lost 3 days after injection. D) Localization of both ED5 signalling and Egr-1 expression in the intra-acinar vessels. Data are presented as mean values ± SEM. * P<0.05. Scale bar represents 50μm.

Egr-1 downregulation in PAH animal model

For the main DNAzyme study 82 rats were used. Blood was drawn peri-operatively for baseline blood analyses. A pilot study revealed that rats needed to receive ED5 treatment every 48 hours (Figure 1C and D and online supplement). Rats were randomly divided to receive intravenous treatment of either: 1) NaCl 0.9% (PAH_VEH; n=24), 2) scrambled DNAzyme-DOPTAP solution (PAH_SCR; n=18), 3) DNAzyme ED5-DOPTAP solution (PAH_ED5; n=20). Treatment started directly after shunt creation (=induction of increased flow) (Figure 2A). Rats received treatment every 48 hours through an externally fixed jugular vein catheter. Randomization was blinded for the investigators. Repeated ED5 delivery did not result in a systemic immune response or decreased liver function (Supplemental Figure E2). For each group, rats were sacrificed 1 week (n=6-12 per group) or 3 weeks (n=10-12 per group) after shunt creation. Sham operated rats served as control and received either NaCl 0.9% (n=12) or ED5-DOTAP solution (n=8). Since no differences were seen between these groups, they were pooled as control (Supplemental Figure E3).

Egr-1 downregulation in non-neointimal PH animal model

In addition, to investigate the effects of Egr-1 downregulation in a non-neointimal PH model, additional rats received a single injection of monocrotaline only. One week later, rats were randomly divided to receive either NaCl 0.9% (MCT_VEH; n=3) or DNAzyme ED5-DOPTAP solution (MCT_ED5; n=3) via externally fixed jugular vein catheters. Rats were sacrificed 3 weeks after monocrotaline injection.

Pioglitazon treatment in PAH animal model

To investigate the effects of the PPAR- γ ligand pioglitazon on pulmonary vascular Egr-1 downregulation in PAH, 24 additional flow-PAH rats were randomly divided to receive either: 1) vehicle treatment (n=6), 2) pioglitazon 20mg/kg (n=9), 3) pioglitazon 100mg/kg (n=9). Treatment was mixed into rat chow and rats were fed ad libitum. Rats were sacrificed 1 day (n=3-5 per group) and 1 week (n=3-4 per group) after start of increased blood flow. Vehicle treated sham rats from the main study served as control.

Echocardiography, hemodynamic measurements, pathology and biomolecular analyses

Echocardiography, hemodynamic measurements, morphometric analyses, immunohistochemistry and RT-PCR technique were performed as previously described [9,10,18,19] and in more detail in the online supplement.

Statistics

Data are presented as mean \pm standard error of the mean. Differences between groups were determined by one-way analysis of variance (ANOVA) with Bonferroni or Dunnet post-hoc test where applicable. For data not normally distributed, Mann Whitney U test was performed. A P-value below 0.05 was considered to be significant.

Results

Increased pulmonary blood flow resulted in progressive PAH with neointimal development

Rats that received monocrotaline administration and an aortocaval shunt (flow-PAH) showed progressive pulmonary vascular remodelling over time (Figure 2A; Table 1). One week after shunt creation (PAH_1wk) intra-acinar vessels exhibited

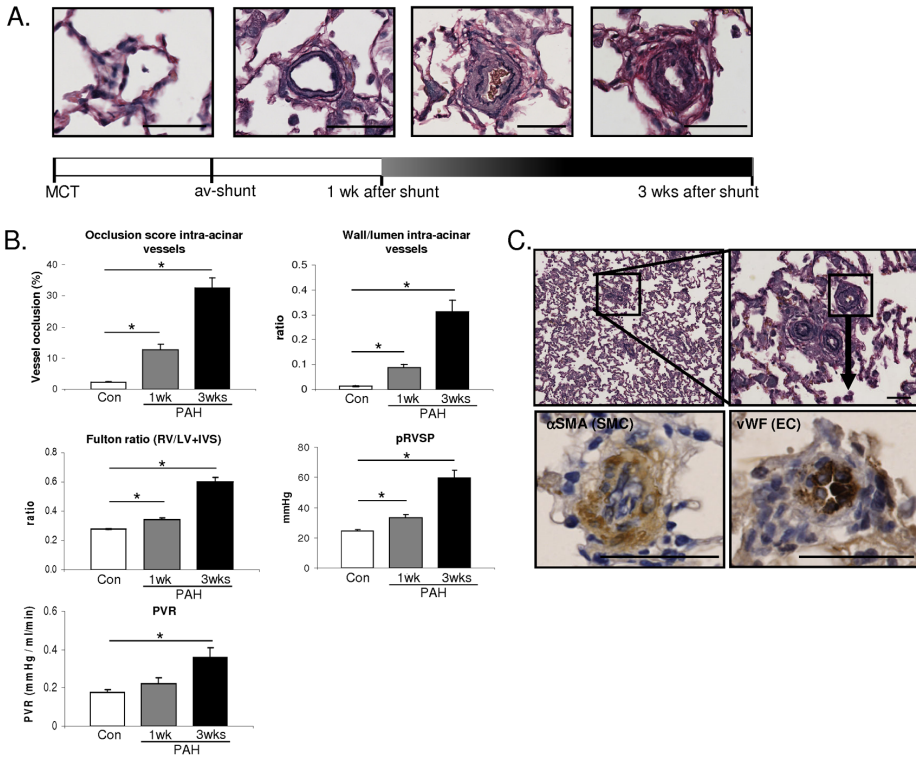


Figure 2. Development of flow-associated PAH. Pulmonary vascular remodelling and disease development in experimental flow-PAH. A) Typical examples of the progression of pulmonary vascular remodelling, including the formation of neointimal lesions after increased pulmonary blood flow. Note the degradation of the lamina elastica interna and the cellular luminal in these neointimal lesions. B) Progressive worsening of vascular remodelling, RV hypertrophy and hemodynamic measurements. C) Occlusive neointimal lesions consisted of ECs (staining positive for vWF) surrounded by SMCs (staining positive for α SMA). Data are presented as mean values \pm SEM. * $P < 0.05$. Scale bar represents 50 μ m.

Table 1. Animal characteristics

	PAH_1wk			PAH_3wks			
	Con	VEH	SCR	ED5	VEH	SCR	ED5
Body weight at sac (g)	361±7	306±6*	304±11	309±6	327±5*	323±5	328±3
RV weight (mg)	0.19±0.00	0.25±0.01*	0.25±0.01	0.19±0.01†	0.49±0.02*	0.49±0.02	0.39±0.02†
LV+IVS weight (mg)	0.68±0.01	0.74±0.17	0.69±0.03	0.71±0.02	0.83±0.02*	0.81±0.02	0.66±0.03 †
RV/BW (mg/g)	0.53±0.01	0.83±0.01*	0.81±0.04	0.60±0.02†	1.49±0.07*	1.53±0.06	1.2±0.06 †
LV+IVS/BW (mg/g)	1.92±0.02	2.44±0.04*	2.33±0.14	2.30±0.05	2.53±0.07*	2.50±0.05	2.53±0.04
atria/BW (mg/g)	0.27±0.01	0.61±0.02	0.48±0.04	0.38±0.02†	0.71±0.04*	0.78±0.02	0.64±0.03†
CO (ml/min)	103±5	131±9*	134±16	135±11	108±9	123±5	127±10
PAAT (ms)	30±1	28±2	24±2	21±3	15±3*	15±2	17±1
TAPSE (mm)	3.0±0.2	3.5±0.1*	3.6±0.6	3.8±0.09	2.5±0.24	2.6±0.2	2.6±0.2
Vascular remodeling							
Pre-acinar							
Outer diameter (µm)	101±8	96±15	104±11	106±10	124±16	115±13	110±10
Wall thickness (µm)	6±1	6±1	5±1	6±1	14±1	13±1	9±1†
Intra-acinar							
Outer diameter (µm)	28±1	36±1*	37±1	35±1	34±1	36±1	35±1
Wall thickness (µm)	0.3±0.0	2.3±0.4*	2.1±0.2	1.0±0.1†	5.6±0.7	5.8±0.7	3.0±0.4†
Remodeling (% of total vessels)							
Non-muscular (%)	79±1	22±3*	24±1	31±8†	13±3	10±2	18±2†
Partially muscularized (%)	26±1	35±3*	35±3	43±3†	13±2	12±2	22±5†
Totally muscularized (%)	6±1	35±3*	33±5	20±2.5†	39±5	41±4	48±4
Occlusive lesions (%)	0±0	12±2*	11±1	2±1†	33±3	32±3	11±2†

PAH: Pulmonary arterial hypertension; Con: control; VEH: vehicle treatment; SCR: scrambled DNazyme treatment; ED5: DNazyme treatment; Sac: sacrifice; RV: right ventricle; LV: left ventricle; IVS: intraventricular septum; BW: body weight; CO: cardiac output; PAAT: pulmonary artery acceleration time; TAPSE: tricuspid annular plane systolic excursion. * $P<0.05$ Con vs VEH; † $P<0.05$ SCR vs ED5. Data presented as mean ± SEM.

muscularization, and sporadic neointimal lesions were observed. In end-stage disease (PAH_3wks) occlusive neointimal lesions were seen in the majority of intra-acinar vessels (Figure 2; Table 1). Vessel occlusion resulted in symptomatic PAH 3 weeks after induction of increased blood flow, including increased peak right ventricular systolic pressure (pRVSP), increased pulmonary vascular resistance, and right ventricular hypertrophy (RVH) (Figure 2B). These parameters correlated with pulmonary vascular remodelling (Supplemental Figure S4).

Four rats did not reach the endpoint of the study: 1 died perioperatively (ED5 group), 3 rats were sacrificed (2 ED5 group; 1 SCR group) because of severe dyspnoea due to air emboli during intravenous injection. These rats were excluded from further analyses.

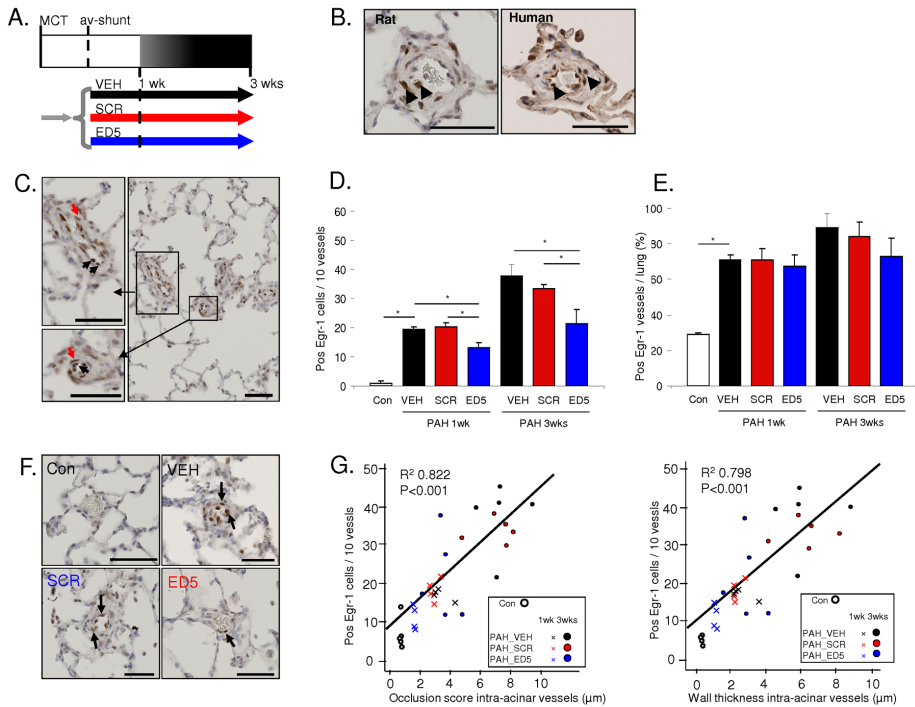


Figure 3. Downregulation of pulmonary vascular *Egr-1* expression. A) Schematic overview of the study design. B) *Egr-1* expression in vehicle and scrambled DNAzyme treated rats showed similarities with *Egr-1* expression in human PAH associated with congenital heart disease. C) *Egr-1* was located in both the medial and endothelial vessel layer in end stage disease (F). D) Chronic ED5 delivery (PAH_ED5) reduced pulmonary vascular *Egr-1* protein expression without reducing the total number of *Egr-1* positive intra-acinar vessels (E). G) Pulmonary vascular *Egr-1* expression correlated with pulmonary vascular remodelling. Data are presented as mean values \pm SEM. * $P < 0.05$. Scale bare represents $50\mu\text{m}$. VEH: vehicle treated rats, SCR: scrambled DNAzyme treated rats, ED5: DNAzyme treated rats.

Intravenous ED5 delivery reduced vascular Egr-1 expression in flow-PAH.

Compared to control, pulmonary vascular *Egr-1* protein expression increased 1 week after increased pulmonary blood flow (PAH_1wk) and progressed during disease development (PAH_3wks) (Figure 3). Chronic ED5 delivery (PAH_ED5) reduced pulmonary vascular *Egr-1* protein expression with 35% and 43% at 1 and 3 weeks after increased flow, respectively (Figure 3D). *Egr-1* was targeted throughout the vessels wall (Supplemental Figure S5). Pulmonary vascular *Egr-1* expression correlated with pulmonary vascular remodelling (Figure 3G).

Egr-1 downregulation attenuated neointimal formation and flow-PAH development

Vascular *Egr-1* downregulation due to ED5 delivery (PAH_ED5) reduced vessel occlusion and wall lumen ratio of the intra-acinar vessels at both 1 week and 3 weeks after induction of increased blood flow (Figure 4, Table 1). *Egr-1* downregulation



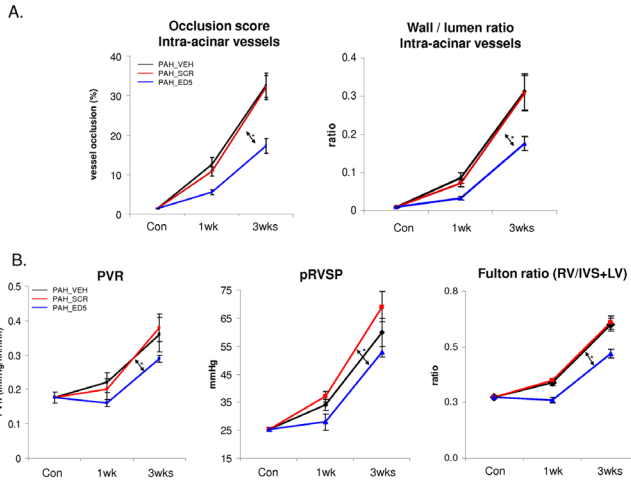


Figure 4. Effects of pulmonary vascular *Egr-1* downregulation. At 1 and 3 weeks after increased flow, *Egr-1* downregulation using ED5 significantly attenuated both (A) pulmonary vascular remodelling and (B) PAH development as shown by a reduction in pulmonary vascular resistance, pRVSP and RV hypertrophy. Data are presented as mean values \pm SEM. * = $P < 0.05$ ED5 vs VEH and SCR.

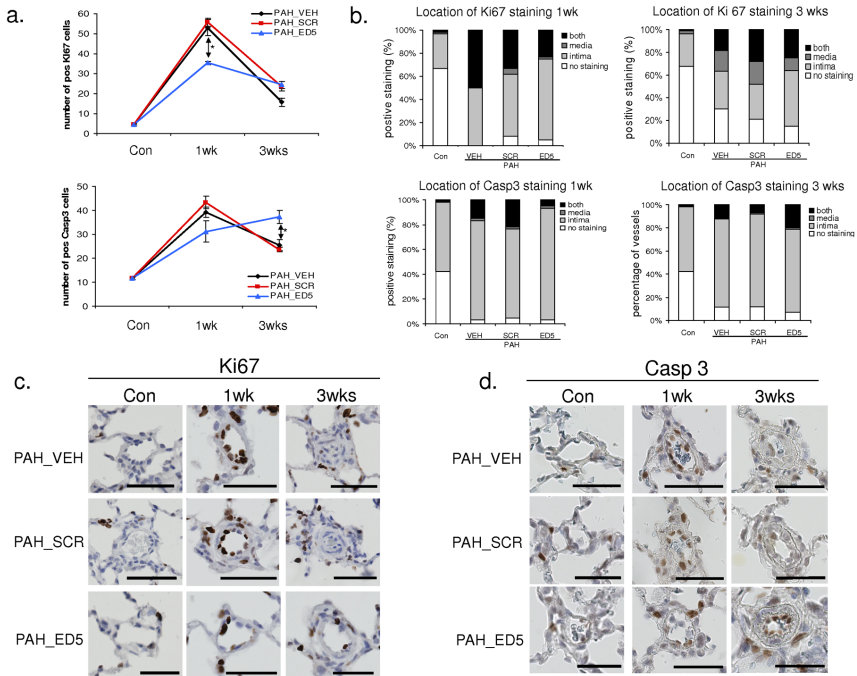


Figure 5. Mechanisms of pulmonary vascular changes due to *Egr-1* downregulation. A) *Egr-1* downregulation resulted in a significant reduction of vascular proliferation (Ki67) 1 week after flow and a significant increase in vascular apoptosis (Caspase 3) 3 weeks after flow. B) Localization of Ki67 and Caspase 3 in the pulmonary vessel. Typical examples of Ki67 (C) and Caspase 3 (D) vascular expression. Data are presented as mean values \pm SEM. * $P < 0.05$. Scale bar represents 50 μ m.

furthermore resulted in a reduction of the pRVSP, pulmonary vascular resistance and RVH (Figure 4B). Scrambled DNAzyme treatment (PAH_SCR) had no effect on any of the vascular remodelling or hemodynamic parameters. ED5 treatment had no effect on left ventricular mass (Table 1).

Egr-1 downregulation attenuated neointimal development through early attenuation of vascular cell proliferation and end stage increase of apoptosis

In vehicle and scrambled DNAzyme treated rats, both vascular proliferation and apoptosis peaked one week after the induction of increased flow (Figure 5A). *Egr-1* downregulation reduced early vascular cell proliferation and increased end staged vascular cell apoptosis, predominantly in the endothelial layer (Figure 5B and Supplemental Figure S6).

Expression of PDGF-B, TGF- β IL-6 and p53, all downstream targets of *Egr-1* and known to play a role in vascular proliferative remodelling in human PAH, was increased in the pulmonary vessels during neointimal development (PAH_VEH and PAH_SCR) at both 1 and 3 weeks (Figure 6, supplemental figure S6). *Egr-1* inhibition (PAH_ED5) resulted in a significant reduction of PDGF-B, TGF- β , IL-6 and p53 expression compared to vehicle and scrambled treatment (Figure 6, supplemental figure S6).

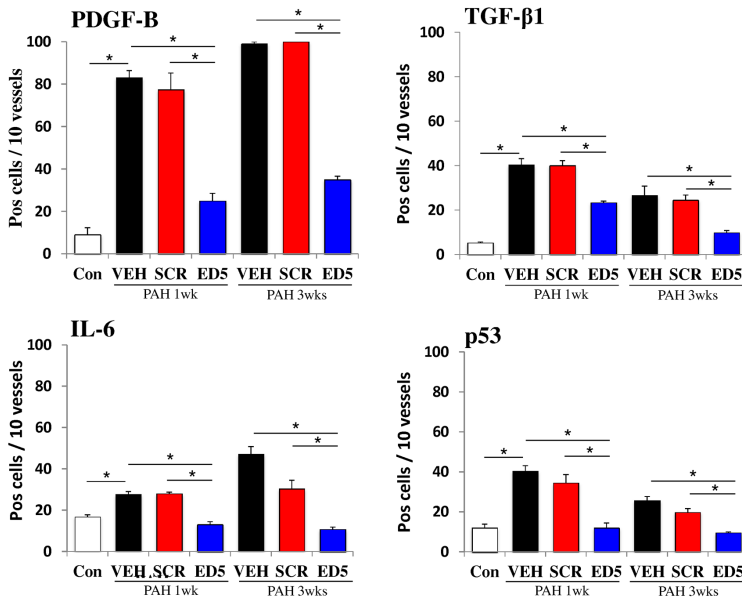


Figure 6. Pulmonary vascular expression of the *Egr-1* downstream genes PDGF-B, TGF- β IL-6 and p53 in the intra-acinar vessels. *Egr-1* inhibition resulted in downregulation of PDGF-B, TGF- β IL-6 and p53 at both 1 and 3 weeks. Histological examples are shown in supplemental Figure S6. Data are presented as mean values \pm SEM. * $P < 0.05$. Scale bar represents 50 μ m.



ED5 delivery has no effect on vascular remodelling in non-neointimal non-flow PH

To further test whether the effects of Egr-1 downregulation are specific for flow-induced neointimal formation, we investigated the effects of ED5 delivery in a non-neointimal, non-flow-associated model of pulmonary hypertension, namely monocrotaline only model (MCT_VEH vs. MCT_ED5) [9]. MCT injection (MCT_VEH) resulted in a significant increase in vessel wall thickness, increased pRVSP and RVH compared to control (Figure 7C). Neointimal lesions were not observed (Figure 7B). In MCT-only PH rats, vascular Egr-1 expression was only sporadically seen compared to its expression in flow PAH rats (Figure 7A). Also, ED5 treatment (MCT_ED5) did not alter vascular remodelling, pRVSP or RVH (Figure 7C) in MCT-only PH rats.

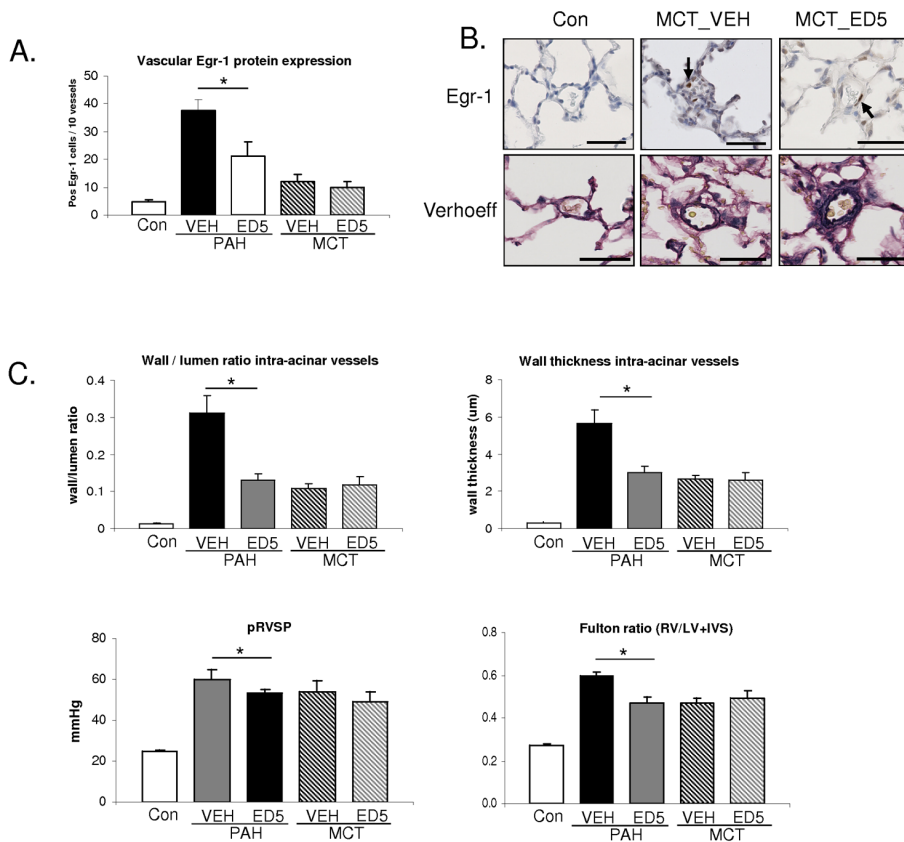


Figure 7. ED5 treatment in non-flow non-neointimal PH. A) Egr-1 protein expression and localization (B) in the intra-acinar vessels at 3 weeks. In rats where pulmonary blood flow was not increased (MCT-only rats), Egr-1 was only sporadically seen and no neointimal lesions were formed. C) In these non-flow non-neointimal rats, ED5 administration had no effect on vascular remodelling, RV hypertrophy or pRVSP. Data are presented as mean values \pm SEM. * $P < 0.05$. Scale bar represents 50 μ m.

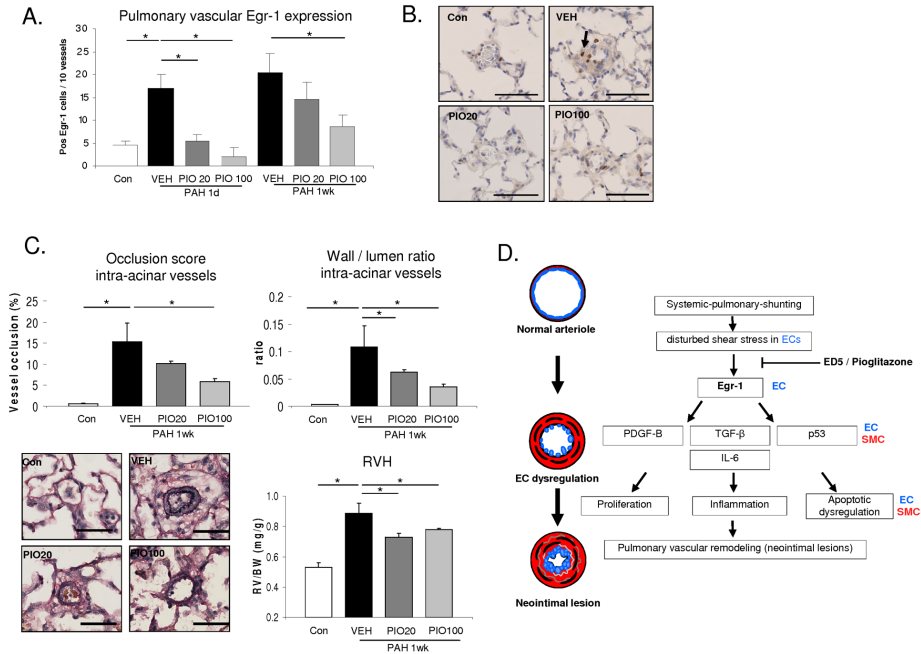


Figure 8. *Egr-1* downregulation using the PPAR- γ ligand pioglitazone. A) *Egr-1* protein expression in the intra-acinar vessels 1 day and 1 week after increased flow. B) Typical examples of *Egr-1* expression 1 week after increased blood flow. C) Preventive pioglitazone treatment attenuated pulmonary vascular remodelling, pRVSP and RV hypertrophy 1 week after increased flow. D) Schematic hypothesis of the role of *Egr-1* and its downstream genes in the development PAH. Data are presented as mean values \pm SEM. * $P < 0.05$. Scale bar represents 50 μ m. PIO 20: 20mg/kg/d pioglitazone treatment, PIO 100: 100mg/kg/d pioglitazone treatment.

Pharmacological downregulation of *Egr-1* using pioglitazone also attenuates vascular remodelling in flow-PAH

Using the PPAR- γ ligand pioglitazone, we investigated whether *Egr-1* could be pharmacologically inhibited. First, pioglitazone treatment activated PPAR- γ , as confirmed by increased PGC1 α (co-activator of PPAR- γ) and MCAD (downstream gene of PPAR- γ) gene expression (Supplemental Figure S7). Pioglitazone reduced vascular *Egr-1* expression in a dose dependent matter 1 day and 1 week after increased pulmonary blood flow (Figure 8A and B). This was accompanied with attenuation of pulmonary vascular remodelling (Figure 8C), including reduction of neointimal lesions and reduction of RVH compared to vehicle treated flow-PAH rats (Figure 8C).



Discussion

This study in experimental flow-associated PAH demonstrates that *in vivo* Egr-1 downregulation, both via intravenous administration of catalytic oligodeoxynucleotides (DNAzymes) and pharmacological intervention using pioglitazone, attenuates pulmonary vascular remodelling including the development of occlusive neointimal lesions, and reduced PAH progression. These results indicate that Egr-1 plays an important role in the induction and development of pulmonary vascular remodelling in flow-associated PAH. Egr-1 is therefore a putative target for future PAH treatment.

Egr-1 is a transcription factor with pleiotropic effects. Egr-1 is poorly expressed in the normal arterial wall but can be activated by various stimuli including changes in shear stress [12,20]. In systemic vessels, Egr-1, once activated, has been shown to act as an early ‘master switch’ during vessel wall remodelling including intimal thickening, vascular proliferation and vessel inflammation [21,22]. A role for Egr-1 in pulmonary vascular remodelling in PAH had not been described until now.

Here we demonstrate, for the first time, a functional role for the transcription factor Egr-1 in pulmonary vascular remodelling in PAH. Our results indicate that Egr-1-inhibition *in vivo* attenuates apoptotic dysregulation and reduces vascular proliferation. In human PAH development, vascular proliferation and apoptosis resistant endothelial cells are recognized hallmarks of pulmonary neointimal formation [2]. Egr-1 has been previously shown to induce neointimal formation in systemic arteries, in atherosclerotic disease and in-stent restenosis, mediated through both anti-apoptosis and pro-proliferative pathways [12,17,21]. PDGF-B and TGF- β 1 are known to induce proliferation of both smooth muscle cells and endothelial cells and are upregulated in human PAH [2]. Egr-1 is known to bind to the promoter regions of these genes resulting in increased expression [12,23]. The results of the current study, showing increased PDGF-B and TGF- β 1 expression in experimental PAH and its reduction through inhibition of Egr-1, support the working mechanism of Egr-1 induced vascular proliferation through PDGF-B and TGF- β 1 (Figure 8D). In addition we show that Egr-1 downregulation results in a reduction of IL-6 (vascular inflammation) and p53 (vascular apoptosis), both downstream targets of Egr-1 and known genes in the pathogenesis of human PAH [2,24].

Egr-1 could be a putative therapeutic target for future PAH treatment. We have previously shown that Egr-1 is upregulated in human end-stage PAH [9]. In these patients Egr-1 was located at sites that are of interest for treatment targeting, namely in vessels with media hypertrophy and in neointimal lesions [9]. The positive effects of Egr-1 inhibition on vascular remodelling and PAH progression in this study supports future outlook of Egr-1 as a treatment target. The fact that these effects were seen in the current PAH model that mimics 1) a human pathological trigger, 2) complex neointimal



development and 3) human PAH progression makes the critical role of Egr-1 in PAH development more convincing [25]. Combined, the observations in both human and now in experimental PAH justify future investigation in Egr-1 intervention either via gene silencing techniques or pharmacological treatment in human PAH.

The rapid developments in the design of gene silencing agents could facilitate a novel approach for therapeutic intervention for the treatment of PAH. First antisense oligonucleotide-based drugs have reached the clinic and have proved to be effective against for instance CMV infections and hypercholesterolemia [26,27]. New generations of oligonucleotides such as DNAzymes or small interfering RNAs (siRNAs) have entered the clinical stage [15]. In the current study we demonstrated that in PAH Egr-1 can be interfered *in vivo* using RNA interfering agents. Several types of clinically suitable carriers for siRNA delivery into pulmonary endothelial cells have been developed [28] and could serve as an alternative for DOTAP mediated delivery in the future and increase specificity. ED5 could possibly have a direct effect on pressure induced RV hypertrophy. However, since we show Egr-1 downregulation 1) attenuates pulmonary vascular resistance in flow-PAH rats 2) has no effect on RV hypertrophy in MCT only treated rats and 3) has no effect on LV mass, it is most likely that the positive effects of ED5 treatment are to Egr-1 downregulation in the pulmonary vasculature.

Pharmacological downregulation of Egr-1 with clinically used drugs could also be an interesting pursuit. One of these pharmacological possibilities is the use of PPAR- γ ligands, such as pioglitazone. PPAR- γ ligands have previously shown to inhibit Egr-1 expression *in vivo* [13,14]. These studies describe Egr-1 as a key repressive target gene of PPAR- γ in different pathophysiological mechanisms. Activation of PPAR- γ has been shown to prevent ERK phosphorylation in endothelial cells [29] and SMCs [30], which may affect Egr-1 activation pathways. In addition, recent studies have suggested that BMPR2 signalling dysfunction in PAH leads to failure of PPAR- γ activation resulting, in SMC proliferation in PAH [31]. PPAR- γ ligands are also shown to have a positive effect on vascular remodelling in other pulmonary hypertension models [32,33]. However, these studies were conducted in a hypoxic PH model that is known to fail to induce the typical neointimal lesions and progressive PAH development, which limits translation to human disease. Our results in a neointimal model of PAH show that pioglitazone prevents pulmonary vascular remodelling and that this positive effect is associated with a downregulation of vascular Egr-1 expression. This justifies further investigation of oral thiazolidinedione PPAR- γ ligands in both preclinical and clinical settings, also focusing on possible side effects.

This study was designed to investigate the mechanistic role of Egr-1 in the development of neointimal lesions. Therefore the question whether targeting Egr-1 also results in reversal of established PAH (when neointimal lesions are already present) should now be addressed. However, since Egr-1 is expressed in remodelled vessels



of both experimental and human end-stage PAH, Egr-1 could very well be a target in established pulmonary vascular remodelling.

Conclusions

This study indicates that the transcription factor Egr-1 governs flow-induced pulmonary vascular remodelling and the development of the characteristic vascular neointimal lesions in flow-associated PAH. Egr-1 therefore is a potential target for future PAH treatment.

Acknowledgments

We thank Michael Weij, Annemieke Smit-van Oosten and Andre Zandvoort for their valuable help with animal operations (aortocaval shunt creation).

Funding Sources

This work was supported by the Netherlands Heart Foundation (grant 2011T057 to MGD).

References

1. M. Humbert, O. Sitbon, A. Chaouat, M. Bertocchi, G. Habib, V. Gressin, A. Yaici, E. Weitzenblum, J.F. Cordier, F. Chabot, C. Dromer, C. Pison, M. Reynaud-Gaubert, A. Haloun, M. Laurent, E. Hachulla, V. Cottin, B. Degano, X. Jais, D. Montani, R. Souza, G. Simonneau, Survival in patients with idiopathic, familial, and anorexigen-associated pulmonary arterial hypertension in the modern management era, *Circulation*. 122 (2010) 156-163.
2. M. Rabinovitch, Molecular pathogenesis of pulmonary arterial hypertension, *J. Clin. Invest.* 122 (2012) 4306-4313.
3. S. Sakao, K. Tatsumi, N.F. Voelkel, Reversible or irreversible remodeling in pulmonary arterial hypertension, *Am. J. Respir. Cell Mol. Biol.* 43 (2010) 629-634.
4. H.J. Bogaard, K. Abe, A. Vonk Noordegraaf, N.F. Voelkel, The right ventricle under pressure: cellular and molecular mechanisms of right-heart failure in pulmonary hypertension, *Chest*. 135 (2009) 794-804.
5. R.M. Berger, M. Beghetti, T. Humpl, G.E. Raskob, D.D. Ivy, Z.C. Jing, D. Bonnet, I. Schulze-Neick, R.J. Barst, Clinical features of paediatric pulmonary hypertension: a registry study, *Lancet*. 379 (2012) 537-546.
6. M.G. Dickinson, B. Bartelds, M.A. Borgdorff, R.M. Berger, The role of disturbed blood flow in the development of pulmonary arterial hypertension: lessons from preclinical animal models, *Am. J. Physiol. Lung Cell. Mol. Physiol.* 305 (2013) L1-14.
7. B. Rondelet, C. Dewachter, F. Kerbaul, X. Kang, P. Fesler, S. Brimiouille, R. Naeije, L. Dewachter, Prolonged overcirculation-induced pulmonary arterial hypertension as a cause of right ventricular failure, *Eur. Heart J.* (2011).
8. K.R. Stenmark, B. Meyrick, N. Galie, W.J. Mooi, I.F. McMurtry, Animal models of pulmonary arterial hypertension: the hope for etiological discovery and pharmacological cure, *Am. J. Physiol. Lung Cell. Mol. Physiol.* 297 (2009) L1013-32.
9. M.G. Dickinson, B. Bartelds, G. Molema, M.A. Borgdorff, B. Boersma, J. Takens, M. Weij, P. Wichers, H. Sietsma, R.M. Berger, Egr-1 expression during neointimal development in flow-associated pulmonary hypertension, *Am. J. Pathol.* 179 (2011) 2199-2209.
10. M.E. van Albada, B. Bartelds, H. Wijnberg, S. Mohaupt, M.G. Dickinson, R.G. Schoemaker,

- K. Kooi, F. Gerbens, R.M. Berger, Gene expression profile in flow-associated pulmonary arterial hypertension with neointimal lesions, *Am. J. Physiol. Lung Cell. Mol. Physiol.* 298 (2010) L483-91.
11. J.I. Pagel, T. Ziegelhoeffer, M. Heil, S. Fischer, B. Fernandez, W. Schaper, K.T. Preissner, E. Deindl, Role of early growth response 1 in arteriogenesis: impact on vascular cell proliferation and leukocyte recruitment in vivo, *Thromb. Haemost.* 107 (2012) 562-574.
 12. L.M. Khachigian, Early growth response-1 in cardiovascular pathobiology, *Circ. Res.* 98 (2006) 186-191.
 13. M. Okada, S.F. Yan, D.J. Pinsky, Peroxisome proliferator-activated receptor-gamma (PPAR-gamma) activation suppresses ischemic induction of Egr-1 and its inflammatory gene targets, *FASEB J.* 16 (2002) 1861-1868.
 14. M. Wu, D.S. Melichian, E. Chang, M. Warner-Blankenship, A.K. Ghosh, J. Varga, Rosiglitazone abrogates bleomycin-induced scleroderma and blocks profibrotic responses through peroxisome proliferator-activated receptor-gamma, *Am. J. Pathol.* 174 (2009) 519-533.
 15. R. Bhindi, R.G. Fahmy, H.C. Lowe, C.N. Chesterman, C.R. Dass, M.J. Cairns, E.G. Saravolac, L.Q. Sun, L.M. Khachigian, Brothers in arms: DNA enzymes, short interfering RNA, and the emerging wave of small-molecule nucleic acid-based gene-silencing strategies, *Am. J. Pathol.* 171 (2007) 1079-1088.
 16. D.A. Baum, S.K. Silverman, Deoxyribozymes: useful DNA catalysts in vitro and in vivo, *Cell Mol. Life Sci.* 65 (2008) 2156-2174.
 17. F.S. Santiago, H.C. Lowe, M.M. Kavurma, C.N. Chesterman, A. Baker, D.G. Atkins, L.M. Khachigian, New DNA enzyme targeting Egr-1 mRNA inhibits vascular smooth muscle proliferation and regrowth after injury, *Nat. Med.* 5 (1999) 1264-1269.
 18. B. Bartelds, R.L. van Loon, S. Mohaupt, H. Wijnberg, M.G. Dickinson, B. Boersma, J. Takens, M. van Albada, R.M. Berger, Mast cell inhibition improves pulmonary vascular remodeling in pulmonary hypertension, *Chest.* 141 (2012) 651-660.
 19. M.A. Borgdorff, B. Bartelds, M.G. Dickinson, B. Boersma, M. Weij, A. Zandvoort, H.H. Sillje, P. Steendijk, M. de Vroomen, R.M. Berger, Sildenafil enhances systolic adaptation, but does not prevent diastolic dysfunction, in the pressure-loaded right ventricle, *Eur. J. Heart Fail.* 14 (2012) 1067-1074.
 20. L.M. Khachigian, K.R. Anderson, N.J. Halnon, M.A. Gimbrone Jr, N. Resnick, T. Collins, Egr-1 is activated in endothelial cells exposed to fluid shear stress and interacts with a novel shear-stress-response element in the PDGF A-chain promoter, *Arterioscler. Thromb. Vasc. Biol.* 17 (1997) 2280-2286.
 21. R.G. Fahmy, L.M. Khachigian, Locked nucleic acid modified DNA enzymes targeting early growth response-1 inhibit human vascular smooth muscle cell growth, *Nucleic Acids Res.* 32 (2004) 2281-2285.
 22. K. Ohtani, K. Egashira, M. Usui, M. Ishibashi, K.I. Hiasa, Q. Zhao, M. Aoki, Y. Kaneda, R. Morishita, A. Takeshita, Inhibition of neointimal hyperplasia after balloon injury by cis-element 'decoy' of early growth response gene-1 in hypercholesterolemic rabbits, *Gene Ther.* 11 (2004) 126-132.
 23. L.A. Rafty, L.M. Khachigian, Zinc finger transcription factors mediate high constitutive platelet-derived growth factor-B expression in smooth muscle cells derived from aortae of newborn rats, *J. Biol. Chem.* 273 (1998) 5758-5764.
 24. M. Levy, C. Maurey, D.S. Celermajer, P.R. Vouhe, C. Danel, D. Bonnet, D. Israel-Biet, Impaired apoptosis of pulmonary endothelial cells is associated with intimal proliferation and irreversibility of pulmonary hypertension in congenital heart disease, *J. Am. Coll. Cardiol.* 49 (2007) 803-810.
 25. G. Kwapiszewska, K. Chwalek, L.M. Marsh, M. Wygrecka, J. Wilhelm, J. Best, B. Egemnazarov, F.C. Weisel, S.L. Osswald, R.T. Schermuly, A. Olschewski, W. Seeger, N. Weissmann, O. Eickelberg, L. Fink, BDNF/TrkB signaling augments smooth muscle cell proliferation in pulmonary hypertension, *Am. J. Pathol.* 181 (2012) 2018-2029.
 26. E. Merki, M.J. Graham, A.E. Mullick, E.R. Miller, R.M. Crouse, R.E. Pitas, J.L. Witztum, S. Tsimikas, Antisense oligonucleotide directed to human apolipoprotein B-100 reduces



- lipoprotein(a) levels and oxidized phospholipids on human apolipoprotein B-100 particles in lipoprotein(a) transgenic mice, *Circulation*. 118 (2008) 743-753.
27. C. Marwick, First "antisense" drug will treat CMV retinitis, *JAMA*. 280 (1998) 871.
28. P.S. Kowalski, N.G. Leus, G.L. Scherphof, M.H. Ruiters, J.A. Kamps, G. Molema, Targeted siRNA delivery to diseased microvascular endothelial cells: cellular and molecular concepts, *IUBMB Life*. 63 (2011) 648-658.
29. G. Cantini, A. Lombardi, E. Borgogni, M. Francalanci, E. Ceni, S. Degl'Innocenti, S. Gelmini, G. Poli, A. Galli, M. Serio, G. Forti, M. Luconi, Peroxisome-proliferator-activated receptor gamma (PPARgamma) is required for modulating endothelial inflammatory response through a nongenomic mechanism, *Eur. J. Cell Biol.* 89 (2010) 645-653.
30. K. Benkirane, F. Amiri, Q.N. Diep, M. El Mabrouk, E.L. Schiffrin, PPAR-gamma inhibits ANG II-induced cell growth via SHIP2 and 4E-BP1, *Am. J. Physiol. Heart Circ. Physiol.* 290 (2006) H390-7.
31. G. Hansmann, V.A. de Jesus Perez, T.P. Alastalo, C.M. Alvira, C. Guignabert, J.M. Bekker, S. Schellong, T. Urashima, L. Wang, N.W. Morrell, M. Rabinovitch, An antiproliferative BMP-2/PPARgamma/apoE axis in human and murine SMCs and its role in pulmonary hypertension, *J. Clin. Invest.* 118 (2008) 1846-1857.
32. J.T. Crossno Jr, C.V. Garat, J.E. Reusch, K.G. Morris, E.C. Dempsey, I.F. McMurry, K.R. Stenmark, D.J. Klemm, Rosiglitazone attenuates hypoxia-induced pulmonary arterial remodeling, *Am. J. Physiol. Lung Cell. Mol. Physiol.* 292 (2007) L885-97.
33. R.E. Nisbet, J.M. Bland, D.J. Kleinhenz, P.O. Mitchell, E.R. Walp, R.L. Sutliff, C.M. Hart, Rosiglitazone attenuates chronic hypoxia-induced pulmonary hypertension in a mouse model, *Am. J. Respir. Cell Mol. Biol.* 42 (2010) 482-490.



Supplementary material and methods

DNAzyme preparation and transfection carrier

For *in vivo* DNAzyme administration we first tested 2 different transfection carriers – 1,2-dioleoyl-3-trimethylammonium-propane (DOTAP; Avanti Polar Lipids, Alabaster, Alabama, USA) and polyethylenimine (in vivo jetPEI; Polyplus transfection, Illkirch, France) – known for targeting the pulmonary vasculature [1]. Sterile DOTAP solution (0.5 mg/ml) was prepared as follows. DOTAP stock solution in chloroform: methanol (9:1) was dried under reduced nitrogen pressure for 10 min and further dried under high vacuum for 30 min. Subsequently, dried lipid film was hydrated in sterile HN buffer (150 mM NaCl, 20 mM HEPES) pH 7.4 for 10 min and vortex vigorously. DOTAP solution was stored at 4 °C under argon gas and used within 4 days. DNAzyme-DOTAP complex was prepared by mixing DOTAP solution with DNAzyme in 1:1 ratio w/w (500ug DNAzyme/500ug DOTAP) and allowing complex to form for 10 min before use. ED5-jetPEI complexes were prepared in 5% glucose according to manufacturer's protocol using 7:1 ratio w/w (DNAzyme/PEI).

In this study we demonstrated that, compared to ED5-jetPEI, a single injection of ED5-DOTAP solution (500ug DNAzyme/500ug DOTAP) in the jugular vein resulted in a significant ED5 uptake in the pulmonary vasculature and a reduction of vascular Egr-1 expression after 24 hours (n= 4 rats; Supplemental Figure S1). For the detection studies of DNAzyme *in vivo*, 6FAM was used as fluorescent label on the 5' terminus of ED5 (Figure 1).

Pilot study: Egr-1 DNAzyme (ED5) delivery to pulmonary vasculature

In a pilot study we aimed to determine whether intravenous administration of the DNAzyme ED5/DOTAP complex would lead to delivery into the pulmonary vasculature and downregulate pulmonary vascular Egr-1 protein expression. To test this, flow-PAH rats (n=4) received a single injection of ED5/6FAM-DOTAP solution (500ug DNAzyme/500ug DOTAP) directly after shunt creation, whereas 3 flow-PAH rats received saline injection. Rats were sacrificed after 1 and 3 days. In contrast to the saline-injected animals, the ED5/6FAM-DOTAP-injected rats, showed ED5 in the endothelial layer of the pulmonary vessels (Figure 1) at day 1 that had diminished at day 3. Accordingly, in these rats ED5 transfection indeed resulted in downregulation of vascular Egr-1 protein expression at day 1 and this effect was lost 3 days after injection (Figure 1C and D). Therefore, in the main study rats received treatment every 48 hours.

Echocardiography

Echocardiography was performed 1 and 3 weeks after start of increased pulmonary blood flow, and in sham operated animals using a Vivid Dimension 7 system and



10S-transducer (GE Healthcare, Waukesha, WI, USA) as described previously [2]. Briefly, cardiac output (CO) was calculated using systolic aorta diameter and pulsed wave Doppler of aorta flow as $(\text{aorta diameter})^2 \times 3.14 \times \text{velocity time integral (VTI)} \times \text{heart rate}$. Pulmonary artery acceleration time (PAAT) was measured in the RV outflow tract, and tricuspid annular plane systolic excursion (TAPSE) was measured in apical 4-chamber view.

Hemodynamic measurements

Rats were anesthetized with 3-5% isoflurane inhalation. A fluid filled pressure catheter was inserted into the right internal jugular vein and guided to the right ventricle under pressure waveform monitoring using a bedside monitor. Mean right atrial pressure and right ventricular systolic pressure were measured. Pulmonary vascular resistance was estimated by dividing the assessed mean pulmonary arterial pressure by the cardiac output as described previously [3].

Pathology and morphometric analysis

Heart and lungs were excised and weighed separately. The right lung was frozen in liquid nitrogen for molecular analysis. The left lung was fixated by passive filling of the airways with 3.6% formalin and embedded in paraffin. Pulmonary vascular morphology (n=6-7 rats per experimental group) was qualitatively and quantitatively analyzed.

Intra-acinar vessels without a clearly defined internal lamina elastica combined with luminal occlusion were defined as occlusive neointimal lesions. Intra-acinar vessels with a double lamina elastica for more than half of its circumference were defined as completely muscular. Intra-acinar vessels with a double lamina elastica for less than half of its circumference were defined as partially muscular. Normal, non-muscular, intra-acinar vessels had a single lamina elastica and no luminal occlusion.

Five-ten randomly chosen pre-acinar vessels ($> 50 \mu\text{m}$) and 40 randomly chosen intra-acinar vessels ($< 50 \mu\text{m}$) were assessed using Image Scope (Aperio Technologies version 10). Three different vascular areas were defined: outer vessel area, inner vessel area and luminal area. The outer vessel area was defined as the area within the lamina elastica externa. The inner vessel area was defined as the area within the lamina elastica interna. The medial area was defined as the outer vessel area minus the inner vessel area.

The occlusion score for the intra-acinar pulmonary vessels was calculated according to the following formula: $(\text{outer vessel area} - \text{luminal area}) / (\text{outer vessel area})$ and presented as the mean (\pm SD) percentage of vessel occlusion per time point.

Muscularization per time point was assessed and presented as the percentage of vessels per degrees of muscularization (including neointimal formation).



Immunohistochemistry

Paraffin-embedded rat lung sections were microwave heated for antigen retrieval. To reduce non-specific staining, sections were preincubated in 0,3% hydrogen peroxide. Sections were then embedded for 1h at room temperature with primary antibodies for aSMA (DAKO, 1:50), von Willebrand Factor (vWF; Abcam, 1:300), Egr-1 (rat: Cell Signaling, 1:50 dilution; human: Abcam, 1:100 dilution), (PDGF)-B (Abcam, 1:100), TGF- β 1 (Abcam, 1:100), IL-6 (Abcam, 1:00), p53 (Abcam, 1:00), Caspase 3 (Cell Signaling, 1:100 dilution) and Ki67 (Abcam, 1:50 dilution). Species-specific immunoglobulin G coupled to peroxidase was used as secondary and tertiary antibodies (DAKO, 1:100 dilution). Sections were stained with diaminobenzidine for 10 min and counterstained with hematoxylin. For immunofluorescence nuclei were stained with DAPI (Vector Laboratories Inc.).

As an example for Egr-1 staining in human PAH, a human lung tissue sample was obtained from an explanted lung from a patient with PAH associated with congenital cardiac shunt (VSD+PDA) that underwent lung transplantation.

Egr-1 positive control staining was performed on prostate adenocarcinoma samples. In addition, bronchial staining of Egr-1 served as positive control within the sample. Negative controls for all secondary antibodies were tested.

Staining was semi-quantified (n=4-6 rats per experimental group) to characterize spatiotemporal expression of the proteins Egr-1, Caspase 3 and Ki67, PDGF-B, TGF- β 1, IL-6 and p53. Twenty intra-acinar vessels were randomly selected per rat. Vessels were scored as followed: a) positive Egr-1 expression (0: no staining; 1: positive staining), b) localization of Egr-1 expression (0: no staining; 1: positive staining mainly in endothelium, 2: positive staining mainly in media and 3: diffuse positive staining) and c) amount of positive Egr-1 cells per vessel. Endothelium was defined as the cell layer bordering the vessel lumen. In non-neointimal vessels, media was defined as the layer between outer elastic layer the cell layer bordering the vessel lumen.

Real-time RT-PCR

For PPAR- γ activation, gene expression of PGC1a (co-activator of PPAR- γ) and MCAD (downstream gene of PPAR- γ) were measured. For real-time RT-PCR of whole lung samples (n=3-5 per group), commercially available kits were used. Total RNA was isolated from pulmonary tissue using TRIzol reagent (Invitrogen). Real-time RT PCR experiments were performed on a CFX384 real time system C1000 Thermal cycler (BioRad Laboratories, Veenendaal, The Netherlands). cDNA was synthesized using QuantiTect Reverse Transcription Kit (Qiagen, Benelux). Real-time RT PCR was conducted using SYBR Green PCR Master Mix according to the manufacturer's instructions (Eurogentec, San Diego, CA). Primer sequences are available on request. Expression levels were obtained from a dilution standard curve and compared with those of cyclophilin or 36B4 RNA in order to calculate the relative expression levels.



References

1. R. Kuruba, A. Wilson, X. Gao, S. Li, Targeted delivery of nucleic-acid-based therapeutics to the pulmonary circulation, *AAPS J.* 11 (2009) 23-30.
2. M.A. Borgdorff, B. Bartelds, M.G. Dickinson, B. Boersma, M. Weij, A. Zandvoort, H.H. Sillje, P. Steendijk, M. de Vroomen, R.M. Berger, Sildenafil enhances systolic adaptation, but does not prevent diastolic dysfunction, in the pressure-loaded right ventricle, *Eur. J. Heart Fail.* 14 (2012) 1067-1074.
3. M.L. Handoko, I. Schaliij, K. Kramer, A. Sebkhii, P.E. Postmus, W.J. van der Laarse, W.J. Paulus, A. Vonk-Noordegraaf, A refined radio-telemetry technique to monitor right ventricle or pulmonary artery pressures in rats: a useful tool in pulmonary hypertension research, *Pflugers Arch.* 455 (2008) 951-959.



Supplementary data

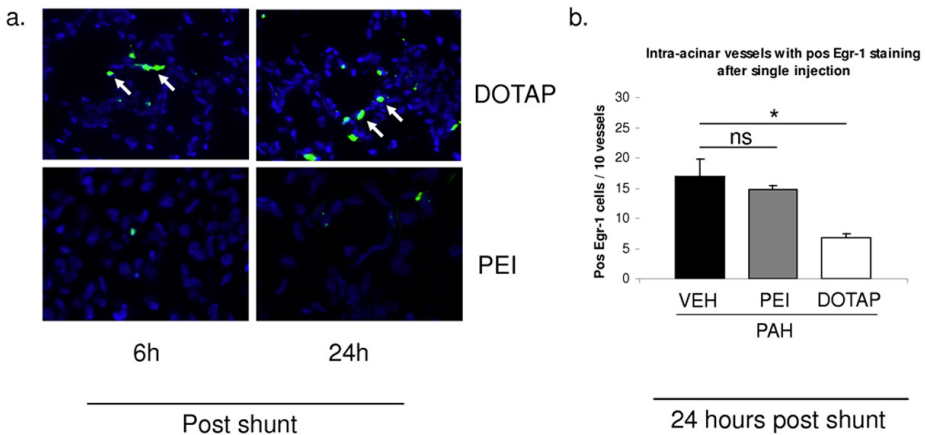


Figure S1. Pilot study: targeting pulmonary vasculature with DNzyme ED5

A) Pulmonary vascular localization of ED5 (6FAM fluorescent signaling) after a single injection combined with either DOTAP or PEI for facilitation of cell transfection. Note the strong presence of ED5 in the combination with DOTAP at 6 and 24 hours post injection. PEI did not result in pulmonary vascular cell transfection. B) transfection of ED5 with DOTAP (PAH_DOTAP) resulted in a reduced pulmonary vascular Egr-1 expression compared to saline injected rats (PAH_VEH). PEI (PAH_PEI) had no effect on Egr-1 expression. Data are presented as mean values \pm SEM. * $P < 0.05$. Scale bar represents 50 μ m.

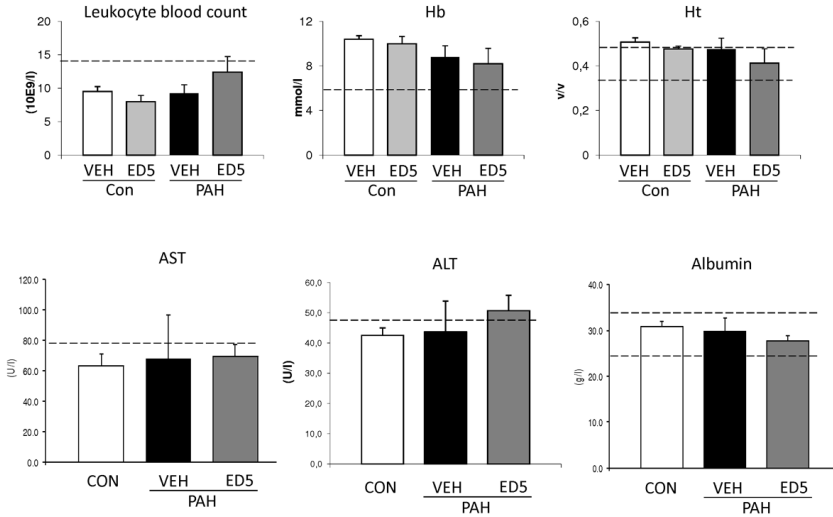


Figure S2. Peripheral blood work results

ED5 treatment did not result in a systemic immune response (as measured by leucocyte count, hematocrit (Ht), hemoglobin (Hb) at 3 weeks) or decreased liver function (as measured by the liver enzymes aspartate transaminase (ASAT), alanine transaminase (ALAT); and albumin production at 1 week) measured in peripheral blood. Data are presented as mean values \pm SEM. Dotted lines indicate normal range for each parameter.

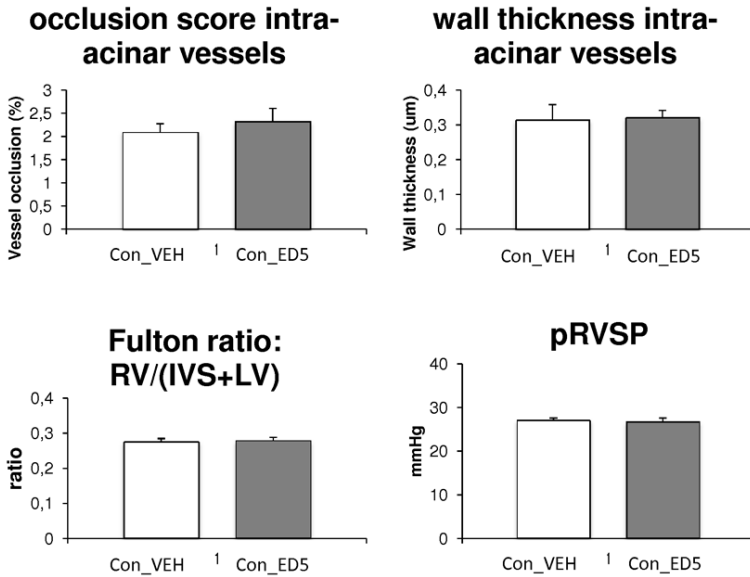


Figure S3. Similarities in sham operated animals at 3 weeks

Pulmonary vascular remodeling (occlusion score, wall thickness), RV hypertrophy (RV/IVS+LV) and peak systolic right ventricular pressure (pRVSP) in sham operated rats that received either vehicle treatment of ED5. ED5 treatment had no effect on pulmonary vascular remodeling, RV remodeling or pRVSP in control animals. Data are presented as mean values \pm SEM.



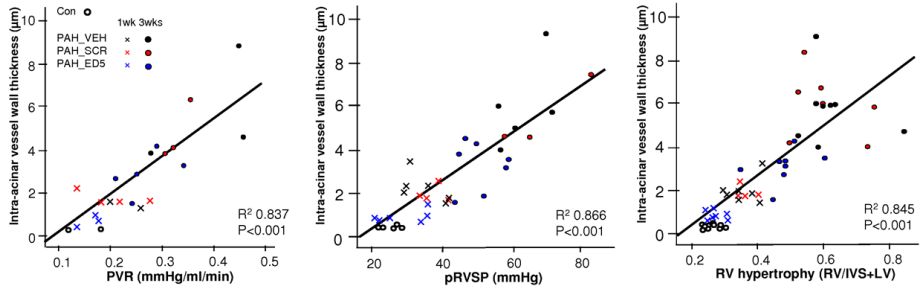


Figure S4. Correlation between the wall thickness of the intra-acinar vessels and hemodynamic parameters and right ventricular hypertrophy. Data are presented as mean values ± SEM. * P < 0.05.

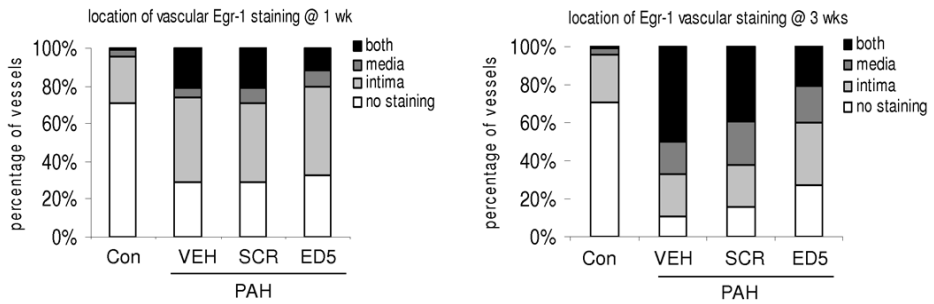


Figure S5. Localization of Egr-1 expression in pulmonary vasculature. At 1 week Egr-1 was found mainly in the intimal layer. At 3 weeks Egr-1 was found throughout the vessel wall. ED5 reduced the expression of Egr-1 throughout the vessel wall.

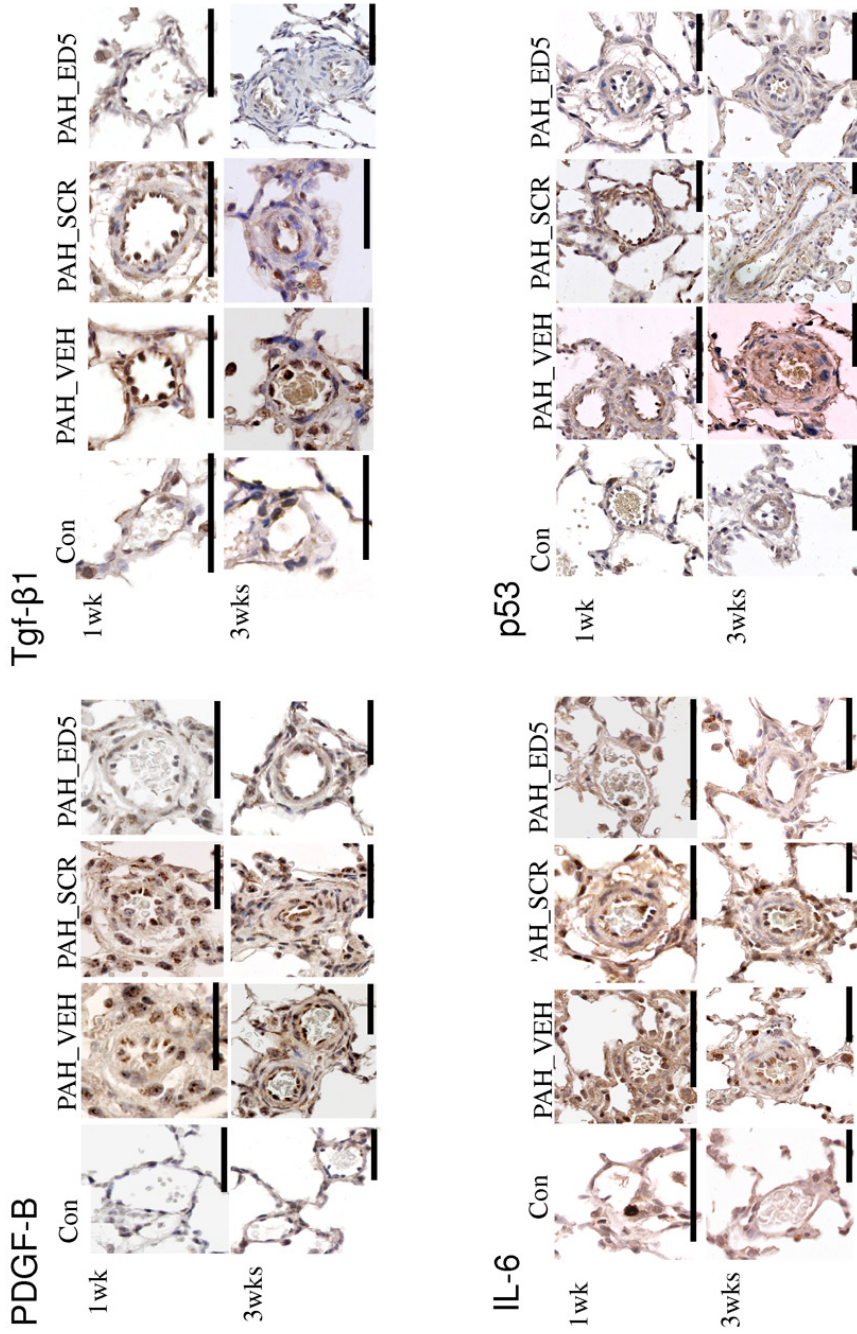


Figure S6. Histological examples of the *Egr-1* downstream genes PDGF-B, TGF- β IL-6 and p53 in the intra-acinar vessels. *Egr-1* inhibition resulted in downregulation of PDGF-B, TGF- β IL-6 and p53 at both 1 and 3 weeks.

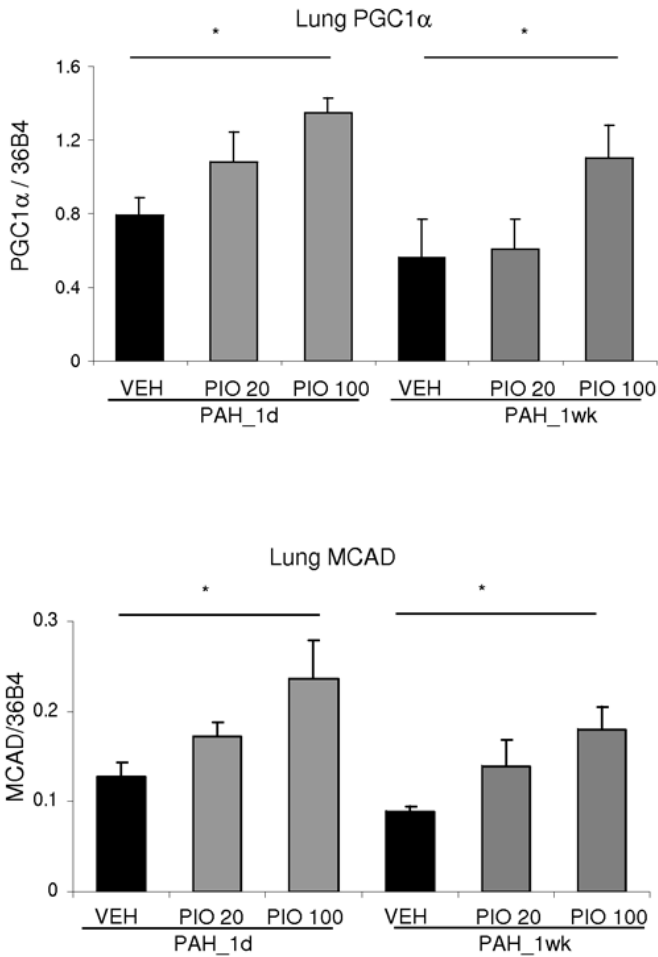


Figure S7. PPAR- γ activation.

Expression of peroxisome proliferator-activated receptor gamma coactivator 1-alpha (PGC1 α) and medium-chain acyl-CoA dehydrogenase (MCAD) as a readout for PPAR- γ activation at 1 day and 1 week after flow. Pioglitazone treatment increased PGC1 α (co-activator of PPAR γ) and MCAD (downstream gene of PPAR γ) expression in a dose dependent manner. Data are presented as mean values \pm SEM. * $P < 0.05$ PAH_PIO100 vs PAH_VEH.



Chapter 4

Anti-VCAM-1 and Anti-E-selectin SAINT-O-Somes for Selective Delivery of siRNA into Inflammation-Activated Primary Endothelial Cells

Piotr S. Kowalski,[†] Lucas L. Lintermans,[†] Henriëtte W. M. Morselt,[†] Niek G. J. Leus,[†] Marcel H. J. Ruiters,^{†,‡} Grietje Molema,[†] and Jan A. A. M. Kamps^{*,†}

Mol Pharm. 2013 Aug 5;10(8):3033-44.

[†]Department of Pathology & Medical Biology, Medical Biology Section, Laboratory for Endothelial Biomedicine & Vascular Drug Targeting Research, University Medical Center Groningen, University of Groningen, Groningen, The Netherlands

[‡]Synvolux Therapeutics, L.J. Zielstraweg 1, Groningen, The Netherlands

Abstract

Activated endothelial cells play a pivotal role in the pathology of inflammatory diseases and present a rational target for therapeutic intervention by endothelial specific delivery of short interfering RNAs (siRNA). This study demonstrates the potential of the recently developed new generation of liposomes based on cationic amphiphile SAINT-C18 (1-methyl-4-(cis-9-dioleyl)methyl-pyridinium-chloride) for functional and selective delivery of siRNA into inflamed primary endothelial cells. To create specificity for inflamed endothelial cells, these so called SAINT-O-Somes were harnessed with antibodies against VCAM-1 respectively E-selectin and tested in TNF- α activated primary endothelial cells from venous and aortic vascular beds. Both targeted SAINT-O-Somes carrying siRNA against the endothelial gene VE-cadherin specifically downregulated its target mRNA and protein without exerting cellular toxicity. SAINT-O-Somes formulated with siRNA formed small particles (106 nm) with a 71% siRNA encapsulation efficiency. SAINT-O-Somes were stable in the presence of serum at 37 °C, protected siRNA from degradation by serum RNases and after i.v. injection displayed pharmacokinetic comparable to conventional long circulating liposomes. These anti-VCAM-1 and anti-E-selectin SAINT-O-Somes are thus a novel drug delivery system that can achieve specific and effective delivery of siRNA into inflamed primary endothelial cells and have physicochemical features that comply with *in vivo* application demands.



Introduction

Gene silencing by means of RNA interference (RNAi) is a powerful technique with a potential for pharmacological application. Short interfering RNAs (siRNAs) are extensively investigated as a new class of molecular drugs due to their highly specific interference with gene expression. However, unmodified or uncomplexed siRNAs (so-called “naked” siRNAs) are subjected to rapid clearance from the circulation by the liver and by renal filtration which limits their usefulness as a therapeutic *per se* [1, 2]. Moreover, the physicochemical properties of siRNAs, including their high molecular weight (~13-15 kDa), polyanionic nature (~40 negatively charged phosphate groups), and their susceptibility to degradation by serum RNases, enforce application of chemical modifications or proper formulation into a delivery system to create potent therapeutics [3, 4]. siRNA carriers have proven to be able of knocking down targets in various diseases *in vivo* including hypercholesterolemia [5], liver cirrhosis [6], and cancer [7]. Moreover, first evidence of successful siRNA mediated gene silencing in humans by systemically delivered siRNA nanoparticles has been published recently [8].

Increased insight in the role of endothelial cells in the pathophysiology of cancer, inflammatory and cardiovascular diseases, has drawn great interest in pharmacological interventions towards the endothelial cells at diseased sites [9, 10]. Their prevalence throughout the body, and accessibility for intravenously administered compounds make them attractive targets for targeted drug delivery approaches. Interfering with molecular processes in diseased endothelial cells by means of siRNA will advance to create novel endothelial cells directed therapies. Santel and Aleku et al. for example, demonstrated that *in vivo* silencing of protein kinase N3 (PKN3) in the tumor vasculature by siRNA containing lipoplexes significantly inhibited growth of various types of tumors as well as formation of metastases [11, 12].

Despite successful attempts of siRNA delivery to tumor endothelium, targeted delivery to endothelial cells in inflamed sites is still ill-addressed. Upon pro-inflammatory stimulation, each organ displays a vascular bed specific pattern of cell adhesion molecules as E-selectin or VCAM-1, providing challenging opportunities to deliver drugs or small RNAs to organ specific (micro)vascular endothelial subsets [13]. E-selectin expression is restricted to endothelial cells and dramatically upregulated during inflammation [14, 15]. Also VCAM-1 is an attractive target as it is strongly upregulated upon inflammatory stimuli and during angiogenesis [16, 17]. In previous studies, we successfully employed immunoliposomes targeted to E-selectin for delivery of the anti-inflammatory drug dexamethasone and the cytotoxic drug doxorubicine to inflamed endothelial cells [18-20].

Limited processing of liposomes and subsequent release of their content displayed by primary endothelial cells remain a serious obstacle to achieve effective drug delivery



[19]. To address this, we recently developed a new generation of liposomes called SAINT-O-Somes, based on formulation of conventional long circulating liposomes and the cationic amphiphilic lipid SAINT-C18 (1-methyl-4-(cis-9-dioleyl)methylpyridinium-chloride). SAINT-O-Somes showed superior intracellular release of their content in endothelial cells compared to conventional liposomes. Moreover, this system displayed the ability to efficiently encapsulate low molecular weight compounds and siRNA [19]. In the current study, we show that siRNA encapsulated in SAINT-O-Somes targeted to VCAM-1 or E-selectin can be successfully delivered into inflamed primary endothelial cells originating from distinct vascular beds (venous and arterial). We investigated the potential of SAINT-O-Somes to specifically deliver siRNA into activated endothelial cells taking into account their physicochemical features (size, stability, protection of siRNA) and target cell conditions as appear *in vivo*. In addition, *in vivo* pharmacokinetic (PK) behavior of siRNA SAINT-O-Somes was studied. Since little is known about the intracellular fate of siRNA delivery systems internalized *via* E-selectin and VCAM-1, we studied the intracellular trafficking of both siRNA and SAINT-O-Somes in the activated endothelial cells. Based on our results, we concluded that SAINT-O-Somes fulfill important requirements for successful targeted delivery of siRNA into inflamed endothelial cells and meet the requirements for *in vivo* application.



Experimental Section

Materials

Lipids 1-palmitoyl-2-oleoyl-sn-glycero-3-phosphocholine (POPC), 1,2-distearoyl-sn-glycero-3-phosphoethanolamine-N-[methoxy(poly-ethylene glycol)-2000]-maleimide (DSPE-PEG₂₀₀₀-Mal), and 2-distearoyl-sn-glycero-3-phosphoethanolamine-N-[methoxy(polyethylene glycol)-2000] (DSPE-PEG₂₀₀₀) were purchased from Avanti Polar Lipids (Alabaster AL, USA). The cationic lipid 1-methyl-4-(cis-9-dioleyl)methyl-pyridinium-chloride (SAINT-C18) was obtained from Synvolux Therapeutics (Groningen, The Netherlands). Cholesterol (Chol) and N-succinimidyl-S-acetylthioacetate (SATA) were obtained from Sigma (St. Louis MO, USA). Nucleic acid stain Hoechst 33342 (trihydrochloride), lipophilic tracers 1,1'-dioctadecyl-3,3,3',3'-tetramethyl-indocarbocyanine perchlorate (DiI), 1,1'-dioctadecyl-3,3,3',3'-tetramethyl-indocarbocyanine perchlorate (DiD), and LysoTracker® Green DND-26 probe were purchased from Molecular Probes (Leiden, The Netherlands). Lipofectamine™ 2000 transfection reagent was purchased from Invitrogen (Breda, The Netherlands). All siRNAs were purchased from Qiagen (Venlo, The Netherlands).

The H18/7-acb (mouse IgG2a anti-human E-selectin) and E1/6-aa2 (mouse IgG1 anti-human VCAM-1 antibody) monoclonal antibody-producing hybridomas were kindly provided by Dr. M. Gimbrone from Harvard Medical School (Boston, MA, USA).

Preparation of siRNA containing SAINT-O-Somes

SAINT-O-Somes were prepared as described previously with slight modifications [19]. In brief, lipids from stock solutions of POPC, SAINT-C18, Chol, DSPE-PEG₂₀₀₀ and DSPE-PEG₂₀₀₀-Mal in chloroform: methanol (9:1) were mixed in a mol% ratio of 37:18:40:4:1. To fluorescently label the liposomal bilayer, DiI or DiD was added to the lipid mixture in a 0.25 mol% ratio of Total Lipid (TL). We prepared SAINT-O-Somes containing VE-cadherin siRNA (Hu_CDH5_2 FlexiTube siRNA, cat No. SI00028483) or control siRNA (AllStars Negative Control, cat No. 1027281), with no homology to any known mammalian gene, with or without a fluorescent label. siRNA was dissolved according to the protocol of the manufacturer and mixed with dried lipids at a ratio of 1 nmol siRNA per 1 μ mol TL. After extrusion through polycarbonate filters (50 nm pore size) nonencapsulated siRNA was removed by ion exchange chromatography on a DEAE Sepharose CL-6B (Sigma, The Netherlands) column using HN buffer (135 mM NaCl, 10 mM HEPES) pH 6.7 as an eluent. The concentration of siRNA encapsulated in liposomes was measured using the Quant-iT™ Ribo-Green® assay (Invitrogen, Breda, The Netherlands) according to the protocol of the manufacturer. The efficiency of siRNA encapsulation into liposomes was calculated based on the measurements of encapsulated siRNA in the presence or absence of 1% (v/v) Triton X-100 (Sigma-Aldrich, Zwijndrecht, The Netherlands). The monoclonal anti-E-selectin and anti-VCAM-1 antibodies were thiolated by means of SATA and coupled to a maleimide group at the distal end of the polyethylene glycol chain by sulfhydryl-maleimide coupling as described before for albumin [21]. SAINT-O-Somes without an antibody were prepared from the same lipid mixture, but instead of being conjugated to the antibody, they were allowed to react with cysteine in a molar ratio twice that of DSPE-PEG₂₀₀₀-Mal to block reactive maleimide groups. The SAINT-O-Somes were characterized by determining the protein concentration using rat IgG as a standard and measuring the total lipid concentration by phosphorus assay [22]. Particle size and Zeta-potential were analyzed using a Nicomp model 380 ZLS submicron particle analyzer. Particle size was measured using dynamic light scattering (DLS) in the volume weighing mode (NICOMP particle sizing systems, Santa Barbara, CA, USA). The Polydispersity index (PDI) was calculated using a Malvern Zetasizer Nano ZSP (Malvern Instruments Ltd., Worcestershire, UK). The number of antibody molecules coupled per liposome was calculated as described before [23]. SAINT-O-Somes were stored at 4 °C under argon gas and were used within 4 weeks.

Cryo-transmission microscopy (Cryo-TEM)

Cryo-TEM analysis of SAINT-O-Somes was performed as described previously [19].



Cell cultures

Human umbilical vein endothelial cells (HUVEC) were obtained from Lonza (Breda, The Netherlands). Cells were cultured in EBM-2 medium supplemented with EGM-2 MV SingleQuot Kit Supplements & Growth Factors (cat No. CC-3202, Lonza,). In all experiments, cells from passage 5 to 7 were used and they were plated on cultures plates (Costar, Corning, NY) at a density of 1.8×10^4 cells/cm² one day before the experiment unless stated differently. Before seeding the cells, culture plates were incubated with EGM2 MV medium for 30 min.

Human aortic endothelial cells (HAEC) were obtained from Cascade Biologics Invitrogen cell culture (Life Technologies, Bleiswijk, The Netherlands). Cells were cultured in Medium 200 (Life Technologies) supplemented with Low Serum Growth Component (LSGS, containing fetal bovine serum, 2% v/v; hydrocortisone, 1 µg/ml; human epidermal growth factor, 10 ng/ml; basic fibroblast growth factor, 3 ng/ml) and heparin 10 µg/ml, streptomycin 100 µg/ml, and penicillin 100 IU/ml). In all experiments, cells from passage 5 to 10 were used and they were plated on cultures plates (Costar) at a density of 2×10^4 cells/cm² one day before the experiment. All cell cultures were maintained by the endothelial cell facility of UMCG.

Influence of serum on particles size stability and siRNA integrity

To determine the influence of temperature and serum on the size of siRNA SAINT-O-Somes, particles were incubated for 2, 4, 6 and 24 h at 37 °C in the presence or absence of 50% human serum. The size of liposomes was measured as described above by dynamic light scattering.


To investigate the integrity of encapsulated siRNA, SAINT-O-Somes containing 160 ng of control siRNA were incubated in presence of 50% human serum for 0.5, 1, 4, 6 and 24 h at 37 °C. An equal amount of naked control siRNA was incubated with human serum for the same period of time as SAINT-O-Somes. At the end of the incubation, 1 % (v/v) Triton X-100 and the gel loading dye (BioLabs, Leiden, The Netherlands) were added to the samples. Subsequently, samples were loaded on 2% agarose gel containing ethidium bromide and run for 15 min at 110 V. Bands were visualized using the ChemiDoc™ XRS system (Bio-rad, Veenendaal, The Netherlands). The integrity of encapsulated siRNA after eight weeks of storage at 4 °C under argon gas was also analyzed by agarose gel electrophoresis as described above.

Investigation of SAINT-O-Somes uptake by flow cytometry and fluorescence microscopy

For flow cytometry experiments, HUVEC and HAEC were seeded in 24-well plates. 10 ng/ml TNF-α (BioSource Europe, Nivelles, Belgium) was added to the cells 2 h before addition of 80 nmol TL/ml of SAINT-O-Somes containing AlexaFluor₄₈₈



siRNA. TNF- α remained present in the medium during further incubation with liposomes. To block E-selectin respectively VCAM-1 protein, a 75-fold excess over the amount of antibodies coupled to the liposomes of anti-E-selectin or anti-VCAM-1 monoclonal antibodies was added to the cells, together with the liposomes. 4 or 24 h after addition of SAINT-O-Somes, cells were washed twice with PBS and detached from the surface using trypsin/EDTA (Sigma, Ayrshire, UK) after which they were immediately transferred to tubes containing 5% FBS (Fetal Bovine Serum, Thermo Scientific HyClone, Cramlington, UK) in PBS and kept on ice. Next, samples were centrifuged for 5 min at 500 g at 4 °C, followed by two washing steps with 3 ml of 5% FBS in PBS, and resuspended in 0.2 ml PBS for flow cytometry analysis (Calibur, BD Biosciences, Franklin Lakes, NJ). When flow cytometry was performed the following day, cells were fixed with 0.5% paraformaldehyde in PBS and stored at 4 °C.



For fluorescence microscopy HUVEC were cultured on Lab-Tek™ Chamber Slides (Nunc, Rochester, NY, USA). Before seeding the cells, chamber slides were incubated with EGM2 MV medium for 30 min. Cells were activated with TNF- α and incubated with liposomes in a similar way as described for the flow cytometry experiments. Targeted and non-targeted SAINT-O-Somes labeled with DiI and containing AlexaFluor₄₈₈ labeled siRNA were used at 80 nmol TL/ml. Nuclei of the cells were stained using Hoechst 33342. At the end of the incubation, cells were washed twice with ice-cold serum-free culture medium, placed on ice and subjected to imaging within 45 min. Fluorescence images of cells were taken with a Leica DM/RXA fluorescence microscope (Wetzlar, Germany) using Quantimet HR600 image analysis software (Leica). Images were taken at excitation/emission wavelengths of 550/570 nm for DiI, 490/520 nm for siRNA AlexaFluor₄₈₈, and 350/461 nm for Hoechst 33342.

Investigation of Intracellular processing of siRNA containing SAINT-O-Somes by confocal microscopy

For confocal laser scanning microscopy (CLSM), HUVEC were cultured on sterile cover glasses (Menzel-Gläser, Braunschweig, Germany) placed into the wells of a 12-well plate. Before seeding the cells, the cover glasses were incubated with EGM2 MV medium for 30 min. Prior to incubation with anti-E-selectin or anti-VCAM-1 SAINT-O-Somes, HUVEC were activated for 4 h with 10 ng/ml of TNF- α . Liposomes containing membrane label (DiD) and/or fluorescent siRNA were incubated with the cells at concentration of 80 nmol TL/ml for the indicated time periods. For staining of acidic organelles, cells were incubated with LysoTracker at a concentration of 75 nM for the last 20 min of the incubation. To stain late endosomal/lysosomal compartments cells were plated at a density of 1.4×10^4 cell/cm² and transfected with 2 μ g/ml pLamp-1-RFP plasmid (obtained from Dr. Walther E. Mothes from Yale School of Medicine,

New Haven, CT, USA) using Lipofectamine 2000, 48 h prior the experiment according to the manufacturer's protocol. At the end of the incubation, cells were washed twice with ice-cold serum-free culture medium, placed on ice and subjected to imaging within 45 min. During this time, there was no change in cell morphology and images taken within this period were reproducible throughout the different experiments. For studying the internalization, cells were fixed with 4% formaldehyde in PBS for 15 min at room temperature (RT) and subsequently slides were mounted with Citi-Fluor AF1 (Citifluor Ltd, London, UK) and kept at 4 °C until analysis. Images were taken with a confocal laser scanning microscope (True Confocal Scanner SP2-AOBS; Leica, Heidelberg, Germany) equipped with argon (Ar) and helium-neon lasers (HeNe) and coupled to a LeicaDM RXE microscope using an HCXPL APO CS 63 x 1.40 oil immersion objective. Continuing scans were taken for fluorophore pairs AlexaFluor₄₈₈/DiD and LysoTracker green/DiD, while sequential scans were obtained for fluorophore pairs AlexaFluor₄₈₈/RFP to avoid bleed through. AlexaFluor₄₈₈ was excited using the 488 nm Ar laser line, AlexaFluor₅₄₆ and RFP were excited using the 543 nm HeNe laser line, and DiD was excited using the 633 nm HeNe laser line. All images were recorded in the linear range, avoiding local saturation, and at an image resolution of 1024x1024 pixels and with pinhole size of 1 Airy unit. A series of xyz-scans with a 0.3 μm step size were taken along the z-axis from top to bottom of the cells. Presented images show a single z-scan or maximum intensity projection of all z-scans from a single series as indicated. Images were analyzed and processed using Leica Confocal Software V2.61 and ImageJ V1.45s.

Gene expression analysis by RT-qPCR

For gene expression analysis, HUVEC and HAEC were seeded in 24-well plates. After 2 h of activation with TNF- α (10 ng/ml), anti-E-selectin or anti-VCAM-1 SAINT-O-Somes containing VE-cadherin specific siRNA or control siRNA were added to the cells at 1 μM siRNA concentration, and incubated for 48 h. TNF- α was present in the medium during the entire incubation period. After 48 h total RNA was isolated using the RNeasy® Mini Plus Kit (Qiagen, Venlo, The Netherlands) according to the protocol of the manufacturer. The amount of RNA was measured by a NanoDrop® ND-1000 Spectrophotometer (Wilmington, DE) and qualitative gel electrophoresis consistently showed intact RNA integrity. cDNA synthesis and quantitative (q) PCR, including data analysis, were performed as described previously [19]. The real-time PCR primers for human VE-cadherin (Hs00174344_m1) and GAPDH (Hs99999905_m1) were purchased as Assay-on-Demand from Applied Biosystems (Nieuwekerk a/d IJssel, The Netherlands). Gene expression levels were normalized to the expression of the reference gene GAPDH and compared to cells treated only with TNF- α .



Protein expression analysis by Western blot and ELISA

HUVEC and HAEC were seeded in 6-well plates and after 2 h of activation with TNF- α (10 ng/ml), anti-E-selectin or anti-VCAM-1 SAINT-O-Somes containing VE-cadherin specific siRNA or control siRNA were added to the cells at 1 μ M siRNA concentration. After 48 h of incubation cells were lysed using RIPA buffer (Sigma-Aldrich, Zwijndrecht, The Netherlands) and lysates were used for Western blot and ELISA. Western blot analysis was performed as described previously [24], with slight modifications. The membrane was horizontally cut through the 70 kDa pre-stained marker and the upper part of the blot was incubated overnight at 4 °C with polyclonal rabbit anti-human VE-cadherin antibody (cat No. #2158, Cell Signaling Technology, Inc, Leiden, The Netherlands). For loading control the lower part of the blot was incubated for 1 h at RT with monoclonal mouse anti-human GAPDH antibody (cat No. #mAbcam 9484, Abcam, Cambridge, UK). Antibody binding was visualized by horseradish peroxidase-conjugated anti-rabbit IgG (cat No. #7074, Cell Signaling Technology, Inc, Leiden, The Netherlands) and anti-mouse IgG H+L (cat No. 1010-05 Southern Biotech, Birmingham, AL, USA). Chemiluminescence (Thermo Scientific, Rockford, IL, USA) signals were quantified by densitometric analysis using Quantity One software (Bio-Rad, Hercules, CA, USA). Protein expression from at least three independent experiments was quantified using DuoSet[®] IC Human Total VE-cadherin ELISA (R&D Systems, Abingdon, UK), according to the manufacturer's protocol.

*Investigation of cellular toxicity by MTS assay*

To investigate the influence of anti-E-selectin and anti-VCAM-1 siRNA SAINT-O-Somes on cell viability, HUVEC and HAEC were seeded in 96-well plates. Incubations with TNF- α and liposomes were performed as described for gene and protein expression analysis. After 48 h cells were washed twice with PBS followed by addition of 100 μ l fresh culture medium and 20 μ l CellTiter 96[®] AQ_{ueous} One Solution reagent (Promega, Leiden, The Netherlands). After 1.5 h, the absorbance at 490 nm was recorded with a Varioskan Flash Multimode reader (Thermo Scientific, Breda, The Netherlands). Absorbance of the activated endothelial cells without addition of SAINT-O-Somes was considered 100%.

Pharmacokinetics of (siRNA) SAINT-O-Somes

Male C57bl/6OlaHsd mice (18-23 g) were purchased from Harlan (Zeist, The Netherlands) and randomly divided into experimental groups. To induce an acute systemic inflammation mice were i.v. injected with 0.2 mg of recombinant mouse TNF- α (mrTNF- α ; Gibco, Camarilo, CA, USA) in 0.9% NaCl, 2 h prior to injection of liposomes. Subsequently, animals received i.v. a single dose (10 mmol TL/kg, 3 mice/group) of [³H]Cholesteryl Hexadecyl Ether (PerkinElmer, Shelton, CT, USA)

labeled SAINT-O-Somes, empty or containing control siRNA. Blood was sampled at 10 min, 30 min, 1 h, 6 h, and 24 h. ^3H radioactivity was measured using a Packard Tri-Carb 2500 TR liquid scintillation analyzer (PerkinElmer Life And Analytical Sciences, Waltham, MA). The total amount of radioactivity in the serum, separated from the blood by centrifugation, was calculated as described previously [21]. Pharmacokinetic parameters were calculated according to population analysis using the Interactive Two-Stage Bayesian program [25]. All animal experiments were performed according to national guidelines and upon approval of the local Animal Care and Use Committee of Groningen University.

Statistical analysis

Statistical analysis of the results was performed by a two-tailed unpaired Student's t-test, assuming equal variances to compare two replicate means, or One-Way ANOVA followed by Bonferroni post-hoc analysis to compare multiple replicate means. Differences were considered significant when $P < 0.05$.

Results

Preparation and characterization of SAINT-O-Somes loaded with siRNA

In the present study we formulated SAINT-O-Somes containing 18 mol% of SAINT-C18 and investigated their potential for effective siRNA delivery into activated primary endothelial cells. The physicochemical properties of SAINT-O-Somes loaded with siRNA are given in Table 1. Using cryo-EM microscopy we demonstrated that siRNA SAINT-O-Somes mainly consist of liposomes. Additionally, disk-like micelles were observed in the population (Fig. 1A), the formation of which could have been induced by the presence of DSPE-PEG₂₀₀₀ >4 mol% TL in the liposome formulation as described by Johnsson et al. [26, 27]. However, based on volume-weighted Gaussian distribution (data not shown) and the presented cryo-EM images, disc-like micelles comprises minor proportion (< 10 %) of siRNA SAINT-O-Somes preparation. The average liposome size defined by DLS method was 106 nm with corresponding polydispersity index of 0.17 which according to multiple sources [28, 29] is considered acceptable for the sample to be homogenous and monodisperse. siRNA SAINT-O-Somes showed good size stability in the presence of 50 % serum and 37 °C (Fig. 1B). Surface charge of targeted SAINT-O-Somes was neutral and particles displayed a siRNA encapsulation efficiency of $71\% \pm 15$ (Table 1). Based on the Ribogreen measurements we estimated that additional 5-6% of siRNA was electrostatically attached to the surface of liposomes. To investigate whether encapsulation into SAINT-O-Somes protects siRNA against RNases, we incubated particles with 50% human serum at 37 °C (Fig. 1C). Nonencapsulated siRNA was entirely degraded in serum



Table 1. Physicochemical properties of siRNA containing SAINT-O-Somes.

Formulation				
POPC : SAINT : Chol : DSPE-PEG : DSPE-PEG-Mal				
37 : 18 : 40 : 4 : 1				
Size	Polydispersity	Zeta Potential	Ab conjugated	siRNA encapsulation
[nm]	Index	[mV]	mol/liposome	efficiency (%)
106 ± 48	0.17 ± 0,03	3.8 ± 5	24 ± 5	71 ± 15

Data are presented as means of 8 preparations ± SD. Ab, average amount for anti-E-selectin or anti-VCAM-1 antibody conjugated to liposome.

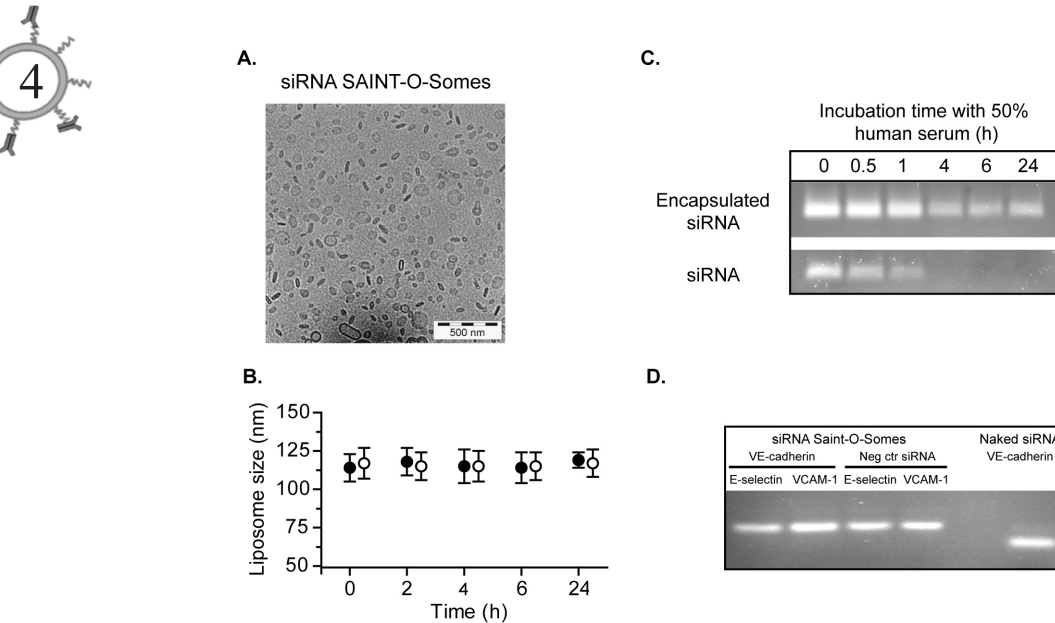


Figure 1. Characterization of siRNA containing SAINT-O-Somes. (A) Cryo-EM images of siRNA containing SAINT-O-Somes; (B) Size stability of siRNA SAINT-O-Somes in (●) presence or (○) absence of 50% serum. Particles were incubated for 2, 4, 6 and 24 h at 37 °C in HN buffer pH 7.4 or in 50% human serum. Data are presented as diameter (nm) ±SD of 3 preparations; Maintenance of siRNA integrity by encapsulation in SAINT-O-Somes was studied by comparison of equal amounts of nonencapsulated and encapsulated siRNA incubated in 50% human serum for 0.5, 1, 4, 6 and 24 h at 37 °C. (C) Agarose gel electrophoresis of nonencapsulated and encapsulated siRNA. (D) Agarose gel electrophoresis of siRNA encapsulated in anti-E-selectin respectively anti-VCAM-1 antibody conjugated SAINT-O-Somes that were stored for 8 weeks at 4 °C, intact naked VE-cadherin siRNA was used a control.

within 4 h, whereas formulation into SAINT-O-Somes preserved the integrity of siRNA for 24 h. Moreover, we demonstrated that SAINT-O-Somes could be stored for at least 8 weeks at 4 °C in HN buffer without loss of siRNA integrity (Fig. 1D) and without change of the particle size (data not shown).

To demonstrate feasibility of SAINT-O-Somes for in vivo administration, we investigated the pharmacokinetic behavior of i.v. injected SAINT-O-Somes both empty and loaded with siRNA. Plasma concentration of the particles showed two-phase clearance kinetic with a short initial half-life ranging from 9-12 min and a secondary half-life of > 11 h (Fig. S1 and Table 2). siRNA SAINT-O-Somes showed longer circulation time than empty SAINT-O-Somes, as indicated by longer secondary half-life and significantly lower plasma clearance and steady state volume of distribution. Coupling of antibody to siRNA SAINT-O-Somes resulted in significantly prolonged secondary half-life from approximately 12 to 17 h and lower plasma clearance.

SAINT-O-Somes targeted to VCAM-1 and E-selectin specifically deliver siRNA into TNF-α activated primary endothelial cells

To achieve specific delivery of siRNA to activated endothelial cells we conjugated SAINT-O-Somes with antibodies directed against E-selectin or VCAM-1. Primary HUVEC and HAEC were used to investigate specificity and efficacy of siRNA delivery. Cells were activated with TNF-α and incubated with targeted SAINT-O-Somes containing fluorescently labeled siRNA. As compared to resting cells, anti-E-selectin and anti-VCAM-1 SAINT-O-Somes showed a 35-fold increase in association (binding and uptake) of siRNA with activated HUVEC and a 25-fold increase with activated HAEC (Fig. 2A, B). HUVEC and HAEC exhibited the highest association with anti-VCAM-1 SAINT-O-Somes after 24 h and comparable association between 4 and 24 h with anti-E-selectin SAINT-O-Somes, which corroborated the protein



Table 2. Pharmacokinetic parameters of siRNA SAINT-O-Somes.

Parameter	SAINT-O-Somes		
	empty	siRNA	siRNA + Ab
C _L , ml/h	2.87 ± 0.07	2.02 ± 0.11*	1.36 ± 0.04#
V _{ss} , ml/g	32.65 ± 0.53	25.92 ± 1.39*	26.09 ± 0.55
t _{1/2} (1), h	0.15 ± 0.01	0.21 ± 0.02	0.21 ± 0.02
t _{1/2} (2), h	11.33 ± 0.06	11.72 ± 0.01*	17.36 ± 1.67#

Data are presented as means values ± SD of 3 mice/group. CL, plasma clearance; V_{ss}, steady-state volume of distribution; t_{1/2} (1), initial half-life; t_{1/2} (2), secondary half-life. * P < 0.05 empty vs siRNA, # P < 0.05 siRNA vs siRNA + Ab (antibody)

expression kinetics of both adhesion molecules (data not shown). In HUVEC, SAINT-O-Somes targeted to E-selectin or VCAM-1 showed comparable siRNA delivery, whereas in HAEC 50% more siRNA was delivered after 24 h by anti-VCAM-1 than by anti-E-selectin SAINT-O-Somes. To prove that association of siRNA in activated endothelial cells was mediated by E-selectin and VCAM-1, we co-incubated cells with an excess of antibodies against both target proteins. This led to a significant decrease in

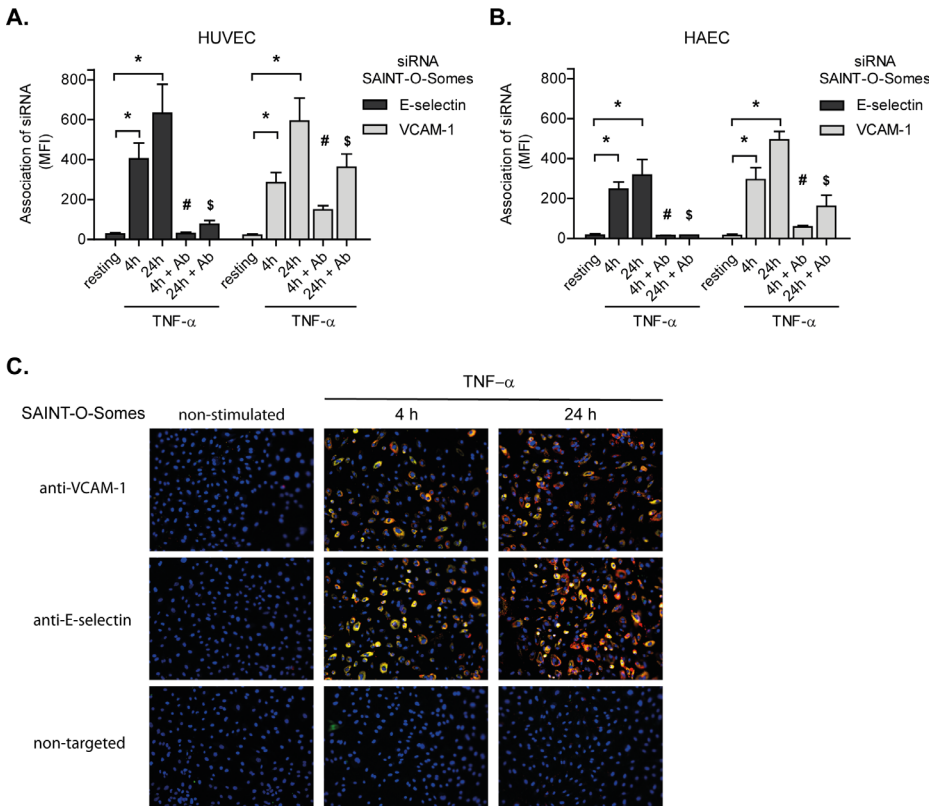


Figure 2. Selective delivery of siRNA to activated primary endothelial cells by targeted SAINT-O-Somes. Quiescent and TNF- α activated (A) HUVEC and (B) HAEC were incubated for 4 or 24 h with anti-E-selectin and anti-VCAM-1 SAINT-O-Somes containing AlexaFluor488 siRNA. Specificity of association to E-selectin respectively VCAM-1, was determined by co-incubation with 75 times excess of anti-E-selectin or anti-VCAM-1 monoclonal antibodies together with the liposomes. The association of siRNA with the cells was quantified by flow cytometric analysis. Data are presented as mean fluorescence intensity (MFI) values \pm SD of three independent experiments. * $P < 0.05$, # $P < 0.05$ - 4h vs 4h + Ab, \$ $P < 0.05$ - 24h vs 24h + Ab. (C) Fluorescence microscopy images of the uptake of targeted and non-targeted SAINT-O-Somes by cultured HUVEC. The liposome membrane was labeled with DiI (red) and encapsulated siRNA was labeled with AlexaFluor488 (green), the nuclei of the cells were stained using Hoechst (blue). The presented data set shows representative images, presented as merged pictures, of three independent experiments. Original magnification 100x.

the siRNA association with the activated cells (Fig. 2A, B). Additionally, in the absence of targeting antibody on the surface of SAINT-O-Somes no association of siRNA was observed either in resting or in activated cells (Fig. 2C and S2. A, B). The uptake of targeted SAINT-O-Somes by activated endothelial cells was confirmed by fluorescence microscopy using DiI (red) labeled liposomes containing fluorescent siRNA (green) (Fig. 2C). The two labels co-localized, indicating uptake of siRNA in conjunction with the carrier.

Intracellular trafficking of anti-VCAM-1 and anti-E-selectin SAINT-O-Somes in endothelial cells

Uptake and intracellular trafficking of the anti-E-selectin and anti-VCAM-1 SAINT-O-Somes loaded with labeled siRNA in TNF- α activated HUVEC was investigated using CLSM. AlexaFluor₅₄₆ siRNA (red) encapsulated in SAINT-O-Somes was binding to the surface of activated HUVEC at 4 °C (Fig. 3A a1, a5) and was internalized at 37 °C (Fig. 3A a2-a4, a6-a8). siRNA SAINT-O-Somes endocytosed via E-selectin and VCAM-1 localized in acidic compartments (late endosomes/lysosomes) within 4 h after start of the incubation with the cells (Fig. 3B, C), as demonstrated by co-localization with LysoTracker (Fig. 3B) or lysosomally expressed Lamp-1-RFP (Fig. 3C). By tracking simultaneously labeled SAINT-O-Somes and the encapsulated siRNA we demonstrated co-localization of the two labels after 4 h and partial dissociation of the siRNA label from the lipid label after 24 h (Fig. S3).

Anti-VCAM-1 and anti-E-selectin SAINT-O-Somes can effectively downregulate target genes in primary endothelial cells

Using anti-E-selectin or anti-VCAM-1 siRNA SAINT-O-Somes we aimed to knock down a gene that is expressed in the endothelial cells and would pose a model for studying the effects of the targeted system. VE-cadherin is an endothelial gene regulating formation of adherent cell junctions [30, 31], the expression of which is restricted to endothelial cells and maintained under TNF- α stimulation (Suppl. Table 1), making it a suitable target gene for this study. TNF- α activated HUVEC and HAEC were incubated for 48 h with SAINT-O-Somes containing VE-cadherin specific siRNA (VE) or control siRNA at 1 μ M concentration. SAINT-O-Somes loaded with VE-cadherin specific siRNA caused up to 60% downregulation of VE-cadherin mRNA in both HUVEC and HAEC, while uncoupled SAINT-O-Somes (data not shown) and SAINT-O-Somes containing control siRNA were devoid of an effect (Fig. 4A, B). Moreover, VE-cadherin downregulation did not alter the expression of the unrelated endothelial genes CD31 or Tie2 in both HUVEC and HAEC (Fig. S4A-D). Furthermore, reduction in VE-cadherin mRNA resulted in up to 50% decrease in protein expression in HUVEC and 25 % in HAEC, as quantified by ELISA (Fig. 4C, D), while no effects were observed with



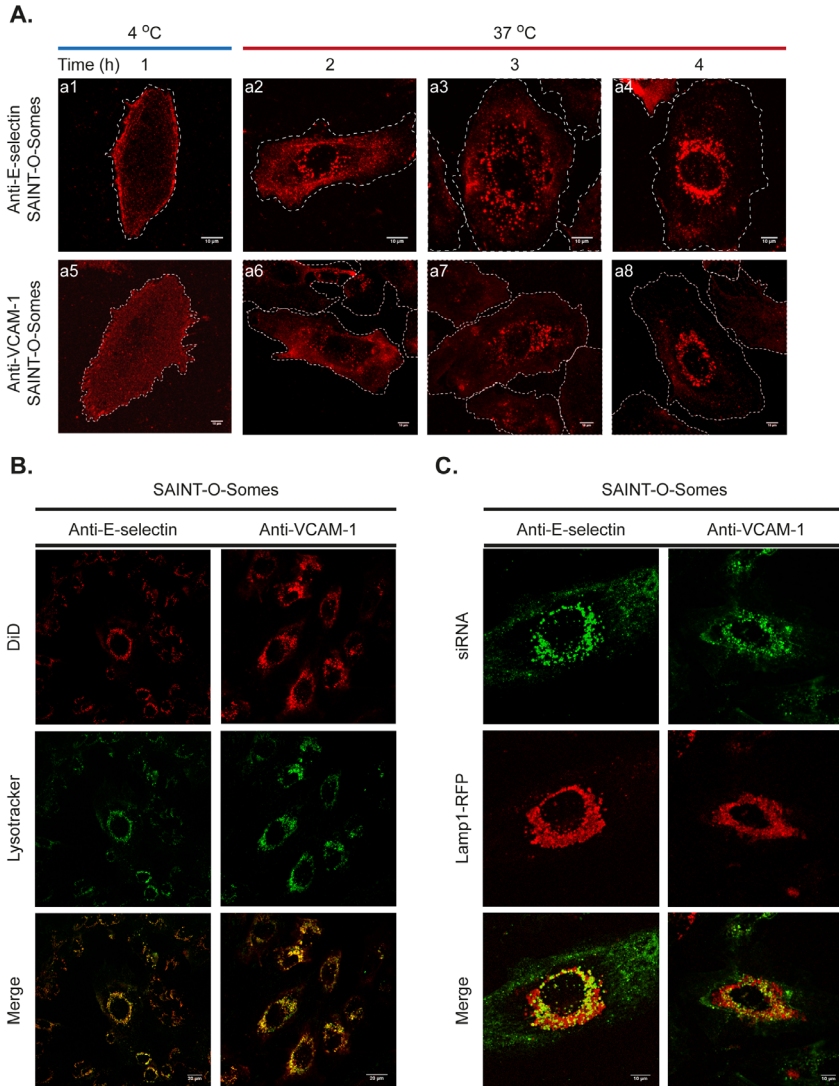


Figure 3. Anti-E-selectin and anti-VCAM-1 targeted SAINT-O-Somes loaded with siRNA are directed to endolysosomal compartments. (A) Encapsulated siRNA labeled with AlexaFluor546 (red) internalized via E-selectin or VCAM-1 displayed perinuclear localization in vesicular structures within 4 h after addition of liposomes (a1-a8). After addition of liposomes, cells were kept at 4 oC to allow binding but inhibit formation of endocytic vesicles (a1, a5). Borders of the cells (white dotted lines) were drawn based on differential interference contrast (DIC) images. Images of the cells were taken using CLSM and are presented as a merge of x-y-z scans using maximum intensity projection; Co-localization of SAINT-O-Somes and siRNA with acidic compartments (late endosomes/lysosomes) in activated HUVEC was demonstrated using (B) LysoTracker. After 4 h of incubation with targeted SAINT-O-Somes labeled with DiD (liposome membrane, red), LysoTracker (green) was added to the cells for 20 min. (C) Co-localization with late endolysosomal compartments was shown using cells transected with a plasmid expressing Lamp-1-RFP protein (red) prior to the experiment as described in 'Experimental Section'. After 4 h of incubation with targeted SAINT-O-Somes containing AlexaFluor488 labeled siRNA (green), cells were visualized using CLSM and are presented as single z-scans. Presented data set show representative images of tree independent experiments.

targeted SAINT-O-Somes containing control siRNA. Specific downregulation of VE-cadherin protein was also confirmed using Western Blot (Fig. 4E, F).

The possibility that targeted siRNA SAINT-O-Somes influence VE-cadherin expression by exerting a toxic effect on the cells was excluded by their negligible effect on endothelial cell viability (Fig. 5A, B). TNF- α activated HUVEC and HAEC were incubated for 48 h with SAINT-O-Somes containing VE-cadherin or control siRNA at 1 μ M concentration. Little or no decrease in cell viability was observed either in cells treated with SAINT-O-Somes containing VE-cadherin specific siRNA or in groups incubated with SAINT-O-Somes loaded with control siRNA.

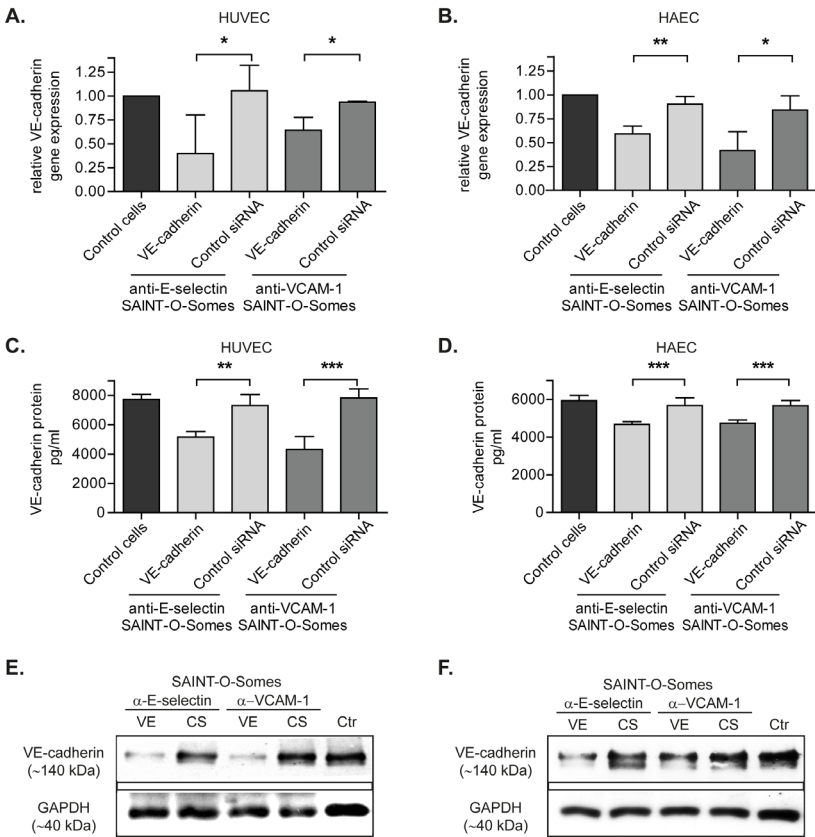


Figure 4. Effective downregulation of VE-cadherin in primary endothelial cells via targeted SAINT-O-Somes siRNA delivery. TNF- α activated HUVEC and HAEC were incubated with targeted SAINT-O-Somes containing VE-cadherin (VE) or control siRNA (CS) at 1 μ M concentration for 48 h. After incubation, RNA or cell lysates were used for RT-qPCR (A,B) respectively ELISA (C,D) and Western blot (E,F) as described in 'Experimental Section'. (A-B) Data are presented as relative expression \pm SD, compared to cells treated only with TNF- α (Ctr), of a minimum of three independent experiments. * $P < 0.05$. (C-D) Data are presented as VE-cadherin protein expression \pm SD of three independent experiments. (E-F) Images show a representative Western Blot.



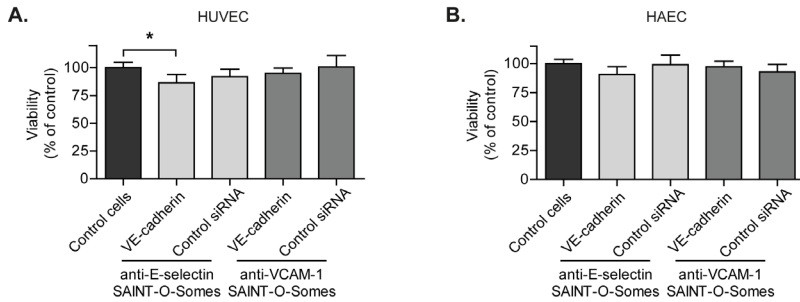


Figure 5. Targeted SAINT-O-Somes delivered siRNA do not affect cell viability. *TNF- α* activated HUVEC (A) and HAEC (B) were incubated with targeted SAINT-O-Somes containing VE-cadherin or control siRNA at 1 μ M concentration for 48 h. After the incubation viability of cells was investigated using CellTiter 96® AQueous One Solution reagent as described in 'Experimental Section'. Viability of activated endothelial cells without addition of SAINT-O-Somes was considered 100%. Data are presented as mean values \pm SD of three independent experiments. * $P < 0.05$.

Discussion

Inflamed endothelial cells play a significant role in the pathology of cancer and inflammatory diseases and present an accessible target for systemically applied drug carriers [13]. As such, development of siRNA delivery devices for pharmacological intervention at the level of inflamed or angiogenic endothelium holds clinical potential. Development of a carrier which selectively delivers siRNA into endothelial cells at the site of inflammation or angiogenesis can enhance pharmacological efficacy and limit possible side effects of the treatment. In the current work we demonstrated that, by using SAINT-C18 based liposomes (SAINT-O-Somes) surface-modified with antibodies specific for the inflammatory adhesion molecules E-selectin or VCAM-1, we were able to selectively deliver siRNA into activated primary endothelial cells. We found that E-selectin and VCAM-1 mediated internalization guided SAINT-O-Somes to endolysosomal compartments and allowed the release of the encapsulated siRNA. Targeted SAINT-O-Somes containing VE-cadherin specific siRNA showed significant downregulation of both the target gene mRNA and protein without exerting cellular toxicity. Furthermore, we demonstrated that the physicochemical properties and in vivo pharmacokinetic behavior of SAINT-O-Somes renders them suitable for in vivo delivery of siRNA. From this study we conclude that anti-E-selectin and anti-VCAM-1 SAINT-O-Somes have the features that allows specific and effective delivery of siRNA to inflamed endothelial cells in vivo, which justifies further in vivo studies on the use of siRNA SAINT-O-Somes to interfere with inflammatory diseases.

SAINT-O-Somes formulated with siRNA and 18 mol% of SAINT-C18 in the liposomal bilayer form small and unilamellar particles. Reported disc-like micelles are not expected to contribute significantly to the physicochemical properties and

findings reported in this manuscript since they comprise <10% of siRNA SAINT-O-Some preparation, that with a polydispersity index of 0.17 is considered homogenous and monodisperse. The here described SAINT-O-Somes are stable in the presence of serum and show siRNA encapsulation efficiency of 71%, that is high compared to other liposomal delivery platforms incorporating cationic lipids [32, 33]. Good stability and encapsulation efficiency are crucial features of *in vivo* siRNA delivery systems. For example, lipoplex formulations can reach > 90% siRNA entrapment efficiency [34], but their limited stability under physiological conditions restricts *in vivo* application [35]. Our results indicated that the integrity of siRNA encapsulated in SAINT-O-Somes is preserved under conditions that resemble the *in vivo* situation (presence of 50% serum and 37 °C) as well as upon long-term storage. We showed that i.v. injected SAINT-O-Somes display a two-phase PK with a long secondary half-life > 11 h, comparable to the PK behavior of conventional long circulating liposomes, that have been successfully used to target endothelial cells *in vivo* [18]. Encapsulation of siRNA significantly influenced the PK parameters and resulted in delayed clearance from the circulation. This could be explained by lower surface charge of SAINT-O-Somes containing negatively charged siRNA. Coupling of antibody to siRNA SAINT-O-Somes prolonged the circulation time from approximately 12 to 17 h. Combined, our results justify use of siRNA SAINT-O-Somes in a follow up *in vivo* studies in the future.

In the current study we focused on primary endothelial cells as they more closely represent endothelial cells *in vivo* than cell lines. Previous studies demonstrated that these cells are difficult to transfect [24] and show limited processing capabilities [19], which makes them a challenging target for our newly designed siRNA carrier. Recently, Whitehead et al. [36] demonstrated that in contrast to cell lines, primary cells were found to yield the most predictive correlations between *in vitro* – *in vivo* siRNA delivery efficacy of lipid nanoparticles. Taking into account the well-established heterogeneity of endothelial cells *in vivo* [37], we included primary cells from two distinct vascular beds in our investigation (HUVEC – venous, HAEC – arterial). Both VCAM-1 and E-selectin have been described as attractive targets for endothelial specific drug delivery [13], however use of VCAM-1 as a target for siRNA delivery to activated endothelial cells has not been demonstrated before. Here we compared association of siRNA encapsulated into E-selectin respectively VCAM-1 targeted SAINT-O-Somes with activated HUVEC and HAEC. We demonstrated that both anti-E-selectin and anti-VCAM-1 SAINT-O-Somes allowed robust and specific siRNA delivery into activated cells and showed comparable downregulation of VE-cadherin mRNA without exerting any cellular toxicity, as often seen with siRNA delivery systems containing cationic amphiphiles [38]. Up to 60% downregulation of VE-cadherin mRNA was reached in both cell types which was associated by 50% decrease in protein expression in HUVEC



and 25 % in HAEC (Fig. 4C-F). Sato et. al [6] demonstrated that 60% downregulation of a target gene mRNA and protein by siRNA-bearing liposomes targeted to hepatic stellate cells, was sufficient to almost completely resolve liver fibrosis and prolonged survival of cirrhotic rats. Thus, demonstrated capacity of targeted SAINT-O-Somes for gene silencing could be sufficient to interfere with the expression of disease-associated genes and requires further investigation in animal models. Differences in the efficacy of protein downregulation between HUVEC and HAEC in our study could not be attributed to differences in mRNA and protein expression levels (Table 2, supplementary data). Since HAEC and HUVEC exerted a similar extent of uptake of siRNA and siRNA delivered by the SAINT-O-Somes did not affect cell viability, possibly the ability of both cells to process SAINT-O-Somes influencing siRNA release is responsible for the observed differences. Moreover, the efficacy of the siRNA delivery can be affected by different molecular aspects that are part of the concept of heterogeneity of endothelial cells [39]. We demonstrated that anti-E-selectin and anti-VCAM-1 SAINT-O-Somes can effectively deliver siRNA to primary endothelial cells originating from different vascular beds, which provides an opportunity for effective targeting of disease-associated endothelial cell subsets in different vascular segments.

Target epitopes residing at the membrane of the target cells should internalize upon ligand binding and allow intracellular release of the siRNA, which is a prerequisite for effective gene downregulation. It was previously shown that both E-selectin and VCAM-1 could mediate internalization of immunoliposomes conjugated with antibodies targeting these proteins [15, 40]. Nevertheless little is known about the intracellular processing of siRNA delivered *via* this route. Therefore we studied the fate of anti-VCAM-1 and anti-E-selectin SAINT-O-Somes containing siRNA after binding to the endothelial cell surface applying confocal microscopy. siRNA endocytosed *via* E-selectin and VCAM-1 localized in endolysosomal compartments in the perinuclear region within 4 h after the start of incubation of cells with SAINT-O-Somes. Our observations are in line with findings describing transport of VCAM-1 and E-selectin ligands mainly *via* clathrin-mediated endocytosis to lysosomes (summarized by Muro et al. [41]) although involvement of other pathways, such as macropinocytosis or cell adhesion molecule endocytosis cannot be excluded. Adrian et al. [19] reported that at low pH (pH<5.5) the SAINT-O-Some bilayer is destabilized, which enhances content release. Within the endolysosomal compartments the low pH may thus be able to facilitate destabilization of the particles and enhance the release of siRNA. Furthermore, cationic lipids such as SAINT can destabilize the endosomal membrane by inducing ‘flipping’ of anionic lipids in the endosomal bilayer which facilitates release of the cargo into the cytoplasm [42]. Under physiological conditions a polyethylene-glycol (PEG) coating limits interaction of particles with the cell membrane by masking their surface charge [43]. Destabilization of SAINT-O-Some bilayer may reduce the effect



of PEG and allow SAINT to interact with the endosomal membrane. Moreover, we showed that SAINT-O-Somes and encapsulated siRNA followed the same route of internalization and partially dissociated after 24h, which indicates limited release of siRNA from the carrier. Up to now, little is known about the relation between siRNA disassembly from the carrier and the efficacy of gene silencing. The first tools to study intracellular disassembly of siRNA nanocomplexes have been developed only recently [44]. Poor processing of liposomes by HUVEC, as reported by Adrian et al. [19], may as well contribute to limited release of siRNA. Based on the intracellular trafficking of SAINT-O-Somes targeted to VCAM-1 and E-selectin, the inclusion of pH-sensitive components in the formulation (e.g. pH-sensitive PEG) might improve the efficacy of siRNA release [33, 45]. Further studies focusing on the exact siRNA release mechanism involving SAINT-O-Somes will shed more light and facilitate the rational design of these SAINT-based carriers.

We here report a liposomal formulation that allows selective and functional siRNA delivery into inflammation activated primary endothelial cells, mediates significant downregulation of a target gene, and is suitable for in vivo application based on their physicochemical and pharmacokinetic features. We demonstrated that both VCAM-1 and E-selectin can serve as an efficient and specific entry route for siRNA delivery to inflamed endothelial cells. Liposomes based on cationic amphiphile SAINT-C18 (SAINT-O-Somes) are a suitable carrier for siRNA and when harnessed with anti-VCAM-1 or anti-E-selectin antibodies allow effective delivery of siRNA to activated primary endothelial cells from venous and aortic vascular beds. anti-VCAM-1 and anti-E-selectin SAINT-O-Somes are thus a novel drug delivery system that provide an opportunity for siRNA delivery to disease-associated endothelial cell subsets in different vascular segments.

Acknowledgements

We thank Henk Moorlag, Peter J. Zwiers and Rianne M. Jongman for excellent technical assistance and Sabine Barnert from the Dept. of Pharmaceutical Technology and Biopharmacy (Albert-Ludwigs University, Freiburg) for her contribution to the cryo-TEM experiments. Dr. Ur Rehman Zia and Dr. Jan Willem Kok from the Dept. of Membrane Cell Biology (UMCG, Groningen) are acknowledged for kindly providing pLamp-1-RFP plasmid and assistance with confocal microscopy. We thank Dr. Ed Talman for providing high quality SAINT-C18 and prof. Gerrit L. Scherphof for editing and proofreading the article.

Microscopic fluorescence imaging was performed at the UMCG Microscopy & Imaging Center (UMIC), which is supported by the Netherlands Organization for Health Research and Development (ZonMW grant 40-00506-98-9021).



This work was supported by EFRO (European Fund for Regional Development) from the European Union, project NTS 068 and 073 Drug Delivery and Targeting. The authors declare no competing financial interests. M.H.J. Ruiters is CEO of Synvolux Therapeutics.


References

1. Y. Huang, J. Hong, S. Zheng, Y. Ding, S. Guo, H. Zhang, X. Zhang, Q. Du, Z. Liang, Elimination pathways of systemically delivered siRNA, *Mol Ther*, 19 (2011) 381-385.
2. R. Juliano, J. Bauman, H. Kang, X. Ming, Biological barriers to therapy with antisense and siRNA oligonucleotides, *Mol Pharm*, 6 (2009) 686-695.
3. K.A. Whitehead, R. Langer, D.G. Anderson, Knocking down barriers: advances in siRNA delivery, *Nat Rev Drug Discov*, 8 (2009) 129-138.
4. M.A. Behlke, Chemical modification of siRNAs for in vivo use, *Oligonucleotides*, 18 (2008) 305-319.
5. M. Frank-Kamenetsky, A. Grefhorst, N.N. Anderson, T.S. Racie, B. Bramlage, A. Akinc, D. Butler, K. Charisse, R. Dorkin, Y. Fan, C. Gamba-Vitalo, P. Hadwiger, M. Jayaraman, M. John, K.N. Jayaprakash, M. Maier, L. Nechev, K.G. Rajeev, T. Read, I. Rohl, J. Soutschek, P. Tan, J. Wong, G. Wang, T. Zimmermann, A. de Fougerolles, H.P. Vornlocher, R. Langer, D.G. Anderson, M. Manoharan, V. Kotliansky, J.D. Horton, K. Fitzgerald, Therapeutic RNAi targeting PCSK9 acutely lowers plasma cholesterol in rodents and LDL cholesterol in nonhuman primates, *Proc Natl Acad Sci U S A*, 105 (2008) 11915-11920.
6. Y. Sato, K. Murase, J. Kato, M. Kobune, T. Sato, Y. Kawano, R. Takimoto, K. Takada, K. Miyanishi, T. Matsunaga, T. Takayama, Y. Niitsu, Resolution of liver cirrhosis using vitamin A-coupled liposomes to deliver siRNA against a collagen-specific chaperone, *Nat Biotechnol*, 26 (2008) 431-442.
7. F. Takeshita, Y. Minakuchi, S. Nagahara, K. Honma, H. Sasaki, K. Hirai, T. Teratani, N. Namatame, Y. Yamamoto, K. Hanai, T. Kato, A. Sano, T. Ochiya, Efficient delivery of small interfering RNA to bone-metastatic tumors by using atelocollagen in vivo, *Proc Natl Acad Sci U S A*, 102 (2005) 12177-12182.
8. M.E. Davis, J.E. Zuckerman, C.H. Choi, D. Seligson, A. Tolcher, C.A. Alabi, Y. Yen, J.D. Heidel, A. Ribas, Evidence of RNAi in humans from systemically administered siRNA via targeted nanoparticles, *Nature*, 464 (2010) 1067-1070.
9. J.A.A.M. Kamps, G. Molema, Targeting Liposomes to Endothelial Cells in Inflammatory Diseases, in: G. Gregoriadis (Ed.) *Interactions of Liposomes with the Biological Milieu*, CRC press, 2007, pp. 127-150.
10. G. Molema, Targeted drug delivery to the tumor neovasculature: concepts, advances, and challenges, in: J. Folkman, W.D. Figg (Eds.) *Angiogenesis: an integrative approach from science to medicine* Cambridge University Press, 2008, pp. 283-297.
11. M. Aleku, P. Schulz, O. Keil, A. Santel, U. Schaeper, B. Dieckhoff, O. Janke, J. Endruschat, B. Durieux, N. Roder, K. Loffler, C. Lange, M. Fechtner, K. Mopert, G. Fisch, S. Dames, W. Arnold, K. Jochims, K. Giese, B. Wiedenmann, A. Scholz, J. Kaufmann, Atu027, a liposomal small interfering RNA formulation targeting protein kinase N3, inhibits cancer progression, *Cancer Res*, 68 (2008) 9788-9798.
12. A. Santel, M. Aleku, N. Roder, K. Mopert, B. Durieux, O. Janke, O. Keil, J. Endruschat, S. Dames, C. Lange, M. Eisermann, K. Loffler, M. Fechtner, G. Fisch, C. Vank, U. Schaeper, K. Giese, J. Kaufmann, Atu027 prevents pulmonary metastasis in experimental and spontaneous mouse metastasis models, *Clin Cancer Res*, 16 (2010) 5469-5480.
13. P.S. Kowalski, N.G. Leus, G.L. Scherphof, M.H. Ruiters, J.A. Kamps, G. Molema, Targeted siRNA delivery to diseased microvascular endothelial cells: cellular and molecular concepts, *IUBMB Life*, 63 (2011) 648-658.



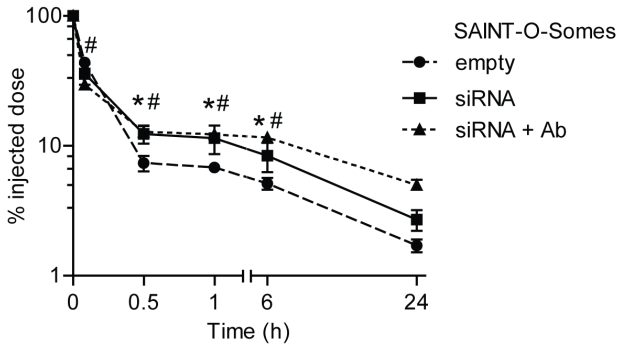
14. M. van Meurs, N.F. Kurniati, F.M. Wulfert, S.A. Asgeirsdottir, I.A. de Graaf, S.C. Satchell, P.W. Mathieson, R.M. Jongman, P. Kumpers, J.G. Zijlstra, P. Heeringa, G. Molema, Shock-induced stress induces loss of microvascular endothelial Tie2 in the kidney which is not associated with reduced glomerular barrier function, *Am J Physiol Renal Physiol*, 297 (2009) F272-281.
15. M. Everts, G.A. Koning, R.J. Kok, S.A. Asgeirsdottir, D. Vestweber, D.K. Meijer, G. Storm, G. Molema, In vitro cellular handling and in vivo targeting of E-selectin-directed immunoconjugates and immunoliposomes used for drug delivery to inflamed endothelium, *Pharm Res*, 20 (2003) 64-72.
16. M. van Meurs, F.M. Wulfert, A.J. Knol, A. De Haes, M. Houwertjes, L.P. Aarts, G. Molema, Early organ-specific endothelial activation during hemorrhagic shock and resuscitation, *Shock*, 29 (2008) 291-299.
17. I. Kim, S.O. Moon, S.H. Kim, H.J. Kim, Y.S. Koh, G.Y. Koh, Vascular endothelial growth factor expression of intercellular adhesion molecule 1 (ICAM-1), vascular cell adhesion molecule 1 (VCAM-1), and E-selectin through nuclear factor-kappa B activation in endothelial cells, *J Biol Chem*, 276 (2001) 7614-7620.
18. S.A. Asgeirsdottir, P.J. Zwiers, H.W. Morselt, H.E. Moorlag, H.I. Bakker, P. Heeringa, J.W. Kok, C.G. Kallenberg, G. Molema, J.A. Kamps, Inhibition of proinflammatory genes in anti-GBM glomerulonephritis by targeted dexamethasone-loaded AbEsel liposomes, *Am J Physiol Renal Physiol*, 294 (2008) F554-561.
19. J.E. Adrian, H.W. Morselt, R. Suss, S. Barnert, J.W. Kok, S.A. Asgeirsdottir, M.H. Ruiters, G. Molema, J.A. Kamps, Targeted SAINT-O-Somes for improved intracellular delivery of siRNA and cytotoxic drugs into endothelial cells, *J Control Release*, 144 (2010) 341-349.
20. S.A. Asgeirsdottir, J.A. Kamps, H.I. Bakker, P.J. Zwiers, P. Heeringa, K. van der Weide, H. van Goor, A.H. Petersen, H. Morselt, H.E. Moorlag, E. Steenbergen, C.G. Kallenberg, G. Molema, Site-specific inhibition of glomerulonephritis progression by targeted delivery of dexamethasone to glomerular endothelium, *Mol Pharmacol*, 72 (2007) 121-131.
21. J.A. Kamps, P.J. Swart, H.W. Morselt, R. Pauwels, M.P. De Bethune, E. De Clercq, D.K. Meijer, G.L. Scherphof, Preparation and characterization of conjugates of (modified) human serum albumin and liposomes: drug carriers with an intrinsic anti-HIV activity, *Biochim Biophys Acta*, 1278 (1996) 183-190.
22. Böttcher CJF, Van Gent CM, Pries C, A rapid and sensitive sub-micro phosphorus determination, *Anal. Chim. Acta*, 24 (1961).
23. J.E. Adrian, J.A. Kamps, G.L. Scherphof, D.K. Meijer, A.M. van Loenen-Weemes, C. Reker-Smit, P. Terpstra, K. Poelstra, A novel lipid-based drug carrier targeted to the non-parenchymal cells, including hepatic stellate cells, in the fibrotic livers of bile duct ligated rats, *Biochim Biophys Acta*, 1768 (2007) 1430-1439.
24. S.A. Asgeirsdottir, E.G. Talman, I.A. de Graaf, J.A. Kamps, S.C. Satchell, P.W. Mathieson, M.H. Ruiters, G. Molema, Targeted transfection increases siRNA uptake and gene silencing of primary endothelial cells in vitro--a quantitative study, *J Control Release*, 141 (2010) 241-251.
25. J.H. Proost, D.J. Eleveld, Performance of an iterative two-stage bayesian technique for population pharmacokinetic analysis of rich data sets, *Pharm Res*, 23 (2006) 2748-2759.
26. M. Johnsson, K. Edwards, Liposomes, disks, and spherical micelles: aggregate structure in mixtures of gel phase phosphatidylcholines and poly(ethylene glycol)-phospholipids, *Biophys J*, 85 (2003) 3839-3847.
27. E. Johansson, A. Lundquist, S. Zuo, K. Edwards, Nanosized bilayer disks: attractive model membranes for drug partition studies, *Biochim Biophys Acta*, 1768 (2007) 1518-1525.
28. J. Seguin, L. Brulle, R. Boyer, Y.M. Lu, M. Ramos Romano, Y.S. Touil, D. Scherman, M. Bessodes, N. Mignet, G.G. Chabot, Liposomal encapsulation of the natural flavonoid fisetin improves bioavailability and antitumor efficacy, *Int J Pharm*, 444 (2013) 146-154.
29. G. Smith, R. Raghunandan, Y. Wu, Y. Liu, M. Massare, M. Nathan, B. Zhou, H. Lu, S. Boddapati, J. Li, D. Flyer, G. Glenn, Respiratory syncytial virus fusion glycoprotein expressed in insect cells form protein nanoparticles that induce protective immunity in cotton rats, *PLoS One*, 7 (2012) e50852.



- 
30. E. Dejana, Endothelial cell-cell junctions: happy together, *Nat Rev Mol Cell Biol*, 5 (2004) 261-270.
 31. C.V. Crosby, P.A. Fleming, W.S. Argraves, M. Corada, L. Zanetta, E. Dejana, C.J. Drake, VE-cadherin is not required for the formation of nascent blood vessels but acts to prevent their disassembly, *Blood*, 105 (2005) 2771-2776.
 32. J.E. Adrian, A. Wolf, A. Steinbach, J. Rossler, R. Suss, Targeted delivery to neuroblastoma of novel siRNA-anti-GD2-liposomes prepared by dual asymmetric centrifugation and sterol-based post-insertion method, *Pharm Res*, 28 (2011) 2261-2272.
 33. D.T. Auguste, K. Furman, A. Wong, J. Fuller, S.P. Armes, T.J. Deming, R. Langer, Triggered release of siRNA from poly(ethylene glycol)-protected, pH-dependent liposomes, *J Control Release*, 130 (2008) 266-274.
 34. A. Singhania, S.Y. Wu, N.A. McMillan, Effective Delivery of PEGylated siRNA-Containing Lipoplexes to Extraperitoneal Tumours following Intraperitoneal Administration, *J Drug Deliv*, 2011 (2011) 192562.
 35. I.S. Zuhorn, W.H. Visser, U. Bakowsky, J.B. Engberts, D. Hoekstra, Interference of serum with lipoplex-cell interaction: modulation of intracellular processing, *Biochim Biophys Acta*, 1560 (2002) 25-36.
 36. K.A. Whitehead, J. Matthews, P.H. Chang, F. Niroui, J.R. Dorkin, M. Severgnini, D.G. Anderson, In vitro-in vivo translation of lipid nanoparticles for hepatocellular siRNA delivery, *ACS Nano*, 6 (2012) 6922-6929.
 37. G. Molema, Heterogeneity in endothelial responsiveness to cytokines, molecular causes, and pharmacological consequences, *Semin Thromb Hemost*, 36 (2010) 246-264.
 38. R.L. Kanasty, K.A. Whitehead, A.J. Vegas, D.G. Anderson, Action and reaction: the biological response to siRNA and its delivery vehicles, *Mol Ther*, 20 (2012) 513-524.
 39. E. Langenkamp, G. Molema, Microvascular endothelial cell heterogeneity: general concepts and pharmacological consequences for anti-angiogenic therapy of cancer, *Cell Tissue Res*, 335 (2009) 205-222.
 40. M. Voinea, I. Manduteanu, E. Dragomir, M. Capraru, M. Simionescu, Immunoliposomes directed toward VCAM-1 interact specifically with activated endothelial cells--a potential tool for specific drug delivery, *Pharm Res*, 22 (2005) 1906-1917.
 41. S. Muro, Challenges in design and characterization of ligand-targeted drug delivery systems, *J Control Release*, (2012).
 42. O. Zelphati, F.C. Szoka, Jr., Mechanism of oligonucleotide release from cationic liposomes, *Proc Natl Acad Sci U S A*, 93 (1996) 11493-11498.
 43. M. Morille, C. Passirani, A. Vonarbourg, A. Clavreul, J.P. Benoit, Progress in developing cationic vectors for non-viral systemic gene therapy against cancer, *Biomaterials*, 29 (2008) 3477-3496.
 44. C.A. Alabi, K.T. Love, G. Sahay, T. Stutzman, W.T. Young, R. Langer, D.G. Anderson, FRET-labeled siRNA probes for tracking assembly and disassembly of siRNA nanocomplexes, *ACS Nano*, 6 (2012) 6133-6141.
 45. S. Simoes, J.N. Moreira, C. Fonseca, N. Duzgunes, M.C. de Lima, On the formulation of pH-sensitive liposomes with long circulation times, *Adv Drug Deliv Rev*, 56 (2004) 947-965.

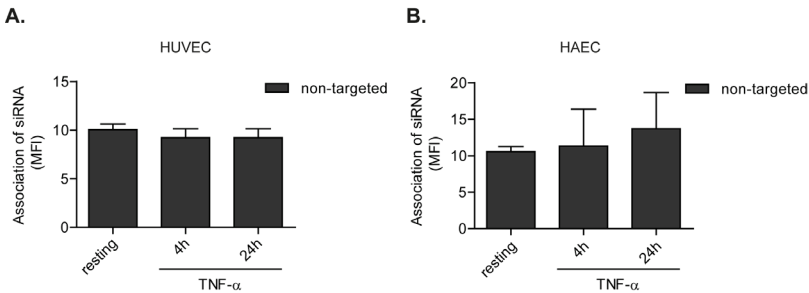
Supplementary data

Figure S1 showing blood clearance of empty and siRNA loaded SAINT-O-Somes. Figure S2 showing association of non-targeted SAINT-O-Somes with endothelial cells. Figure S3 showing CLSM images of intracellular co-localization of SAINT-O-Somes and siRNA in activated HUVEC. Figure S4 showing expression of endothelial genes CD31 and Tie-2 in HUVEC and HAEC after transfection with anti-E-selectin and anti VCAM-1 SAINT-O-Somes containing VE-cadherin specific or control siRNA. Supplementary Table 1 showing basal expression of VE-cadherin, CD31 and Tie-2 in resting or TNF- α activated cells. This information is available free of charge via the Internet at <http://pubs.acs.org/>.



S1. Blood clearance of empty and siRNA loaded SAINT-O-Somes.

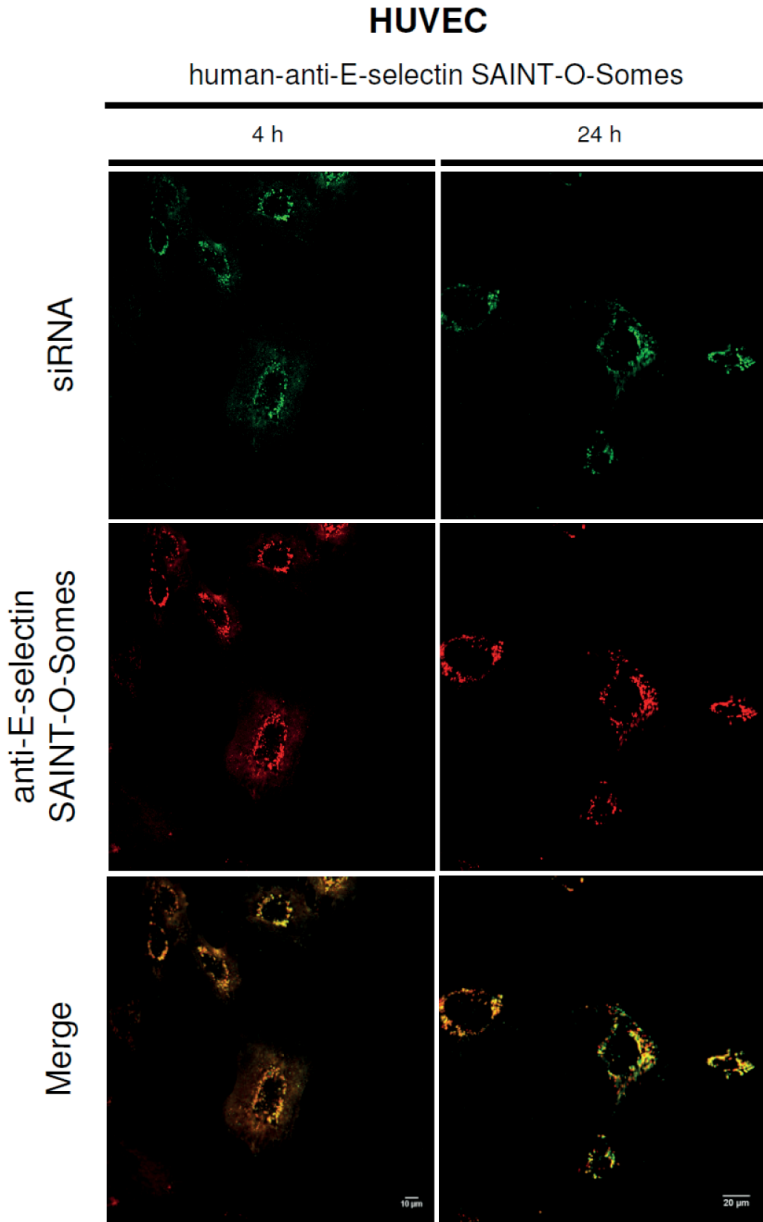
C57BL/6 mice were injected with 10 $\mu\text{mol}/\text{kg}$ of ^3H labeled SAINT-O-Somes, empty or containing siRNA. ^3H radioactivity was measured in the plasma to determine clearance kinetic. Data are presented as mean values \pm SD of 3 mice/group. * $P < 0.05$ empty vs siRNA; # $P < 0.05$ empty vs siRNA + Ab (antibody).



S2. Association of non-targeted SAINT-O-Somes with endothelial cells.

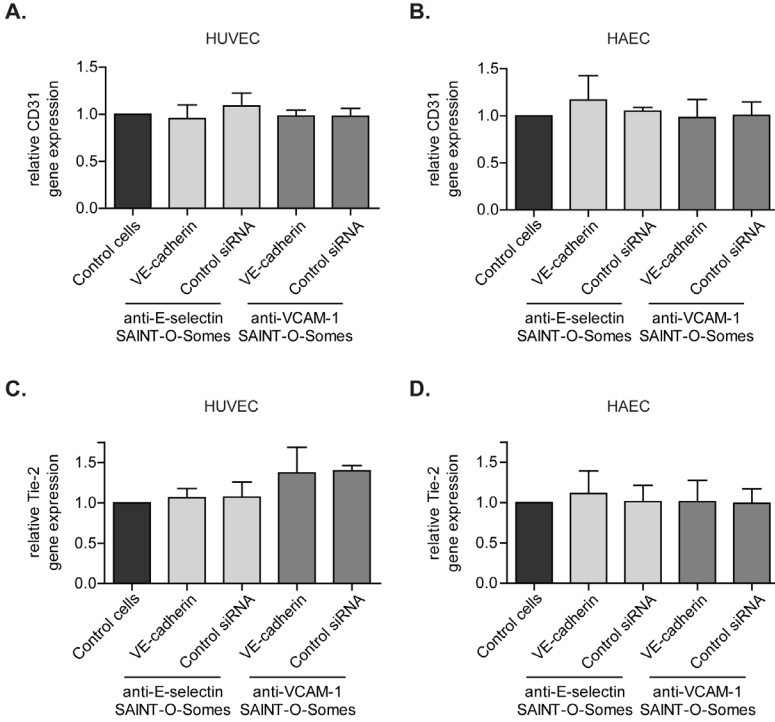
Activated and non-activated HUVEC (A) and HAEC (B) were incubated with SAINT-O-Somes containing AlexaFluor488 siRNA for 4 h or 24 h at a concentration of 80 nmol TL/ml. The association was quantified by flow cytometry as described in 'Experimental Section'. Data are presented as MFI (mean fluorescence intensity) values \pm SD of three independent experiments.





S3. SAINT-O-Somes and siRNA co-localize intracellularly in activated HUVEC.

Cells were activated with TNF- α for 2 h, and subsequently incubated for 4 or 24 h with an anti-E-selectin SAINT-O-Somes labeled with DiD (red) and containing AlexaFluor488 labeled siRNA (green). Cells were visualized live using CLSM. Presented data sets show representative single z-plane images of three independent experiments.



S4. Transfection of HUVEC and HAEC with siRNA specific VE-cadherin does not alter expression of unrelated endothelial genes (CD31 and Tie-2).

TNF- α activated HUVEC (A, C) and HAEC (B, D) incubated with targeted SAINT-O-Somes containing VE-cadherin or control siRNA at 1 μ M concentration for 48 h. After incubation, RNA was isolated from the cells for RT-qPCR as described in 'Experimental Section'. The real-time PCR primers for human CD31 (Hs00169777_m1) and Tie-2 (Hs00176096_m1) were purchased as Assay-on-Demand from Applied Biosystems. Data are presented as mean relative expression \pm SD, compared to cells treated only with TNF- α , of a minimum of three independent experiments. * $P < 0.05$.

Table 1. Basal expression of VE-cadherin, CD31 and Tie-2 in resting or TNF- α activated cells.

	VE-cadherin		CD31		Tie-2	
	- TNF- α	+ TNF- α	- TNF- α	+ TNF- α *	- TNF- α	+ TNF- α
HUVEC	0.37 \pm 0.02	0.39 \pm 0.01	0.23 \pm 0.02	0.17 \pm 0.04*	0.011 \pm 0.005	0.017 \pm 0.005
HAEC	0.11 \pm 0.01	0.12 \pm 0.03	0.07 \pm 0.02	0.05 \pm 0.02	0.010 \pm 0.003	0.019 \pm 0.006*

Basal gene expression levels relative to GAPDH

HUVEC and HAEC were incubated with or without TNF- α for 48 h. After incubation, RNA was isolated from the cells for RT-qPCR as described in 'Experimental Section'. Compared to CD31 and Tie-2, VE-cadherin is abundantly expressed in HUVEC and HAEC, and its expression was not affected by TNF- α stimulation. mRNA levels are presented as relative to GAPDH \pm SD of a minimum of three independent experiments.

* $P < 0.05$, - TNF- α vs. + TNF- α .



Chapter 5

Anti-VCAM-1 SAINT-O-Somes enable endothelial-specific delivery of siRNA and downregulation of inflammatory genes in activated endothelium in vivo

Piotr S. Kowalski¹, Peter J. Zwiers¹, Henriëtte W.M. Morselt¹, Joanna M. Kuldo¹, Niek G.J. Leus¹, Marcel H.J. Ruiters^{1,2}, Grietje Molema¹, Jan A.A.M. Kamps¹

J Control Release. 2014 Jan 3;176C:64-75.

¹ *University of Groningen, University Medical Center Groningen, Dept. of Pathology & Medical Biology, Medical Biology section, Laboratory for Endothelial Biomedicine & Vascular Drug Targeting research, Groningen, the Netherlands*

² *Synvolux Therapeutics, L.J. Zielstraweg 1, Groningen, the Netherlands*

Abstract

The pivotal role of endothelial cells in the pathology of inflammatory diseases raised interest in the development of short interfering RNA (siRNA) delivery devices for selective pharmacological intervention in the inflamed endothelium. The current study demonstrates endothelial specific delivery of siRNAs and downregulation of inflammatory genes in activated endothelium *in vivo*, applying a novel type of targeted liposomes based on the cationic amphiphile SAINT-C18 (1-methyl-4-(cis-9-dioleyl) methyl-pyridinium-chloride). To create specificity for inflamed endothelial cells, these so-called SAINT-O-Somes were harnessed with antibodies against vascular cell adhesion protein 1 (VCAM-1). In TNF α challenged mice, intravenously administered anti-VCAM-1 SAINT-O-Somes exerted long circulation times and homed to VCAM-1 expressing endothelial cells in inflamed organs. The formulations were devoid of liver and kidney toxicity. Using anti-VCAM-1 SAINT-O-Somes we successfully delivered siRNA to knock down VE-cadherin mRNA in inflamed renal microvasculature, as demonstrated by using laser microdissection of different microvascular beds prior to analysis of gene expression. Using the same strategy, we demonstrated local attenuation of endothelial inflammatory response towards lipopolysaccharide in kidneys of mice treated with anti-VCAM-1 SAINT-O-Somes containing NF κ B p65 specific siRNA. This study is a first demonstration of a novel, endothelial specific carrier that is suitable for selective *in vivo* delivery of siRNAs into inflamed microvascular segments and interference with disease associated endothelial activation.



Introduction

The interest to therapeutically target inflammatory processes is stirred by widespread devastating chronic diseases, including atherosclerosis, type 2 diabetes, and sepsis, that share a pathophysiologically important inflammatory component [1, 2]. Endothelium is an attractive target for anti-inflammatory therapy by virtue of its active engagement in the inflammatory process and its role in the pathophysiology of these (chronic) inflammatory diseases [3]. Activated endothelial cells at the site of inflammation play a central role in the recruitment of leukocytes from the blood primarily via the production of cytokines, chemokines and adhesion molecules [4]. Expression of these molecules is often triggered by pro-inflammatory cytokines such as tumor necrosis factor (TNF) α , interleukin (IL)-1b or bacterial endotoxins like lipopolysaccharide (LPS). This occurs mainly via activation of nuclear factor (NF) κ B and p38 mitogen-activated protein kinase (MAPK) signaling cascades, as shown for various inflammatory diseases [5-7].

Various pharmacological approaches to counteract (endothelial) cell activation are already applied in the clinic, tested in clinical trials, or are in preclinical development. These include corticosteroids, nonsteroidal anti-inflammatory drugs (NSAIDs), and inhibitors of NF κ B and p38 MAPK signaling (reviewed by Kuldo et al. [8]). Although existing therapies improve disease status, they often evoke adverse effects due to the lack of cellular and molecular specificity and carry a substantial risk of systemic toxicity [9]. New molecular drugs such as small interfering RNAs (siRNAs) offer high molecular specificity and potent gene silencing of disease associated genes [10]. The physicochemical properties of siRNAs demand their formulation into a delivery system that allows modification of the pharmacokinetic profile of the siRNA, reduces off-target toxicity, and improves the therapeutic index, thereby creating potent therapeutics [11, 12]. siRNA nano-carriers targeted to subsets of inflammatory leukocytes and monocytes have already shown their anti-inflammatory potential of gene silencing and their ability to attenuate disease progression in mouse models of intestinal inflammation [13], atherosclerosis, and myocardial infarction [14]. Development of siRNA based drug delivery approaches to inhibit endothelial activation in inflammation may create an additional translational avenue to therapeutically address inflammatory diseases and offer improvement over existing therapies. Attractive molecular targets for selective gene silencing in the endothelial cells are the members of the NF κ B and p38 MAPK family [6, 15] or enzymes generating reactive oxygen species (e.g. NADPH oxidase) [16], based on their inherent association with inflammatory activation of the endothelium.

Upon inflammatory stimulation, each organ displays a vascular bed specific pattern of cell adhesion molecules expression including E-selectin and vascular cell adhesion protein 1 (VCAM-1) [4], providing a challenging gateway to deliver small RNAs to



organ-specific (micro)vascular endothelial subsets [17]. To this end, we developed a new generation of liposomes called SAINT-O-Somes by combining cationic SAINT-C18 (1-methyl-4-(cis-9-dioleyl)methyl-pyridinium-chloride) amphiphile with conventional liposome technology, that showed superior intracellular release of their content in endothelial cells compared to conventional liposomes [18]. We furthermore recently demonstrated that SAINT-O-Somes targeted to VCAM-1 and E-selectin can selectively and functionally deliver siRNA into inflammation activated endothelial cells *in vitro*, and are suitable for *in vivo* application based on their physicochemical and pharmacokinetic features [19]. E-selectin has been previously applied as a molecular target to direct liposomes and viruses to glomerular endothelium in mouse kidney inflammatory disease [20, 21], but the data regarding the use of VCAM-1 as a target on inflamed endothelium *in vivo* are scarce [22].

In the current study we aimed to show that anti-VCAM-1 ($\text{Ab}_{\text{VCAM-1}}$) targeted SAINT-O-Somes carrying siRNA enable cell specific gene downregulation in inflamed endothelium *in vivo*. We studied the pharmacokinetic (PK) behavior, biodistribution, and *in vivo* toxicity of $\text{Ab}_{\text{VCAM-1}}$ SAINT-O-Somes in TNF α challenged mice. Focusing on kidneys as our organ of interest, we investigated the potential of $\text{Ab}_{\text{VCAM-1}}$ SAINT-O-Somes to deliver VE-cadherin and NF κ B p65 (RelA) specific siRNAs to the inflamed renal vasculature of those mice. Using SAINT-O-Somes containing RelA specific siRNA we demonstrated both *in vitro* and *in vivo* proof-of-concept of attenuation of an endothelial inflammatory response towards LPS by knocking down the signal transduction pathway, which is pivotal in endothelial cell activation. In addition, we provide new insights into the use of VCAM-1 as a target for drug delivery to inflamed endothelium *in vivo*. Taking all data together, we demonstrate here that $\text{Ab}_{\text{VCAM-1}}$ SAINT-O-Somes can be used for selective delivery of siRNA into inflamed microvascular endothelial cells *in vivo* to functionally interfere with disease associated endothelial activation.

Materials and methods

Materials

Lipids, 1-palmitoyl-2-oleoyl-sn-glycero-3-phosphocholine (POPC), 1,2-distearoyl-sn-glycero-3-phosphoethanolamine-N-[methoxy(polyethylene glycol)-2000]-maleimide (DSPE-PEG₂₀₀₀-Mal), and 2-distearoyl-sn-glycero-3-phosphoethanolamine-N [methoxy(polyethylene glycol)-2000] (DSPE-PEG₂₀₀₀) were purchased from Avanti Polar Lipids (Alabaster AL, USA). The cationic lipid 1-methyl-4-(cis-9-dioleyl)methyl-pyridinium-chloride (SAINT-C18) was obtained from Synvolux Therapeutics (Groningen, The Netherlands). Cholesterol (Chol) and N-succinimidyl-S-acetylthioacetate (SATA) were obtained from Sigma (St. Louis, MO, USA). Radioactive tracer [³H]Cho-



lesteryl Hexadecyl Ether [Cholesteryl-1,2-3H(N)] was purchased from PerkinElmer (Shelton, CT, USA). Nucleic acid stain DAPI was obtained from Roche Diagnostics (Manheim, Germany). Lipofectamine™ 2000 transfection reagent was purchased from Invitrogen (Breda, The Netherlands). All siRNAs were purchased from Qiagen (Venlo, The Netherlands).

The M/K-2.7 (rat IgG1a anti-mouse VCAM-1) producing hybridoma was obtained from American Type Culture Collection (ATCC, Manassas, VA, USA). Rat IgG antibody (irrelevant IgG) was purchased from Sigma-Aldrich (Zwijndrecht, The Netherlands).

Preparation of siRNA containing SAINT-O-Somes

SAINT-O-Somes were prepared as described previously with slight modifications [19]. In brief, lipids from stock solutions of POPC, SAINT-C18, Chol, DSPE-PEG₂₀₀₀ and DSPE-PEG₂₀₀₀-Mal in chloroform:methanol (9:1) were mixed in a molar ratio of 37:18:40:4:1. Radioactively labeled SAINT-O-Somes were prepared by adding a trace amount (2.5 mCi/μmol of total lipid) of [³H]Cholesteryl Hexadecyl Ether ([³H]CHE) to the formulation. SAINT-O-Somes were prepared containing siRNA specific for VE-cadherin (Mm_Cdh5_2 FlexiTube siRNA, target sequence 5'-AAGGATCAAGTCCAATCTAAA-3'), RelA (Hs_REL A_7 FlexiTube siRNA, 5'-CCGGATTGAGGAGAAACGTAA-3'; Mm_Rela_3 FlexiTube siRNA, 5'-CACCATCAAGATCAATGGCTA-3') or control siRNA (AllStars Negative Control, cat No. 1027281), with no homology to any known mammalian gene. VE-cadherin respectively RelA specific siRNAs used for the experiments were selected from a pool of four pre-designed siRNAs based on the specificity and efficacy of target gene downregulation. siRNA was dissolved according to the protocol of the manufacturer and mixed with dried lipids at a ratio of 1 nmol siRNA per 1 μmol total lipid (TL). After extrusion through polycarbonate filters (50 nm pore size) nonencapsulated siRNA was removed by ion exchange chromatography on a DEAE Sepharose CL-6B column (Sigma, The Netherlands) using HN buffer (135 mM NaCl, 10 mM HEPES) pH 6.7 as an eluent. The concentration of siRNA encapsulated in liposomes was measured using the Quant-iT™ Ribo-Green® assay (Invitrogen, Breda, The Netherlands) according to the protocol of the manufacturer. The efficiency of siRNA encapsulation into liposomes was calculated based on the measurements of encapsulated siRNA in the presence or absence of 1% (v/v) Triton X-100 (Sigma-Aldrich, Zwijndrecht, The Netherlands). The anti-VCAM-1 and irrelevant IgG antibodies were thiolated by means of SATA and coupled to a maleimide group at the distal end of the polyethylene glycol chain by sulfhydryl-maleimide coupling as described before for albumin [23]. SAINT-O-Somes without an antibody were prepared from the same lipid mixture, but instead of being conjugated to the antibody, they were allowed to react with cysteine in a molar ratio twice that of DSPE-PEG₂₀₀₀-Mal to block reactive maleimide groups. The



SAINT-O-Somes were characterized by determining the protein concentration using rat IgG as a standard and measuring the total lipid concentration by phosphorus assay [24]. Particle size and Zeta-potential were analyzed using a Nicomp model 380 ZLS submicron particle analyzer. Particle size was measured using dynamic light scattering (DLS) in the volume weighing mode (NICOMP particle sizing systems, Santa Barbara, CA, USA). The Polydispersity index (PDI) was analyzed using a Malvern Zetasizer Nano ZSP (Malvern Instruments Ltd., Worcestershire, UK). The number of antibody molecules coupled per liposome was calculated as described before [25]. SAINT-O-Somes were stored at 4 °C under argon gas and were used within 4 weeks.

Cell cultures

Human umbilical vein endothelial cells (HUVEC) were obtained from Lonza (Breda, The Netherlands). Cells were cultured in EBM-2 medium supplemented with EGM-2 MV SingleQuot Kit Supplements & Growth Factors (cat No. CC-3202, Lonza). In all experiments, cells from passage 5 to 7 were used. Cells were plated on culture plates (Costar, Corning, NY) at a density of 1.8×10^4 cells/cm² one day before the experiment unless stated differently. Before seeding the cells, culture plates were incubated with EGM2 MV medium for 30 min. Cell cultures were maintained by the Endothelial Cell Facility of UMCG.

Animals

Male C57bl/6OlaHsd mice (18-23 g) were purchased from Harlan (Zeist, The Netherlands) and randomly divided into experimental groups. Animals were group housed and maintained on a mouse chow diet, in a temperature and light-dark cycle controlled environment (24 °C, 12:12 h). All intravenous (i.v.) injections were performed in the orbital plexus under anesthesia (inhalation of isoflurane/O₂). To induce acute systemic inflammation mice received i.v. 0.2 µg recombinant mouse TNFα (rmTNFα; Gibco, Camarillo, CA, USA) in sterile 0.9% NaCl. For induction of endotoxemia, mice were intraperitoneally (i.p) injected with LPS (Escherichia coli, serotype 0.26:B6l; Sigma, St. Louis, MO, USA) in 0.9% NaCl at 1.5 mg/kg (450 EU/g). At the end of the experiment mice were sacrificed under anesthesia, blood was collected via heart puncture and organs were immediately snap frozen in liquid nitrogen or embedded in paraffin. Frozen organs were stored at -80 °C until analysis. All animal experiments were performed according to national guidelines and upon approval of the local Animal Care and Use Committee of Groningen University (DEC 6150B).

Pharmacokinetics and biodistribution of SAINT-O-Somes

2h prior to injection of liposomes, mice were challenged with rmTNFα. Subsequently, animals received i.v. a single dose (10 µmol TL/kg, 3 mice/group) of [³H]CHE-labeled



SAINT-O-Somes containing control siRNA (~ 0.12 mg siRNA/kg), conjugated with either anti-VCAM-1 or irrelevant IgG antibody (Ab_{VCAM-1} or IgG siRNA SAINT-O-Somes). Blood was sampled at 10 min, 30 min, 1 h, 6 h, and 24 h. At 24 h mice were sacrificed and liver, spleen, kidney, lungs, heart and brain were removed and processed for measurement of radioactivity as described previously [23]. 3H radioactivity was measured using a Packard Tri-Carb 2500 TR liquid scintillation analyzer (PerkinElmer Life And Analytical Sciences, Waltham, MA). The total amount of radioactivity in the serum was calculated as described previously [20]. Pharmacokinetic parameters were calculated according to population analysis and the Interactive Two-Stage Bayesian approach [26] using the Multifit program (Dr J.H. Proost, Department of Pharmacokinetics and Drug Delivery, University Center for Pharmacy, University of Groningen).

Immunohistochemical and immunofluorescent detection of VCAM-1 protein and localization of Ab_{VCAM-1} siRNA SAINT-O-Somes in mouse tissues

Tissue cryo-sections (5 μ m) were fixed in acetone for 10 min, non-specific binding was blocked by 1 h incubation with PBS containing 1% BSA (Bovine Serum Albumin; Sigma-Aldrich, Zwijndrecht, The Netherlands) and 2% FCS (Fetal Calf Serum; Thermo Scientific HyClone, Cramlington, UK). For detection of VCAM-1 protein tissues were incubated for 60 min with rat anti-mouse VCAM-1 antibody (10 μ g/ml) diluted in PBS/1% BSA supplemented with 2% FCS. Endogenous peroxidase activity was blocked using the EnVision kit (EnVision + System-HRP (AEC), DAKO, Carpinteria, CA, USA). Subsequently, sections were incubated for 30 min with rabbit anti-rat antibody (Vector Laboratories, Burlingame, CA, USA) at 10 μ g/ml in PBS supplemented with 5% normal mouse serum (NMS; DAKO). Detection was performed with anti-rabbit labeled polymer-HRP antibody from the EnVision kit. Peroxidase activity was detected with 3-amino-9-ethylcarbazole (AEC; DAKO) and sections were counterstained with Mayer's hematoxylin (Merck, Darmstadt, Germany). Isotype-matched controls were consistently found to be devoid of staining. Immunohistochemical detection of Ab_{VCAM-1} and IgG siRNA SAINT-O-Somes after i.v. administration was performed on the cryo-sections with rabbit anti-rat antibody (Vector) in PBS/5% NMS and using EnVision kit to detect peroxidase activity as described above.

Immunofluorescence double staining for immunoliposomes and CD31 was performed as previously described [20]. Endogenous biotin was blocked by a Biotin Blocking System (Dako, Glostrup, Denmark). Ab_{VCAM-1} and IgG siRNA liposomes were detected with AlexaFluor₅₄₆-conjugated goat anti-rat antibodies (1 h incubation, 20 μ g/ml PBS; Molecular Probes, Leiden, The Netherlands). CD31 was detected with biotin-labeled rat anti-mouse CD31 (clone 390, 5 μ g/ml PBS; eBioscience, San Diego, CA), followed by AlexaFluor₄₈₈-conjugated streptavidin (50 μ g/ml PBS Molecular Probes).



All incubation steps were carried out in the presence of 5% NMS. Sections were mounted with Citi-Fluor AF1 (Citifluor Ltd, London, UK) and examined using a confocal laser scanning microscope (CLSM) equipped with a true confocal scanner (TCS SP2-AOBS; Leica, Heidelberg, Germany) coupled to a LeicaDM RXE microscope with an HCXPL APO CS 63 x 1.40 oil immersion objective. Sequential scans were obtained to avoid bleed through. AlexaFluor₄₈₈ was excited using the 488 nm Ar laser line, AlexaFluor₅₄₆ was excited using the 543 nm HeNe laser line. All images were recorded in the linear range, avoiding local saturation, at an image resolution of 1024x1024 pixels and with pinhole size of 1 Airy unit. A series of xyz-scans with a 0.3 µm step size were taken along the z-axis from top to bottom of the tissue. Presented images show a single z-scan from a single series. Images were analyzed and processed using ImageJ V1.45s.

Investigation of NFκB p65 (RelA) downregulation in vitro

For downregulation of RelA using targeted siRNA SAINT-O-Somes, HUVEC were activated with 10 ng/ml TNFα (Boehringer, Ingelheim, Germany) for 6 h prior to addition of liposomes. Ab_{VCAM-1} SAINT-O-Somes containing RelA specific siRNA or control siRNA were added to the cells at 1 or 1.5 µM siRNA concentration, and incubated for 24 h. TNFα was present in the medium during the entire incubation period. Subsequently, cells were washed and cultured for an additional 24 h in the absence of TNFα. At the 48 h time point cells were re-challenged with LPS (1 µg/ml) for 4 h. Subsequently cells were washed twice with PBS and total RNA was isolated for gene expression analysis.

For protein analysis, HUVEC were seeded in 6-well plates, challenged with TNFα and incubated with Ab_{VCAM-1} siRNA SAINT-O-Somes as described above. After 48 h of incubation cells were lysed using RIPA buffer (Sigma-Aldrich, Zwijndrecht, The Netherlands) and lysates were used for Western blot performed as described previously [27], with slight modifications. The membrane was horizontally cut through the 50 kDa pre-stained marker and the upper part of the blot was incubated overnight at 4 °C with rabbit anti-RelA antibody (Cell Signaling Technology). For loading control the lower part of the blot was incubated overnight at 4 °C with rabbit anti-GAPDH antibody (cat No. sc-25778, Santa Cruz Biotechnology, Dallas, TX, USA). Antibody binding was visualized by horseradish peroxidase-conjugated anti-rabbit IgG (cat No. #7074, Cell Signaling Technology, Inc, Leiden, The Netherlands). Chemiluminescence (Thermo Scientific, Rockford, IL, USA) signals were quantified by densitometric analysis using Quantity One software (Bio-Rad, Hercules, CA, USA). A representative Western Blot of two independent experiments is presented.

For immunofluorescent staining of RelA, HUVEC were cultured on sterile cover glasses (Menzel-Gläser, Braunschweig, Germany) placed into the wells of a 12-well plate. Cells were challenged with TNFα and incubated with Ab_{VCAM-1} siRNA SAINT-O-



Somes as described above. After 48 h, cells were challenged LPS for 25 min and fixed with 1 % formaldehyde in PBS for 20 min. Subsequently, cells were permeabilized by 5 min incubation with 0.25% TritonX-100 in PBS, then blocked with PBS/3% BSA for 30 min at RT and later incubated with rabbit anti-RelA antibody (cat No. #8242, Cell Signaling Technology) diluted 1:50 in PBS/0.5 % BSA/0.05% Tween 20 (Sigma, St. Louis, MO, USA). Next, coverslips were washed with PBS and incubated for 1 h with 20 $\mu\text{g}/\text{ml}$ of AlexaFluor₄₈₈-conjugated goat anti-rabbit antibody (Molecular Probes, Eugene, Oregon, USA). At the end of the incubation, coverslips were washed with PBS and mounted using Aqua Poly/Mount medium (Polysciences, Warrington, PA, USA) containing DAPI, air dried for 24 h, and stored in the dark at 4 °C. Fluorescence images were taken with a Leica DM/RXA fluorescence microscope (Wetzlar, Germany) using Quantimet HR600 image analysis software (Leica). Images were taken at excitation/emission wavelengths 490/520 nm for AlexaFluor₄₈₈, and 350/460 nm for DAPI.

In vivo gene downregulation using anti-VCAM-1 siRNA SAINT-O-Somes

2 h prior to administration of SAINT-O-Somes mice were challenged with rmTNF α (treatment group; 3 mice/group), while untreated animals (n=3) received 0.9% NaCl. Subsequently, treatment groups received a single i.v. dose (50 $\mu\text{mol TL}/\text{kg}$) of Ab_{VCAM-1} SAINT-O-Somes containing either VE-cadherin specific siRNA (VE-cadherin group) or RelA specific siRNA (RelA group) at a dose of 0.6 mg siRNA/kg. Control mice were i.v. injected either with an equivalent dose of Ab_{VCAM-1} SAINT-O-Somes containing control siRNA or with sterile HN buffer pH 7.4 (vehicle). 48 h after injection of the liposomes, the VE-cadherin group and corresponding control groups were sacrificed, while the RelA group and corresponding control groups received an i.p. LPS challenge and were sacrificed 4 h later. Blood and organs were collected for further analysis.

Examination of liver and kidney toxicity

Toxicity parameters were measured in EDTA-treated plasma obtained from peripheral blood of rmTNF α challenged mice treated with targeted siRNA SAINT-O-Somes (50 $\mu\text{mol TL}/\text{kg}$, 0.6 mg siRNA/kg) and control mice. Liver toxicity was analyzed by determining levels of liver enzymes ALAT (alanine aminotransferase) and ALP (alkaline phosphatase), kidney toxicity by urea and creatinine measurements. All tests were performed with assays from Roche Diagnostics (Mannheim, Germany), and were measured using a Hitachi automatic analyzer (Modular Analytics, Roche diagnostics, Mannheim, Germany).

Laser dissection microscopy of renal microvascular segments

9 μm cryo-sections were mounted on 1.35 μm polyethylene-naphthalene membranes attached to normal 1-mm slides (P.A.L.M. Microlaser Technologies GmbH, Bernried,



Germany). Sections were fixed in a cold acetone, air-dried and stained with Mayer's hematoxylin. Stained sections were briefly washed with diethyl pyrocarbonate-treated tapwater, air-dried and stored at 4°C. Endothelial cells from arterioles (area $5 \times 10^5 \mu\text{m}^2$), postcapillary venules (area $1 \times 10^6 \mu\text{m}^2$), and glomeruli (area $1 \times 10^6 \mu\text{m}^2$) were dissected using the Leica LMD6500 Laser Microdissection System (Leica Microsystems, Wetzlar, Germany). Microdissected material was collected directly in AdhesiveCap 0.5 ml tubes (Carl Zeiss, Göttingen, Germany) and stored at -80 °C prior to RNA isolation.

Gene expression analysis by RT-qPCR

Total RNA from *in vitro* experiments was isolated using the RNeasy® Mini Plus Kit (Qiagen, Venlo, The Netherlands) and total RNA from laser microdissected material was isolated using RNeasy® Micro Plus Kit (Qiagen) according to manufacturer's protocols. The integrity of RNA isolated from whole tissue, LMD samples and cell culture material was analyzed by qualitative gel electrophoresis and was consistently found intact. cDNA synthesis and real-time PCR, including data analysis, were performed as described previously [18]. The real-time PCR primers (supplementary Table 1) were purchased as Assay-on-Demand from Applied Biosystems (Nieuwekerk a/d IJssel, The Netherlands). Gene expression levels were normalized to the expression of the reference gene glyceraldehyde-3-phosphate dehydrogenase (GAPDH), which was not influenced by the experimental conditions. Enrichment of the endothelial marker gene CD31 in the laser microdissected material as compared to the whole tissue was found to be consistent for each vascular compartment (enrichment in arterioles ~ 65 fold, glomeruli ~ 11 fold, venules ~ 3 fold).

Analysis of leukocyte attraction to kidney venules

Paraffin embedded mouse kidneys from the *in vivo* study in which $\text{Ab}_{\text{VCAM-1}} \text{siRNA}_{\text{RelA}}$ SAINT-O-Somes were administered as described above (paragraph 2.8) were used for immunohistochemical detection of CD45 positive cells. 5 μm paraffin sections were de-paraffinized and microwaved (300 W) for 15 min in citrate buffer (10 mM, pH 6) for antigen retrieval. Subsequently, endogenous peroxidase activity was blocked using the EnVision kit (DAKO) and sections were incubated for 1 h with 3.5 $\mu\text{g}/\text{ml}$ of rat anti-mouse CD45 antibody in PBS/1% BSA (cat No. #550539, BD Pharmingen, San Diego, CA, USA). Next sections were incubated with rabbit anti-rat antibody (Vector) in PBS/5% NMS for 30 min. Peroxidase activity was detected using the EnVision kit as described above. Sections were counterstained with Mayer's hematoxylin and slides were scanned using NanoZoomer (Hamamatsu Photonics, Higashi-ku, Hamamatsu, Japan) with 40x magnification. Isotype-matched controls were consistently found to be devoid of staining. Leukocyte attraction to the postcapillary venules was scored by



3 independent researchers. CD45⁺ cells that were in direct contact with the endothelial cells at the luminal or basal site of postcapillary venules were counted in 10 randomly selected kidney venules, for all mice, and values were arranged per group.

Statistical analysis

Statistical analysis of the results was performed by a two-tailed unpaired Student's t-test, assuming equal variances to compare two replicate means, or One-Way ANOVA followed by Bonferroni post-hoc analysis to compare multiple replicate means. Differences were considered significant when $p < 0.05$.

Results

Characterization of TNF α induced VCAM-1 expression *in vivo*.

TNF α is a well characterized cytokine and a potent inducer of the inflammatory response in the vasculature. We therefore used mice systemically challenged with TNF α as a model to study VCAM-1 mediated siRNA delivery to inflammation activated endothelial cells *in vivo*. I.v. injection of TNF α resulted in induction of VCAM-1 mRNA in main organs (kidneys ~ 27 fold, brain ~ 6 fold, heart ~ 32 fold, liver ~ 20 fold, lungs ~ 39 fold) [28] and consequent elevated protein expression at 2 h post challenge, as compared to untreated mice. 2 h after administration of TNF α , VCAM-1 was abundantly expressed in arterioles and venules of all organs. Furthermore, liver sinusoidal endothelium and kidney peritubular capillary endothelium as well as some scattered capillaries in the brain expressed VCAM-1 protein (Fig. 1).

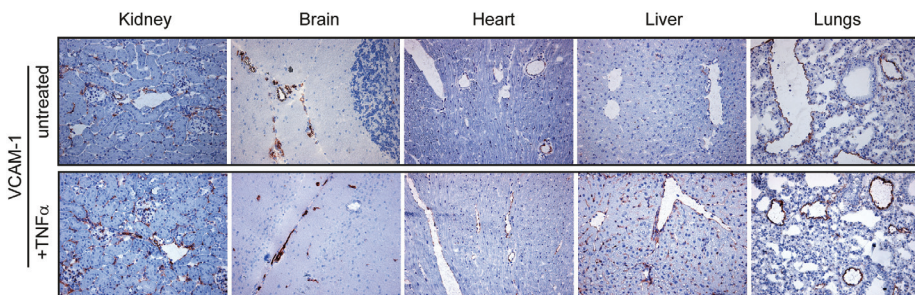


Figure 1. Adhesion molecule expression *in vivo* 2 h after systemic administration of TNF α . VCAM-1 protein expression (red staining) in mouse organs 2 h after i.v. injection of mTNF α and in untreated controls, assessed by immunohistochemistry as described in 'Materials and Methods'.

Table 1. Characterization of antibody conjugated SAINT-O-Somes containing siRNA.

Formulation					
POPC : SAINT : Chol : DSPE-PEG : DSPE-PEG-Mal					
37 : 18 : 40 : 4 : 1					
SAINT-O-Somes	Size [nm]	Polydispersity Index	Zeta Potential [mV]	Ab conjugated mol/liposome	siRNA encapsulation efficiency (%)
Ab _{VCAM-1}	116 ± 49	0.16 ± 0.02	3.8 ± 5	26 ± 8	74 ± 14
IgG	118 ± 48	0.16 ± 0.03	2.1 ± 7	22 ± 10	74 ± 16

Data are presented as means of 3-6 preparations ± SD.

Pharmacokinetic properties and tissue distribution of Ab_{VCAM-1} siRNA SAINT-O-Somes in TNF α challenged mice.

The physicochemical properties of targeted siRNA SAINT-O-Somes that were administered to mice are presented in Table 1. Ab_{VCAM-1} and IgG SAINT-O-Somes containing control siRNA were i.v. injected into mice 2 h after administration of TNF α . SAINT-O-Somes plasma concentration curves showed two-phase disappearance kinetics (Fig. 2A) with a short initial half-life (8 min for IgG and 10 min for Ab_{VCAM-1}) and a long secondary half-life (11 h for IgG and 25 h for Ab_{VCAM-1}) (Table 2). Plasma clearance and steady state volume of distribution for Ab_{VCAM-1} siRNA SAINT-O-Somes were approximately 1.5 fold higher than those of IgG siRNA SAINT-O-Somes.

At 24 h, the whole body distribution of Ab_{VCAM-1} siRNA SAINT-O-Somes showed increased accumulation in tissues of TNF α challenged mice as reflected by the targeting ratio (% of injected dose/gram tissue of Ab_{VCAM-1} divided by % of injected dose/gram tissue of IgG siRNA SAINT-O-Somes) (Fig. 2B). Accumulation of Ab_{VCAM-1} siRNA SAINT-O-Somes in TNF α activated kidneys, heart and lungs was more than 3 times higher than that of IgG siRNA SAINT-O-Somes, while in the brain this accumulation was 7.3 times higher. The accumulation of both preparations in the liver was comparable, whereas in the spleen Ab_{VCAM-1} siRNA SAINT-O-Somes accumulated to a somewhat higher extent than IgG siRNA SAINT-O-Somes. The total recovery of the radioactivity from the collected tissues ranged from 75-80% for both preparations (data not shown).

Localization of Ab_{VCAM-1} siRNA SAINT-O-Somes in the tissues of TNF α challenged mice follows VCAM-1 expression.

Immunohistochemical staining was performed to determine the intra-organ localization of the Ab_{VCAM-1} and IgG siRNA SAINT-O-Somes in the tissues of TNF α challenged mice, 6 h after i.v. injection of liposomes (Fig. 3A). Homing of Ab_{VCAM-1} siRNA SAINT-O-Somes followed the heterogenic VCAM-1 expression in the kidneys,



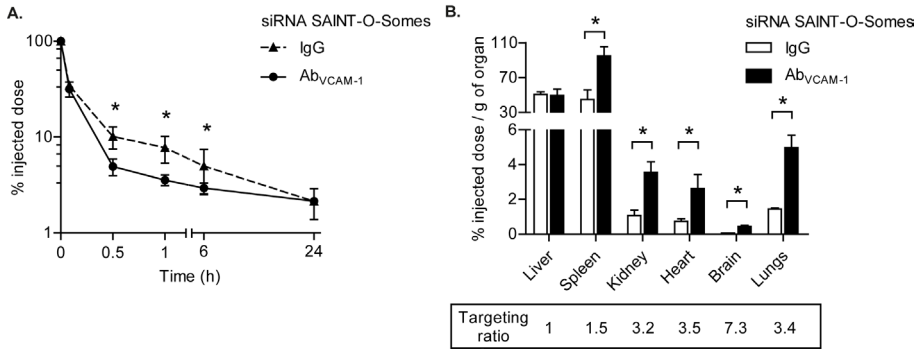


Figure 2. Tissue distribution and pharmacokinetic properties of targeted siRNA SAINT-O-Somes in TNF α challenged mice. C57BL/6 mice were i.v. challenged with 0.2 μ g rmTNF α 2 h later 10 μ mol TL/kg of [3 H] cholesteryl hexadecyl ether-labeled siRNA SAINT-O-Somes conjugated with anti-VCAM-1 (Ab_{VCAM-1}) or irrelevant IgG antibodies (IgG) were administered i.v. (A) Disappearance from blood in time. (B) Tissue distribution 24 h after administration of targeted siRNA SAINT-O-Somes. Fold-increase in accumulation of Ab_{VCAM-1} versus IgG siRNA SAINT-O-Somes is represented by the targeting ratio. Data are presented as mean values \pm SD of 3 mice/group. * $p < 0.05$.

heart and lungs (Fig. 3B), whereas IgG siRNA SAINT-O-Somes mainly accumulated in the glomerular compartment of the kidneys and were not detected in lungs and heart. Both Ab_{VCAM-1} and IgG SAINT-O-Somes furthermore accumulated in liver and spleen (Fig. 3B). In these latter organs Ab_{VCAM-1} siRNA SAINT-O-Somes localized mainly in the vascular compartments, in venules and sinusoidal endothelium in the liver, and in the red pulp of the spleen. In contrast, IgG siRNA SAINT-O-Somes were mostly found in the Kupffer cells and in the white pulp, respectively (Fig. 3B). In addition, with CLSM we could show that Ab_{VCAM-1} siRNA SAINT-O-Somes co-localized with endothelial cells (stained for endothelial marker CD31) in the venules and arterioles of TNF α challenged mouse kidneys (Fig. 3C). No co-localization with those vascular compartments was observed for IgG siRNA SAINT-O-Somes.

Table 2. Pharmacokinetic parameters of targeted siRNA SAINT-O-Somes.

Parameter	siRNA SAINT-O-Somes	
	Ab_{VCAM-1}	IgG
C_l , ml/h	3.41 \pm 0.11	2.89 \pm 0.25*
V_{ss} , ml/g	58.6 \pm 3.6	35.8 \pm 2.1*
$t_{1/2}$ (1), h	0.13 \pm 0.01	0.17 \pm 0.03*
$t_{1/2}$ (2), h	25.7 \pm 4.5	11.5 \pm 0.4*

Data are presented as mean values \pm SD of 3 mice/group. C_l , plasma clearance; V_{ss} , steady-state volume of distribution; $t_{1/2}$ (1), initial half-life; $t_{1/2}$ (2), secondary half-life. * $p < 0.05$ Ab_{VCAM-1} vs IgG.

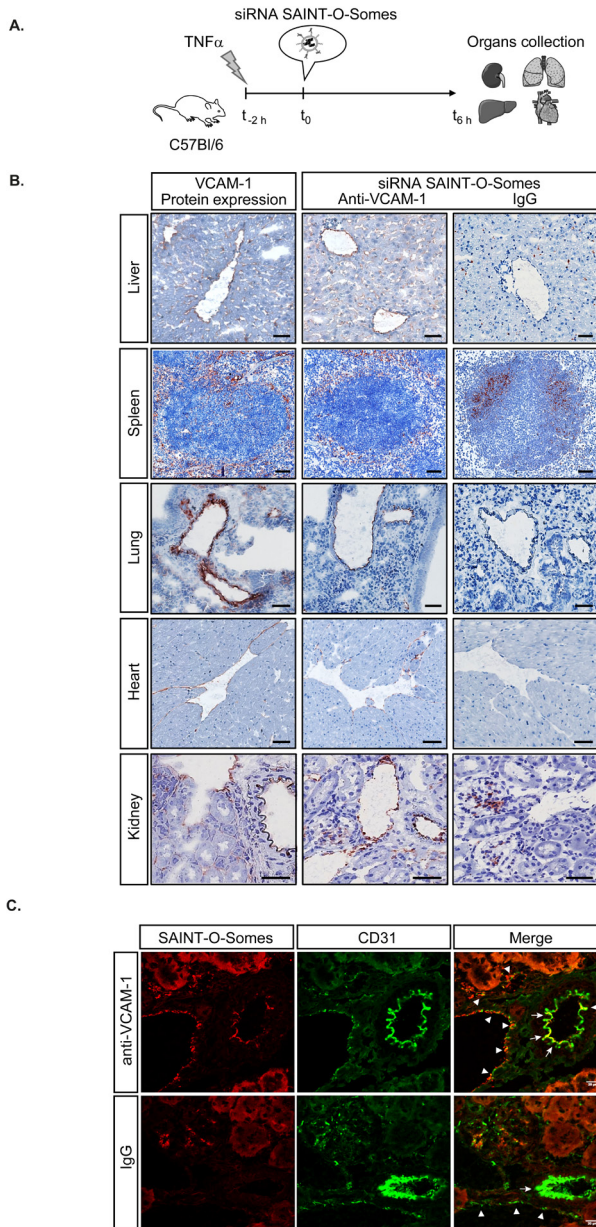


Figure 3. Homing of Ab_{VCAM-1} siRNA SAINT-O-Somes follows heterogenic VCAM-1 expression in the different organs. (A) Schematic representation of the experimental setup. (B) Immunohistochemical detection of VCAM-1 protein expression and Ab_{VCAM-1} and IgG siRNA SAINT-O-Somes localization (red staining) in tissues of TNF α challenged mice, 6 h after i.v. injection of SAINT-O-Somes. Original magnification 200x, scale bar represents 50 μ m. (C) Confocal microscopy images of double immunofluorescent staining for endothelial marker CD31 (green) and Ab_{VCAM-1} siRNA SAINT-O-Somes (red) in kidney of TNF α challenged mice. White arrowheads point at venules and arrows at arterioles. Presented data sets show representative images of 2 mice/group.

Ab_{VCAM-1} siRNA SAINT-O-Somes are not toxic and enable effective siRNA delivery to specific vascular segments in mouse kidneys.

No significant changes in the plasma levels of ureum, creatinine, ALAT and ALP (kidney and liver toxicity parameters) or in the weight of the animals (data not shown) were detected after a single dose (50 $\mu\text{mol TL/kg}$, 0.6 mg/kg siRNA) of Ab_{VCAM-1} siRNA SAINT-O-Somes, as compared to TNF α challenged mice (Table 3). Although a significant decrease in the ALP levels was found in the group treated with control siRNA, the levels of all the parameters presented in Table 3, including ALP, were not significantly different from untreated healthy mice.

In a previous study we used VE-cadherin as a model gene for studying the effects of the targeted SAINT-O-Somes in endothelial cells *in vitro*, since its expression is restricted to endothelial cells and maintained under TNF α stimulation [19]. In the present study, using Ab_{VCAM-1} siRNA_{VEcad} SAINT-O-Somes we also chose the VE-cadherin as a target gene in mouse microvessels and validated endothelial specific gene downregulation *in vivo*. TNF α challenged mice were i.v. injected with a single dose of Ab_{VCAM-1} SAINT-O-Somes containing VE-cadherin specific or control siRNA (0.6 mg/kg) and were sacrificed after 48 h. Downregulation of VE-cadherin in the vascular compartments, as demonstrated using laser microdissection, corroborated the accumulation of Ab_{VCAM-1} siRNA SAINT-O-Somes in these compartments (Fig. 4A). The VE-cadherin siRNA treated group showed 40% downregulation of VE-cadherin mRNA in postcapillary venules and 30% downregulation in arterioles, as compared to the group that received control siRNA (Fig. 4B-D). No difference in VE-cadherin expression was detected in the glomerular compartment, which corroborated the minor accumulation of SAINT-O-Somes in that compartment.

Table 3. Kidney and liver toxicity parameters measured in plasma after treatment with Ab_{VCAM-1} SAINT-O-Somes (50 $\mu\text{mol TL/kg}$) containing (0.6 mg/kg) VE-cadherin specific or control siRNA.

Parameter	- TNF α	+TNF α	Ab _{VCAM-1} SAINT-O-Somes	
			VE-cadherin	Control siRNA
Ureum (mmol/l)	7.7 \pm 0.7	7.3 \pm 0.1	8.3 \pm 1.7	8.5 \pm 1.1
Creatinine ($\mu\text{mol/l}$)	9 \pm 2.5	7 \pm 1	7.9 \pm 1	6 \pm 1
ALAT (U/l)	23.1 \pm 5	30.3 \pm 2.9	24.3 \pm 5.7	20.7 \pm 3.8
ALP (U/l)	70 \pm 11.4	80 \pm 5.7	70 \pm 4.7	61 \pm 7.8*

Data are presented as mean values \pm SD of 3 mice/group. ALAT, alanine aminotransferase; ALP, alkaline phosphatase. * $p < 0.05$ vs TNF α

*Downregulation of RelA gene expression by siRNA attenuates endothelial inflammatory response to TNF α and LPS *in vitro*.*

To demonstrate proof of concept of endothelial specific siRNA delivery based therapeutic intervention we chose RelA as a target gene to inhibit endothelial activation in inflammation. We first investigated *in vitro* the consequences of RelA downregulation on the inflammatory status of endothelial cells after TNF α and LPS challenge. In HUVEC transfected with RelA specific siRNA and exposed to TNF α or LPS, 98% downregulation of RelA mRNA was achieved (Fig. S1A), which was paralleled by nearly complete inhibition of RelA protein expression (Fig. S1B) and absence of RelA in the nucleus after the challenge (Fig. S1C), while transfection with control siRNA was devoid of such effects. Interference with NF κ B signaling led to attenuation of the inflammatory response towards TNF α and LPS as demonstrated by robust inhibition of expression of the pro-inflammatory genes E-selectin, VCAM-1, ICAM-1, IL-8 and IL-6, and MCP-1 (Fig. S1D, E). Moreover, downregulation of RelA resulted in 70-80% inhibition of IL-8 protein and 50-60% inhibition of IL-6 protein production by endothelial cells exposed to TNF α resp. LPS (Fig. S2). Comparable effects of RelA downregulation were found in the mouse heart endothelial cell line (H5V), implying that attenuation of the inflammatory response using RelA siRNA can also be achieved in mouse endothelial cells (Fig. S3).

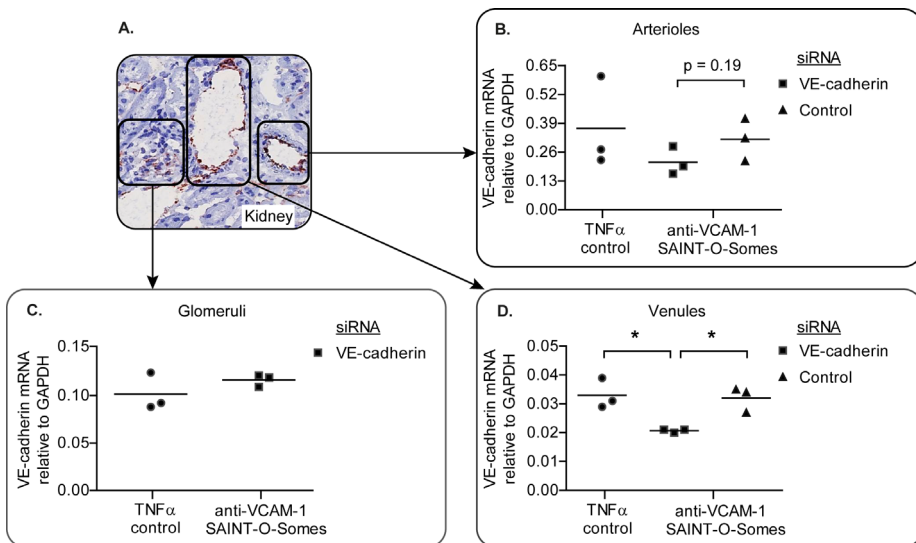


Figure 4. Ab_{VCAM-1} siRNA_{VEcadh} SAINT-O-Somes downregulate target gene VE-cadherin in specific vascular segments. TNF α challenged mice were injected with Ab_{VCAM-1} SAINT-O-Somes containing (0.6 mg/kg) VE-cadherin or control siRNA and sacrificed 48 h later. (A) Accumulation of Ab_{VCAM-1} siRNA SAINT-O-Somes in the kidney. (B-D) VE-cadherin gene expression in specific vascular segments, laser microdissected from kidney cryo-sections prior to analysis by RT-qPCR. Data of 3 mice/group and mean values are presented. * p < 0.05.

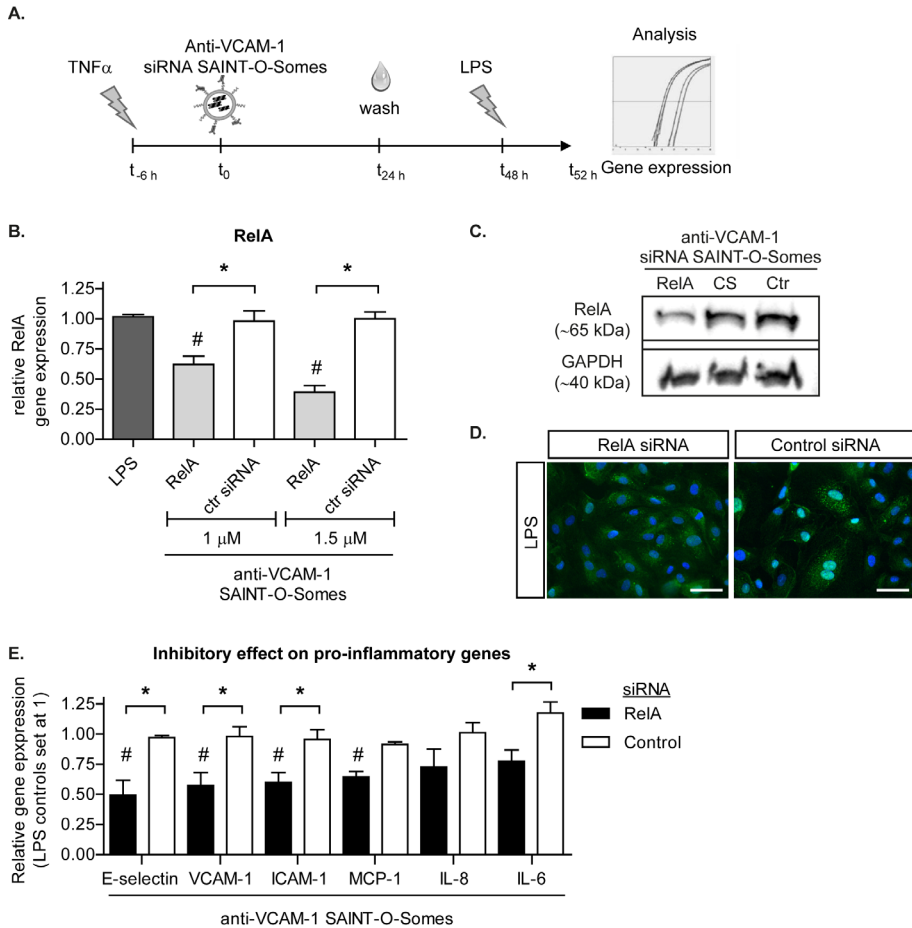


Figure 5. Ab_{VCAM-1} $siRNA_{RelA}$ SAINT-O-Somes reduce the expression of pro-inflammatory genes in LPS activated endothelial cells. (A) Schematic representation of the experimental setup. HUVEC were activated with $TNF\alpha$ (10 ng/ml) and subsequently incubated with Ab_{VCAM-1} SAINT-O-Somes containing RelA specific or control siRNA (CS) for 24 h. After an additional 24 h incubation period, cells were stimulated with LPS (1 mg/ml) for the last 4 h of the experiment. (B) siRNA concentration dependent downregulation of RelA mRNA. (C) Downregulation of RelA protein expression by Ab_{VCAM-1} $siRNA_{RelA}$ SAINT-O-Somes at 1.5 mM resulted in (D) decreased nuclear translocation of RelA in LPS stimulated HUVEC and (E) attenuation of pro-inflammatory gene expression upon LPS stimulation. (B, E) Data are presented as mean values \pm SD of three independent experiments. * $p < 0.05$, # $p < 0.05$ RelA vs LPS; (C) Image shows a representative Western Blot; (D) Immunofluorescence data set shows representative images of one of three independent experiments, original magnification 400x. Scale bar represents 50 μ m.

Ab_{VCAM-1} SAINT-O-Somes containing siRNA against RelA attenuate the endothelial inflammatory response to LPS in vitro and in vivo.

HUVEC were challenged with TNF α for 6 h to induce expression of VCAM-1 and subsequently incubated with Ab_{VCAM-1} siRNA_{RelA} SAINT-O-Somes for 24 h. After an additional 24 h cells were exposed to LPS for 4 h (Fig. 5A). Ab_{VCAM-1} siRNA_{RelA} SAINT-O-Somes showed a dose dependent downregulation of RelA mRNA up to 60 % at 1.5 μ M of siRNA, as compared to control siRNA (Fig. 5B). Inhibition of gene expression was corroborated by downregulation of RelA protein expression (Fig. 5C) and led to a decrease in RelA nuclear translocation upon LPS stimulation (Fig. 5D). In parallel, a 40-50 % downregulation of adhesion molecules (E-selectin, VCAM-1, ICAM-1), 35 % downregulation of MCP-1, and 30-40 % downregulation of IL-8 and IL-6 was observed (Fig. 5E). Non-targeted siRNA_{RelA} SAINT-O-Somes were devoid of the above effect (data not shown).

To determine whether Ab_{VCAM-1} siRNA_{RelA} SAINT-O-Somes can attenuate the endothelial inflammatory response to LPS *in vivo*, we used the TNF α challenged mouse model, to allow SAINT-O-Somes homing, followed by LPS challenge. TNF α challenged mice were injected with a single dose of Ab_{VCAM-1} SAINT-O-Somes containing (0.6 mg/kg) RelA specific or control siRNA and re-challenged with LPS after 48 h. Local pharmacological effects of the siRNA treatment were analyzed in laser microdissected vascular compartments of the kidneys (Fig. 6A). The extent of RelA downregulation was analyzed in mice sacrificed prior to LPS treatment (at 48 h time point). 48 h after an acute TNF α challenge the expression of most pro-inflammatory genes is restored to basal (low) levels, therefore, to show the consequences of RelA downregulation on the expression of downstream pro-inflammatory genes, the second challenge was required. As previously observed for VE-cadherin, the major effects of siRNA treatment were observed in postcapillary venules. We found 46% downregulation of RelA mRNA in kidney venules 48 h after administration of Ab_{VCAM-1} siRNA_{RelA} SAINT-O-Somes, compared to controls (Fig. 6B). LPS challenged mice treated with Ab_{VCAM-1} siRNA_{RelA} SAINT-O-Somes further showed a significant downregulation of E-selectin, MCP-1, and IL-6 gene expression in the venules to approx. 40%, as compared to LPS challenged group that received control siRNA (Fig. 6C-E). We did not observe significant differences in the expression of these genes in glomeruli and renal arterioles (Fig. S4). Furthermore, no significant differences were found in the expression of VCAM-1, ICAM-1, and IL-8 in the venules of LPS challenged mice that received Ab_{VCAM-1} siRNA_{RelA} SAINT-O-Somes (data not shown). The molecular effects in the venules were accompanied by a significantly reduced number of adhering/infiltrating CD45+ cells in mice treated with Ab_{VCAM-1} siRNA_{RelA} SAINT-O-Somes, as compared to LPS re-challenged control mice (Fig. 6F). The effect on leukocyte attraction was though not significantly different from mice treated with control siRNA.



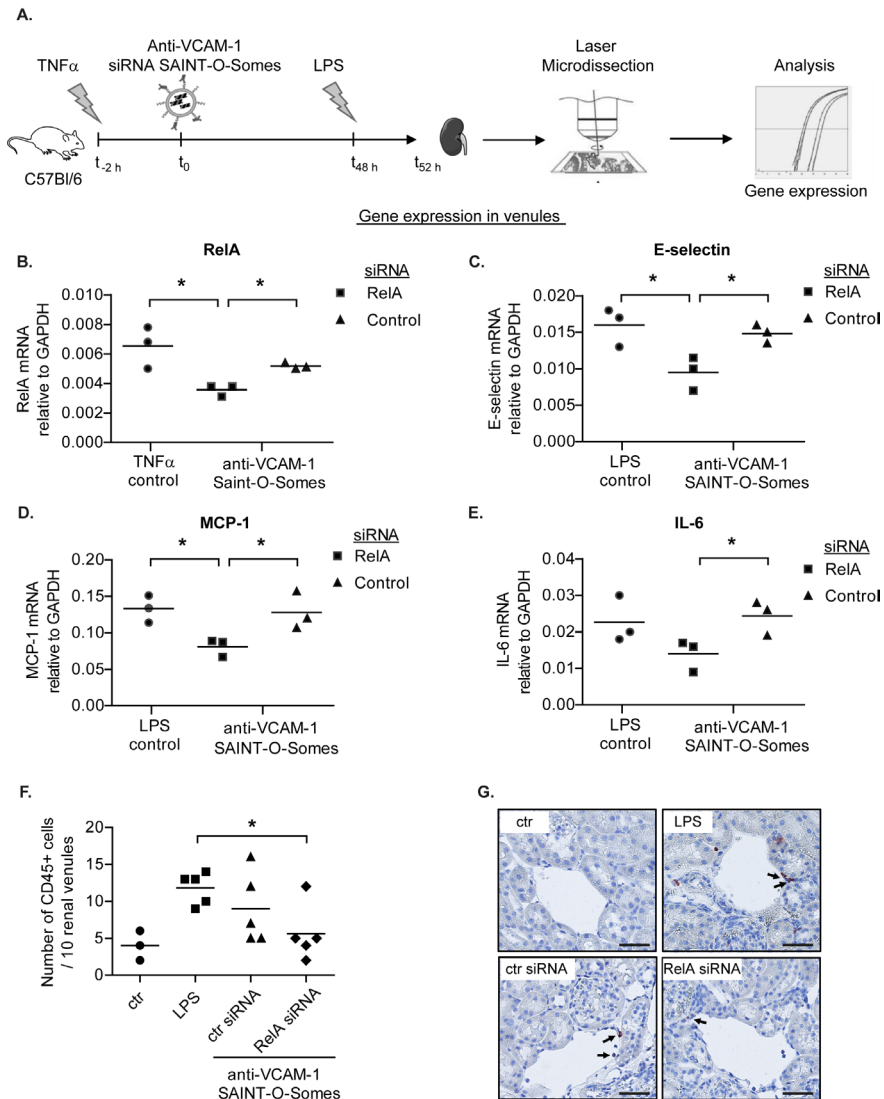


Figure 6. Local attenuation of endothelial inflammatory response towards LPS challenge in vivo by endothelial specific RelA downregulation. (A) Schematic representation of the experimental setup. (B) RelA mRNA expression in kidney venules of TNF α challenged mice 48 h after administration of Ab_{VCAM-1} SAINT-O-Somes containing (0.6 mg/kg) RelA specific or control siRNA. (C-E) Inhibition of pro-inflammatory gene expression in renal postcapillary venules of TNF α / LPS challenged mice by Ab_{VCAM-1} siRNA_{RelA} SAINT-O-Somes. Kidney venules were laser microdissected prior to analysis by RT-qPCR. Data of 3 mice/group and mean values are presented. * $p < 0.05$. (F-G) Leukocyte (CD45+ cells) attraction to kidney venules. Number of CD45+ cells in contact with vessel wall (black arrows (G)) was scored in 10 randomly selected postcapillary venules per kidney as described in 'Material and Methods'. Data are presented as mean values of 3-5 mice/group. * $p < 0.05$. Scale bar represents 50 μ m.

Discussion

Microvascular endothelial cells at a site of inflammation are both active participants and regulators of acute and chronic inflammatory processes, thus endothelial specific delivery of therapeutics presents a promising approach for anti-inflammatory intervention. In the current work we demonstrate that it is feasible to selectively deliver siRNAs to inflamed endothelial cells *in vivo* using SAINT-C18 based liposomes (SAINT-O-Somes), surface-modified with antibodies specific for the inflammatory adhesion protein VCAM-1, and we show their potential to interfere with disease associated endothelial cell activation. Ab_{VCAM-1} SAINT-O-Somes selectively homed to VCAM-1 expressing endothelial cells in specific microvascular segments in organs of TNF α challenged mice and effectively delivered VE-cadherin and NF κ B p65 (RelA) specific siRNAs to the renal vasculature without exerting liver and kidney toxicity. The resulting knock down of RelA led to attenuation of the endothelial inflammatory response towards LPS and exerted local therapeutic effects represented by inhibition of pro-inflammatory gene expression and leukocyte attraction to kidney venules. From this study we conclude that Ab_{VCAM-1} SAINT-O-Somes are suitable for functional delivery of siRNAs to inflamed microvascular segments and attenuation of endothelial inflammatory responses *in vivo*.

NF κ B is a key regulator of the inflammatory response in endothelial cells, and its activation is involved in the pathogenesis of many diseases with an underlying inflammatory component such as sepsis and atherosclerosis [29, 30]. Activation of NF κ B by pro-inflammatory cytokines, free radicals or pathogens, leads to the expression of a variety of pro-inflammatory genes encoding cytokines, chemokines and adhesion molecules [31]. Targeting members of the NF κ B signaling pathway is a promising therapeutic strategy, yet a specific intervention is an important requisite as systemic inhibition of its biological function has for example detrimental effects on the performance of the immune system and the maintenance of liver homeostasis upon acute inflammation [32, 33]. Many currently used small molecule inhibitors of NF κ B lack cellular and molecular specificity and exert systemic toxicity [8]. Endothelial specific inhibition of NF κ B activity may therefore enhance the efficacy of anti-inflammatory treatment by attenuating the inflammation while reducing adverse effects of the intervention. For example, Ye et al. showed that mice with genetically engineered endothelial-selective blockade of NF κ B activation were resistant to septic shock and sepsis-related death yet retained a normal capacity to clear pathogenic bacteria [6]. Other studies in transgenic mice with endothelial cell-restricted depletion of NF κ B demonstrated its protective role in the development of atherosclerosis [31] and hypertension-induced renal damage [5].



Targeting inflamed vasculature has been attempted using a variety of targets including PECAM-1, ICAM-1, and E-selectin, each representing different vascular specificity and heterogeneity of expression in quiescence and inflammatory diseases (reviewed by Simone et. al. [34]). VCAM-1 presents an attractive target for endothelial specific drug delivery as it is expressed at low levels by resting endothelium and is strongly induced by inflammatory stimuli, such as pro-inflammatory cytokines or growth factors [4]. TNF α challenged mice showed induced VCAM-1 mRNA and protein expression in all vascular segments of major organs at 2-8 h post challenge. In the kidney VCAM-1 protein was expressed in arterioles and venules but not in glomeruli, corroborating findings in models of hemorrhagic shock [35] and LPS induced sepsis [36]. Our data indeed indicate limited use of VCAM-1 for targeting glomerular endothelium, whereas venous and arteriolar endothelial cells were accessible through VCAM-1. Strong induction of VCAM-1 expression was also found at the sites of pathological inflammation in atherosclerosis [37], autoimmune diseases [38], and on tumor vasculature [39], offering multiple applications for siRNA delivery devices targeted to VCAM-1.

We showed that Ab_{VCAM-1} siRNA SAINT-O-Somes display the required physicochemical properties and pharmacokinetic behavior to target VCAM-1 expressing microvascular endothelial cells in TNF α challenged mice. Circulation kinetics of i.v. injected siRNA SAINT-O-Somes were comparable to long circulating liposomes that do not contain the cationic SAINT-C18 [20]. Ab_{VCAM-1} siRNA SAINT-O-Somes showed higher plasma clearance than IgG conjugated SAINT-O-Somes, which is likely due to specific binding to VCAM-1 on activated endothelial cells. Compared to IgG SAINT-O-Somes, a significantly higher accumulation of Ab_{VCAM-1} SAINT-O-Somes was found in the inflamed microvasculature of kidneys, heart and lungs and brain. In all organs, the localization of Ab_{VCAM-1} SAINT-O-Somes corroborated the TNF α induced VCAM-1 expression on the endothelium, whereas IgG SAINT-O-Somes were mainly associated with the phagocytic cells of the reticuloendothelial system (RES) in the liver and spleen. The glomerular presence of IgG SAINT-O-Somes possibly occurred due to uptake by mesangial cells possessing phagocytic properties [40].

We previously showed that targeted SAINT-O-Somes containing siRNA at 1 μ M concentration had no influence on the viability of endothelial cells *in vitro*, after 48 h exposure [19]. *In vivo*, no toxicity was observed after administration of a single dose (50 μ mol TL/kg, 0.6 mg/kg siRNA) of Ab_{VCAM-1} siRNA SAINT-O-Somes to mice, as indicated by the absence of weight loss or unchanged plasma levels of the indicators of liver and kidney damage. The toxicity of lipid based formulations is often attributed to their positive surface charge, determined by the type and the content of cationic lipid, as well as presence of the helper lipids facilitating endosomal escape such as DOPE (reviewed by Borja et al. [41]). It is highly likely that the absence of toxic effects of SAINT-O-Somes in our study is a consequence of the relatively low SAINT-C18



content (18 mol%), in combination with PEG shielding of the surface charge, and the absence of DOPE in the formulation.

Upon pro-inflammatory stimulation, the kidney vasculature displays a heterogeneous expression of VCAM-1 in distinct vascular beds (Fig 1 and 3B), which allowed us to study the local effects of Ab_{VCAM-1} siRNA SAINT-O-Somes in kidney vasculature. The tool of laser microdissection in combination with quantitative RT-PCR enabled analysis of vascular bed-specific pharmacological effects, that were masked when whole kidney homogenates were analyzed (data not shown). Whole organ effects of Ab_{VCAM-1} SAINT-O-Somes delivered VE-cadherin and RelA specific siRNAs were also investigated in lungs and liver but no downregulation of the targeted genes was found (data not shown). Likely the siRNA effects in these organs are also restricted to the endothelium which comprises a small part of the whole tissue but have not been studied yet. Targeted delivery of VE-cadherin or RelA specific siRNAs by Ab_{VCAM-1} SAINT-O-Somes resulted in downregulation of VE-cadherin and RelA mRNA expression predominantly in renal venules, whereas gene expression in glomeruli was unaltered. This local effects of siRNA can be explained by the fact that a majority of Ab_{VCAM-1} siRNA SAINT-O-Somes accumulated in the kidney venules, while only minor amounts were found in the glomeruli. Interestingly, despite detectable accumulation of Ab_{VCAM-1} siRNA SAINT-O-Somes in the kidney arterioles, we did not observe a significant downregulation of VE-cadherin and RelA gene expression. Possibly insufficient accumulation of Ab_{VCAM-1} SAINT-O-Somes at the highly endothelial-dense arterial wall is underlying this effect, which is also experimentally reflected by the immunofluorescent data (Fig. 3C). Recent studies demonstrated the effects of flow related shear stress on endothelial endocytosis of nanocarriers targeted to PECAM-1 [42] and ICAM-1 [43], showing a higher rate of endocytosis in vascular segments with lower shear stress. It may be possible that hydrodynamic differences between the vascular segments may also play a role in differential uptake and concomitant effects of Ab_{VCAM-1} siRNA SAINT-O-Somes. The differences between arterial and venous endothelial cells with regard to siRNA release such as the ability to intra-cellularly process Ab_{VCAM-1} SAINT-O-Somes, as implied by data in our previous study [19], may also contribute to the observed preferential gene silencing capacity *in vivo* in the venous segments.

A single dose of Ab_{VCAM-1} SAINT-O-Somes (0.6 mg/kg siRNA) was sufficient to achieve approximately 40% reduction of the VE-cadherin and RelA mRNA expression *in vivo*, 48 h post administration. This result corroborates downregulation of mRNA expression of the above genes found in HUVEC, which *in vitro* was followed by inhibition of protein expression ([19] and Fig 5 A-D). *In vivo*, however, we did not detect changes in protein expression in whole kidney protein extracts (data not shown). Lack of the differences in RelA protein expression may be explained by the fact that the effects of Ab_{VCAM-1} siRNA_{RelA} SAINT-O-Somes are localized in a minority of cells



within the kidney. We could show, though, the downstream effects of RelA knockdown by $\text{Ab}_{\text{VCAM-1}} \text{siRNA}_{\text{RelA}}$ SAINT-O-Somes in kidney venules, represented by inhibition of LPS induced E-selectin, MCP-1, and IL-6 gene expression, and a decrease in leukocyte attraction to kidney venules. Absence of VCAM-1 and ICAM-1 downregulation *in vivo* may possibly be explained by a more complex regulation of the inflammatory gene expression in subsets of microvascular endothelium *in vivo* than described for *in vitro* cell culture systems [4]. The inhibitory effect of RelA siRNA on leukocyte attraction in the venules may be a result of both inhibition of gene expression and binding of $\text{Ab}_{\text{VCAM-1}}$ conjugated to SAINT-O-Somes to its target that may affect leukocyte interaction with the vessel wall. The contribution of the latter is however not likely, as $\text{Ab}_{\text{VCAM-1}}$ SAINT-O-Somes were hardly detectable in kidney venules 48 h after administration, being the time point at which the LPS challenge took place (data not shown).

Until now drug delivery based selective NF κ B interference with activated endothelium has only been demonstrated using adenoviral gene therapy [21, 44], whereas only a few non-viral carriers are currently available for *in vivo* siRNA delivery into endothelial cells [17, 45]. Most studies regarding those carriers focus on siRNA delivery to tumor vasculature that is markedly transformed by the tumor microenvironment, often leaky and not considered normal vasculature [46]. It is therefore difficult to compare gene silencing efficacy of $\text{Ab}_{\text{VCAM-1}} \text{siRNA}_{\text{RelA}}$ SAINT-O-Somes with those systems. siRNA delivery into the vasculature was previously demonstrated using non-targeted lipoplexes that were taken up via interaction of positively charged cationic lipids with the endothelial cells [47]. With those lipoplexes, based on cationic lipid AtuFECT01, Santel et. al. demonstrated silencing of gene and protein expression of endothelial specific genes PECAM-1 and Tie-2 in liver, lungs, and heart vasculature. Mice were treated i.v. with a daily siRNA dose of 1.88 mg/kg for 4 consecutive days [47]. Contrary to cationic lipoplexes, $\text{Ab}_{\text{VCAM-1}}$ SAINT-O-Somes facilitate selective siRNA delivery via antibody/antigen specific interaction solely to disease associated endothelial cell subsets. Future studies need to evaluate the duration of *in vivo* gene silencing and the influence of multiple dosing on silencing efficiency and duration, as well as the maintenance of VCAM-1 specificity to vascular segments.

In summary, this study reports on a novel, endothelial specific carrier suitable for selective delivery of siRNAs to inflamed microvascular endothelial cells and interference with disease associated endothelial activation. We showed that VCAM-1 can serve as a specific entry route for this delivery and we demonstrated proof-of-concept of pharmacological effects represented by attenuation of the endothelial inflammatory responses towards LPS by $\text{Ab}_{\text{VCAM-1}} \text{siRNA}_{\text{RelA}}$ SAINT-O-Somes mediated inhibition of NF κ B p65. Future studies on pharmacological effects of $\text{Ab}_{\text{VCAM-1}} \text{siRNA}_{\text{RelA}}$ SAINT-O-Somes in relevant models of inflammatory diseases will disclose more details on the potential of this system for broad therapeutic application.



Acknowledgements

We thank Arjen H. Petersen, Rianne M. Jongman and Henk Moorlag for excellent technical assistance. Dr. Jill Moser from the Dept. of Critical Care (UMCG, Groningen) is acknowledged for assistance with scoring of leukocyte attraction to kidney venules. We thank Dr. Ed Talman for providing high quality SAINT-C18 and prof. Gerrit L. Scherphof for editing and proofreading the manuscript.

Microscopic fluorescence imaging was performed at the UMCG Microscopy & Imaging Center (UMIC), which is supported by the Netherlands Organization for Health Research and Development (ZonMW grant 40-00506-98-9021). This work was supported by EFRO (European Fund for Regional Development) from the European Union, project NTS 068 and 073 Drug Delivery and Targeting. The authors declare no competing financial interests. M.H.J. Ruiters is CEO of Synvolux Therapeutics.

References

1. I. Tabas, C.K. Glass. Anti-inflammatory therapy in chronic disease: challenges and opportunities, *Science*, 339 (2013) 166-172.
2. D.C. Angus. The lingering consequences of sepsis: a hidden public health disaster?, *JAMA*, 304 (2010) 1833-1834.
3. J.S. Pober, W.C. Sessa. Evolving functions of endothelial cells in inflammation, *Nat Rev Immunol*, 7 (2007) 803-815.
4. G. Molema. Heterogeneity in endothelial responsiveness to cytokines, molecular causes, and pharmacological consequences, *Semin Thromb Hemost*, 36 (2010) 246-264.
5. N. Henke, R. Schmidt-Ullrich, R. Dechend, J.K. Park, F. Qadri, M. Wellner, M. Obst, V. Gross, R. Dietz, F.C. Luft, C. Scheidereit, D.N. Muller. Vascular endothelial cell-specific NF-kappaB suppression attenuates hypertension-induced renal damage, *Circ Res*, 101 (2007) 268-276.
6. X. Ye, J. Ding, X. Zhou, G. Chen, S.F. Liu. Divergent roles of endothelial NF-kappaB in multiple organ injury and bacterial clearance in mouse models of sepsis, *J Exp Med*, 205 (2008) 1303-1315.
7. C. Stambe, R.C. Atkins, P.A. Hill, D.J. Nikolic-Paterson. Activation and cellular localization of the p38 and JNK MAPK pathways in rat crescentic glomerulonephritis, *Kidney Int*, 64 (2003) 2121-2132.
8. J.M. Kuldo, K.I. Ogawara, N. Werner, S.A. Asgeirsdottir, J.A. Kamps, R.J. Kok, G. Molema. Molecular pathways of endothelial cell activation for (targeted) pharmacological intervention of chronic inflammatory diseases, *Curr Vasc Pharmacol*, 3 (2005) 11-39.
9. F. Buttgerit, G.R. Burmester, B.J. Lipworth. Optimised glucocorticoid therapy: the sharpening of an old spear, *Lancet*, 365 (2005) 801-803.
10. G.R. Rettig, M.A. Behlke. Progress toward in vivo use of siRNAs-II, *Mol Ther*, 20 (2012) 483-512.
11. R.L. Kanasty, K.A. Whitehead, A.J. Vegas, D.G. Anderson. Action and reaction: the biological response to siRNA and its delivery vehicles, *Mol Ther*, 20 (2012) 513-524.
12. Z. Cheng, A. Al Zaki, J.Z. Hui, V.R. Muzykantov, A. Tsourkas. Multifunctional nanoparticles: cost versus benefit of adding targeting and imaging capabilities, *Science*, 338 (2012) 903-910.
13. D. Peer, E.J. Park, Y. Morishita, C.V. Carman, M. Shimaoka. Systemic leukocyte-directed



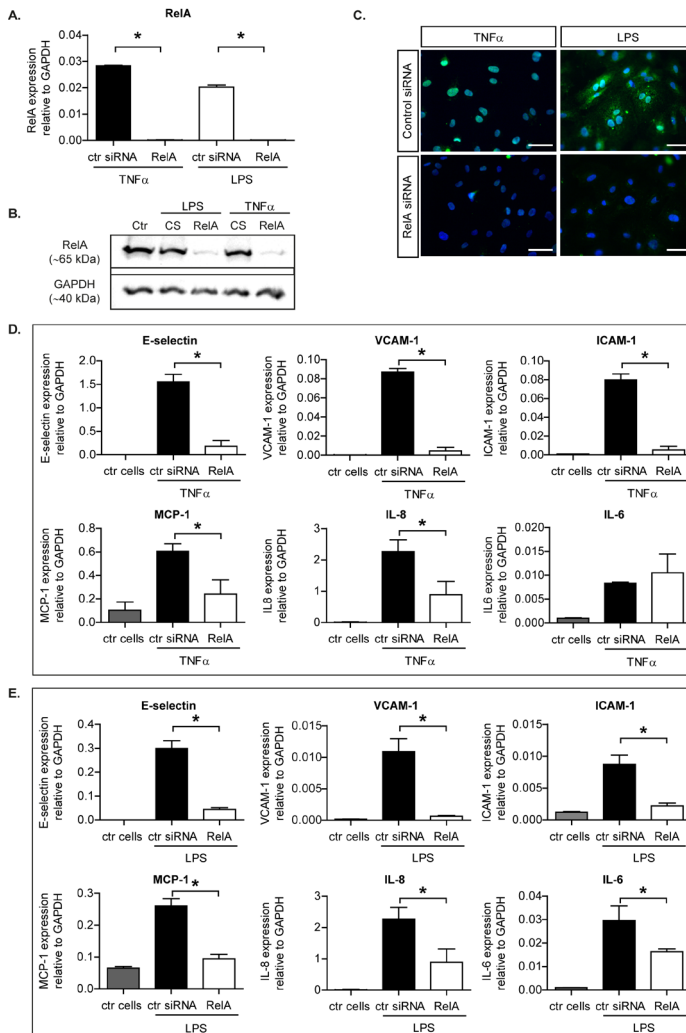
- siRNA delivery revealing cyclin D1 as an anti-inflammatory target, *Science*, 319 (2008) 627-630.
14. F. Leuschner, P. Dutta, R. Gorbatov, T.I. Novobrantseva, J.S. Donahoe, G. Courties, K.M. Lee, J.I. Kim, J.F. Markmann, B. Marinelli, P. Panizzi, W.W. Lee, Y. Iwamoto, S. Milstein, H. Epstein-Barash, W. Cantley, J. Wong, V. Cortez-Retamozo, A. Newton, K. Love, P. Libby, M.J. Pittet, F.K. Swirski, V. Kotliansky, R. Langer, R. Weissleder, D.G. Anderson, M. Nahrendorf. Therapeutic siRNA silencing in inflammatory monocytes in mice, *Nat Biotechnol*, 29 (2011) 1005-1010.
 15. J. Zhang, B. Shen, A. Lin. Novel strategies for inhibition of the p38 MAPK pathway, *Trends Pharmacol Sci*, 28 (2007) 286-295.
 16. E.D. Hood, C.F. Greineder, C. Dodiá, J. Han, C. Mesaros, V.V. Shuvaev, I.A. Blair, A.B. Fisher, V.R. Muzykantov. Antioxidant protection by PECAM-targeted delivery of a novel NADPH-oxidase inhibitor to the endothelium in vitro and in vivo, *J Control Release*, 163 (2012) 161-169.
 17. P.S. Kowalski, N.G. Leus, G.L. Scherphof, M.H. Ruiters, J.A. Kamps, G. Molema. Targeted siRNA delivery to diseased microvascular endothelial cells: cellular and molecular concepts, *IUBMB Life*, 63 (2011) 648-658.
 18. J.E. Adrian, H.W. Morselt, R. Suss, S. Barnert, J.W. Kok, S.A. Asgeirsdottir, M.H. Ruiters, G. Molema, J.A. Kamps. Targeted SAINT-O-Somes for improved intracellular delivery of siRNA and cytotoxic drugs into endothelial cells, *J Control Release*, 144 (2010) 341-349.
 19. P.S. Kowalski, L.L. Lintermans, H.W. Morselt, N.G. Leus, M.H. Ruiters, G. Molema, J.A. Kamps. Anti-VCAM-1 and Anti-E-selectin SAINT-O-Somes for Selective Delivery of siRNA into Inflammation-Activated Primary Endothelial Cells, *Mol Pharm*, 10 (2013) 3033-3044.
 20. S.A. Asgeirsdottir, P.J. Zwiers, H.W. Morselt, H.E. Moorlag, H.I. Bakker, P. Heeringa, J.W. Kok, C.G. Kallenberg, G. Molema, J.A. Kamps. Inhibition of proinflammatory genes in anti-GBM glomerulonephritis by targeted dexamethasone-loaded AbEsel liposomes, *Am J Physiol Renal Physiol*, 294 (2008) F554-561.
 21. J.M. Kuldo, S.A. Asgeirsdottir, P.J. Zwiers, A.R. Bellu, M.G. Rots, J.A. Schalk, K.I. Ogawara, C. Trautwein, B. Banas, H.J. Haisma, G. Molema, J.A. Kamps. Targeted adenovirus mediated inhibition of NF-kappaB-dependent inflammatory gene expression in endothelial cells in vitro and in vivo, *J Control Release*, 166 (2013) 57-65.
 22. A. Tsourkas, V.R. Shinde-Patil, K.A. Kelly, P. Patel, A. Wolley, J.R. Allport, R. Weissleder. In vivo imaging of activated endothelium using an anti-VCAM-1 magnetooptical probe, *Bioconjug Chem*, 16 (2005) 576-581.
 23. J.A. Kamps, P.J. Swart, H.W. Morselt, R. Pauwels, M.P. De Bethune, E. De Clercq, D.K. Meijer, G.L. Scherphof. Preparation and characterization of conjugates of (modified) human serum albumin and liposomes: drug carriers with an intrinsic anti-HIV activity, *Biochim Biophys Acta*, 1278 (1996) 183-190.
 24. Böttcher CJF, Van Gent CM, Pries C. A rapid and sensitive sub-micro phosphorus determination, *Anal. Chim. Acta*, 24 (1961).
 25. J.E. Adrian, J.A. Kamps, G.L. Scherphof, D.K. Meijer, A.M. van Loenen-Weemaes, C. Reker-Smit, P. Terpstra, K. Poelstra. A novel lipid-based drug carrier targeted to the non-parenchymal cells, including hepatic stellate cells, in the fibrotic livers of bile duct ligated rats, *Biochim Biophys Acta*, 1768 (2007) 1430-1439.
 26. J.H. Proost, D.J. Eleveld. Performance of an iterative two-stage bayesian technique for population pharmacokinetic analysis of rich data sets, *Pharm Res*, 23 (2006) 2748-2759.
 27. S.A. Asgeirsdottir, E.G. Talman, I.A. de Graaf, J.A. Kamps, S.C. Satchell, P.W. Mathieson, M.H. Ruiters, G. Molema. Targeted transfection increases siRNA uptake and gene silencing of primary endothelial cells in vitro--a quantitative study, *J Control Release*, 141 (2010) 241-251.
 28. G. Molema. Heterogeneity in responses of microvascular endothelial cells during inflammation, in: S.M. Dauphinee, A. Karsan (Eds.) *Endothelial Dysfunction and Inflammation*, Birkhäuser, Basel, 2010, pp. 15-35.
 29. M.P. de Winther, E. Kanters, G. Kraal, M.H. Hofker. Nuclear factor kappaB signaling in atherogenesis, *Arterioscler Thromb Vasc Biol*, 25 (2005) 904-914.



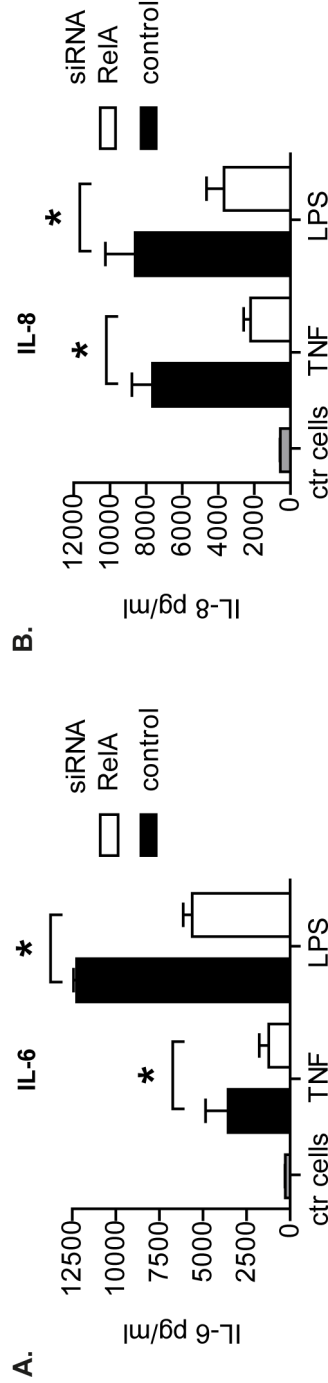
30. S.F. Liu, A.B. Malik. NF-kappa B activation as a pathological mechanism of septic shock and inflammation, *Am J Physiol Lung Cell Mol Physiol*, 290 (2006) L622-L645.
31. R. Gareus, E. Kotsaki, S. Xanthoulea, I. van der Made, M.J. Gijbels, R. Kardakaris, A. Polykratis, G. Kollias, M.P. de Winther, M. Pasparakis. Endothelial cell-specific NF-kappaB inhibition protects mice from atherosclerosis, *Cell Metab*, 8 (2008) 372-383.
32. J. Wang, R.A. Barke, R. Charboneau, S. Roy. Morphine impairs host innate immune response and increases susceptibility to *Streptococcus pneumoniae* lung infection, *J Immunol*, 174 (2005) 426-434.
33. T. Luedde, J. Heinrichsdorff, R. de Lorenzi, R. De Vos, T. Roskams, M. Pasparakis. IKK1 and IKK2 cooperate to maintain bile duct integrity in the liver, *Proc Natl Acad Sci U S A*, 105 (2008) 9733-9738.
34. E. Simone, B.S. Ding, V. Muzykantov. Targeted delivery of therapeutics to endothelium, *Cell Tissue Res*, 335 (2009) 283-300.
35. M. van Meurs, F.M. Wulfert, A.J. Knol, A. De Haes, M. Houwertjes, L.P. Aarts, G. Molema. Early organ-specific endothelial activation during hemorrhagic shock and resuscitation, *Shock*, 29 (2008) 291-299.
36. N.I. Shapiro, K. Yano, M. Sorasaki, C. Fischer, S.C. Shih, W.C. Aird. Skin biopsies demonstrate site-specific endothelial activation in mouse models of sepsis, *J Vasc Res*, 46 (2009) 495-502.
37. A. Broisat, S. Hernot, J. Toczek, J. De Vos, L.M. Riou, S. Martin, M. Ahmadi, N. Thielens, U. Wernery, V. Caveliers, S. Muyldermans, T. Lahoutte, D. Fagret, C. Ghezzi, N. Devoogdt. Nanobodies targeting mouse/human VCAM1 for the nuclear imaging of atherosclerotic lesions, *Circ Res*, 110 (2012) 927-937.
38. J.L. Tlaxca, J.J. Rychak, P.B. Ernst, P.R. Konkalmatt, T.I. Shevchenko, T.T. Pizzaro, J. Rivera-Nieves, A.L. Klibanov, M.B. Lawrence. Ultrasound-based molecular imaging and specific gene delivery to mesenteric vasculature by endothelial adhesion molecule targeted microbubbles in a mouse model of Crohn's disease, *J Control Release*, 165 (2013) 216-225.
39. S. Gosk, T. Moos, C. Gottstein, G. Bendas. VCAM-1 directed immunoliposomes selectively target tumor vasculature in vivo, *Biochim Biophys Acta*, 1778 (2008) 854-863.
40. Anatomy of the kidney. in: B.M. Brenner (Ed.) *The Kidney*, Saunders, Philadelphia, PA, 2004, pp. 3-72.
41. B. Ballarin-Gonzalez, K.A. Howard. Polycation-based nanoparticle delivery of RNAi therapeutics: Adverse effects and solutions, *Adv Drug Deliv Rev*, 64 (2012) 1717-1729.
42. J. Han, B.J. Zern, V.V. Shuvaev, P.F. Davies, S. Muro, V. Muzykantov. Acute and chronic shear stress differently regulate endothelial internalization of nanocarriers targeted to platelet-endothelial cell adhesion molecule-1, *ACS Nano*, 6 (2012) 8824-8836.
43. T. Bhowmick, E. Berk, X. Cui, V.R. Muzykantov, S. Muro. Effect of flow on endothelial endocytosis of nanocarriers targeted to ICAM-1, *J Control Release*, 157 (2012) 485-492.
44. K. Ogawara, J.M. Kuldo, K. Oosterhuis, B.J. Kroesen, M.G. Rots, C. Trautwein, T. Kimura, H.J. Haisma, G. Molema. Functional inhibition of NF-kappaB signal transduction in alphavbeta3 integrin expressing endothelial cells by using RGD-PEG-modified adenovirus with a mutant IkappaB gene, *Arthritis Res Ther*, 8 (2006) R32.
45. J. Kaufmann, K. Ahrens, A. Santel. RNA interference for therapy in the vascular endothelium, *Microvasc Res*, 80 (2010) 286-293.
46. E. Langenkamp, G. Molema. Microvascular endothelial cell heterogeneity: general concepts and pharmacological consequences for anti-angiogenic therapy of cancer, *Cell Tissue Res*, 335 (2009) 205-222.
47. A. Santel, M. Aleku, O. Keil, J. Endruschat, V. Esche, G. Fisch, S. Dames, K. Loffler, M. Fechtner, W. Arnold, K. Giese, A. Klippel, J. Kaufmann. A novel siRNA-lipoplex technology for RNA interference in the mouse vascular endothelium, *Gene Ther*, 13 (2006) 1222-1234.



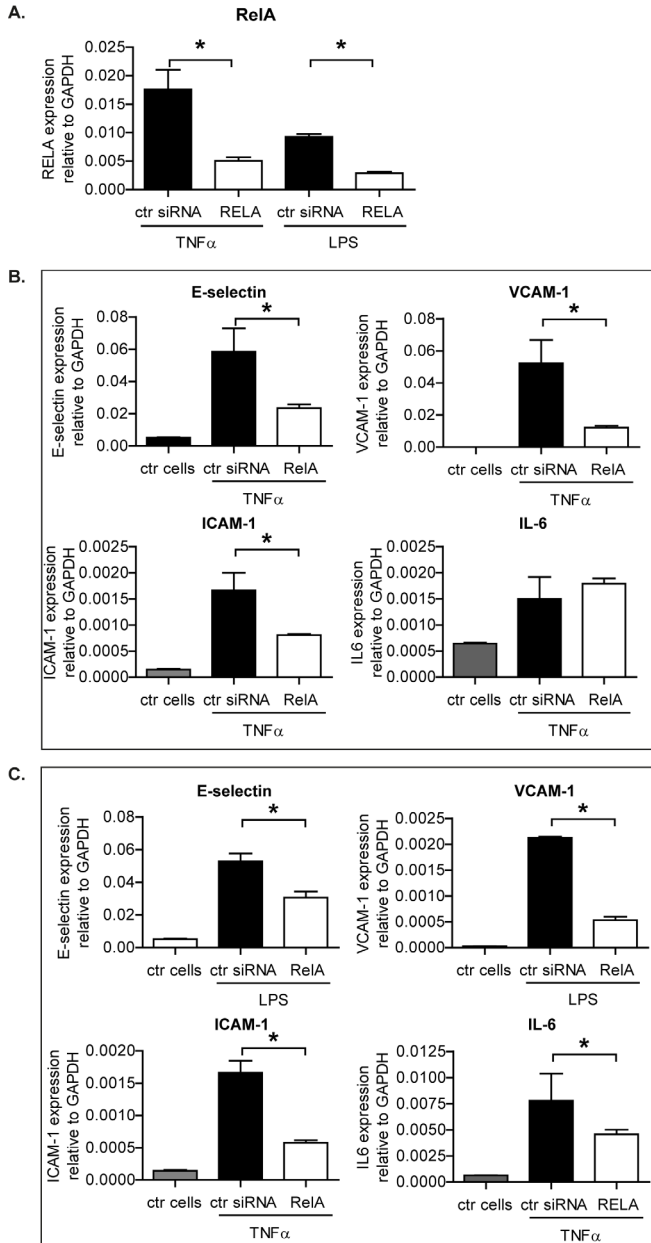
Supplementary data



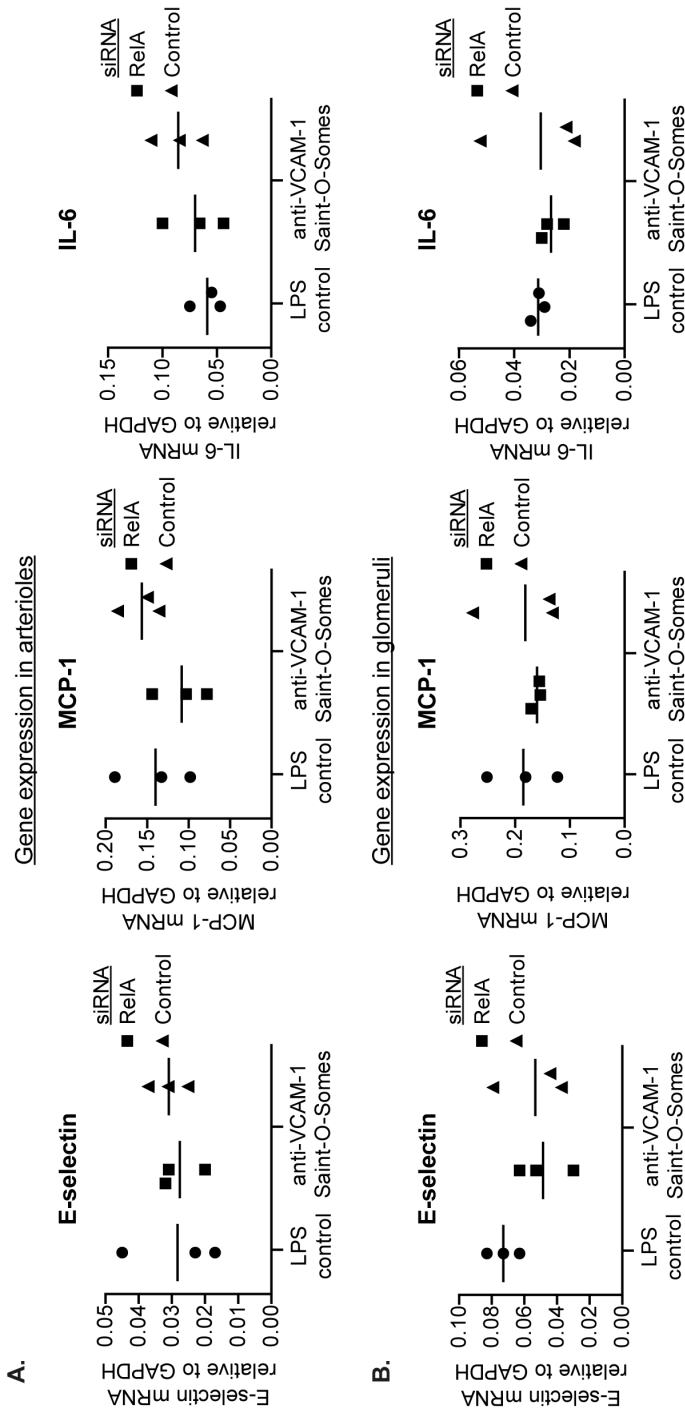
S1. Downregulation of NF κ B p65 (RelA) using siRNA attenuates the inflammatory response to TNF α and LPS in human endothelial cells. HUVEC were transfected with 60 nM of RelA specific or control siRNA (CS) using Lipofectamine 2000, according to the manufacturer's protocol. After 48 h, cells were challenged with either TNF α (10 ng/ml; Boehringer) or LPS (1 mg/ml) for the following 4 h or 25 min for immunofluorescent detection of RelA. Subsequent analysis of gene and protein expression was performed as described in 'Materials and Methods'. siRNA mediated downregulation of RelA (A) mRNA and (B) protein expression. Image shows a representative Western Blot of two independent experiments; (C) Absence of RelA in the nucleus upon pro-inflammatory activation. (D, E) Attenuation of pro-inflammatory gene expression in TNF α or LPS stimulated HUVEC upon downregulation of RelA. All RT-qPCR data are presented as mean values \pm SD, n=3. * $p < 0.05$; (C) Presented immunofluorescence data set show images from three independent experiments, original magnification 400x. Scale bar represents 50 μ m.



S2. Downregulation of RelA in endothelial cells inhibits TNF α and LPS induced production of pro-inflammatory cytokines IL-6 and IL-8. HUVEC were transfected with RelA or control siRNA using Lipofectamine 2000 and after 48 h they were exposed to TNF α or LPS for 4h as described for S1. IL-6 and IL-8 content in culture media, collected at the end of the experiment, was quantified using human IL-6 and IL-8 ELISA Max Standard Sets (BioLegend, San Diego, CA, USA). Inhibition of (A) IL-6 and (B) IL-8 production in TNF α or LPS activated HUVEC by downregulation of RelA. Data are presented as mean values \pm SD, n=4.



S3. Downregulation of RelA using siRNA attenuates inflammatory response to TNF α and LPS in mouse endothelial cells. H5V mouse heart endothelial cells were transfected with RelA or control siRNA using Lipofectamine 2000 and after 48 h they were exposed to *mr*TNF α (100 ng/ml) or LPS (1 μ g/ml) for 4 h. (A) siRNA mediated downregulation of RelA mRNA. (B, C) Attenuation of pro-inflammatory gene expression in TNF α or LPS stimulated cells upon downregulation of RelA. All RT-qPCR data are presented as mean values \pm SD, $n=3$. * $p < 0.05$.



S4. *Ab_{VCAM-1} siRNA_{RelA} SAINT-O-Somes treatment did not affect E-selectin, MCP-1 and IL-6 gene expression in kidney arterioles and glomeruli of LPS challenged mice. Mice were challenged with *mrTNF α* for 2 h, subsequently injected with anti-VCAM-1 SAINT-O-Somes containing (0.6 mg/kg) RelA specific or control siRNA and 48 h later re-challenged with LPS for 4 h, as described in 'Material and Methods'. (A) Kidney arterioles and (B) glomeruli were laser microdissected and samples were analyzed by RT-qPCR for E-selectin, MCP-1 and IL-6 gene expression. Data are presented as mean values \pm SD of 3 mice/group. * $p < 0.05$.*



Table 1. qPCR primers used for gene expression analysis

Primer	Cat. No.
<i>Housekeeping genes</i>	
GAPDH	Hs99999905_m1 Mm99999915_g1
<i>Adhesion molecules</i>	
E-selectin	Hs00174057_m1 Mm00441278_m1
VCAM-1	Hs00365486_m1 Mm00449197_m1
ICAM-1	Hs00164932_m1 Mm00516023_m1
PECAM-1 (CD31)	Hs00169777_m1 Mm00476702_m1
P-selectin	Mm00441295_m1
<i>Cytokines/chemokines</i>	
MCP-1	Hs00234140_m1 Mm00446190_m1
IL-6	Hs00174131_m1 Mm00433859_m1
IL-8	Hs00174131_m1 Mm00433859_m1
<i>Others</i>	
RelA (NFκB p65)	Hs00153294_m1 Mm00501346_m1
VE-cadherin	Mm00486938_m1

Species - Human (Hs), mouse (Mm).





Chapter 6

SAINT-Liposome-Polycation particles, a new carriers for improved delivery of siRNAs to inflamed endothelial cells

Piotr S. Kowalski¹, Praneeth R. Kuninty¹, Klaas T. Bijlsma¹, Marc C.A. Stuart³, Niek G.J. Leus¹, Marcel H.J. Ruiters^{1,2}, Grietje Molema¹, Jan A.A.M. Kamps¹

manuscript in preparation

¹University of Groningen, University Medical Center Groningen, Dept. of Pathology & Medical Biology, Medical Biology section, Laboratory for Endothelial Biomedicine & Vascular Drug Targeting research, Groningen, the Netherlands

²Synvolux Therapeutics, L.J. Zielstraweg 1, Groningen, the Netherlands

³University of Groningen, Centre for Systems Chemistry, Stratingh Institute, Groningen, the Netherlands

Abstract

Interference with acute and chronic inflammatory processes by means of delivery of siRNAs into microvascular endothelial cells at a site of inflammation demands specific, non-toxic and effective siRNA delivery system. In the current work we describe the design and characterization of siRNA carriers based on cationic pyridinium-derived lipid 1-methyl-4-(cis-9-dioleyl)methyl-pyridinium-chloride) (SAINT-C18) and the transfection enhancer protamine, complexed with siRNA/carrier DNA or siRNA only. These carriers, called SAINT-liposome-polycation-DNA (S-LPD) and SAINT-liposome-polycation (S-LP), have a high efficiency of siRNA encapsulation, low cellular toxicity, and superior efficacy of gene downregulation in endothelial cells *in vitro* as compared to DOTAP-LPD. Incorporation of 10 mol% PEG and anti-E-selectin antibody in these formulations resulted in selective siRNA delivery into activated endothelial cells. Furthermore, we showed that the physicochemical characteristics of S-LPD and S-LP, including size-stability and maintenance of the siRNA integrity in the presence of serum at 37 °C, comply with requirements for *in vivo* application.



Introduction

Nucleic acids such as short interfering RNAs (siRNA) are a promising new class of therapeutics, enabling specific interference with gene expression [1]. They can be therapeutically exploited for the inhibition of disease associated genes and provide the opportunity to address so far unmet therapeutic needs. However, unmodified or uncomplexed siRNAs (so-called “naked” siRNAs) are subjected to rapid clearance from the circulation by the liver and renal filtration, and are sensitive to degradation by serum RNases, which limits their application *in vivo* [2]. Therefore for the development of clinically suitable siRNA therapeutics, safe and effective delivery systems that are specifically taken up by diseased cells, are crucial.

The pivotal role of endothelial cells in the pathology of inflammatory diseases and cancer along with the identification of disease-associated molecular targets (e.g., E-selectin, VCAM-1, $\alpha_v\beta_3$ -integrins) on the endothelial cells [3] raised interest in the development of siRNA delivery devices for selective pharmacological intervention in the diseased endothelium. Systemic administration of siRNA via the bloodstream is a feasible route to reach the vascular endothelium, though only a few types of carriers suitable for *in vivo* siRNA delivery into endothelial cells have been developed so far [4]. We recently demonstrated specific delivery of siRNA to inflamed endothelial cells using two types of carriers based on cationic pyridinium-derived lipid 1-methyl-4-(cis-9-dioleyl)methyl-pyridinium-chloride (SAINT-C18), called SAINT-O-Somes and SAINTargs [4-6]. SAINT-C18 by itself is capable of delivering nucleic acids, and in combination with the helper-lipid 1,2-dioleoyl-sn-glycero-3-phosphoethanolamine (DOPE) it forms complexes with nucleic acids that are characterized by high transfection efficiency in the presence of serum and low toxicity *in vitro* [7]. Notably, administration of SAINT:DOPE (SD) also did not elicit any immune response or toxicity in mice [8, 9]. For *in vivo* application addition of polyethylene-glycol (PEG) to an siRNA carrier is often essential, to avoid RES and improve carrier stability in the serum [10]. However, PEGylation of SD lipoplexes significantly reduces their transfection efficacy [5] and enforces formulation of the particles only with a low amount of PEG (2 mol%), resulting in short blood circulation times (personal communication with N.G.J. Leus).

A major advantage of SD is the capacity to transfect not only siRNA or DNA but also proteins. Van der Gun et al. demonstrated that SD enables serum-insensitive protein delivery to various cell types, in contrast to other commercially available protection compounds [11]. Protamine is a small cationic protein with high arginine content that is FDA approved for parenteral administration [12]. Protamine aids DNA condensation and stabilization in sperm cells [13] and has attracted much attention as a nucleic acid transfection enhancer for gene delivery [12]. It was employed by Huang and coworkers to develop siRNA delivery systems called liposome-polycation-DNA (LPD) [14], that



comprise of siRNA and carrier DNA complexed with protamine and lipids. These formulations show gene silencing at relatively low doses (0.15-0.45 mg siRNA/kg), display a more uniform size than lipoplexes, and could be grafted with up to 20 mol% of PEG allowing a substantial reduction of clearance by the RES [15].

In order to improve the efficacy of gene silencing in endothelial cells and *in vivo* suitability of SAINT-based carriers, we formulated and characterized particles composed of a protamine complexed with siRNA/ctDNA or siRNA only, and encapsulated by SD liposomes, called SAINT-liposome-polycation-DNA (S-LPD) and SAINT-liposome-polycation (S-LP). These particles were examined for size, stability and influence of PEG grafting. Toxicity and VE-cadherin gene silencing efficacy in endothelial cells of S-LPD and S-LP was compared to liposome-polycation-DNA particles based on DOTAP : Cholesterol liposomes. When conjugated with anti-E-selectin antibodies, S-LPD and S-LP demonstrated selective siRNA delivery to activated endothelium. We showed that this novel SAINT-based systems allow efficient and specific siRNA delivery to inflamed endothelial cells and have physicochemical features that comply with demands for *in vivo* application.

Materials and methods

Materials

Lipids, 1,2-dioleoyl-3-trimethylammonium-propane (DOTAP), 1,2-dioleoyl-*sn*-glycero-3-phosphoethanolamine (DOPE), 1,2-distearoyl-*sn*-glycero-3-phosphoethanolamine-N-[methoxy(polyethylene glycol)-2000]-maleimide (DSPE-PEG₂₀₀₀-Mal), and 2-distearoyl-*sn*-glycero-3-phosphoethanolamine-N [methoxy(polyethylene glycol)-2000] (DSPE-PEG₂₀₀₀) were purchased from Avanti Polar Lipids (Alabaster AL, USA). The cationic lipid 1-methyl-4-(*cis*-9-dioleoyl)methyl-pyridinium-chloride (SAINT-C18) was obtained from Synvolux Therapeutics (Groningen, The Netherlands). Cholesterol (Chol), protamine (sulphate salt from Salmon), calf-thymus DNA (ct-DNA) and N-succinimidyl-S-acetylthioacetate (SATA) were purchased from Sigma (St. Louis, MO, USA). Nucleic acid stain DAPI was obtained from Roche Diagnostics (Manheim, Germany). All siRNAs were purchased from Qiagen (Venlo, The Netherlands).

The H18/7-acb (mouse IgG2a anti-human E-selectin) producing hybridoma was kindly provided by Dr. M. Gimbrone from Harvard Medical School (Boston, MA, USA).



Liposome preparation

Liposomes composed of SAINT and DOPE or DOTAP and Cholesterol in a molar ratio of 1:1 were prepared by lipid film hydration. Lipids were dissolved in chloroform/methanol (9:1, v/v) and dried under reduced nitrogen pressure and vacuum for 30 minutes. The dried lipid film was hydrated with RNase free water (Qiagen) for 10 minutes. Liposome size was reduced by repeated extrusion through a polycarbonate membrane (Whatman, Maidstone Kent, UK), pore size 100 nm, using a high pressure extruder (Lipex, Vancouver, Canada). The liposomes were stored at 4 °C under Argon gas.

Preparation of LPD and LP particles

To prepare SAINT : DOPE based LPD and LP, referred to as S-LPD respectively S-LP, protamine (1 mg/ml) and nucleic acids (NA) were mixed at a ratio of 0.75 (w/w) and incubated for 10 minutes at room temperature (RT). A 1:1 (w/w) mixture of siRNA (0.3 mg/ml) and calf thymus DNA (1 mg/ml) in RNase free water was used to form LPD, while an equivalent total NA amount of siRNA only was used for LP. Liposomes (10 mM) were added to the mixture at a ratio of 0.025 ($\mu\text{mol TL}/\mu\text{g NA}$). Samples were vortexed and incubated for 30 min at RT. DOTAP : Cholesterol based LPD were prepared as described by Li et al. [16] and are here referred to as DOTAP-LPD. Particles were PEGylated by post insertion of DSPE-PEG₂₀₀₀ micelles (3.56 mM) for 10 min at 50 °C. DSPE-PEG₂₀₀₀ micelles were prepared by lipid film hydration, as described for liposomes in paragraph 2.2., and added to the particles at indicated mol% PEG ratios. LPD and LP were used for the experiments within 1 hour after preparation.

Targeted S-LPD and S-LP were prepared by simultaneous post insertion of anti-E-selectin DSPE-PEG₂₀₀₀ micelles in a 1:4,000 molar ratio of protein/TL and non-targeted DSPE-PEG₂₀₀₀ micelles at indicated mol% PEG ratio. To prepare anti-E-selectin DSPE-PEG₂₀₀₀ micelles, antibodies were thiolated by means of SATA and coupled to the maleimide group at the distal end of the polyethylene glycol (DSPE-PEG₂₀₀₀-Mal) chain by sulfhydryl-maleimide coupling [17]. In brief, SATA-modified antibodies containing free sulfhydryl groups were added to DSPE-PEG₂₀₀₀-Mal micelles at a molar ratio of 1:20 and incubated at room temperature for 1 h. Excess of free DSPE-PEG₂₀₀₀-Mal micelles was removed by Zeba™ Desalt Spin Columns, 7K MWCO (Thermo Fisher Scientific, Rockford, IL, USA). Protein concentration of the anti-E-selectin DSPE-PEG₂₀₀₀ micelles was determined by measuring absorbance at 280 nm using NanoDrop® ND 1000 spectrophotometer (Thermo Fisher Scientific, Wilmington, DE, USA).



Characterization of S-LPD and S-LP particles

Particle size and ζ -potential were analyzed using a Nicomp 380 ZLS submicron particle analyzer (NICOMP particle sizing systems, Santa Barbara, CA, USA). Particle size was measured using dynamic light scattering (DLS) in the volume weighing mode. The Polydispersity index (PDI) was analyzed using a Malvern Zetasizer Nano ZSP (Malvern Instruments Ltd., Worcestershire, UK). S-LPD and S-LP particles were freshly prepared using control siRNA (Qiagen, AllStars Negative Control, cat No. 1027281) and, when indicated, formulated with various amounts of PEG-DSPE₂₀₀₀. The siRNA encapsulation efficiency was measured using the Quant-iT™ Ribo-Green® assay (Invitrogen, Breda, The Netherlands). For gel retardation, particles containing 200 ng siRNA were mixed with 1 % (v/v) Triton X-100 and 1% (v/v) SDS, and subsequently loaded on 2% agarose gel containing ethidium bromide (60 μ g/ml). Electrophoresis was performed at 15 min at 110 V. Images of the gel were taken using the ChemiDoc XRS system (Bio-rad, Veenendaal, The Netherlands).

Cryo-transmission electron microscopy (Cryo-TEM)

The morphology of S-LPD and S-LP particles was determined by transmission cryo-EM. Samples were applied on glow discharged holey carbon-coated grids (Quantifoil 3.5/1), and the excess of liquid was blotted away by filter paper. The specimens were frozen in liquid ethane using a vitrobot (FEI, Eindhoven, The, Netherlands) the frozen hydrated samples were mounted in a Gatan (mol 626) CRYOSTAGE and examined in a Philips CM 120 cryo-electron microscope, operating at 120 kV or in a FEI Tecnai 20 cryo-electron microscope operating at 200 kV. Images were recorded under low-dose conditions with a slow-scan CCD camera.

Cell cultures

Human umbilical vein endothelial cells (HUVEC) were obtained from Lonza (Breda, The Netherlands) and the Endothelial Cell Facility of UMCG. HUVEC obtained from Lonza were used for functional and uptake studies. Cells were cultured in EBM-2 medium supplemented with EGM-2 MV SingleQuote Kit Supplements & Growth Factors (cat No. CC-3202, Lonza). In all experiments, cells from passage 5 to 7 were used. Cells were plated on culture plates (Costar, Corning, NY) at a density of 1.8×10^4 cells/cm² one day before the experiment unless stated otherwise. Before seeding the cells, culture plates were coated with EGM2 MV medium for 30 min. Primary HUVEC isolated from two umbilical cords, to circumvent donor bias, were used to demonstrate siRNA delivery capacity of anti-E-selectin targeted LP particles. Isolated HUVEC showed higher induction of E-selectin expression upon TNF α stimulation, as compared to one obtained from Lonza. Cells were plated one day before the experiment at a density of 2.2×10^4 cells/cm² on 1% gelatin-precoated culture plates (Costar) and cultured in



EC-medium consisting of RPMI 1640 (Lonza, Verviers, Belgium) supplemented with 20% (v/v) heat inactivated fetal calf serum (FCS, Hyclone, Logan, UT, USA), 2 mM L-glutamine (GIBCO-BRL), 5 U/ml heparin (Leo Pharma, Breda, the Netherlands), 100 IU/ml penicillin (Yamanouchi Pharma, Leiderdorp, the Netherlands), 100 µg/ml streptomycin (Radiumfarma-Fisiopharma, Milano, Italy), and 20 µg/ml endothelial cell growth factor (ECGF) extracted from bovine brain (Maciag et al., 1982). Freshly isolated HUVEC were used between passage 1 and 4. All cell cultures were maintained by the Endothelial Cell Facility of UMCG.

Influence of serum on particles size-stability and siRNA integrity

To determine the effect of serum and temperature on size of the S-LPD and S-LP, particles were formulated with 10% DSPE-PEG₂₀₀₀ and incubated for 1, 4, and 24 h at 37 °C in the presence or absence of 50% human serum. The size of the particles was measured by DLS as described above.

To investigate the ability of S-LPD and S-LP to protect siRNA from degradation by serum RNases, particles containing 200 ng of control siRNA (Qiagen) were incubated in the presence of 50% human serum for different time periods up to 24 h at 37 °C. An equal amount of naked control siRNA was incubated with 50% human serum for the same period of time. siRNA integrity was analyzed by agarose gel electrophoresis as described above.

Cellular uptake of S-LPD and S-LP by endothelial cells

For the flow cytometry experiments, HUVEC were seeded in 24-well plates at a density of 2.2×10^4 cells/cm². 2 hours prior siRNA delivery cells were activated with TNF α (10 ng/ml), that remained present in the medium during the experiment. S-LPD and S-LP or DOTAP-LPD particles complexed with AlexaFluor₄₈₈ labeled control siRNA (Qiagen) were added to the cells for 4 hours at 50 nM siRNA. To demonstrate specificity of E-selectin mediated uptake cells were pre-incubated for 5 min with 75-fold excess of anti-E-selectin antibody. At 4 after transfection, cells were washed twice with PBS and detached from the surface using trypsin/EDTA (Sigma, Ayrshire, UK), subsequently they were transferred to tubes containing 5% FBS (fetal bovine serum, Thermo Scientific HyClone, Cramlington, UK) in PBS and kept on ice. Next, samples were centrifuged for 5 min at 500 g at 4 °C, washed twice with 5% FBS in PBS and resuspended in 0.5% paraformaldehyde/PBS. Cells were stored at 4 °C until flow cytometry (Calibur, BD Biosciences, Franklin Lakes, NJ). The results were analyzed using FlowJo software v7.6.5.



Gene expression analysis by RT-qPCR

For gene expression analysis, HUVEC were seeded in 24-well plates. After 2 h of activation with TNF α (10 ng/mL), S-LPD and S-LP or DOTAP-LPD particles containing VE-cadherin specific siRNA (Hs_CDH5_2 FlexiTube siRNA, target sequence 5'-ACGTATTATTATCACAATAACGAA-3') or control siRNA, with no homology to any known mammalian gene, were added to the cells at 25-300 nM and incubated for 4 h. TNF α was present in the medium during the entire incubation period. After 48 h total RNA was isolated using the RNeasy Mini Plus Kit (Qiagen, Venlo, The Netherlands) according to the protocol of the manufacturer. The concentration of RNA was measured by a NanoDrop ND-1000 spectrophotometer, and qualitative gel electrophoresis consistently showed intact RNA integrity. cDNA synthesis and quantitative (q) PCR, including data analysis, were performed as described previously [18]. The real-time PCR primers for human VE-cadherin (Hs00174344_m1) and GAPDH (Hs99999905_m1) were purchased as Assay-on-Demand from Applied Biosystems (Nieuwekerk a/d IJssel, The Netherlands). Gene expression levels were normalized to the expression of the reference gene GAPDH.

Investigation of cellular toxicity by MTS assay

HUVEC were seeded in 96-well plates. Incubations with TNF α and particles were performed as described in 2.9. After 48 h, cells were washed with PBS and incubated with CellTiter 96® AQueous One Solution reagent (Promega, Leiden, The Netherlands) diluted 1:5 (v/v) in culture medium. After 1.5 h, the absorbance at 490 nm was recorded with a Varioskan Flash Multimode reader (Thermo Scientific, Breda, The Netherlands). Absorbance of the activated endothelial cells without the addition of particles was set as 100%.

Statistical analysis

Statistical analysis of the results was performed by a two-tailed unpaired Student's t-test, assuming equal variances to compare two replicate means, or One-Way ANOVA followed by Bonferroni post-hoc analysis to compare multiple replicate means. Differences were considered significant when $p < 0.05$.



Results

Preparation and optimization of SAINT-LPD and LP particles

In the present study we aimed to formulate SAINT-based LPD and LP particles composed of a protamine/nucleic acids (NA) core complex encapsulated by SAINT:DOPE liposomes, called S-LPD and S-LP (Fig. 1). Prior to formulation of the S-LPD and S-LP, core complexes were prepared with varying ratios of protamine, calf thymus DNA and siRNA to study the influence on the core size and z-potential (Fig 2). Cores including siRNA and ctDNA showed a smaller mean size and increase in z-potential with an increasing ratio of protamine/NA (Fig. 2A, B). Cores containing only siRNA exhibited an increase in z-potential but no change in mean particle sizes upon increasing the ratio of protamine/NA (Fig. 2C, D). A protamine/NA ratio of 0.75 resulted in cores with a mean size of approximately 200 nm, z-potential close to -10 mV and good NA complexation (Fig. S1), and was considered optimal to formulate S-LPD and S-LP particles. Core complexes prepared using the selected ratio of protamine/NA ratio were subsequently complexed with SAINT:DOPE liposomes forming S-LPD and S-LP particles. S-LP based on protamine/siRNA formed significantly smaller particles, of approximately 150 nm, with lower z-potential as compared to S-LPD, prepared using protamine/ctDNA + siRNA (Table 1).

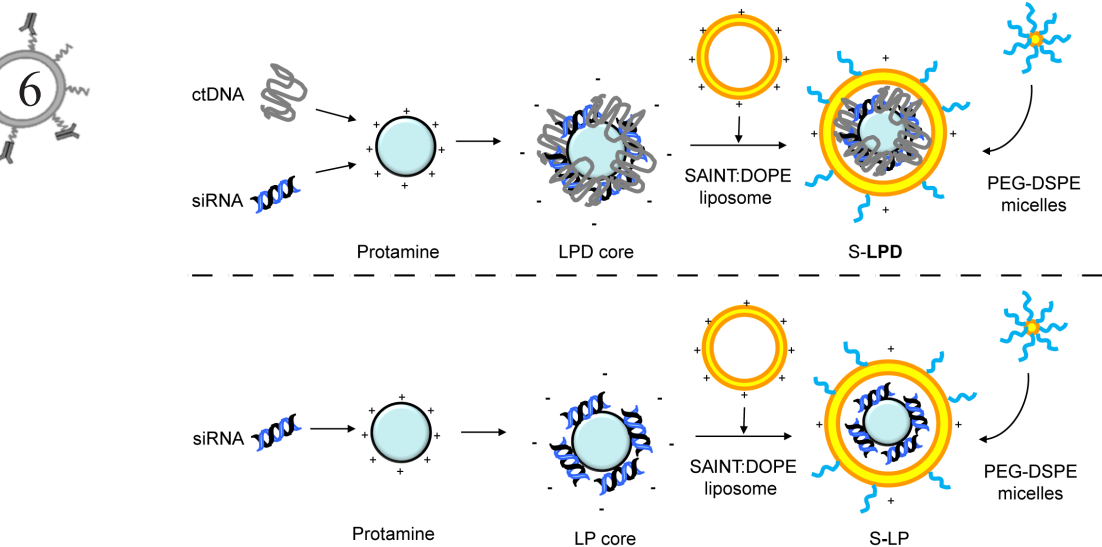


Figure 1. Hypothetical schematic overview of SAINT-LPD and LP particle formulation.

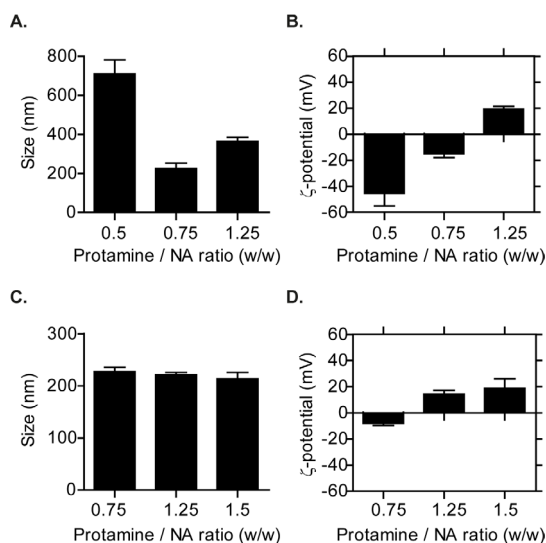


Figure 2. Optimization of the particle core by varying protamine/NA ratios. Mean size and ζ -potential of the particle cores prepared with varying ratios of protamine/nucleic acid (NA). (A, B) Protamine/ctDNA + siRNA based particle core, (C, D) protamine/siRNA based particle core. Data are presented as mean values of three independent preparations \pm SD.

Table 1. Physicochemical properties of SAINT-LPD (S-LPD) and SAINT-LP (S-LP) particles containing various amounts of PEG

	Size [nm]	Polydispersity Index	Zeta Potential [mV]
S-LP	144 \pm 8@	0.17 \pm 0.02	25.6 \pm 5@
S-LP 5% PEG	155 \pm 14@	0.16 \pm 0.02	27.8 \pm 10
S-LP 10% PEG	199 \pm 3*@	0.19 \pm 0.04	11.2 \pm 5*@
S-LP 20% PEG	256 \pm 16*@	0.26 \pm 0.05*@	0.5 \pm 4*
S-LPD	202 \pm 7	0.19 \pm 0.02	37.3 \pm 5
S-LPD 5% PEG	216 \pm 6	0.18 \pm 0.01	17.3 \pm 3*
S-LPD 10% PEG	225 \pm 13*	0.19 \pm 0.02	23.3 \pm 8*
S-LPD 20% PEG	285 \pm 8*	0.39 \pm 0.04*	2.6 \pm 5*

Data are presented as means of 3 preparations \pm SD. * $P < 0.05$ vs 0% PEG; @ $P < 0.05$ vs S-LPD.



Steric stabilization of S-LPD and S-LP particles by PEGylation

Particles were PEGylated by the post-insertion method with 5-20 mol% PEG-DSPE₂₀₀₀. Increasing PEG in the formulation resulted in a significant decrease in z-potential of both S-LPD and S-LP particles down to 0.5-2.6 mV with 20 mol% PEG (Table 1). The siRNA delivery capacity of S-LPD and S-LP to endothelial cells was hampered by an increasing amount of PEG in the formulation (Fig. S2) up to 10 mol% PEG. Formulations with 20 mol% PEG showed an increase in size and polydispersity compared to one with 10 mol% PEG (Table 1). 10% surface density of PEG was thus considered optimal for PEGylated formulations. 10% PEG S-LP and S-LPD presented comparable siRNA delivery capacity to endothelial cells, while S-LP displayed significantly smaller mean particle size (199 ± 3 nm) and lower z-potential (11.2 ± 5 mV) than S-LPD (Table 1).

Characterization of the nanoparticles

The morphology of S-LPD and S-LP nanoparticles was characterized using Cryo-EM microscopy (Fig. 3A). Both S-LPD and S-LP formed uniform particles with a lipid bilayer surrounding an irregularly shaped core (Fig. 3A a1, a2). A few particles with a typical electron-dense fingerprint structure, which reflects a hexagonal organization of the lipid bilayer (H_{II}), were seen in the populations. The influence of 10% PEG on the morphology of particles is currently being investigated (data not shown).

Both non-PEGylated and 10% PEG S-LPD and S-LP displayed a high efficiency of siRNA encapsulation, as demonstrated in the gel retardation assay (Fig. 3B, C).

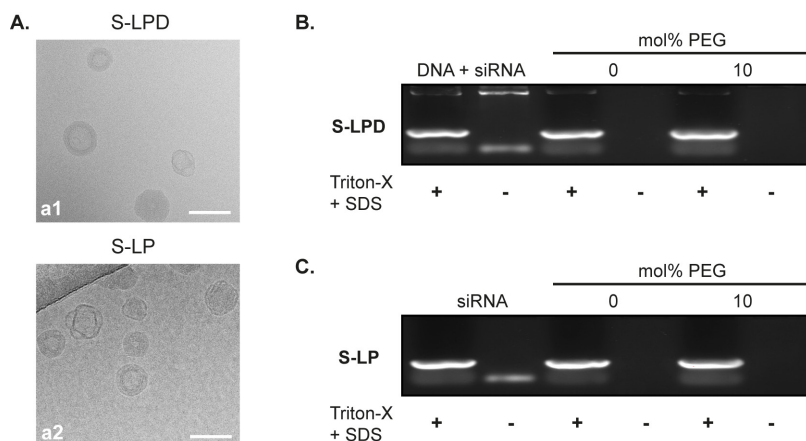


Figure 3. Characterization of the S-LPD and S-LP particles. (A) Cryo-EM images of S-LPD and S-LP particles formulated without PEG (a1, a2). The ability of non-PEGylated and PEGylated (B) S-LPD and (C) S-LP particles to encapsulate siRNA was investigated by 2% agarose gel electrophoresis.

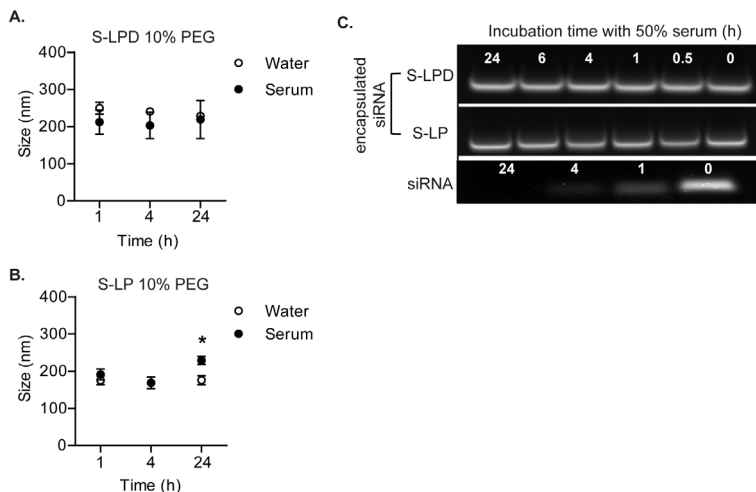


Figure 4. Influence of serum on particle size-stability and siRNA integrity. Size stability of (A) S-LPD and (B) S-LP formulated with 10 mol% PEG-DSPE2000 was determined in the (●) presence or (○) absence of 50% serum at different time points at 37 °C. Data are presented as the mean diameter (nm) \pm SD of three preparations. (C) Maintenance of siRNA integrity encapsulated in the particles was studied by agarose gel electrophoresis of equal amounts of nonencapsulated and encapsulated siRNA incubated in 50% human serum at 37 °C.

Based on the RiboGreen assay, the siRNA encapsulation efficiency of S-LP was 98% (data not shown), while exact siRNA encapsulation efficiencies of S-LPD could not be determined due to interference of ctDNA with the assay.

To investigate the Influence of serum on size-stability and maintenance of siRNA integrity by 10% PEG S-LPD and S-LP, particles were incubated with 50% human serum at 37 °C (Fig. 4). Both 10% PEG S-LPD and S-LP showed good size stability in the presence of serum for 24 h (Fig. 4A, B). Additionally, nonencapsulated siRNA was entirely degraded in the serum within 4 h, whereas formulation into S-LPD and S-LP preserved the integrity of siRNA for 24 h (Fig. 4C).

10% PEG S-LPD and S-LP show low toxicity and high efficacy of gene downregulation in endothelial cells.

We used VE-cadherin, the expression of which is restricted to endothelial cells and maintained under TNF α stimulation [4, 19], as a model gene to investigate the capacity of gene downregulation by S-LPD and S-LP. HUVEC cells were incubated for 4 h with non-PEGylated respectively 10% PEG S-LPD or S-LP or DOTAP-LPD particles containing VE-cadherin specific or control siRNA at siRNA concentrations ranging from 25-300 nM. Non-PEGylated S-LP had the least effect on cell viability as compared to S-LPD and DOTAP-LPD particles (Fig. 5A-C) and showed efficient VE-cadherin gene silencing with an approximated IC₅₀ of 34 nM siRNA, which is a 3-fold



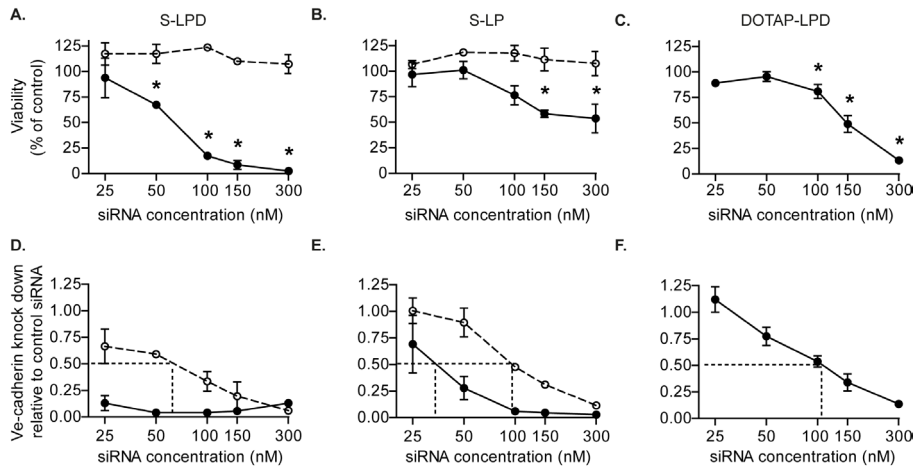


Figure 5. Toxicity of S-LPD and S-LP particles and their capacity to downregulate VE-cadherin in endothelial cells. HUVEC were incubated for 4 h with non-PEGylated S-LPD, S-LP and DOTAP LPD particles (●) or S-LPD and S-LP formulated with 10 mol% PEG-DSPE2000 (○), containing VE-cadherin specific or control siRNA at siRNA concentrations ranging from 25-300 nM. (A - C). Viability of the cells was analyzed after 48 h as described in M&M section. Viability of the cells without addition of the particles was set at 100%. Data are presented as mean values \pm SD (n=3). * $P < 0.05$ vs control; (D-E) VE-cadherin downregulation by (●) non-PEGylated or (○) 10% PEG S-LPD, S-LP or DOTAP-LPD particles. 48 h after incubation with the particles RNA was isolated and VE-cadherin gene expression was determined by RT-qPCR. Data are presented as mean values \pm SD of three independent experiments. Dotted lines indicate estimated IC50.

lower than the IC50 of DOTAP-LPD (108 nM) (Fig. 5D-F). The IC50 of S-LPD could not be determined in the selected concentration range, moreover siRNA delivery at siRNA concentrations higher than 25 nM resulted in a profound decrease in endothelial cell viability (Fig. 5A). Post insertion of 10 mol% PEG diminished toxicity associated with S-LPD and S-LP siRNA delivery (Fig. 5A, B) but led to a decrease in efficacy of gene downregulation (Fig. 5D, E). 10% PEG S-LPD had an estimated IC50 of 62 nM, while the IC50 of 10% PEG S-LP was 92 nM.

Selective siRNA delivery to activated primary endothelial cells by anti-E-selectin 10% PEG S-LPD and S-LP particles.

To achieve specific delivery of siRNA to activated endothelial cells, 10% PEG S-LPD and 10% PEG S-LP particles were conjugated with antibodies directed against E-selectin. Uptake of the particles formulated with AlexaFluor₄₈₈ siRNA was investigated in resting and TNF α activated HUVEC by flow cytometry. As compared to the resting cells, both anti-E-selectin 10% PEG S-LPD and anti-E-selectin 10% PEG S-LP showed a 8-10 fold increase in siRNA uptake in TNF α activated HUVEC (Fig. 6A, B), while uptake of IgG and non-targeted particles in quiescent and in activated cell

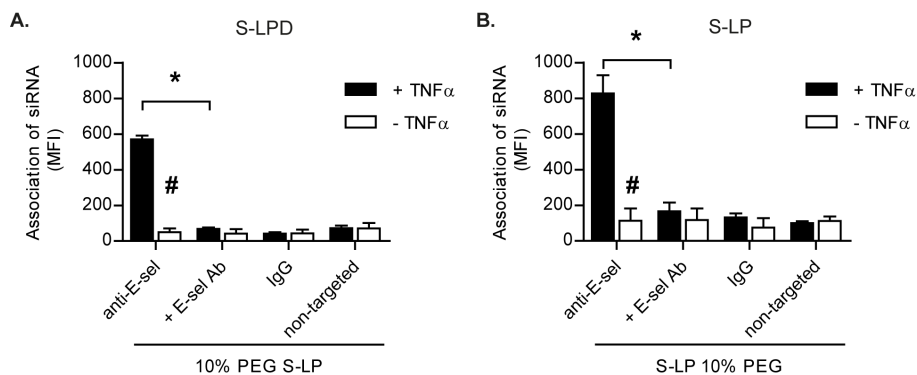


Figure 6. Selective delivery of siRNA to activated primary endothelial cells by anti-E-selectin targeted S-LPD and S-LP particles. Quiescent and TNF α activated HUVEC were incubated for 4 h with anti-E-selectin 10 mol% PEG (A) S-LPD and (B) S-LP particles containing AlexaFluor488 siRNA. Specificity of association to E-selectin, was shown by co-incubation of the cells with excess of anti-E-selectin monoclonal antibodies together with the particles. The association of siRNA with the cells was quantified by flow cytometry. Data are presented as mean fluorescence intensity (MFI) values \pm SD of three independent experiments. * $P < 0.05$, # $P < 0.05$ - TNF α vs + TNF α .

was comparable. Specificity of association was demonstrated by blocking E-selectin with an excess of anti-E-selectin antibodies prior to incubation with the particles. This resulted in an almost complete decrease in the uptake of siRNA by activated endothelial cells (Fig. 6A, B).

Discussion

Specific and effective delivery without exerting toxicity is a key challenge and the most significant barrier for siRNA technology to become therapeutically applicable. Interference with acute and chronic inflammatory processes by means of downregulation of key controllers of endothelial cells activation at a site of inflammation demands, therefore, a suitable siRNA delivery system. In the current work we describe the design and characterization of siRNA carriers which combine SAINT-technology with protamine as a transfection enhancer, and show their ability for the delivery of siRNA into inflammation-activated endothelial cells. These so called, S-LPD and S-LP particles showed high efficacy of siRNA encapsulation, low *in vitro* toxicity and efficient gene downregulation in endothelial cells, that were compared to conventional LPD particles based on DOTAP : Cholesterol [14]. Incorporation of 10 mol% PEG and anti-E-selectin antibody in the formulation of the carriers resulted in selective siRNA delivery into TNF α activated endothelial cells. Furthermore, we showed that the physicochemical characteristics of S-LPD and S-LP, including size-stability and maintenance of siRNA



integrity in the presence of serum at 37 °C, comply with demands for *in vivo* application.

LPD particles originally formulated by the group of Huang et al, with DOTAP : Cholesterol liposomes, offer several advantages for *in vivo* siRNA delivery over conventional lipoplexes such as good stability in physiological milieu and low RES uptake [20]. Due to the above properties, LPD were primarily applied in experimental RNAi-based tumor therapy. Several studies demonstrated high tumor targeting using anisamide-coated PEGylated LPD [1, 16], and recently RGD-targeted PEGylated LPD formulations were used to silence expression of VEGFR-2 receptor in angiogenic endothelial cells *in vitro* [21]. Still, these particles demonstrated moderate cellular toxicity as well as moderate efficacy of gene silencing due to poor intracellular release of siRNA [15]. Toxicity of LPD formulation was reduced by replacement of carrier DNA with hyaluronic acid [22], but efficacy of intracellular siRNA release still remains an issue. Here we prepared targeted S-LPD and S-LP based on protamine-siRNA/carrier DNA or protamine-siRNA core, that were complexed with SAINT : DOPE liposomes and engrafted with DSPE-PEG₂₀₀₀. The optimized protamine/NA ratios for S-LPD and S-LP was 0.75 (Fig. 2). Further increasing these ratio resulted in core formulations with positive net charge that would interfere in the interaction with cationic lipids and hamper the core complexation by the liposomes. Addition of SD liposomes to the cores yielded uniform particles with a diameter of 150-200 nm and a double lipid bilayer structure, as revealed by Cryo-TEM, comparable to DOTAP-LPD [20]. We further demonstrated that S-LPD and S-LP formulations displayed higher gene silencing potency than DOTAP-LPD, reflected by a 3-fold lower siRNA concentration required to silence a target gene VE-cadherin mRNA to 50% of control expression. Since DOTAP-LPD delivered more siRNA to the endothelial cells than S-LPD and S-LP (Fig. S2) and all particles displayed comparable sizes (120 - 200 nm), the observed differences in VE-cadherin silencing were likely related to the ability of the particles to intracellularly release the siRNA. It has been shown that SD lipoplexes facilitate intermembrane interactions by adopting a hexagonal phase at physiological conditions [7, 23], promoted by the lipid membrane destabilizing effect of DOPE [24]. Therefore, the use of SAINT : DOPE in the formulation of S-LPD and S-LP could significantly improve siRNA release from the carrier and the endosomes [25] by allowing more effective hexagonal phase transition than DOTAP : Cholesterol formulations. Further studies focusing on the intracellular siRNA release mechanism involving S-LPD and S-LP are needed to validate this hypothesis.

S-LPD were approximately 4-fold more potent in VE-cadherin silencing than S-LP (Fig. 5B). This increase in potency may result from the weaker interaction of the siRNA with the protamine caused by the presence of high molecular weight ctDNA, enabling more efficient siRNA release, or improved particle stability enabled by higher core compaction as advocated by Li et al. [14]. S-LPD on the other hand caused a dose



dependent decrease in the endothelial cell viability, starting at 50 nM siRNA, while S-LP affected the cell viability starting at 3-fold higher siRNA concentrations. S-LP were also less harmful for the cells than DOTAP-LPD (Fig 5A). Greater toxicity of S-LPD and DOTAP-LPD likely results from the presence of ctDNA in the formulation, which as a foreign DNA may elicit toxicity related to the presence of immunostimulatory CpG motifs [26]. Toxicity of the S-LPD and S-LP particles was reduced by addition of 10 mol% PEG to the formulation, however, that decreased delivery of siRNA and ctDNA to the cells.

In many studies, lipoplexes containing DOPE showed reduced stability and activity *in vivo* [27]. DOPE also significantly decreased the *in vivo* activity of DOTAP-LPD by decreasing the stability of lipid bilayer, resulting in high association with the serum proteins and increase in particle size [28]. In our study S-LPD and S-LP were grafted with 10% PEG to limit their toxicity and increase the stability in physiological conditions. 10% PEG S-LPD did not show any increase in size, while the size of S-LP only slightly increased after 24 h incubation with serum at 37 °C. Moreover, both particles were able to maintain siRNA integrity for the whole incubation period. Demonstrated particle and siRNA stability in the presence of serum indicates that S-LPD and S-LP comply with demands for *in vivo* application. In contrast, SD lipoplexes significantly lose their siRNA delivery capacity to HUVEC when grafted with 2 mol% PEG [5], S-LPD and S-LP maintained their siRNA delivery ability even with 10 mol% PEG (Fig 5). Comparison of the morphology of PEGylated SD lipoplexes with PEGylated S-LPD and S-LP using Cryo-TEM and studying their phase transition with differential scanning calorimetry may shed more light on the distinct influence of PEGylation on both types of particles. While addition of 10 mol% PEG hampered interaction of the S-LPD and S-LP particles with activated endothelial cells (Fig. 6 and S2), the combination with post insertion of anti-E-selectin DSPE-PEG₂₀₀₀ micelles allowed us to create specificity for these cells via interaction with E-selectin. 8 to 10 fold more siRNA was delivered to activated HUVEC by anti-E-selectin S-LPD and S-LP as compared to IgG conjugated particles. Specificity to E-selectin was demonstrated by co-incubation of the cells with an excess of anti-E-selectin antibodies together with the anti-E-selectin S-LPD and S-LP.

Other siRNA delivery systems based on SAINT-C18, such as SAINT-O-Somes and SAINTarg are already in the later stage of development and have been tested *in vivo*, thus for an adequate comparison further *in vivo* studies with S-LP and S-LPD need to be performed. Based on our *in vitro* result, S-LPD and S-LP were more potent in VE-cadherin silencing than SAINT-O-Somes (approx. 10–fold) and could accommodate more PEG on the particle surface without substantial loss of silencing potency as compared to SAINTargs. Moreover, anti-E-selectin S-LPD and S-LP showed comparable selectivity of siRNA delivery to activated endothelial cells as other



SAINT-based systems. High silencing potency and 98% siRNA encapsulation efficacy presented by S-LPD and S-LP allows the use of multiple therapeutic siRNAs in one formulation without the need for substantial dose increase, in order to reach the effective siRNA concentration in the target cells. Targeted LPD co-formulated with combination of siRNAs against c-Myc, MDM2, and vascular endothelial growth factor (VEGF) significantly reduced the lung metastasis and increased the survival time of the tumor-bearing animals [29]. Attractive molecular targets for simultaneous gene silencing in the endothelial cells may be the members of the NF κ B and p38 MAPK families, based on their inherent association with inflammatory activation of the endothelium.

In summary, this study reports on new SAINT-based carriers formulated with protamine, that allow selective and functional siRNA delivery into inflammation activated endothelial cells, mediate potent downregulation of a target gene, and are suitable for *in vivo* application based on their physicochemical and features. S-LPD and S-LP are thus novel SAINT-based siRNA delivery systems that can offer an improvement in *in vivo* siRNA delivery to disease-associated endothelial cell subsets in different vascular segments, although thorough validation of this system in animal models is essential.

Acknowledgements

We thank Henk Moorlag and Peter J. Zwiers for excellent technical assistance. Dr. Ed Talman is acknowledged for providing high quality SAINT-C18.

This work was supported by EFRO (European Fund for Regional Development) from the European Union, project NTS 068 and 073 Drug Delivery and Targeting. The authors declare no competing financial interests. M.H.J. Ruiters is CEO of Synvolux Therapeutics.

References

1. K.A. Whitehead, R. Langer, D.G. Anderson, Knocking down barriers: advances in siRNA delivery, *Nat Rev Drug Discov*, 8 (2009) 129-138.
2. Y. Huang, J. Hong, S. Zheng, Y. Ding, S. Guo, H. Zhang, X. Zhang, Q. Du, Z. Liang, Elimination pathways of systemically delivered siRNA, *Mol Ther*, 19 (2011) 381-385.
3. E. Simone, B.S. Ding, V. Muzykantov, Targeted delivery of therapeutics to endothelium, *Cell Tissue Res*, 335 (2009) 283-300.
4. P.S. Kowalski, L.L. Lintermans, H.W. Morselt, N.G. Leus, M.H. Ruiters, G. Molema, J.A. Kamps, Anti-VCAM-1 and Anti-E-selectin SAINT-O-Somes for Selective Delivery of siRNA into Inflammation-Activated Primary Endothelial Cells, *Mol Pharm*, 10 (2013) 3033-3044.
5. N.G. Leus, E.G. Talman, P. Ramana, P.S. Kowalski, T.E. Woudenberg-Vrenken, M.H. Ruiters, G. Molema, J.A. Kamps, Effective siRNA delivery to inflamed primary vascular



- endothelial cells by anti-E-selectin and anti-VCAM-1 PEGylated SAINT-based lipoplexes, *Int J Pharm*, 459 (2014) 40-50.
6. S.A. Asgeirsdottir, E.G. Talman, I.A. de Graaf, J.A. Kamps, S.C. Satchell, P.W. Mathieson, M.H. Ruiters, G. Molema, Targeted transfection increases siRNA uptake and gene silencing of primary endothelial cells in vitro--a quantitative study, *J Control Release*, 141 (2010) 241-251.
 7. I. van der Woude, A. Wagenaar, A.A. Meekel, M.B. ter Beest, M.H. Ruiters, J.B. Engberts, D. Hoekstra, Novel pyridinium surfactants for efficient, nontoxic in vitro gene delivery, *Proc Natl Acad Sci U S A*, 94 (1997) 1160-1165.
 8. S. Audouy, D. Hoekstra, Cationic lipid-mediated transfection in vitro and in vivo (review), *Mol Membr Biol*, 18 (2001) 129-143.
 9. S.A. Audouy, L.F. de Leij, D. Hoekstra, G. Molema, In vivo characteristics of cationic liposomes as delivery vectors for gene therapy, *Pharm Res*, 19 (2002) 1599-1605.
 10. V.P. Torchilin, Recent advances with liposomes as pharmaceutical carriers, *Nat Rev Drug Discov*, 4 (2005) 145-160.
 11. B.T. van der Gun, A. Monami, S. Laarmann, T. Rasko, K. Slaska-Kiss, E. Weinhold, R. Wasserkort, L.F. de Leij, M.H. Ruiters, A. Kiss, P.M. McLaughlin, Serum insensitive, intranuclear protein delivery by the multipurpose cationic lipid SAINT-2, *J Control Release*, 123 (2007) 228-238.
 12. Y. Tsuchiya, T. Ishti, Y. Okahata, T. Sato, Characterization of protamine as a transfection accelerator for gene delivery, *J Bioact. Compat. Polym.*, 21 (2006) 519-537.
 13. R.E. Braun, Packaging paternal chromosomes with protamine, *Nat Genet*, 28 (2001) 10-12.
 14. S.D. Li, L. Huang, Targeted delivery of antisense oligodeoxynucleotide and small interference RNA into lung cancer cells, *Mol Pharm*, 3 (2006) 579-588.
 15. S. Zhang, D. Zhi, L. Huang, Lipid-based vectors for siRNA delivery, *J Drug Target*, 20 (2012) 724-735.
 16. S.D. Li, S. Chono, L. Huang, Efficient gene silencing in metastatic tumor by siRNA formulated in surface-modified nanoparticles, *J Control Release*, 126 (2008) 77-84.
 17. J.A. Kamps, P.J. Swart, H.W. Morselt, R. Pauwels, M.P. De Bethune, E. De Clercq, D.K. Meijer, G.L. Scherphof, Preparation and characterization of conjugates of (modified) human serum albumin and liposomes: drug carriers with an intrinsic anti-HIV activity, *Biochim Biophys Acta*, 1278 (1996) 183-190.
 18. J.E. Adrian, H.W. Morselt, R. Suss, S. Barnert, J.W. Kok, S.A. Asgeirsdottir, M.H. Ruiters, G. Molema, J.A. Kamps, Targeted SAINT-O-Somes for improved intracellular delivery of siRNA and cytotoxic drugs into endothelial cells, *J Control Release*, 144 (2010) 341-349.
 19. E. Dejana, Endothelial cell-cell junctions: happy together, *Nat Rev Mol Cell Biol*, 5 (2004) 261-270.
 20. S.D. Li, L. Huang, Nanoparticles evading the reticuloendothelial system: role of the supported bilayer, *Biochim Biophys Acta*, 1788 (2009) 2259-2266.
 21. P. Vader, B.J. Crielaard, S.M. van Dommelen, R. van der Meel, G. Storm, R.M. Schiffelers, Targeted delivery of small interfering RNA to angiogenic endothelial cells with liposome-polycation-DNA particles, *J Control Release*, 160 (2012) 211-216.
 22. S. Chono, S.D. Li, C.C. Conwell, L. Huang, An efficient and low immunostimulatory nanoparticle formulation for systemic siRNA delivery to the tumor, *J Control Release*, 131 (2008) 64-69.
 23. I.S. Zuhorn, V. Oberle, W.H. Visser, J.B. Engberts, U. Bakowsky, E. Polushkin, D. Hoekstra, Phase behavior of cationic amphiphiles and their mixtures with helper lipid influences lipoplex shape, DNA translocation, and transfection efficiency, *Biophys J*, 83 (2002) 2096-2108.
 24. J. Smisterova, A. Wagenaar, M.C. Stuart, E. Polushkin, G. ten Brinke, R. Hulst, J.B. Engberts, D. Hoekstra, Molecular shape of the cationic lipid controls the structure of cationic lipid/dioleoylphosphatidylethanolamine-DNA complexes and the efficiency of gene delivery, *J Biol Chem*, 276 (2001) 47615-47622.
 25. L.K. Medina-Kauwe, J. Xie, S. Hamm-Alvarez, Intracellular trafficking of nonviral vectors, *Gene Ther*, 12 (2005) 1734-1751.
 26. D.A. Schwartz, T.J. Quinn, P.S. Thorne, S.



- Sayeed, A.K. Yi, A.M. Krieg, CpG motifs in bacterial DNA cause inflammation in the lower respiratory tract, *J Clin Invest*, 100 (1997) 68-73.
27. Y. Liu, L.C. Mounkes, H.D. Liggitt, C.S. Brown, I. Solodin, T.D. Heath, R.J. Debs, Factors influencing the efficiency of cationic liposome-mediated intravenous gene delivery, *Nat Biotechnol*, 15 (1997) 167-173.
28. S. Li, M.A. Rizzo, S. Bhattacharya, L. Huang, Characterization of cationic lipid-protamine-DNA (LPD) complexes for intravenous gene delivery, *Gene Ther*, 5 (1998) 930-937.
29. S.D. Li, S. Chono, L. Huang, Efficient oncogene silencing and metastasis inhibition via systemic delivery of siRNA, *Mol Ther*, 16 (2008) 942-946.

Supplementary data

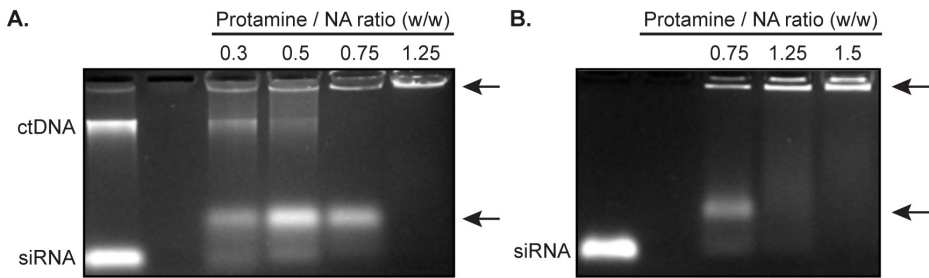


Figure S1. Gel retardation of protamine/NA particle cores. Cores composed of (A) protamine/ctDNA+siRNA and (B) protamine/siRNA were prepared with various ratios of protamine/ NA (w/w) and were resolved on 2% agarose gel by electrophoresis. Arrows indicate positions of the core in the gel. Data show a representative image of the gel.

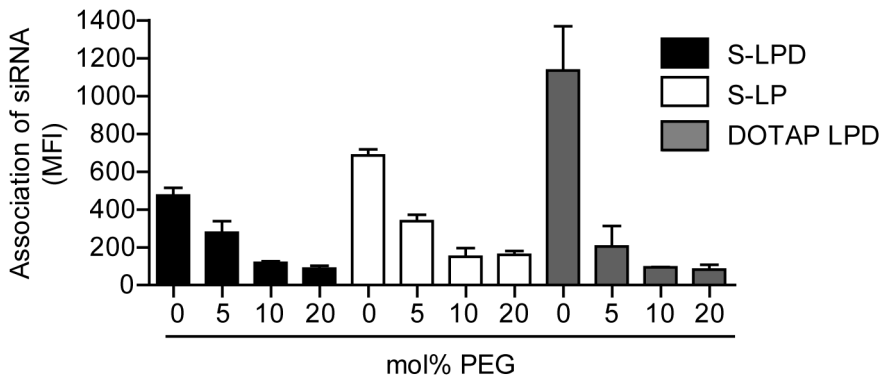


Figure S2. Delivery of siRNA by S-LPD or S-LP particles to endothelial cells. HUVEC were incubated for 4 h with S-LP, S-LPD or DOTAP LPD particles formulated with various amounts of PEG-DSPE2000 and containing AlexaFluor488 siRNA at 50 nM concentration. The uptake of siRNA by the cells was quantified by flow cytometry. Data are presented as mean fluorescence intensity (MFI) values \pm SD ($n=3$).



Chapter 7

Summary, Conclusions and
Future perspectives

Summary

The discovery and application of RNA interference (RNAi) has transformed basic research and markedly advanced our understanding of eukaryotic gene regulation and function. Until now, short interfering RNAs (siRNAs) have proven to be the most effective and widely used tool for specific inhibition of gene expression, and as a result they are being translated into the clinic with an unprecedented speed [1]. The ultimate goal, achieving siRNA-based therapies for life-threatening or debilitating diseases, can, however, not be attained without improving the safety, efficiency and target specificity of siRNA delivery systems. This thesis focuses on the development of a lipid-based carrier suitable for endothelial-specific *in vivo* delivery of siRNA. Our aims were to design and characterize a liposomal targeted siRNA carrier system based on the cationic amphiphile SAINT-C18, study suitability of E-selectin and VCAM-1 for specific siRNA delivery into inflamed endothelium and validate molecular targets for siRNA mediated anti-inflammatory intervention, and finally to investigate the potential of this system for interference with disease associated endothelial activation *in vivo*.

Microvascular endothelial cells at the site of inflammation are both active participants and regulators of acute and chronic inflammatory processes, thus endothelial specific delivery of siRNA presents a promising approach for anti-inflammatory intervention and for a better understanding of the role of endothelial cells in inflammatory diseases. In **chapter 2** we reviewed recent developments in the design of siRNA delivery strategies aiming to therapeutically affect diseased endothelium and introduced the general consideration of endothelial heterogeneity in relation to disease state and its consequences for targeted therapeutic interventions. We discussed obstacles central to our work that are limiting the clinical application of siRNA for treatment of chronic inflammatory diseases. This includes intracellular fate of endothelium targeted delivery systems and microvascular bed dependent heterogeneity of endothelial responses to pro-inflammatory stimuli or pharmacological treatment. Upon inflammatory challenge, different vascular beds display a heterogeneous expression of adhesion molecules, including e.g., E-selectin, VCAM-1, and ICAM-1 [2]. Thus identification of the disease-specific makeup of potential target epitopes in vascular segments is crucial for the outcome of endothelial targeted treatment. Ideally, target epitope expression should be restricted to diseased endothelium and the protein becomes internalized upon ligand binding, allowing internalization of the carrier and cytoplasmic release of siRNA. Knowledge about the intracellular processing of carriers internalized by endothelial adhesion molecules is still limited. Finally, we discussed novel technologies that may aid further development of targeted delivery systems toward clinical application such as the use of tissue slices and application of laser microdissection (LMD). Tissue slices enable analysis of the pharmacological effects in the complexity of the whole human



organ [3] while LMD allows studying local pharmacological effects by enrichment of endothelial cells from (micro)vascular segments prior to analysis [4], which can be an essential strategy to provide proof of concept of *in vivo* siRNA delivery effects.

Lack of suitable animal models to study gene function in relevant diseases is a major problem for researchers, often embarked upon by generating transgenic animals at a vast expense of time and money. RNAi tools combined with a proper delivery system can aid investigations into gene function and identification/validation of therapeutic targets *in vivo*. In **chapter 3** we formulated catalytic oligodeoxynucleotides (DNAzymes) that bind to target RNA sequences resulting in specific RNA degradation [5], with cationic lipid, to study the role of early growth response protein 1 (Egr-1) in a rat model of pulmonary arterial hypertension (PAH). Pulmonary arterial hypertension (PAH) is characterized by the development of unique neointimal lesions in small pulmonary arteries, leading to increased right ventricular (RV) afterload and heart failure. PAH is regarded incurable when neointimal lesions have formed, thus therapeutic strategies are needed to prevent formation of these lesions. We intravenously administered DNAzymes formulated with cationic lipid 1,2-dioleoyl-3-trimethylammonium-propane (DOTAP) to rats with experimental flow-associated PAH. This resulted in downregulation of Egr-1 in pulmonary vasculature and attenuated pulmonary vascular remodeling, including the development of occlusive neointimal lesions, and subsequent reduction of pulmonary vascular resistance, RV systolic pressure, and RV hypertrophy. We showed that hampered expression of Egr-1 target genes (PDGF-B, TGF- β , IL-6 and p53) and concomitant decrease in vascular proliferation and increased apoptosis was associated with the attenuation of neointimal development. These data imply that Egr-1 plays a critical role during vascular remodeling in PAH, and as indicated by our results, that it can serve as a therapeutic target for biologics such as DNAzymes or siRNAs. Such a pharmacological approach can benefit from improved specific delivery into pulmonary endothelium using targeted delivery systems.

In **chapter 4** we set out on an attempt to develop a targeted carrier for selective delivery of siRNA into inflamed endothelial cells. For this purpose we employed a new type of liposomes called SAINT-O-Somes, which are based on formulation of conventional long circulating liposomes with the cationic lipid 1-methyl-4-(*cis*-9-dioleoyl)methyl-pyridiniumchloride (SAINT-C18). SAINT-O-Somes showed superior intracellular release of small molecules in endothelial cells as compared to conventional liposomes and displayed good siRNA encapsulation efficacy due to the presence of 20 mol% of cationic SAINT-C18 [6]. In line with our aims, we confirmed the suitability of vascular cell adhesion protein 1 (VCAM-1) respectively E-selectin as targets for selective siRNA delivery into inflamed endothelium by studying the uptake and the intracellular trafficking of SAINT-O-Somes harnessed with antibodies against these adhesion molecules in TNF α activated primary endothelial cells. Both VCAM-1 and



E-selectin guided SAINT-O-Somes to endolysosomal compartments where (a limited) release of the encapsulated siRNA from the carrier was found after 24h. We showed that anti-VCAM-1 and anti-E-selectin SAINT-O-Somes carrying siRNA against the endothelial gene VE-cadherin specifically downregulated its target mRNA and protein expression without exerting cellular toxicity. Notably, SAINT-O-Somes were stable in the presence of serum and protected siRNA from degradation by serum RNases, and when i.v. injected displayed a pharmacokinetic profile comparable to conventional long circulating immunoliposomes, with a circulation half-life of approximately 17 h. This study demonstrated the capacity of anti-VCAM-1 and anti-E-selectin SAINT-O-Somes to selectively deliver siRNA into inflamed endothelial cells and their suitability for *in vivo* application.

Our findings from chapter 4 prompted the *in vivo* study on the use of anti-VCAM-1 ($\text{Ab}_{\text{VCAM-1}}$) siRNA SAINT-O-Somes to interfere with disease associated endothelial activation, which is described in **chapter 5**. To demonstrate proof of concept of endothelial specific siRNA based therapeutic intervention we chose NF κ B p65 (RelA), which is a key component of a signal transduction pathway pivotal in endothelial cell activation, as a target gene to inhibit endothelial activation in inflammation. I.v. administered $\text{Ab}_{\text{VCAM-1}}$ SAINT-O-Somes selectively homed to VCAM-1 expressing endothelial cells in specific microvascular segments in inflamed organs of TNF α challenged mice. In the renal vasculature they effectively delivered VE-cadherin and RelA specific siRNAs without exerting liver and kidney toxicity. The resulting knock down of RelA led to attenuation of the endothelial inflammatory response in kidney venules towards LPS and exerted local therapeutic effects represented by inhibition of pro-inflammatory gene expression (E-selectin, IL-6, MCP-1) and leukocyte attraction. Employing laser microdissection allowed to unravel vascular bed-specific pharmacological effects of siRNA, that were masked when whole kidney homogenates were analyzed. This study showed that $\text{Ab}_{\text{VCAM-1}}$ siRNA_{RelA} SAINT-O-Somes are suitable for functional *in vivo* delivery of siRNAs to inflamed microvascular segments leading to attenuation of endothelial inflammatory responses and provides proof-of concept that siRNA-based approaches directed to inflamed endothelium may create new prospects to therapeutically address (chronic) inflammatory diseases.

Finally in **chapter 6**, we described the design of, and characterized new SAINT-based siRNA carriers incorporating protamine, a small cationic protein used as a transfection enhancer, with the aim to improve the efficacy of *in vivo* gene silencing. The concept for the design of these carriers was based on the ability of SAINT-C18, formulated with the helper-lipid 1,2-dioleoyl-sn-glycero-3-phosphoethanolamine (DOPE), to efficiently deliver DNA, siRNA as well as proteins into cells in the presence of serum and with low toxicity *in vitro*, thus being potentially interesting for *in vivo* application [7]. So called SAINT-liposome-polycation-DNA (S-LPD) and SAINT-liposome-polycation (S-LP)



were formulated by complexing protamine with siRNA and carrier DNA or siRNA only and subsequent addition of SAINT:DOPE liposomes allowing encapsulation of the protamine assemblies. S-LPD and S-LP had high efficiency of siRNA encapsulation, low *in vitro* toxicity and superior efficacy of gene downregulation in endothelial cells as compared to liposome-polycation-DNA based on DOTAP : Cholesterol, developed by Huang and coworkers [8]. Incorporation of 10 mol% PEG and anti-E-selectin antibody in the formulation of the carriers enabled selective siRNA delivery into activated endothelial cells. Furthermore, the physicochemical characteristics of S-LPD and S-LP, including size-stability and maintenance of siRNA integrity in the presence of serum at 37 °C, complied with *in vivo* application demands, thus encouraging further validation of this system *in vivo*.

Conclusions

Since the discovery of RNAi more than a decade ago, many efforts have been undertaken to harness gene silencing for application to endothelium engaged in widespread (chronic) diseases, e.g., in age related macular degeneration and cancer [9]. Endothelium is regarded as a relevant therapeutic target that is directly accessible for intravenously administered compounds, though, so far only a few non-viral carriers for *in vivo* siRNA delivery into endothelial cells are in pre-clinical development [9, 10]. Our work has yielded novel SAINT-C18 lipid-based carriers called SAINT-O-Somes, S-LPD, and S-LP, that we characterized and optimized for selective *in vivo* delivery of siRNA into inflammation activated endothelium [11]. The *in vivo* study performed with anti-VCAM-1 SAINT-O-Somes containing RelA specific siRNA provided proof of concept of microvascular specific siRNA delivery based anti-inflammatory intervention [12]. We showed that selective interference with NF κ B signaling in endothelium by means of siRNA, until now only demonstrated using adenoviral gene therapy or modular fusion protein SCL1 [13, 14], can offer an alternative approach to therapeutically address inflammatory diseases. Even though the downregulation of RelA was not complete, a ~50% inhibition of upregulation of RelA controlled pro-inflammatory genes was found upon LPS challenge, which had an impact on one of the key processes in inflammation, namely the recruitment of leukocytes. Dose finding and efficacy studies in more clinically relevant animal models are necessary to investigate the real therapeutic impact of the our siRNA delivery approaches for further development into broad therapeutic applications in inflammatory diseases.



Future perspectives

The last decade also brought an unprecedented expansion in development of new nanoparticles for treatment of numerous diseases. This development was largely driven by the discovery of RNAi and the expenditure on application of RNAi-based therapies assisted by the advancement in the design of new materials and technologies, e.g., lipidoids, microfluidics, and biomimetics. Although the full therapeutic potential of RNAi has not yet been exploited, it ensures new RNAi-based therapies. The future demand for multifunctional nanoparticles featuring targeting ligands, auxiliary moieties, and gene silencing capability, will grow stirred by implementation of personalized approaches towards treatment of diseases and development of affordable clinical scale manufacturing methods for nanoparticles [15].

Disease models for validation of endothelial specific siRNA-based anti-inflammatory intervention

Our experiments provided the first evidence that inflamed endothelial cells that actively engage in the pathology of widespread chronic diseases may benefit from siRNA-based therapies. Validation of Ab_{VCAM-1} siRNA_{RelA} SAINT-O-Somes in relevant animal models of disease is necessary to prove their therapeutic potential. Specifically, diseases with a strong inflammatory component underlying their pathology such as atherosclerosis or sepsis, are rational choices for this validation. Atherosclerotic plaques exhibit strong induction of VCAM-1 and endothelial-restricted depletion of NFκB signaling was demonstrated to reduce the atherosclerotic plaque formation [16]. Atherosclerosis models such as ApoE^{-/-} or ApoE/LdL^{-/-} mice may therefore be of interest to investigate the effect of Ab_{VCAM-1} siRNA_{RelA} SAINT-O-Somes on the plaque formation or their inversion in developed atherosclerosis. Also experimental sepsis mouse models such as cecal ligation and puncture or systemic injection of bacterial endotoxin (LPS) may offer a platform for validation of anti-inflammatory effects of Ab_{VCAM-1} siRNA_{RelA} SAINT-O-Somes. During septic shock VCAM-1 is overexpressed on the surface of endothelial cells in all major organs [17] and genetically engineered mice with an endothelial selective blockade of NFκB activation show resistance to septic shock and sepsis-related death [18]. Importantly, a great deal of clinical research in sepsis, including more than 40 human clinical trials, so far did not result in FDA-approved drugs for use in sepsis [19]. Development of effective siRNA-based anti-inflammatory therapeutics may thus significantly aid the treatment of sepsis.

Pulmonary arterial hypertension (PAH) may also benefit from a targeted siRNA delivery approach. As demonstrated in this thesis, formation of neointimal lesions in a PAH model can be attenuated by inhibition of Egr-1 expression in the pulmonary vasculature, where Egr-1 downregulation restricts vascular remodeling by increase of



apoptosis and reduction of proliferation in endothelial and smooth muscle cells. Egr-1 is expressed in remodeled vessels, also in human end-stage PAH, and could therefore very well be a target in established disease. Identification of suitable target epitopes on remodeled vessels in neointimal lesions of PAH patients enabling specific delivery of biologics targeting Egr-1 in the lesions is a prerequisite for treatment of established PAH. So far, no studies described potential targets for such approach. However, inflammation has been suggested to play a role in PAH as well as in the development of neointimal lesions [20], that was also reflected in our study by elevated IL-6 expression in remodeled vessels. This suggests that elevated expression of endothelial activation markers such as E-selectin, VCAM-1, or ICAM-1 may also be present in those lesions and could be exploited for target drug delivery. Reducing inflammation has also been shown to attenuate the development of PAH [21] justifying future exploration of the anti-inflammatory therapies for PAH next to, or in combination with Egr-1 inhibition.

Improving gene silencing efficacy of SAINT-O-Somes

Our data showed that micromolar concentrations of siRNA encapsulated into SAINT-O-Somes were required to downregulate the target genes in endothelial cells. This was in line with our observations that limited intracellular release of siRNA from the carrier is taking place [11]. Using high concentrations of siRNA carrier for target gene silencing is not cost effective and may lead to toxicity [22], therefore improvement of the siRNA release properties of SAINT-O-Somes should be a key subject for the further development of this system. The enhancements introduced should, however, not radically challenge the carrier properties such as size, siRNA encapsulation efficacy, capacity of antibody conjugation, or stability *in vivo*. Modification of these properties may influence the pharmacokinetic behavior of SAINT-O-Some and may result in decrease of their specificity for inflamed endothelial cells. Based on our knowledge on the intracellular trafficking of SAINT-O-Somes targeted to VCAM-1 and E-selectin, inclusion of pH responsive components in the formulation (e.g., pH-sensitive PEG or cell-penetrating peptides) might improve the intracellular efficacy of siRNA release [23]. At low endolysosomal pH, the liposomes will lose their PEG coating and will protrude the endolysosomal membrane more efficiently via exposed cationic lipid head groups or cell-penetrating peptide moieties. Those modification will increase the complexity of the system, thus for clinical purpose the benefit of introduced pH-sensitivity should compensate for the higher development and production costs of the particles.

The silencing efficacy could also be improved by refining the payload of siRNA. Recently developed RNAi-microsponges present a means of rapidly generating large amounts of siRNA densely packed into crystalline particles of 2 μm in size, using rolling circle transcription and RNA polymerization [24]. By encapsulation into a



positively charged polycation such as polyethylenimine (PEI), RNAi-microsponges can be condensed to a size of 200 nm. Using RNAi-microsponge/PEI particles, roughly three orders of magnitude less carrier was required to achieve the same degree of gene silencing as with conventional particle-based vehicle [25]. Given the high cost of therapeutic siRNA and the need for high silencing efficiency, this approach can significantly reduce the difficulties of achieving high loading efficiency for siRNA, which in combination with enhanced siRNA efficacy and low cytotoxicity may synergize to improve the overall delivery system performance. Furthermore, the ease of modification of the polymeric RNA composition enables the introduction of multiple RNA species into a single RNAi-microsponge for combination therapies.

Alternative approaches for silencing endothelial activation

A number of mediators and overlapping signaling pathways contribute to the control of the inflammatory response in the endothelial cells. As a result many agents that target proteins in distinct signaling pathways, including NF κ B, p38 MAPK, COX2, and mTOR, have been developed to inhibit endothelial activation in inflammation [26]. The complexity of this regulatory mechanism is also associated with microvascular segment specific engagement of the endothelial cells in disease and their heterogeneous response to treatment [2]. Therefore, using a single target to efficiently inhibit inflammatory processes in the endothelium is likely not feasible. In this thesis we demonstrated that Ab_{VCAM-1} SAINT-O-Somes mediated delivery of RelA specific siRNA attenuated the expression of pro-inflammatory genes in endothelial cells and reduced attraction of the leukocytes via the kidney venules [12]. Not all inflammatory molecules were however inhibited by the RelA downregulation. Combination of multiple siRNA species against several inflammatory targets may enhance the therapeutic potential of siRNA anti-inflammatory therapy. Simultaneous inhibition of NF κ B and p38MAPK would block many downstream effector molecules [27], which from a pharmacological point of view is beneficial compared to mono-target therapy against a single inflammatory signaling protein. SiRNA encapsulation and release efficacy are the limiting factors for suitability of the carrier for such an approach as the amount of intracellularly released siRNAs should reach the concentration required for effective gene silencing. S-LPD and S-LP developed and described in this thesis display a higher siRNA encapsulation efficacy and 10-fold greater gene silencing potency in HUVEC than SAINT-O-Somes, thus they meet the requirements for combined siRNA therapies.

MicroRNAs (miRNAs) have emerged as a novel class of endogenous, noncoding short RNA molecules (about 22 nt) that regulate gene expression at the post-transcriptional level, via degradation or translational inhibition of their target mRNAs [28]. In contrast to siRNA, miRNA recognition of the target mRNA is imperfect, that results in binding of many target mRNAs and silencing of multiple target genes by



one single miRNA [1]. Recent studies indicate the contribution of specific miRNAs, including e.g., miR-10a and miR-126, to vascular inflammation and diseases [29, 30]. Elevated levels of miR-10a have been shown to inhibit the pro-inflammatory phenotype in atherosusceptible endothelium *in vivo* and *in vitro* by regulating the I κ B/NF κ B signaling pathway [31], while miR-126 negatively regulates the expression of VCAM-1 protein, which mediates leukocyte adherence to ECs in vascular inflammation [32]. Delivery of anti-inflammatory miRNAs that are deficient in diseased endothelial cells, to increase their presence to a similar or higher level than found in healthy cells, may present an alternative approach to address the complexity of the inflammatory diseases. Double stranded miRNA equivalent to the dicer products, which is a structural analogues of siRNA, can be delivered directly to the cytoplasm of the cells for loading into the RNA-induced silencing complex (RISC) [33]. miRNA mimics siRNA in most of its features and the delivery challenges met for siRNA are the same for miRNA (reviewed by [34]). Although functionality of the miRNA may have more advantages for treatment of complex inflammatory diseases, efficacy of target suppression by miRNA molecules has yet to be verified in animal models of clinically relevant diseases.

The fact that endothelial cells exhibit different proliferation rates ranging from days to years [35] is an important aspect of rational application of a post-transcriptional silencing mechanism for target gene inhibition. Silencing effects of siRNA can last from 3-7 days in rapidly dividing cells and up to 3 weeks in slow/non-dividing cells. The duration of the effect will also depend on the target gene expression kinetics, the level of expression, delivered dose and the treatment frequency [36]. Resolution of inflammation in chronic diseases may thus require repeated intravenous administration of the siRNA therapeutics on a weekly to monthly basis. Advanced genome editing technologies such as zinc finger nucleases (ZFNs), transcription activator-like effector nucleases (TALENs) and clustered regularly interspaced short palindromic repeat (CRISPR)-based systems will complement gene silencing methods and broaden our toolkit to understand and treat diseases [37]. These chimeric nucleases enable efficient, precise and irreversible genome modification by inducing targeted DNA double-strand breaks that stimulate the cellular DNA repair mechanisms [38]. This approach allows correcting the underlying cause of the disease, therefore permanently eliminating the disease symptoms. So far, there is no evidence that this would be a desired therapy for attenuation of endothelial activation in chronic inflammatory diseases though, lack of understanding of the underlying causes of many inflammatory diseases will be the key factor that limits therapeutic use of genome engineering tools. To date, ZFNs have been used to correct the disease-causing mutations in X-linked severe combined immune deficiency (SCID) [39], hemophilia B [40], and α_1 -antitrypsin deficiency [41]. Unlike ZFNs and TALENs that are protein-guided, the specificity of CRISPR/Cas9 targeting is RNA-guided [42]. Early studies indicate that CRISPR/Cas9 can be used to edit



genomes in human cells, zebrafish [43] and bacteria [44] with comparable activity to TALENS, but show higher off-target effects [45]. Delivery of those tools to the cells is achieved by transfection/transduction of DNA, but RNA delivery is also an on-going area of investigation. Overall, utility of site-specific nucleases is currently limited mainly to production and manipulation of induced pluripotent stem cells but further development of this technology will ultimately open numerous new directions for gene therapy. Specificity of target recognition of each nuclease platform and the optimal methods for delivering DNA or mRNA sequences encoding these nucleases into cells and organisms are a critical areas of future research. So far, the packaging capacity of large DNA fragments into viral vectors is limited, while efficacy of DNA delivery by non-viral vectors is insufficient.

New technologies facilitating clinical translation of siRNA nanoparticles

Despite great progress in nanoparticle development, their translation to the clinic has been slow compared with small molecule drugs. New applications require tailoring of the properties of the carrier such as size, shape, surface charge, and its content, that are important parameters for optimizing cellular delivery and *in vivo* pharmacokinetics. Therefore upscalable formulation methods yielding tunable carriers at limited costs, displaying well-defined and reproducible features, will aid the design of effective nanoparticle-based therapies. Particle fabrication by the so called Particle Replication in Non-wetting Templates (PRINT) process is a robust, well-established, and scalable approach for rapidly manufacturing particles with exquisite control over particle geometry and composition [46]. Also recent advances in microfluidics are expected to improve the synthesis of nanoparticles and accelerate their transition to the clinic [47]. Formulation of Lipid nanoparticles (LNP), that are at present the leading systems for *in vivo* delivery of siRNA, employs microfluidic mixing techniques to produce systems of 20-100 nm diameter or larger, that have variable siRNA encapsulation efficiencies and homogeneity [48]. Moreover, biomimetic microfluidic technologies are capable of representing organ-level functions on a chip such as those observed in the lung, liver and kidneys [49]. These technologies could serve the evaluation of particle toxicity and its therapeutic efficacy, and screen for the most potent formulations prior to entering *in vivo* trials.

The versatile fabrication methods using nucleic acids as building blocks make nucleic acids one of the most popular construction materials for nano-scale objects [50]. Nanoobjects formed from DNA, such as DNA origami, may be designed in almost any 3D shape [51]. The geometry and size of DNA assemblies can be accurately designed due to the well-known self-recognition properties of DNA and the knowledge of the exact structure of the double helix at the atomic level. Moreover, DNA nanostructures composed of nucleic acid hybrid materials, e.g, DNA-gold nanoparticles or DNA block



copolymer micelles, permit to implement extra functionalities (including imaging agents), and offer multiple possibilities for drug incorporation with control over the payload release [52, 53]. For example, anticancer drugs, e.g., doxorubicin, paclitaxel, and cisplatin (reviewed by de Vries [50]) or antisense DNA have been successfully conjugated to these nanoparticles. Similarly, gold-nanoconjugates functionalized with densely packed RNA are a potent material for siRNA delivery due to high serum stability without the need for chemical modification of RNA and efficient gene silencing [54].

Above mentioned carrier systems composed of high density DNA or RNA show low immunogenicity and can be taken up by the cells without the need for a transfection agents, mainly via scavenger-receptor-dependent endocytosis [50, 55]. These system may therefore in the near future become the new frontier in the field of biomedicine. To date, use of DNA and RNA nanostructures for drug delivery is in pre-clinical stage and more effort is necessary to achieve the pharmaceutical grade and manufacturing scale established in pharmaceutical industry for other delivery platforms, such as lipid based carriers.

In summary, many new technologies are now available to assist in the design and development of superior siRNA delivery systems for clinical application, that may or may not be made endothelial-specific, and their potential needs further exploration.

References

1. D. Castanotto, J.J. Rossi, The promises and pitfalls of RNA-interference-based therapeutics, *Nature*, 457 (2009) 426-433.
2. G. Molema, Heterogeneity in endothelial responsiveness to cytokines, molecular causes, and pharmacological consequences, *Semin Thromb Hemost*, 36 (2010) 246-264.
3. I.A. de Graaf, P. Olinga, M.H. de Jager, M.T. Merema, R. de Kanter, E.G. van de Kerkhof, G.M. Groothuis, Preparation and incubation of precision-cut liver and intestinal slices for application in drug metabolism and toxicity studies, *Nat Protoc*, 5 (2010) 1540-1551.
4. E. Langenkamp, J.A. Kamps, M. Mrug, E. Verpoorte, Y. Niyaz, P. Horvatovich, R. Bischoff, H. Struijker-Boudier, G. Molema, Innovations in studying in vivo cell behavior and pharmacology in complex tissues--microvascular endothelial cells in the spotlight, *Cell Tissue Res*, 354 (2013) 647-669.
5. D.A. Baum, S.K. Silverman, Deoxyribozymes: useful DNA catalysts in vitro and in vivo, *Cell Mol Life Sci*, 65 (2008) 2156-2174.
6. J.E. Adrian, H.W. Morselt, R. Suss, S. Barnert, J.W. Kok, S.A. Asgeirsdottir, M.H. Ruiters, G. Molema, J.A. Kamps, Targeted SAINT-O-Somes for improved intracellular delivery of siRNA and cytotoxic drugs into endothelial cells, *J Control Release*, 144 (2010) 341-349.
7. B.T. van der Gun, A. Monami, S. Laarmann, T. Rasko, K. Slaska-Kiss, E. Weinhold, R. Wasserkort, L.F. de Leij, M.H. Ruiters, A. Kiss, P.M. McLaughlin, Serum insensitive, intranuclear protein delivery by the multipurpose cationic lipid SAINT-2, *J Control Release*, 123 (2007) 228-238.
8. S.D. Li, L. Huang, Targeted delivery of antisense oligodeoxynucleotide and small interference RNA into lung cancer cells, *Mol Pharm*, 3 (2006) 579-588.
9. J. Kaufmann, K. Ahrens, A. Santel, RNA interference for therapy in the vascular endothelium, *Microvasc Res*, 80 (2010) 286-293.
10. P.S. Kowalski, N.G. Leus, G.L. Scherphof, M.H. Ruiters, J.A. Kamps, G. Molema, Targeted



- siRNA delivery to diseased microvascular endothelial cells: cellular and molecular concepts, *IUBMB Life*, 63 (2011) 648-658.
11. P.S. Kowalski, L.L. Lintermans, H.W. Morselt, N.G. Leus, M.H. Ruiters, G. Molema, J.A. Kamps, Anti-VCAM-1 and Anti-E-selectin SAINT-O-Somes for Selective Delivery of siRNA into Inflammation-Activated Primary Endothelial Cells, *Mol Pharm*, 10 (2013) 3033-3044.
 12. P.S. Kowalski, P.J. Zwiers, H.W. Morselt, J.M. Kuldo, N.G. Leus, M.H. Ruiters, G. Molema, J.A. Kamps, Anti-VCAM-1 SAINT-O-Somes enable endothelial-specific delivery of siRNA and downregulation of inflammatory genes in activated endothelium in vivo, *J Control Release*, 176C (2014) 64-75.
 13. J.M. Kuldo, S.A. Asgeirsdottir, P.J. Zwiers, A.R. Bellu, M.G. Rots, J.A. Schalk, K.I. Ogawara, C. Trautwein, B. Banas, H.J. Haisma, G. Molema, J.A. Kamps, Targeted adenovirus mediated inhibition of NF-kappaB-dependent inflammatory gene expression in endothelial cells in vitro and in vivo, *J Control Release*, 166 (2013) 57-65.
 14. B. Sehnert, H. Burkhardt, J.T. Wessels, A. Schroder, M.J. May, D. Vestweber, J. Zwerina, K. Warnatz, F. Nimmerjahn, G. Schett, S. Dubel, R.E. Voll, NF-kappaB inhibitor targeted to activated endothelium demonstrates a critical role of endothelial NF-kappaB in immune-mediated diseases, *Proc Natl Acad Sci U S A*, 110 (2013) 16556-16561.
 15. Z. Cheng, A. AlZaki, J.Z. Hui, V.R. Muzykantov, A. Tsourkas, Multifunctional nanoparticles: cost versus benefit of adding targeting and imaging capabilities, *Science*, 338 (2012) 903-910.
 16. R. Gareus, E. Kotsaki, S. Xanthoulea, I. van der Made, M.J. Gijbels, R. Kardakaris, A. Polykratis, G. Kollias, M.P. de Winther, M. Pasparakis, Endothelial cell-specific NF-kappaB inhibition protects mice from atherosclerosis, *Cell Metab*, 8 (2008) 372-383.
 17. J.W. Fries, A.J. Williams, R.C. Atkins, W. Newman, M.F. Lipscomb, T. Collins, Expression of VCAM-1 and E-selectin in an in vivo model of endothelial activation, *Am J Pathol*, 143 (1993) 725-737.
 18. S.F. Liu, A.B. Malik, NF-kappa B activation as a pathological mechanism of septic shock and inflammation, *Am J Physiol Lung Cell Mol Physiol*, 290 (2006) L622-L645.
 19. P.A. Ward, New approaches to the study of sepsis, *EMBO Mol Med*, 4 (2012) 1234-1243.
 20. M.E. van Albada, B. Bartelds, H. Wijnberg, S. Mohaupt, M.G. Dickinson, R.G. Schoemaker, K. Kooi, F. Gerbens, R.M. Berger, Gene expression profile in flow-associated pulmonary arterial hypertension with neointimal lesions, *Am J Physiol Lung Cell Mol Physiol*, 298 (2010) L483-491.
 21. B. Bartelds, R.L. van Loon, S. Mohaupt, H. Wijnberg, M.G. Dickinson, B. Boersma, J. Takens, M. van Albada, R.M. Berger, Mast cell inhibition improves pulmonary vascular remodeling in pulmonary hypertension, *Chest*, 141 (2012) 651-660.
 22. D.R. Caffrey, J. Zhao, Z. Song, M.E. Schaffer, S.A. Haney, R.R. Subramanian, A.B. Seymour, J.D. Hughes, siRNA off-target effects can be reduced at concentrations that match their individual potency, *PLoS One*, 6 (2011) e21503.
 23. V.P. Torchilin, Recent approaches to intracellular delivery of drugs and DNA and organelle targeting, *Annu Rev Biomed Eng*, 8 (2006) 343-375.
 24. J.B. Lee, J. Hong, D.K. Bonner, Z. Poon, P.T. Hammond, Self-assembled RNA interference microsponges for efficient siRNA delivery, *Nat Mater*, 11 (2012) 316-322.
 25. A. Elbakry, A. Zaky, R. Liebl, R. Rachel, A. Goepferich, M. Breunig, Layer-by-layer assembled gold nanoparticles for siRNA delivery, *Nano Lett*, 9 (2009) 2059-2064.
 26. J.S. Pober, W.C. Sessa, Evolving functions of endothelial cells in inflammation, *Nat Rev Immunol*, 7 (2007) 803-815.
 27. J. Zhang, B. Shen, A. Lin, Novel strategies for inhibition of the p38 MAPK pathway, *Trends Pharmacol Sci*, 28 (2007) 286-295.
 28. V.N. Kim, MicroRNA biogenesis: coordinated cropping and dicing, *Nat Rev Mol Cell Biol*, 6 (2005) 376-385.
 29. C. Urbich, A. Kuehbachner, S. Dimmeler, Role of microRNAs in vascular diseases, inflammation, and angiogenesis, *Cardiovasc Res*, 79 (2008) 581-588.
 30. B. Qin, H. Yang, B. Xiao, Role of microRNAs



- in endothelial inflammation and senescence, *Mol Biol Rep*, 39 (2012) 4509-4518.
31. Y. Fang, C. Shi, E. Manduchi, M. Civelek, P.F. Davies, MicroRNA-10a regulation of proinflammatory phenotype in atherosusceptible endothelium in vivo and in vitro, *Proc Natl Acad Sci U S A*, 107 (2010) 13450-13455.
 32. T.A. Harris, M. Yamakuchi, M. Ferlito, J.T. Mendell, C.J. Lowenstein, MicroRNA-126 regulates endothelial expression of vascular cell adhesion molecule 1, *Proc Natl Acad Sci U S A*, 105 (2008) 1516-1521.
 33. J.J. Rossi, New hope for a microRNA therapy for liver cancer, *Cell*, 137 (2009) 990-992.
 34. M. Muthiah, I.K. Park, C.S. Cho, Nanoparticle-mediated delivery of therapeutic genes: focus on miRNA therapeutics, *Expert Opin Drug Deliv*, 10 (2013) 1259-1273.
 35. B. Hobson, J. Denekamp, Endothelial proliferation in tumours and normal tissues: continuous labelling studies, *Br J Cancer*, 49 (1984) 405-413.
 36. D.W. Bartlett, M.E. Davis, Insights into the kinetics of siRNA-mediated gene silencing from live-cell and live-animal bioluminescent imaging, *Nucleic Acids Res*, 34 (2006) 322-333.
 37. T. Gaj, C.A. Gersbach, C.F. Barbas, 3rd, ZFN, TALEN, and CRISPR/Cas-based methods for genome engineering, *Trends Biotechnol*, 31 (2013) 397-405.
 38. C. Wyman, R. Kanaar, DNA double-strand break repair: all's well that ends well, *Annu Rev Genet*, 40 (2006) 363-383.
 39. F.D. Urnov, J.C. Miller, Y.L. Lee, C.M. Beausejour, J.M. Rock, S. Augustus, A.C. Jamieson, M.H. Porteus, P.D. Gregory, M.C. Holmes, Highly efficient endogenous human gene correction using designed zinc-finger nucleases, *Nature*, 435 (2005) 646-651.
 40. H. Li, V. Haurigot, Y. Doyon, T. Li, S.Y. Wong, A.S. Bhagwat, N. Malani, X.M. Anguela, R. Sharma, L. Ivanciu, S.L. Murphy, J.D. Finn, F.R. Khazi, S. Zhou, D.E. Paschon, E.J. Rebar, F.D. Bushman, P.D. Gregory, M.C. Holmes, K.A. High, In vivo genome editing restores haemostasis in a mouse model of haemophilia, *Nature*, 475 (2011) 217-221.
 41. K. Yusa, S.T. Rashid, H. Strick-Marchand, I. Varela, P.Q. Liu, D.E. Paschon, E. Miranda, A. Ordonez, N.R. Hannan, F.J. Rouhani, S. Darche, G. Alexander, S.J. Marciniak, N. Fusaki, M. Hasegawa, M.C. Holmes, J.P. Di Santo, D.A. Lomas, A. Bradley, L. Vallier, Targeted gene correction of alpha1-antitrypsin deficiency in induced pluripotent stem cells, *Nature*, 478 (2011) 391-394.
 42. J.M. Campbell, K.A. Hartjes, T.J. Nelson, X. Xu, S.C. Ekker, New and TALENed genome engineering toolbox, *Circ Res*, 113 (2013) 571-587.
 43. W.Y. Hwang, Y. Fu, D. Reyon, M.L. Maeder, S.Q. Tsai, J.D. Sander, R.T. Peterson, J.R. Yeh, J.K. Joung, Efficient genome editing in zebrafish using a CRISPR-Cas system, *Nat Biotechnol*, 31 (2013) 227-229.
 44. W. Jiang, D. Bikard, D. Cox, F. Zhang, L.A. Marraffini, RNA-guided editing of bacterial genomes using CRISPR-Cas systems, *Nat Biotechnol*, 31 (2013) 233-239.
 45. Y. Fu, J.A. Foden, C. Khayter, M.L. Maeder, D. Reyon, J.K. Joung, J.D. Sander, High-frequency off-target mutagenesis induced by CRISPR-Cas nucleases in human cells, *Nat Biotechnol*, 31 (2013) 822-826.
 46. D.A. Canelas, K.P. Herlihy, J.M. DeSimone, Top-down particle fabrication: control of size and shape for diagnostic imaging and drug delivery, *Wiley Interdiscip Rev Nanomed Nanobiotechnol*, 1 (2009) 391-404.
 47. P.M. Valencia, O.C. Farokhzad, R. Karnik, R. Langer, Microfluidic technologies for accelerating the clinical translation of nanoparticles, *Nat Nanotechnol*, 7 (2012) 623-629.
 48. N.M. Belliveau, J. Huft, P.J. Lin, S. Chen, A.K. Leung, T.J. Leaver, A.W. Wild, J.B. Lee, R.J. Taylor, Y.K. Tam, C.L. Hansen, P.R. Cullis, Microfluidic Synthesis of Highly Potent Limit-size Lipid Nanoparticles for In Vivo Delivery of siRNA, *Mol Ther Nucleic Acids*, 1 (2012) e37.
 49. D. Huh, H.J. Kim, J.P. Fraser, D.E. Shea, M. Khan, A. Bahinski, G.A. Hamilton, D.E. Ingber, Microfabrication of human organs-on-chips, *Nat Protoc*, 8 (2013) 2135-2157.
 50. J.W. de Vries, F. Zhang, A. Herrmann, Drug delivery systems based on nucleic acid



- nanostructures, *J Control Release*, 172 (2013) 467-483.
51. P.W. Rothemund, Folding DNA to create nanoscale shapes and patterns, *Nature*, 440 (2006) 297-302.
52. A. Rodriguez-Pulido, A.I. Kondrachuk, D.K. Prusty, J. Gao, M.A. Loi, A. Herrmann, Light-triggered sequence-specific cargo release from DNA block copolymer-lipid vesicles, *Angew Chem Int Ed Engl*, 52 (2013) 1008-1012.
53. P.K. Lo, P. Karam, F.A. Aldaye, C.K. McLaughlin, G.D. Hamblin, G. Cosa, H.F. Sleiman, Loading and selective release of cargo in DNA nanotubes with longitudinal variation, *Nat Chem*, 2 (2010) 319-328.
54. P.C. Patel, L. Hao, W.S. Yeung, C.A. Mirkin, Duplex end breathing determines serum stability and intracellular potency of siRNA-Au NPs, *Mol Pharm*, 8 (2011) 1285-1291.
55. N.L. Rosi, D.A. Giljohann, C.S. Thaxton, A.K. Lytton-Jean, M.S. Han, C.A. Mirkin, Oligonucleotide-modified gold nanoparticles for intracellular gene regulation, *Science*, 312 (2006) 1027-1030.



Chapter 8

Nederlandse samenvatting

Nederlandse samenvatting

Algemene inleiding (hoofdstuk 1)

De ontdekking en de toepassing van “RNA interferentie” (RNAi) heeft het fundamentele onderzoek naar functie en regulatie van eukaryote genen in een stroomversnelling gebracht en onze inzichten daarin aanzienlijk vergroot. Tot nu toe zijn “short interfering RNAs” (siRNAs) de meest effectieve instrumenten gebleken voor het specifiek onderdrukken van gen expressie met als gevolg dat hun klinische toepassing in snel tempo toeneemt [1]. Het uiteindelijke doel hiervan, dat wil zeggen het ontwerpen van effectieve op siRNA gebaseerde therapieën voor levensbedreigende of ernstige invaliderende ziekten, zal echter niet worden bereikt zonder de efficiëntie, target specificiteit en veiligheid van siRNA afgifte systemen verder te verbeteren.

Het in dit proefschrift beschreven onderzoek richt zich op de ontwikkeling van een op lipiden gebaseerd siRNA drager systeem dat geschikt is voor de specifieke in vivo aflevering van siRNAs in de endotheelcellen van bloedvaten. Voor dat doel werd een dragersysteem voor siRNA ontwikkeld op basis van het kationische amfifiele lipide SAINT-18 met als potentiële targets de endotheel-specifieke eiwitten E-selectine en vasculair cel adhesie molecuul (VCAM)-1, die met name tot expressie komen op ontstoken bloedvatendotheel. Vervolgens werd nagegaan of, en in hoeverre dit systeem kan worden toegepast om de ontstekingsreactie in vivo met specifiek siRNA te onderdrukken.

Het is bekend dat microvasculaire endotheelcellen niet slechts participant zijn in zowel acute als chronische ontstekingen maar ook een belangrijke rol als regulator in ontstekingsprocessen vervullen. We verwachtten daarom dat de mogelijkheid om siRNA specifiek aan deze cellen af te leveren zou kunnen leiden tot een beter begrip van de rol van endotheliale cellen in het ontstekingsproces.

In **hoofdstuk 2** wordt een overzicht gegeven van recente ontwikkelingen in het ontwerpen van verschillende strategieën gericht op de (therapeutische) behandeling van (chronische) ontstekingen via interventie op het niveau van het vaatendotheel. In dit verband wordt het concept geïntroduceerd van endotheliale heterogeniteit met betrekking tot het betreffende ziektebeeld en de typen bloedvaten die betrokken zijn, en de consequenties daarvan voor doel-specifieke *therapeutische interventies*.

Obstakels die een belemmering vormen voor de klinische toepassing van siRNA voor de behandeling van chronische ontstekingsprocessen (inflammatie) staan centraal in deze discussie. Daarbij komen met name de intracellulaire afhandeling van de naar het microvasculaire endotheel gestuurde afgiftesystemen aan de orde, evenals de heterogeniteit van dat endotheel met betrekking tot zijn respons op pro-inflammatoire prikkels en farmacologisch ingrijpen.



In reactie op een inflammatoire prikkel brengen vaatendothelcellen verschillende adhesie eiwitten zoals E-selectine, VCAM-1 en intercellulair adhesie molecuul (ICAM)-1 in verschillende mate tot expressie op het celoppervlak. De exacte opmaak van adhesie-eiwit expressie is afhankelijk van het type endotheel dat reageert[2]. Daarom is inzicht in en kennis van de mogelijke target epitopen op het aangedane endotheel van essentieel belang voor het resultaat van een endotheel-specifieke therapie. Idealiter komt het beoogde target epitooop uitsluitend tot expressie op het aangedane endotheel en wordt het betreffende eiwit in de cel opgenomen na interactie met het ligand dat bindt aan het eiwit. De kennis hierover en over de intracellulaire verwerking van aldus opgenomen carriersystemen is echter nog zeer beperkt.

In samenhang hiermee worden nieuwe technologieën besproken die de verdere ontwikkeling van cel- of weefselspecifieke afgiftesystemen tot aan de klinische toepassing kunnen bevorderen, zoals de toepassing van dunne weefselplakjes en de zogenaamde laser microdissectie (LMD). Het gebruik van weefselplakjes maakt het mogelijk de farmacologische effecten van een behandeling te analyseren in een systeem waarin de complexiteit van het intacte organisme (d.w.z. het proefdier of de mens) dicht benaderd wordt. LMD op zijn beurt maakt het mogelijk lokale farmacologische effecten op het endotheel te analyseren in geslecteerde (micro)vasculaire segmenten.

Het ontbreken van geschikte diermodellen is een probleem voor het onderzoeken van de betrokkenheid van bepaalde genen bij het ontstaan van pathologische afwijkingen. Bij gebrek aan beter wordt hierbij vaak gebruik gemaakt van transgene proefdieren, een zeer kostbare en tijdrovende benadering. Het gebruik van RNA interferentie technieken in combinatie met geschikte cel-specifieke afgiftesystemen zou een aantrekkelijk alternatief daarvoor kunnen vormen en kunnen bijdragen aan de identificatie van geschikte therapeutische targetmoleculen voor in vivo toepassing.

Hoofdstuk 3 gaat over de formulering van katalytische oligodeoxynucleotiden (“DNAzymes”), in complexen met kationische lipiden met als doel de rol van het “early growth response protein-1” (Egr-1) te onderzoeken in een rattenmodel voor pulmonaire arteriële hypertensie (PAH). DNAzymes kunnen binden aan bepaalde target RNA sequenties met als resultaat specifieke afbraak van (m)RNA en dus onderdrukking van de expressie van bepaalde genen.

PAH wordt getypeerd door de vorming van unieke beschadigingen in de intima van kleine arteriën in de long die leiden tot een toename van de afterload van het rechter ventrikel (RV) met als ultiem gevolg hartfalen. De aandoening is niet meer behandelbaar als de laesies eenmaal zijn gevormd en dus is er een dringende behoefte aan een strategie die de vorming van deze laesies kan voorkomen.

Complexen van Egr-1-specifiek DNAzyme met het kationische lipide 1,2-dioleoyl-3-trimethylammonium-propaan (DOTAP) werden intraveneus toegediend aan ratten



met een experimentele flow-geïnduceerde PAH. Dit resulteerde in een down-regulatie van Egr-1 in de pulmonale vasculatuur en onderdrukte de pulmonaire vasculaire remodellering, inclusief de vorming van afsluitende neo-intima laesies. Dit ging gepaard met afnames van de pulmonaire vaatweerstand, de RV systolische druk en RV hypertrofie.

Aangetoond werd dat de onderdrukte expressie van de Egr-1 target genen PDGF-B, TGF- β , IL-6 en p53 en de daarmee gepaard gaande afname in vaatproliferatie en toegenomen apoptose samen gaat met een verminderde neo-intima vorming. Deze waarneming impliceert dat Egr-1 een belangrijke rol speelt tijdens de bij PAH optredende vasculaire remodellering.

In **hoofdstuk 4** worden pogingen beschreven een carrier systeem te ontwerpen voor de selectieve afgifte van siRNA in aan inflammatie onderhevige endotheelcellen. Voor dat doel werd een nieuw type liposomen gebruikt, genaamd SAINT-O-Somen, gebaseerd op de combinatie van conventionele lang-circulerende liposomen en het kationische lipide 1-methyl-4-(cis-9-dioleyl)methyl-pyridiniumchloride (SAINT-C18).

SAINT-O-Somen met 20% SAINT-C18 lieten zien niet alleen een goede siRNA insluitingsefficiëntie te bezitten maar daarnaast ook superieur te zijn aan conventionele liposomen wat betreft effectiviteit van intracellulaire afgifte van kleine moleculen. Geheel in overeenstemming met de gestelde doelen kon worden aangetoond dat de adhesie eiwitten VCAM-1 en E-selectine geschikt zijn als targets voor de selectieve afgifte van siRNA in ontstoken endotheel. Daartoe werden siRNA-bevattende SAINT-O-Somen, die aan hun oppervlak waren voorzien van antilichamen tegen deze adhesie eiwitten, geïncubeerd met tumornecrosefactor (TNF)- α geactiveerde primaire endotheelcellen. Zowel met anti-VCAM-1 als met anti-E-selectine gemodificeerde SAINT-O-Somen werden na opname door de cellen aangetroffen in endolysosomale compartimenten, van waaruit over een periode van 24 uur het ingesloten siRNA ten dele in het cytosol werd vrijgemaakt. Er kon worden aangetoond dat beide SAINT-O-Somen met daarin ingesloten een siRNA dat specifiek is voor het endotheliale VE-cadherine gen het betreffende target mRNA en daarmee de expressie van het VE-cadherine kunnen down-reguleren zonder enige toxiciteit. Met het oog op de in vivo toepassing van dit carrier systeem is het voorts van belang dat kon worden vastgesteld dat de SAINT-O-Somen stabiel zijn in aanwezigheid van serum en het ingesloten siRNA volledig beschermen tegen afbraak door serum Rnases. Na intraveneuze toediening in de muis lieten de SAINT-O-Somen een farmacokinetisch profiel zien dat vergelijkbaar is met dat van conventionele lang-circulerende liposomen met een halfwaarde tijd van ca. 17 uur. Samenvattend: deze waarnemingen laten zien dat de met anti-VCAM-1 of anti-E-selectine antilichaam gemodificeerde SAINT-O-Somen een in principe geschikt dragersysteem vormen voor de selectieve en functionele in vivo afgifte van siRNA in ontstoken endotheelcellen.



Hoofdstuk 5 toont de conceptuele bruikbaarheid aan van siRNA-bevattende anti-VCAM-1 (Ab_{VCAM-1}) SAINT-O-Somen in met TNF- α behandelde muizen als in vivo model voor ziekte-gerelateerde endotheel activatie. Als anti-inflammatoir target gen voor endotheel-specifieke therapeutische interventie werd NF κ B p65 (ReIA) gekozen. Dit is een sleutel component van een signaal transductie pad dat een essentiële rol speelt in endotheel activering. Intraveneus toegediende Ab_{VCAM-1} SAINT-O-Somen bleken selectief te worden afgeleverd aan endotheelcellen die VCAM-1 tot expressie brengen in specifieke microvasculaire segmenten in ontstoken organen van met TNF- α behandelde muizen. SiRNAs specifiek voor ReIA werden effectief afgeleverd in de vasculatuur van de nier zonder noemenswaardige toxiciteit voor lever en nier. De daarmee gepaard gaande onderdrukking van ReIA expressie veroorzaakte in renale microvasculatuur een vermindering van de inflammatoire respons na LPS toediening. Bovendien werden lokale therapeutische effecten vastgesteld in de vorm van remming van expressie van de pro-inflammatoire genen E-selectine, interleukine-6 en macrofagen aantrekkend eiwit (MCP)-1 en van leukocyten mobilisatie. Met behulp van laser microdissectie konden we vaatbed-specifieke farmacologische effecten onderscheiden die gemaskeerd werden wanneer hele-nier homogenaten werden geanalyseerd. Deze studie laat zien dat op siRNA gebaseerde therapeutische behandeling van ontstoken endotheel zeer wel mogelijk is en biedt goede vooruitzichten op bruikbare strategieën voor de behandeling van (chronische) inflammatoire aandoeningen.

Tenslotte wordt in **hoofdstuk 6** een nieuw op SAINT gebaseerd siRNA carrier systeem beschreven met daarin ingebouwd een klein kationisch eiwit, protamine, als transfectie versterker, met als doel verbetering van de efficiëntie van in vivo siRNA vrijmaking uit het carriersysteem en onderdrukking van gen expressie.

Het concept voor dit type carrier is gebaseerd op het vermogen van SAINT-18 om, in combinatie met het helper lipide 1,2-dioleoyl-sn-glycero-3-phosphoethanolamine (DOPE) en in aanwezigheid van serum, op efficiënte wijze DNA en siRNA, maar ook eiwitten in cellen binnen te brengen zonder toxiciteitsverschijnselen te veroorzaken[7]. Dergelijke zogenaamde SAINT-liposoom-polykation-DNA (S-LPD) en SAINT-liposoom-polykation (S-LP) complexen werden gemaakt door protamine met siRNA, en eventueel carrier DNA, te complexeren en vervolgens SAINT-DOPE liposomen toe te voegen, met als gevolg dat de protamine/siRNA/(DNA) complexen hierin worden ingebouwd. Deze S-LP(D) complexen blijken siRNA met hoge efficiëntie in te bouwen, vertonen geringe toxiciteit op cellulair niveau en een superieur vermogen tot gen down-regulatie in endotheelcellen in vergelijking met de op DOTAP/cholesterol gebaseerde liposoom-polykation-DNA (LPD) partikels ontwikkeld door Huang en medewerkers [8].



Aangetoond werd dat inbouw van 10 mol% PEG en koppeling van het anti-E-selectine antilichaam in de S-LP(D) partikels selectieve siRNA afgifte in geactiveerde endotheelcellen mogelijk maakten. Meting van fysicochemische parameters van deze S-LPD en S-LP partikels, zoals stabiliteit in partikel afmeting en siRNA structuur in aanwezigheid van serum bij 37 °C, laat zien dat de eigenschappen van deze partikels compatibel zijn met in vivo vigerende omstandigheden. Dit rechtvaardigt verdere validering van deze systemen voor in vivo toepassingen.

Samengevat laten de studies in dit promotieonderzoek zien dat op SAINT-gebaseerde siRNA carriersystemen uitermate geschikt zijn voor in vivo aflevering van siRNA in endotheelcellen in ontstekingsweefsel. Vervolgonderzoek zal duidelijk moeten maken in hoeverre deze nieuwe benadering therapeutisch gewin oplevert voor de behandeling van (chronische) ontstekingsziekten in hiervoor relevante proefdiermodellen.



Appendices

Streszczenie

Curriculum Vitae

List of publications

Acknowledgements

Streszczenie

Odkrycie zjawiska interferencji RNA (ang. RNA interference, RNAi) i jego zastosowanie w badaniach podstawowych zmieniły dotychczasowe poglądy na mechanizmy regulacji ekspresji genów oraz przyspieszyły poznawanie funkcji genów. Jak dotąd małe interferujące RNA (ang. small interfering RNA, siRNA) stanowią najbardziej efektywne narzędzie pozwalające w precyzyjny sposób wyciszyć ekspresję dowolnego genu poprzez degradację cząsteczek mRNA, co skutkuje obniżoną produkcją białka. siRNA są małymi, około 22-nukleotydowymi, dwuniciowymi cząsteczkami RNA o 100%-owej homologii do docelowego mRNA, powstałymi w wyniku syntezy chemicznej. Terapeutyczny potencjał siRNA wzbudza ogromne zainteresowanie, jednak skuteczne terapie z użyciem siRNA wymagają zastosowania wydajnych oraz bezpiecznych nośników umożliwiających użycie siRNA wewnątrz żywego organizmu (in vivo). Aplikacja tzw. „nagiego siRNA” – bez użycia nośnika – skutkuje jego degradacją przez enzymy odpowiedzialne za rozkład RNA oraz jego niemal natychmiastowym (5-10 min) wydalaniem z krwiobiegu.

Komórki śródbłonna naczyń stanowią wysoce wyspecjalizowaną wyściółkę naczyń krwionośnych i pełnią kluczową rolę w utrzymywaniu wewnętrznej homeostazy organizmu poprzez regulację ważnych procesów biologicznych takich jak np. krzepnięcie krwi, angiogeneza, odpowiedź zapalna oraz regulacja ciśnienia tętniczego i ukrwienia tkanek. Szczególnie istotną rolę komórek śródbłonna naczyń jest regulacja odpowiedzi zapalnej, gdzie odpowiadają one za rekrutację leukocytów z krwiobiegu do ogniska zapalnego oraz pośredniczą w ich migracji do przyległych tkanek. Kontrola odpowiedzi prozapalnej przez komórki śródbłonna naczyń odbywa się poprzez ich aktywację pod wpływem bodźców prozapalnych np. bakteryjnych lipopolisacharydów (LPS), co indukuje produkcję białek z rodziny selektyn (P-selektyny, E-selektyny), białek adhezyjnych (ang. Vascular cell adhesion protein 1; VCAM-1, Intercellular Adhesion Molecule 1; ICAM-1) oraz wydzielanie cytokin prozapalnych (m.in. interleukiny-6 i 8; IL-6, IL-8). Selektyny i białka adhezyjne uczestniczą w adhezji leukocytów do aktywowanych komórek śródbłonna, podczas gdy interleukiny odpowiadają za pobudzenie procesu zapalnego i aktywację leukocytów.

Terapie przeciwzapalne, stosowane obecnie w leczeniu przewlekłych lub ostrych stanów zapalnych towarzyszących np. miażdżycy, cukrzycy typu 2 czy sepsie, charakteryzuje brak selektywności molekularnej i komórkowej. Działają one systemowo na wiele komórek organizmu oraz blokują wiele różnych mechanizmów wewnątrzkomórkowych, co prowadzi do niepożądanych efektów ubocznych takich jak obniżenie odporności biologicznej organizmu, osteoporoza, zwiększone

ryzyko zawału mięśnia sercowego i problemy z układem pokarmowym. Opracowanie nowego typu nośników pozwalających na selektywne dostarczanie siRNA do aktywowanych komórek śródbłonka naczyń, w celu obniżenia ekspresji czynników prozapalnych, umożliwiłoby terapię przeciwzapalną o wysokiej specyficzności molekularnej i komórkowej. Szczególnie obiecujące pod tym względem są nośniki lipidowe, ze względu na ich niską toksyczność w próbach klinicznych oraz wysoką wydajnością w transfekcji siRNA *in vivo*.

Cele badań opisanych w niniejszej pracy były następujące:

- Zaprojektowanie oraz scharakteryzowanie nośnika lipidowego opartego na lipidzie kationowym SAINT-C18, który umożliwiłby efektywne i specyficzne dostarczanie siRNA do komórek śródbłonka naczyń w stanie zapalnym.
- Zbadanie przydatności białek adhezyjnych (VCAM-1 oraz E-selektyny) do selektywnego wprowadzania nośników siRNA do aktywowanych komórek śródbłonka naczyń.
- Zbadanie potencjału opracowanych nośników z siRNA do selektywnego wyciszania prozapalnych genów w komórkach śródbłonka naczyń w stanie zapalnym oraz zademonstrowanie ich efektów przeciwzapalnych *in vivo*.

Rozdział 1 zawiera ogólne wprowadzenie do podjętej tematyki badań oraz informacje dotyczące celów badawczych niniejszej pracy.

Rozdział 2 zawiera przegląd literatury dotyczącej aktualnie dostępnych nośników umożliwiających dostarczanie siRNA do komórek śródbłonka naczyń oraz porusza kwestie istotne dla terapii z użyciem siRNA, takie jak właściwości nośnika siRNA wpływające na wydajność transfekcji oraz na uwalnianie siRNA wewnątrz komórki. Rozdział ten prezentuje także koncept zróżnicowania komórek śródbłonka naczyń w poszczególnych organach pod względem ich odpowiedzi prozapalnej oraz dyskutuje konsekwencje tego zjawiska dla potencjalnych terapii z użyciem siRNA celowanych w komórki śródbłonka naczyń. W rozdziale 2 podejmujemy również dyskusję dotyczącą wykorzystania nowych technologii, takich jak laserowe pozyskiwanie mikroskrawków (ang. laser microdissection, LMD) oraz plastrów tkankowych do badań nad nośnikami siRNA w celu przyspieszenia ich zastosowania klinicznego.

Celem **rozdziału 3** było zbadanie funkcji czynnika transkrypcyjnego early growth response protein-1 (Egr-1) w rozwoju nadciśnienia płucnego (ang. pulmonary arterial hypertension, PAH). Chorobę tę cechują charakterystyczne zmiany w błonie wewnętrznej naczyń płucnych (ang. neointimal lesions) prowadzące do podwyższenia ciśnienia w krążeniu płucnym oraz przerostu prawego przedsionka serca, a z czasem

do jego niewydylności i śmierci pacjenta. Obecnie nie istnieją skuteczne sposoby leczenia pacjentów z PAH, dlatego niezbędne są badania nad przyczynami rozwoju i nowymi terapiami tej choroby. Dostarczenie do komórek śródbłonka naczyń płucnych katalitycznych nukleotydów (DNAzymów) degradujących mRNA genu Egr-1, w połączeniu z nośnikiem lipidowym 1,2-dioleilo-3-trimetyloamoniopropan (DOTAP), umożliwiło wyciszenie ekspresji tego genu w naczyniach płucnych szczurów z PAH. Wyciszenie ekspresji Egr-1 zahamowało powstawanie zmian w naczyniach płucnych oraz zaskutkowało zmniejszeniem ciśnienia płucnego i utrzymaniem prawidłowej funkcji prawego przedsionka. Zaobserwowano także związek pomiędzy zmniejszoną ekspresją Egr-1 oraz obniżoną ekspresją genów będących pod kontrolą Egr-1 (PDGF-B, TGF- β , IL-6 and p53), co mogło mieć wpływ na obniżenie proliferacji i zwiększenie apoptozy komórek w naczyniach płucnych. Wyniki te zostały również potwierdzone z użyciem pioglitazonu – leku, który poprzez aktywację PPAR γ hamuje ekspresję Egr-1. Wyniki te wskazują, że Egr-1 pełni istotną rolę w rozwoju PAH i może posłużyć jako cel dla przyszłych terapii, zarówno genowych, opartych na siRNA lub DNAzymach, lub też farmakologicznych, z użyciem aktywatorów PPAR γ (np. pioglitazonu).

W **rozdziale 4** stworzono oraz scharakteryzowano nośnik lipidowy oparty na lipidzie kationowym SAINT-C18, tzw. SAINT-O-Somes, oraz zbadano jego potencjał do efektywnego i specyficznego dostarczania siRNA do komórek śródbłonka naczyń w stanie zapalnym. Konstrukcja nośnika opierała się na wykorzystaniu liposomów: pęcherzyków powstających samoistnie z fosfolipidów w środowisku wodnym, mających formę podwójnej warstwy lipidowej otaczającej hydrofilowe wnętrze. Dodanie lipidu kationowego SAINT-C18 do kompozycji konwencjonalnych liposomów nadało im właściwości niezbędne dla nośnika siRNA, m.in. umożliwiło wydajne inkorporowanie siRNA do wnętrza liposomów. W rozdziale tym scharakteryzowano właściwości fizykochemiczne nośnika zawierającego siRNA takie jak rozmiar, stabilność w obecności surowicy, wydajność inkorporowania siRNA oraz jego ochrona przed degradacją. Potwierdzono także przydatność VCAM-1 oraz E-selektyny jako białek, które mogą służyć do specyficznego dostarczania siRNA do komórek śródbłonka naczyń aktywowanych przez TNF α (czynnik nekrozy nowotworów; ang. tumor necrosis factor). W tym celu nośnik wyposażono w przeciwciała specyficznie rozpoznające VCAM-1 lub E-selektynę na powierzchni aktywowanych komórek śródbłonka naczyń i badano specyficzność i efektywność dostarczania siRNA do tych komórek. Inkubacja aktywowanych komórek z nośnikiem zawierającym siRNA specyficznym dla VE-kadheryny (ang. VE-cadherin) skutkowało 60% wyciszeniem ekspresji mRNA oraz białka tego genu. Zbadano też właściwości farmakokinetyczne radioaktywnie wyznakowanego nośnika poprzez jego dożylną iniekcję u myszy. Wyniki potwierdziły, że SAINT-O-Somes umożliwiają specyficzne i efektywne wyciszenie

genów w komórkach śródbłonna naczyń oraz spełniają wymogi stawiane nośnikom siRNA przeznaczonym do aplikacji *in vivo*.

W **rozdziale 5** kontynuowano badania nad SAINT-O-Somes w mysim modelu stanu zapalnego. Celem badań było ustalenie czy SAINT-O-Somes wyposażone w przeciwciała rozpoznające VCAM-1 oraz zawierające siRNA przeciwko podjednostce p65 (RelA) czynnika transkrypcyjnego NFκB są w stanie zahamować aktywację komórek śródbłonna naczyń przez bodźce prozapalne (np. LPS). Wykazano, iż nośniki wyposażone w przeciwciała rozpoznające VCAM-1 umożliwiają specyficzne dostarczanie siRNA do mysich komórek śródbłonna naczyń wykazujących podwyższoną ekspresję VCAM-1, wywołaną dożylnym podaniem TNFα. Zastosowanie technologii laserowego pozyskiwania mikroskrawków do izolacji komórek śródbłonna naczyń żylnych nerek umożliwiło zlokalizowaną analizę ekspresji genów i wykazanie lokalnego efektu siRNA w tych naczyniach. Nośniki zawierające siRNA specyficzne dla VE-kadheryny lub p65 pozwoliły na 40% wyciszenie ich ekspresji. Zahamowanie ekspresji p65 spowodowało osłabienie odpowiedzi prozapalną komórek śródbłonna naczyń żylnych nerek stymulowanych LPS, objawiające się zmniejszoną ekspresją mRNA dla E-selektyny, MCP-1 i IL-6 oraz zmniejszoną adhezją leukocytów do ścian tych naczyń. Wyniki te pokazały, że SAINT-O-Somes wyposażone w przeciwciała rozpoznające VCAM-1 oraz zawierające siRNA przeciwko p65 są zdolne do specyficznego zahamowania ekspresji genu p65 w aktywowanych komórkach śródbłonna naczyń oraz do zahamowania odpowiedzi prozapalnej *in vivo*. Jest to także pierwsza prezentacja zastosowania siRNA do terapii przeciwzapalnej celowanej w komórki śródbłonna naczyń.

Rozdział 6 przedstawia konstrukcję nośnika siRNA z wykorzystaniem lipidu kationowego SAINT-C18 oraz białka protaminy. Celem badań było stworzenie nośnika odznaczającego się wysoką wydajnością transfekcji siRNA do komórek śródbłonna naczyń. Idea konstrukcji tego nośnika została oparta na zdolności SAINT-C18, w kombinacji z lipidem 1,2- dioleilo-sn-glicero-3-fosfatydyloetanolamina (DOPE) w stosunku molowym 1:1, do efektywnej transfekcji DNA, siRNA oraz białka do komórek z niską toksycznością. Protamina to białko o niskiej masie cząsteczkowej bogate w argininę i wspomagające upakowanie DNA w plemnikach u niektórych ssaków. Silna kationowość protaminy sprawia, że jest ona stosowana w warunkach klinicznych do osłabiania właściwości antykoagulacyjnych heparyny oraz do konstrukcji nośników transportujących kwasy nukleinowe (np. DNA). Skonstruowane przez nas nośniki SAINT-liposome-polycation-DNA (S-LPD) and SAINT-liposome-polycation (S-LP) powstały w wyniku tworzenia kompleksów protaminy z siRNA oraz DNA, lub jedynie z siRNA, a następnie inkorporacji powstałych kompleksów przez liposomy o kompozycji

SAINT:DOPE. S-LPD i S-LP wykazywały się wysoką wydajnością inkorporacji siRNA, niską toksycznością oraz wysoką wydajnością transfekcji siRNA do komórek śródbłonka naczyń. Dodanie do mieszaniny nośników 10 mol% poli(tlenku etylenu) (PEG) oraz wyposażenie ich w przeciwciała rozpoznające E-selektynę umożliwiło specyficzne dostarczanie siRNA do komórek śródbłonka naczyń aktywowanych przez TNF α . Ponadto pokazano, że właściwości fizykochemiczne prezentowane przez S-LPD i S-LP spełniają wymogi stawiane nośnikom siRNA przeznaczonym do zastosowania *in vivo*.

Rozdział 7 podsumowuje wyniki opisane w poprzedzających rozdziałach oraz przedstawia perspektywy przyszłych badań.

Podsumowując, wyniki badań niniejszej pracy demonstrują, że zaprezentowane nośniki siRNA oparte na lipidzie kationowym SAINT-C18 umożliwiają specyficzne dostarczanie siRNA *in vivo* do komórek śródbłonka naczyń w stanie zapalnym. Przyszłe badania w stosownych modelach zwierzęcych pozwolą ocenić korzyści płynące z zastosowania terapii opartych na siRNA w leczeniu przewlekłych chorób zapalnych.

About the author – Curriculum Vitae

Piotr Kowalski was born on 7th of May 1985 in Lezajsk, Poland. He completed his secondary school education with distinction in 2004, specializing in mathematics and informatics, and started studies at Jagiellonian University (Kraków, Poland) at the Faculty of Biology and Earth Science. He specialized in Biochemistry and conducted his master research project at the Department of Medical Biotechnology, under the supervision of Prof. Alicja Józkowicz and Prof. Józef Dulak. In 2009 he defended his master thesis entitled “Improvement of viral transduction methods for overexpression of cytoprotective genes in endothelial progenitor cells”. As a master student, he participated in the international research programs, including Leonardo da Vinci and Undergraduate Research Experience and Knowledge Award (UREKA). Within the framework of Leonardo da Vinci he spent three months in the Institute Clinique de La Souris (France) at the laboratory for Genetic Engineering and Model Validation, where under supervision of Dr. Xavier Warot, he worked on implementation of Bacterial Artificial Chromosome recombineering technology for generation of transgenic mouse models. During UREKA he spent three months in the laboratory of Dr. Margaret Worrall at University College Dublin (Ireland), where he investigated protein-protein interactions of tumor associated serpins (serine protease inhibitors) SCCA2 and leupin. He also experienced research from the industrial perspective by working for six months in a biotech company BioTe21. In August 2009 he started his PhD studies at the University of Groningen (The Netherlands). He joined the department of Pathology and Medical Biology and conducted his research in the Laboratory for Endothelial Biomedicine and Vascular Drug Targeting under the supervision of Prof. Grietje Molema and Dr. Jan Kamps. His PhD research focused on the development of novel lipid-based system for specific in vivo delivery of siRNA to inflamed endothelium. His work provided new insights into the use of SAINT-O-Somes and adhesion molecules such as VCAM-1 for delivering siRNA into activated ECs and presented proof of concept for microvascular segment specific, siRNA delivery based anti-inflammatory therapeutic intervention. In the same group he also worked as a postdoc for five months investigating the potential of targeted SAINT-O-Somes, formulated with anti-inflammatory drugs, for inhibition of endothelial activation in sepsis mouse models.

List of publications

Published papers:

1. **Kowalski PS**; Zwiers PJ; Morselt HW; Kuldo JM; Leus NG; Ruiters MH; Molema G; Kamps JA, Anti-VCAM-1 SAINT-O-Somes enable endothelial-specific delivery of siRNA and downregulation of inflammatory genes in activated endothelium *in vivo*. *J Control Release*. **2014** Feb 28;176:64-75.
2. Leus NG; Talman EG; Ramana P; **Kowalski PS**; Woudenberg-Vrenken TE; Ruiters MH; Molema G; Kamps JA, Effective siRNA delivery to inflamed primary vascular endothelial cells by anti-E-selectin and anti-VCAM-1 PEGylated SAINT-based lipoplexes. *Int J Pharm*. **2014** Jan 1;459(1-2):40-50.
3. **Kowalski PS**; Lintermans LL; Morselt HW; Leus NG; Ruiters MH; Molema G; Kamps JA, Anti-VCAM-1 and Anti-E-selectin SAINT-O-Somes for Selective Delivery of siRNA into Inflammation-Activated Primary Endothelial Cells. *Mol Pharm*. **2013** Aug 5;10(8):3033-44.
4. **Kowalski PS**; Leus NG; Scherphof GL; Ruiters MH; Kamps JA; Molema G, Targeted siRNA delivery to diseased microvascular endothelial cells: cellular and molecular concepts. *IUBMB Life* **2011** Aug;63(8):648-58.
5. Higgins WJ; Fox DM; **Kowalski PS**; Nielsen JE; Worrall DM, Heparin enhances serpin inhibition of the cysteine protease cathepsin L. *J Biol Chem*. **2010** Feb 5;285(6):3722-9.

Submitted:

6. Dickinson MG; **Kowalski PS**; Bartelds B; Borgdorff MA; Sietsma H; Molema G; Kamps JA; Berger R M, Egr-1 downregulation using Catalytic Oligodeoxynucleotides Attenuates Neointimal Development and Disease Progression in Experimental Pulmonary Arterial Hypertension. *Under revision for Cardiovascular research*
7. Leus NG; Morselt HW; Zwiers PJ; **Kowalski PS**; Ruiters MH; Molema G; Kamps JA, VCAM-1 specific PEGylated SAINT-based lipoplexes deliver siRNA to activated endothelium *in vivo*. *Under revision for International Journal of Pharmaceutics*.

Manuscript in preparation:

8. **Kowalski PS**; Kuninty PR; Bijlsma KT; Stuart MC; Leus NG; Ruiters MH; Molema G; Kamps JA, SAINT-Liposome-Polycation particles, a new carriers for improved delivery of siRNAs to inflamed endothelial cells.

Acknowledgements

One cannot underestimate the importance of teamwork while doing a PhD, as said by Michael Jordan, one of the greatest basketball players of our times, “Talent wins games, but teamwork and intelligence wins championships”. The completion of this thesis would not have been possible without the help of many people who have been a part of my PhD, and to which I would like to express my sincere gratitude.

First and foremost I would like to thank my promoter Prof. Grietje Molema and co-promoter Dr. Jan Kamps for giving me the opportunity to perform this research and their esteemed guidance. Dear Ingrid, thank you for your great mentorship, good advices and showing me how to be a good scientist and mentor for others. You influenced me to keep my learning curve steep and set the bar high for future challenges. Dear Jan, thank you for your constant support and always being available to discuss all burning issues. You taught me how to make my research scientifically sound, how to stay enthusiastic even when the data was depressing, and you always encouraged me to enjoy and spend more time outside the lab, for which I am very grateful. I would also like to thank Prof. Gerrit Scherphof for his temporary supervision of my PhD during the first year and for his input in proofreading of my manuscripts and translating my Dutch summary.

My sincere gratitude to the members of the reading committee, Prof. Alicja Józkwicz, Prof. Geert Storm, and Prof. Andreas Herrmann, for their time and effort put into reading and approving my thesis. Especially, I would like to thank Prof. Józkwicz for coming all the way from Kraków to Groningen to be an opponent at my defense.

My utmost thanks to all people from the EBVDT group and the Medical Biology department who helped me during these four and a half years. Special thanks to my paranymphs Dr. Jill Moser and Dr. Matijs van Meurs. Thank you for being my support at this very special moment. Jill, I will always cherish your sense of humor and our scientific discussions during the coffee breaks and I truly believe that one of your many brilliant ideas will make you famous, so stay in touch! J Matijs, thank you for all your support and encouragement to excel. Many thanks to Rianne Jongman for making this lovely book and for her skilled technical assistance in the lab. Henriëtte, you have taught me nearly everything I know about the liposomes. I appreciate your dedication to research and your eagerness to help me with the experiments, thank you. Peter Zwiers, thank you for your professional help and guidance with the laser microdissection and the animal experiments. It was always fun to work with you. Henk (a.k.a. Mr. HUVEC), I am very grateful for your help with the cell culturing and many other things in the lab, you have golden hands and a golden heart. Peter Heeringa, thank

you for organizing great New year's events and for always being willing to supply the "EBVDT entertainment" crew your HD camera and iMac. I would also like to thank Miriam, Nikola, Ganesh, Sigga, Anita, Guido, Linda, Martin, Jasper, Pytrick, Marja, Bart, Geert, Roelof Jan, Teo and Jelleke for answering my numerous questions and for always being willing to share your precious protocols.

Many thanks to my students Lucas, Tiede and Praneeth for helping to develop my mentor skills and for many hours of hard work and fun, which lead to completion of this book. Good luck with your scientific careers. Karin, Rieza, Marijn, Linda and Koen thanks for your active participation in the social and scientific life of the EBVDT group.

Special thanks to my office mates: Niek, Roel, Gopi, Titia, Elise, Neng, Betty and Gesiena. It was a pleasure to work with you all. You were the most friendly and amusing people I have worked with. Above all, you are my good friends and I hope we will stay in touch. Niek, my friend, we share not only the authorship on papers but also a lot of great memories from the lab, conferences, and social events. I am grateful for all your help and wish you all the best with your postdoc and defense of your thesis. Roel, thanks for taking over the role of being the youngest AIO in the room and for your enthusiasm for carrying this responsibility ;). Gopala, thank you for the opportunity to experience the defense ceremony as your paranymph. I now feel more prepared for my own defense ;). Best of luck with your postdoc and your wedding. Titia, thanks for your enthusiasm at work and good advice. Good luck with your teaching career. Elise, many thanks for our scientific discussions and amusing skiing/cycling trips. Good luck with choosing the best career path. Neng, I miss your loempia's and other delicious food that you were making and bringing to work. I hope you enjoy being home and you will soon become a professor. Betty, thanks for nice conversations and for staying in touch with the group after your PhD. Good luck with your clinical chemist residency. Gesiena, thanks for being a driving force for our social events and introducing me to the "cafe world" ;). Best of luck with your M.D. career.

I would also like to thank my collaborators Dr. Beatrijs Bertelds and Dr. Michael Dickinson from the department of Pediatric Cardiology. I have a high regard for the work we did together and I believe that it will soon be published in a very good journal. Michael, we both share the passion for research thus I hope you will find the time in your busy M.D. schedule to connect with science and we will stay in touch. Many thanks to Rebecca, you were an invaluable assistance and a superb collaborator during my short postdoc project. I am confident that we will get a nice paper out of these results which will also be a part of your thesis. Thanks for your hard work and good luck with your promotion.

Many thanks to all my fellow PhD student and colleagues from the other groups or departments: Zia, Bispo, Hande, Federico, Akshay, Monika, Ewa, Kasia, Marcin, Ania, Nato, Nikola, Marta, Paulina, Anouk, Christian, Rutger, Fahimeh, Ee soo, Ghazaleh, Mojtaba, Vaishali, Genaro, David, Roland, Eelke, Marlies, Floor, Jan Renier, Kasia, Antek, Milind, Justin, Saritha and Vikram. Thanks for always being willing to share your protocols, for all the volleyball tournaments and lab days, for coffee breaks, movie evenings and other scientific and social events that we shared. I wish you all the best with your projects and scientific careers.

I would like to express my appreciation to the team of the animal facility: Miriam van der Meulen-Frank, Arjen Petersen, Michel Weij, Annemieke Smit-van Oosten, and Marloes for their assistance in planning and execution of my animal experiments. Many thanks to Klaas Sjollema from the UMCG Microscopy and Imaging Center for his help with handling various types of microscopes and obtaining high quality images.

My sincere gratitude to my colleagues and team mates from volleyball club APSAZ. Thank you for all the trainings, games, tournaments and social events that allowed me to unwind after the rough days in the lab.

I would like to thank my Parents, Małgorzacie i Adamowi Kowalskim. Kochani Rodzice, dziękuję za Wasze ogromne wsparcie w trakcie mojego doktoratu. Dzięki Wam zawsze mogłem rozwijać swoje pasje i zainteresowania, dlatego mój doktorat jest także Waszym osiągnięciem. Dziękuję że zawsze mogłem i wciąż mogę na Was polegać. Many thanks to my Sister Monika for always supporting my choices and visiting me in Groningen. Good luck with getting your PhD degree soon.

Finally, I would like to thank my beloved Małgosia for being there for me when I needed it the most, and for making me a better person. Achieving this PhD would have been much more difficult without your support. I am certain that together we can overcome all future challenges.

Piotr